Investigation into Strategies for Harvesting Chemical Based Information using Digital Imaging and Infra-red Sensors for Environmental and Health Applications

— by —

Cormac Fay

B.Eng. in Mechatronic Engineering

M.Eng. in Telecommunications Engineering

Thesis submitted for the degree of:

Doctor of Philosophy

— Supervised by —

Dr. Brian Corcoran (School of Mechanical Engineering);

Prof. Noel O'Connor (School of Electronic Engineering);

Prof. Dermot Diamond (School of Chemical Sciences);

"Yaaaay/ Got away with it again!"

Declaration

I hereby certify that this material, which I now submit for assessment on the programme of study leading to the award of Doctor of Philosophy is entirely my own work, that I have exercised reasonable care to ensure that the work is original, and does not to the best of my knowledge breach any law of copyright, and has not been taken from the work of others save and to the extent that such work has been cited and acknowledged within the text of my work.

Signed: _____

ID No.: **51577204** Date: 18^{th} **of September 2013**

Dedication

— To the craziest people I know: —

My Parents:

Nualer and Jimmy;

Brothers & Sisters:

Jamie, Yaya, Aggie, Merzer, Ed, Mick, and Nunu;

Nieces & Nephews:

Eoin, Niamh, Craig, Con, Aoife, Stephanie, Emma, Sé, Holly, Róisín, and James (Jr.);

To those that didn't make it:

Máire, Marie, Hugh, and Joe (R.I.P.);

This is for you, dedicated to you, and kept secret from you for years.

Lastly, to the love of my life, my soul mate, and the greatest person in the world: Me, without whom this thesis would have been written years ago.

Quotes

"It is not the critic who counts: not the man who points out how the strong man stumbles or where the doer of deeds could have done better. The credit belongs to the man who is actually in the arena, whose face is marred by dust and sweat and blood, who strives valiantly, who errs and comes up short again and again, because there is no effort without error or shortcoming, but who knows the great enthusiasms, the great devotions, who spends himself for a worthy cause; who, at the best, knows, in the end, the triumph of high achievement, and who, at the worst, if he fails, at least he fails while daring greatly, so that his place shall never be with those cold and timid souls who knew neither victory nor defeat."

— Theodore Roosevelt, Citizenship in a Republic, Speech at the Sorbonne, Paris, April 23, 1910

"But we were born of risen apes, not fallen angels, and the apes were armed killers besides. And so what shall we wonder at? Our murders and massacres and missiles, and our irreconcilable regiments? Or our treaties whatever they may be worth; our symphonies however seldom they may be played; our peaceful acres, however frequently they may be converted into battlefields; our dreams however rarely they may be accomplished. The miracle of man is not how far he has sunk but how magnificently he has risen. We are known among the stars by our poems, not our corpses."

— Robert Ardrey

"The greatest danger for most of us is not that our aim is too high and we miss it, but that it is too low and we reach it."

— Michelangelo Buonarroti

> *"... Ask ten different scientists about the environment, population control, genetics ... and you'll get ten different answers, but there's one thing every scientist on the planet agrees on. Whether it happens in a hundred years or a thousand years or a million years, eventually our Sun will grow cold and go out. When that happens, it won't just take us. It'll take Marilyn Monroe and Lao-Tzu, and Einstein, and Morobuto, and Buddy Holly, and Aristophanes ... and all of this ... all of this was for nothing unless we go to the stars."*
>
> — Jeffrey Sinclair

"Do not be afraid to ask dumb questions; they are easier to handle than dumb mistakes."

— Unknown

> *"Necessity is the mother of invention."*
>
> — Plato

"All truths are easy to understand once they are discovered; the point is to discover them."

— Galileo Galilei

> *"If you are not prepared to be wrong you will never come up with anything original."*
>
> — *Sir Ken Robinson, TED 2010*

"During each show a control audience is locked in an identical, adjoining room without comedians. The Comedy Research Project then assesses whether this audience has laughed more or less than the experimental audience. The CRP audience is not, however, protected by Home Office animal welfare regulations."

— Dr. Helen Pilcher, The Comedy Research Project

"... This is Ankh-Morpork,... A sprawling place, home to a million people, greatest of cities on the Discworld, located on either side of the river Ankh, a waterway so muddy that it looks as if it is flowing upside down... The river Ankh is probably the only river in the universe on which the investigators can chalk the outline of the corpse..."

"An education was a bit like a communicable sexual disease. It made you unsuitable for a lot of jobs and then you had the urge to pass it on."

"Light thinks it travels faster than anything but it is wrong. No matter how fast light travels, it finds the darkness has always got there first, and is waiting for it."

"Seeing, contrary to popular wisdom, isn't believing. It's where belief stops, because it isn't needed any more."

— Sir Terence David John "Terry" Pratchett

"One of the advantages of being disorderly is that one is constantly making exciting discoveries."

— A. A. Milne

Publications

Journal (Published)

[1] Monika Czugala, Cormac Fay, Noel E. O'Connor, Brian Corcoran, Fernando Benito-Lopez, and Dermot Diamond. **Portable integrated microfluidic analytical platform for the monitoring and detection of nitrite**. *Talanta*, **116**:997 – 1004, 2013.

[2] Larisa Florea, Cormac Fay, Emer Lahiff, Thomas Phelan, Noel E O'Connor, Brian Corcoran, Dermot Diamond, and Fernando Benito-Lopez. **Dynamic pH mapping in microfluidic devices by integrating adaptive coatings based on polyaniline with colorimetric imaging techniques**. *Lab Chip*, pages –, 2013.

[3] Vincenzo F. Curto, Cormac Fay, Shirley Coyle, Robert Byrne, Corinne O'Toole, Caroline Barry, Sarah Hughes, Niall Moyna, Dermot Diamond, and Fernando Benito-Lopez. **Real-time sweat pH monitoring based on a wearable chemical barcode microfluidic platform incorporating ionic liquids**. *Sensors and Actuators B: Chemical*, **171-172**(0):1327 – 1334, 2012.

[4] Cormac Fay, Salzitsa Anastasova, Conor Slater, Sandra Teodora Buda, Roderick Shepherd, Brian Corcoran, Noel E. O'Connor, Gordon G. Wallace, Aleksandar Radu, and Dermot Diamond. **Wireless Ion-Selective Electrode Autonomous Sensing System**. *IEEE Sensors Journal*, **11**(10):2374–2382, OCT 2011.

[5] Cormac Fay, Aiden R. Doherty, Stephen Beirne, Fiachra Collins, Colum Foley, John Healy, Breda M. Kiernan, Hyowon Lee, Damien Maher, Dylan Orpen, Thomas Phelan, Zhengwei Qiu, Kirk Zhang, Cathal Gurrin, Brian Corcoran, Noel E. O'Connor,

Alan F. Smeaton, and Dermot Diamond. **Remote Real-Time Monitoring of Subsurface Landfill Gas Migration**. *Sensors*, **11**(7):6603–6628, JUL 2011.

[6] Cormac Fay, King-Tong Lau, Stephen Beirne, Ciaran O. Conaire, Kevin McGuinness, Brian Corcoran, Noel E. O'Connor, Dermot Diamond, Scott McGovern, Greg Coleman, Rod Shepherd, Gursel Alici, Geoff Spinks, and Gordon Wallace. **Wireless aquatic navigator for detection and analysis (WANDA)**. *Sensors and Actuators B-Chemical*, **150**(1):425–435, SEP 21 2010.

[7] Dylan Orpen, Stephen Beirne, Cormac Fay, King Tong Lau, Brian Corcoran, and Dermot Diamond. **The optimisation of a paired emitter-detector diode optical pH sensing device**. *Sensors and Actuators B-Chemical*, **153**(1):182–187, MAR 31 2011.

[8] Isabel M. Perez de Vargas-Sansalvador, Cormac Fay, M. D. Fernandez-Ramos, Diamond Diamond, Fernando Benito-Lopez, and Luis Fermin Capitan-Vallvey. **LED-LED portable oxygen gas sensor**. *Analytical and Bioanalytical Chemistry*, **0**:1–8, 2012.

[9] Benjamin Schazmann, Deirdre Morris, Conor Slater, Stephen Beirne, Cormac Fay, Ronen Reuveny, Niall Moyna, and Dermot Diamond. **A wearable electrochemical sensor for the real-time measurement of sweat sodium concentration**. *Analytical Methods*, **2**(4):342–348, 2010.

[10] Isabel M. Vargas-Sansalvador, Cormac Fay, Thomas Phelan, M.D. Fernández-Ramos, Luis Fermin Capitan-Vallvey, Dermot Diamond, and Fernando Benito-Lopez. **A new light emitting diode - light emitting diode portable carbon dioxide gas sensor based on an interchangeable membrane system for industrial applications**. *Analytica Chimica Acta*, **699**(2):216 – 222, 2011.

Journal (In Preparation)

[11] Cormac Fay, Kevin McGuinness, Martina O'Toole, Brian Corcoran, Noel E. O'Connor, Gordon Wallace, and Dermot Diamond. **Investigation into the Effects of Compression Algorithms on Chemical Sensing via Imaging Techniques**. *In Preparation*, 2013.

[12] Cormac Fay, Aiden R. Doherty, Brian Corcoran, Noel E. O'Connor, Alan F. Smeaton, and Dermot Diamond. **An integrated**

approach to event detection, categorisation and visualisation for heterogeneous sensor data sources. *Submitted*, 2012.

[13] Claudio Zuliani, Cormac Fay, Giusy Matzeu, Gavin Power, Brian Corcoran, and Dermot Diamond. **Development towards a sensorised gum shield for real-time pH salivary sensing**. *Submitted*, 2012.

[14] Cormac Fay, John Healy, Aiden R. Doherty, Damien Maher, Fiachra Collins, Dylan Orpen, Brian Corcoran, Noel E. O'Connor, Alan F. Smeaton, and Dermot Diamond. **Remote monitoring of gas pressure levels at landfill waste sites and presentation of the data on-line through the use of an autonomous sensing platform**. *In Preparation*, 2012.

[15] Cormac Fay, Brian Corcoran, Noel E. O'Connor, Gordon Wallace, and Dermot Diamond. **Investigation into the Saturation component of the Hue colour model for colorimetric chemical analysis via digital imaging techniques**. *In Preparation*, 2013.

[16] Anshika Agarwal, Cormac fay, Vincenzo Curto, Dermot Diamond, T S Natarajan, and TS Chandra. **Development of pH sensitive electrospun nanofibers to detect spoilage of the milk**. *In Preparation*, 2013.

Book Chapter

[17] Dermot Diamond, Fiachra Collins, John Cleary, Claudio Zuliani, and Cormac Fay. *Autonomous Sensor Networks: Collective Sensing Strategies for Analytical Purposes*, **Vol. 13** of *Springer Series on Chemical Sensors and Biosensors*. Springer, first edition, February 2013.

Conference

[18] John Cleary, Cormac Fay, Thomas Phelan, Ted McCormack, Owen Naughton, Paul Johnston, Laurence Gill, and Dermot Diamond. **Kinvarra bay data fusion project**. In *SmartBay Principal Investigator Workshop*, 12 Jun 2013.

[19] Cormac Fay, John Healy, Aiden Doherty, Damien Maher, Fiachra Collins, Dylan Orpen, Brian Corcoran, Noel E. O'Connor, Alan F. Smeaton, and Dermot Diamond. **Remote monitoring of gas pressure levels at landfill waste sites and presentation of the data**

on-line through the use of an autonomous sensing platform. *Project Report. Environmental Protection Agency*, 2010.

[20] T. Radu, C. Slater, D. Kim, C. Fay, and D. Diamond. **Smart Dust: Autonomous sensors for environmental monitoring-detection of heavy metals in dust**. In *Environmental Sensing Simposium*, NCSR, DCU, Ireland, 25th November 2008.

[21] T. Radu, Lau-K.T. Fay, C., and D. Diamond. **PROeTEX Project: Advanced e-textiles for firefighters and civilian victims**. In *Environmental Sensing Simposium*, NCSR, DCU, Ireland, 25th November 2008.

[22] C. Slater, C. Fay, B. Corcoran, and D. Diamond. **Low power microcontroller based platform for the development of remote environmental monitoring**. In *Environmental Sensing Simposium*, NCSR, DCU, 25th November.

[23] S. McGovern, C. Fay, G. Coleman, R. Shepherd, G. Alici, D. Spinks, Diamond, G., and G. Wallace. **Wireless aquatic navigator for detection and analysis (WANDA)**. In *Actuators for Bionics and Biomimetics Symposium*, 29th May 2009.

[24] C. Fay, S. Beirne, King-Tong. Lau, B. Corcoran, N.E. O'Connor, D. Diamond, S. McGovern, G. Coleman, R. Multu, G. Alici, G. Spinks, and G. Wallace. **Wireless aquatic navigator for detection and analysis (WANDA)**. In *Dublin Innovation week*, 14th-20th October 2009.

[25] M. O'Toole, C. Fay, B. Paull, and D. Diamond. **A highly sensitive LED based miniaturised photometric detector applied to liquid chromatography**. In *CLARITY Science Open Day - Bringing Information to Life*, O'Reilly Hall University Colleege Dublin, 23rd November 2009.

[26] D. Orpen, Beirne S., C. Fay, King-Tong. Lau, B. Corcoran, and D. Diamond. **Development of a Low-Cost Optical Test Platform for Inkjet Printed Chemical Sensing Films**. In *Dublin Innovation week*, Dublin, 14th-20th October 2009.

[27] C. Fay, S. McGovern, S. Beirne, G. Coleman, R. Shepherd, G. Alici, G. Spinks, G. Wallace, and D. Diamond. **WANDA**. In *International Simposium on Functional Nanomaterials*, NCSR, DCU, Ireland, 10th - 11th September 2009.

[28] C. Fay, S. Beirne, King-Tong. Lau, B. Corcoran, N.E. O'Connor, D. Diamond, S. McGovern, G. Coleman, R. Multu, G. Alici,

G. Spinks, and G. Wallace. **Wireless aquatic navigator for detection and analysis (WANDA)**. In *Dublin City University Faculty Research Day*, Dublin, Ireland., 12th May 2010.

[29] D. Orpen, Beirne S., C. Fay, King-Tong. Lau, B. Corcoran, and D. Diamond. **The Development Of Low-Cost, Robust, Reproducible Optical Chemical Sensors Using Inkjet Printing**. In *UNCSR 2nd Annual Symposium*, September 29th 2010.

[30] D. Orpen, C. Fay, Beirne S., King-Tong. Lau, B. Corcoran, and D. Diamond. **The Development Of Low-Cost, Robust, Reproducible Optical Chemical Sensors Using Inkjet Printing**. In *CLARITY Science Open Day - Bringing Information to Life*, The Helix, Dublin, Ireland., November 19th 2010.

[31] Kiernan-B. Healey, J., C. Fay, S. Beirne, and D. Diamond. **Autonomous Gas Monitoring System**. In *CLARITY Science Open Day - Bringing Information to Life*, The Helix, Dublin, Ireland., November 19th 2010.

[32] B. Kiernan, C. Fay, C. Slater, and D. Diamond. **SMART Landfill: An autonomous approach for environmental gas monitoring**. In *EPA Conference in the RHK*, Museum of Modern Art, Kilmainham, Dublin, 6th - 7th of February 2008.

[33] C. Fay, S. Beirne, G. Wallace, and D. Diamond. **Automated domestic appliance recognition for the elderly**. In *Collaborative Research Opportunities Workshop Enabling Technologies for Active Ageing*, Innovation Campus, Squires Way, North Wollongong, Australia, 14th February 2011.

[34] D. Morris, B. Schazmann, Zhijun Wang, C. Fay, S. Beirne, C. Slater, K.-T. Lau, G. Wallace, and D. Diamond. **Wearable technology for the real-time analysis of sweat during exercise**. In *Applied Sciences on Biomedical and Communication Technologies, 2008. ISABEL '08. First International Symposium on*, pages 1–2, 2008.

[35] D. Morris, B. Schazmann, Y.a Wu, S. Coyle, S. Brady, J. Hayes, C. Slater, C. Fay, K.T. Lau, G. Wallace, and D. Diamond. **Wearable sensors for monitoring sports performance and training**. In *5th International Workshop on Wearable and Implantable Body Sensor Networks, BSN 2008, in conjunction with the 5th International Summer School and Symposium on Medical Devices and Biosensors, ISSS-MDBS 2008*, Hong Kong, 1-3 June 2008.

[36] D. Morris, B. Schazmann, R. Reuveny, Y. Wu, S. Coyle, C. Fay, J. Hayes, N. Moyna, G. Wallace, K.T. Lau, and D. Diamond. **Development and Testing of Textile Bsed Biochemical Sensors Designed for Personal Health and Sports Applicatoins**. In *The Second International Scientific Conference Textiles of the Future (Futuro Textiel)*, Kortrijk, Belguim, 13-15 Nov 2008.

[37] D. Maher, J. Cleary, J. Healy, C. Fay, G. Carroll, and D. Diamond. **A field deployable autonomous wet chemistry analyzer for in situ water quality monitoring**. In *9th Annual IEEE Conference on Sensors*, 1-4 November 2010.

[38] A. Radu, S. Anastasova, C. Fay, D. Diamond, J. Bobacka, and A. Lewenstam. **Low cost, calibration-free sensors for in situ determination of natural water pollution**. In *Sensors, 2010 IEEE*, pages 1487–1490, 2010.

[39] D. Diamond, R. Byrne, F.B. Lopez, J. Cleary, D. Maher, J. Healy, C. Fay, Jungho Kim, and K.-T. Lau. **Biomimetics and materials with multiple personalities - The foundation of next generation molecular sensing devices**. In *Sensors, 2010 IEEE*, pages 1079–1082, 2010.

[40] N. Lopez-Ruiz, V. F. Curto, C. Fay, L.F. Capitan-Vallvey, D. Diamond, A.J. Palma, and F. Benito-Lopez. **Multianalyte colourimetric water analysis, using a mobile phone, in a paper microfluidic**. In *Biosensing Technology*, Sitges, Spain, 12 - 15 May 2013.

[41] Tanja Radu, Cormac Fay, King-Tong Lau, and Dermot Diamond. **Wearable gas sensors**. In *pHealth 2009 - International Workshop on Wearable Micro and Nano Technologies for the Personalised Health*, Oslo, Norway., 24-26 June 2009.

[42] Tanja Radu, Cormac Fay, King-Tong Lau, Rhys Waite, and Dermot Diamond. **Wearable CO2 sensor**. In *Smart Textiles Salon*, Gent, Belgium, 25 September 2009.

[43] Tanja Radu, Cormac Fay, King-Tong Lau, Rhys Waite, and Dermot Diamond. **Wearable sensing application- carbon dioxide monitoring for emergency personnel using wearable sensors**. In *ICESE 2009 - International Conference on Environmental Systems Engineering*, Venice, Italy, 28-30 October 2009.

[44] Damien Maher, John Cleary, John Healy, Cormac Fay, Gary Carroll, and Dermot Diamond. **Commercialisation of an autonomous**

phosphate analyser. In *ENVIRON 2010*, Limerick, Ireland, 17-19 February 2010.

[45] Stephen Beirne, Breda M. Kiernan, Cormac Fay, Colum Foley, Brian Corcoran, Alan F. Smeaton, and Dermot Diamond. **Autonomous greenhouse gas measurement system for analysis of gas migration on landfill sites**. In *SAS 2010 - IEEE Sensors Applications Symposium*, Limerick , Ireland, 23–25 February 2010.

[46] Breda M. Kiernan, Stephen Beirne, Cormac Fay, and Dermot Diamond. **Monitoring of gas emissions at landfill sites using autonomous gas sensors**. *Project Report. STRIVE, Environmental Protection Agency*, 2010.

[47] Dylan Orpen, Cormac Fay, Stephen Beirne, King-Tong Lau, Brian Corcoran, and Dermot Diamond. **The development of low-cost, robust, reproducible optical chemical sensors using inkjet printing**. In *Sensor Systems for Environmental Monitoring*, London, England., 14 October 2010.

[48] Isabel M. Perez de Vargas-Sansalvador, Cormac Fay, Thomas Phelan, M. D. Fernández-Ramosa, Luis Fermin Capitán-Vallveya, Dermot Diamond, and Fernando Benito-Lopez. **A new LED-LED portable CO2 gas sensor based on an interchangeable membrane system for industrial applications**. In *CASi*, The Helix, Dublin, Ireland., 21 February 2011.

[49] Cormac Fay, Stephen Beirne, Ciarán Ó Conaire, Kevin Mc Guinness, Scott McGovern, Greg Coleman, Rod Shepherd, King-Tong Lau, Brian Corcoran, Noel E. O'Connor, Gursel Alici, Geoff Spinks, Gordon Wallace, and Dermot Diamond. **WANDA: A Radically New Approach for Low-Cost Environmental Monitoring**. In *ACES Electromaterials Symposium*, AIIM/IPRI, Innovation Campus, University of Wollongong, Australia., February 9th - 11th 2011.

[50] Stephen Beirne, Cormac Fay, Brian Corcoran, Noel E. O'Connor, Geoff Spinks, Dermot Diamond, and Gordon Wallace. **The role of rapid prototyping technology in the development of electromaterial demonstrator projects**. In *ACES Electromaterials Symposium*, Wollongong, Australia, 11 Feb 2011.

[51] Dylan Orpen, Cormac Fay, Damien Maher, Thomas Phelan, Eoin Hurrell, Colm Foley, Alan F. Smeaton, and Dermot Diamond.

Remote monitoring of landfill gases from solid waste landfill (including real time data integration to a web based data portal). In *Conference on Analytical Sciences (CASi, 2011)*, Dublin, Ireland., 21 - 22 February 2011.

[52] Dylan Orpen, Cormac Fay, T Phelan, Eoin Hurrell, C Foley, Alan F. Smeaton, and Dermot Diamond. **Remote monitoring of landfill gases from solid waste landfill**. In *Conference on Analytical Sciences*, Dublin, Ireland, 21-22 Feb 2011.

[53] Fiachra Collins, Dylan Orpen, Damien Maher, John Cleary, Cormac Fay, and Dermot Diamond. **Distributed chemical sensor networks for environmental sensing**. In *Sensor Devices 2011 - The Second International Conference on Sensor Device Technologies and Applications*, Nice/Saint Laurent du Var, France, 21-27 Aug 2011.

[54] Dylan Orpen, Cormac Fay, Stephen Beirne, Martina O'Toole, King-Tong Lau, Brian Corcoran, and Dermot Diamond. **Ultra low cost LED based gas sensing**. In *Photonics Ireland 2011*, The Grand Hotel, Malahide, Dublin, 7-9 Sept 2011.

[55] Vincenzo F. Curto, Cormac Fay, Shirley Coyle, Robert Byrne, Dermot Diamond, and Fernando Benito-Lopez. **Wearable microfluidic pH sweat sensing device based on colorimetric imaging techniques**. In *MicroTas 2011*, Seattle, USA, 2-6 Oct 2011.

[56] Vincenzo F. Curto, Cormac Fay, Shirley Coyle, Dermot Diamond, and Fernando Benito-Lopez. **Wearable micro-fluidic pH sweat sensing device based on clorimetric imaging techniques**. In *Seminar in Microfluidics*, University of California, Berkeley, CA, 10 Oct 2011.

[57] Monika Czugala, Cormac Fay, Dermot Diamond, and Fernando Benito-Lopez. **Photoactuated ionogel microvalves for water quality on-chip analysis**. In *QUESTOR - DCU Workshop*, Dublin, Ireland., 2 March 2012.

[58] Fiachra Collins, Dylan Orpen, Cormac Fay, and Dermot Diamond. **Analysis of landfill gas migration by use of autonomous gas monitoring platforms**. In *The 27th International Conference on Solid Waste Technology and Management*, Philadelphia, USA, 10-14 Mar 2012.

[59] Monika Czugala, Pedro Ortiz, Cormac Fay, Andreu Llobera, Fernando Benito-Lopez, and Dermot Diamond. **Photo-actuated**

ionogel microvalves for real-time water quality analysis in a microfluidic device. In *Lab on a Chip European Congress*, Edinburgh, UK, 28-29 Mar 2012.

[60] I.M. Perez de Vargas-Sansalvador, Cormac Fay, M.D. Fernandez-Ramos, Dermot Diamond, Fernando Benito-Lopez, and L.F. Capitan-Vallvey. **LED-LED portable oxygen gas sensor**. In *Europtrode*, Barcelona, 1-4 Apr 2012.

[61] Vincenzo F. Curto, Cormac Fay, Shirley Coyle, and Dermot Diamond. **Microfluidic device for colorimetric analysis of sweat**. In *Body Sensor Networks*, London, UK., 10-13 May 2012.

[62] Monika Czugala, Cormac Fay, Pedro Ortiz, Andreu Llobera, Dermot Diamond, and Fernando Benito-Lopez. **Photo-actuated ionogel microvalves for real-time water quality analysis in a microfluidic device**. In *2nd International Symposium on Functional Nanomaterials*, Dublin, Ireland, 6-7th Sept 2012.

[63] Fiachra Collins, Dylan Orpen, Eoghan McNamara, Cormac Fay, and Dermot Diamond. **Landfill gas monitoring network - development of wireless sensor network platforms.** In *SENSORNETS*, Barcelona, Spain., 19 - 21 Feb 2013.

[64] Breda M. Kiernan, Cormac Fay, Stephen Beirne, and Dermot Diamond. **Development of an Autonomous Greenhouse Gas Monitoring System**. In *Proceedings of World Academy of Science, Engineering and Technology*, **20**, pages 153 – 157. World Academy of Science, Engineering and Technology, 2008.

[65] Jung Ho Kim, King Tong Lau, C. Fay, and D. Diamond. **Development of optical sensing system for detection of Fe ions using conductive polymer actuator based microfluidic pump**. In *Sensors, 2008 IEEE*, pages 1155 –1158, oct. 2008.

[66] Breda M. Kiernan, Stephen Beirne, Cormac Fay, and Dermot Diamond. **Landfill gas monitoring at borehole wells using an autonomous environmental monitoring system**. In *Proceedings of World Academy of Science, Engineering and Technology*, **19**, pages 166 – 171. World Academy of Science, Engineering and Technology, 2008.

[67] Deirdre Morris, Benjamin Schazmann, Yangzhe Wu, Shirley Coyle, Sarah Brady, Cormac Fay, Jer Hayes, King Tong Lau, Gordon Wallace, and Dermot Diamond. **Wearable technology for**

bio-chemical analysis of body fluids during exercise. In *Engineering in Medicine and Biology Society, 2008. EMBS 2008. 30th Annual International Conference of the IEEE*, pages 5741 –5744, aug. 2008.

[68] Breda M. Kiernan, Stephen Beirne, Cormac Fay, and Dermot Diamond. **Measurement of representative landfill gas migration samples at landfill perimeters: a case study**. In *The 24th International Conference on Solid Waste Technology and Management*, **SESSION 6A Landfill Studies**, pages 15–18 March, Philadelphia, PA, USA, 2009. The Journal of Solid Waste Technology and Management.

News

[69] Expertguide. **Researchers reveal new robot: a fish called WANDA**. Online (Expertguide.com.au), 28th May 2009.

[70] ACES Newsletter. **A fish called WANDA**. Online, 28th May 2009.

[71] UOW news website. **Story and photos included on website**. Online, 29th May 2009.

[72] ABC Illawarra Radio. **Multimedia footage/photos on blog**. Online, 29th May 2009.

[73] Machines Like Us. **Robot fish ready to swim**. Online (machineslikeus.com), 29th May 2009.

[74] Tha Hindu News Update Service. **Want to look underwater? Use robo fish**. Online (hindu.com), 29th May 2009.

[75] Tha Indian News. **Want to look underwater? Use robo fish**. Online, 29th May 2009.

[76] The Engineer Online. **A fish called Wanda**. Online (theengineer.co.uk), 29th May 2009.

[77] Insciences Organisation. **Researchers reveal new robot: a fish called WANDA**. Online, 29th May 2009.

[78] Science Alert. **Robot fish ready to swim**. Online (sciencealert.com.au), 29th May 2009.

[79] WIN TV News. **Story including footage of WANDA fish**. Online, 29th May 2009.

[80] Channel 9 News. **Story including footage of WANDA fish**. Online, 29th May 2009.

[81] SBS News. **Story including footage of WANDA fish**. Online, 29th May 2009.

[82] **Robot Fish?** Online (DivePhotoGuide.com), 30th May 2009.

[83] **Robo-fish put through paces**. Online (Illawarra Mercury), 30th May 2009.

[84] **Robofish on Small Scale - Daily Telegraph**. Online, 30th May 2009.

[85] C. Fay. **Robotic fish - Science Spin**. Online (www.sciencespin.com), 2009.

[86] C. Fay. **A robot fish called Wanda**. Online (http://www.irishtimes.com/), September 10th 2009.

[87] T. Radu, C. Fay, K. Lau, R. Waite, and D. Diamond. **Wearable CO2 sensor**. Online (www.underdresswholesale.com), November 2010.

[88] Tanja Radu, Cormac Fay, King-Tong Lau, and Dermot Diamond. **Detecting Hazardous Gases in Emergency Disaster Scenarios using Wearable Sensors**. ERCIM News Online, January 2009.

Presented Publications

Paper	Chapter	Title	DOI
1	2	Remote Real-Time Monitoring of Subsurface Landfill Gas Migration	10.3390/s110706603
2	3	Wireless Aquatic Navigator for Detection and Analysis (WANDA)	10.1016/j.snb.2010.06.021
3	4	Real-time Sweat pH Monitoring Based on a Wearable Chemical Barcode Micro-fluidic Platform Incorporating Ionic Liquids	10.1016/j.snb.2012.06.048
4	5	Dynamic pH Mapping in Microfluidic Devices by Integrating Adaptive Coatings Based on Polyaniline with Colorimetric Imaging Techniques	10.1039/C2LC41065F

Abstract

Chemical sensing offers a gateway into the complex world of molecular based information. Sensing strategies are paramount in achieving this outside the confines of restrictive laboratory settings. Two key strategies are adopted in this work, which are generically applicable across multiple applicable areas.

This work initially focused on the application of networked sensors for monitoring greenhouse gas emissions from landfill sites at a sampling rate of 4/day. The findings of this study showed that the existing practice of sampling (4/year) is inadequate for detecting emission breaches and offers more information towards understanding landfill dynamics.

Digital imaging may offer a lower cost alternative to the current sensing model due to the recent pervasive nature of technologies such as mobile phones. However, chemical sensing employing this technology remains largely unexplored. This study examines the potential of this new area of chemical sensing using several exemplar platforms. Firstly, a mobile sensing robotic fish is used to patrol a water body detecting chemical contaminants en-route. Secondly, imaging of wearable colour-responsive sensors is explored as a means to monitor the pH of an athlete's sweat in real time. Finally, analysis of chemical gradients along microfluidic channels is evaluated through digital imaging of chemo-responsive films.

Contents

List of Tables

List of Figures

Nomenclature

CH_4 Methane

CO_2 Carbon Dioxide

3G Third Generation of Mobile Telecommunications Technology

µTAS Micro Total Analysis Systems

ANN Artifical Neural Network

BCG Bromocresol Green

BSN Body Sensor Network

CCD Charge-Coupled Device

GHG Greenhouse Gas

GPRS General Packet Radio Service

GSM Global System for Mobile Communications

HCl Hydrochloric Acid

HSV Hue, Saturation and Value

IC Integrated Circuit

IR Infrared

ISS Internet Scale Sensing

KOH Potassium Hydroxide

LEL Lower Explosive Limit

LOC Lab-on-a-Chip

LOC Lab-on-a-Chip

PANI Polyaniline

pH Power of Hydrogen

RGB Red, Green and Blue

US United States

WFD Water Framework Directive

WSN Wireless Sensor Network

1 Introduction

"In the begining there was nothing, and it exploded."

— Terry Pratchett (on the big bang theory).

Contents

1.1 Motivation

IT HAS LONG BEEN UNDERSTOOD that the activities of humans in recent history can have a negative effect on the Earth's ecological and geological stability. Evidence of this has been observed through carbon deposits in the atmosphere [155], the acidification of oceans [154], studies reporting the mass extinction of species [153, 152], deforestation [151], disintegration of polar ice shelves [150], a dramatic change in the Earth's weather patterns [149], amongst a number of other indicators. Two key issues have subsequently emerged. The first is a concern with the ecology of the natural environment and the sustainability of industrialism. The second, which has become more profound recently, is a question related to the sustainability of the Earth's rapidly growing human population with respect to the availability and consumption of resources.

1.1.1 Waste & Landfills

One contributing factor to the climate crisis, and relevant to the work presented in this thesis, is the management of our waste. Although it is less appreciated than other major sources, it is important to note that waste activities accounts for ca. 5% of global greenhouse gas contribution [125, 136]. For instance, in Europe alone this results in 3 billion tonnage to address per year of which 90 millions tonnes are considered hazardous (according to Eurostat Statistics 2011 [113, 114]). The treatment of this waste is conducted in many forms to include: incineration [107], export [127], recycling [128], and also by means of landfilling [136]. Landfilling has been recognised in many parts of the world as a cost effective way of disposal/storage of waste. Moreover, it continues to be the most common disposal method in many countries [124, 112]. However, the pollution of landfilling have been well documented - especially older sites ill-equipped with modern environmental technology - to include leaching of hazardous substances [115], underground fires [131], and atmospheric greenhouse gas emissions [132, 135, 133] contributing to global warming [129, 140]. Furthermore, due to the growing human population, especially in densely populated areas such as megacities [89], the amount of waste is expected to increase. Furthermore, lack of available land space is increasing becoming an issue which may interfere with city expansions [144] and also pose a public health risk to the surrounding population [104]. As a result of all of these concerns, modern landfill site design must take measures to control and treat the emissions from the waste body [111].

Despite necessary safeguards, poorly managed/monitored sites can have significant environmental and public health impacts and resulting recovery processes can be costly. Franzidis *et al.* [116] have reported a study of a landfill site activity at the city of Montreal, Canada, lasting three years in duration. Their findings suggested

that the build up of landfill gas was associated with a number of factors such as the time of year, surface status, and/or atmospheric conditions. Furthermore, they reported that overall size of the lateral gas plumes increased in magnitude each year along with strong migration events associated with the annual maintenance of the site's gas collection system [116]. Significant property damage and loss of life was reported by Drouin *et al.* [109] due to the accumulation and explosive effects of CH_4. In 1986, a house at Loscoe in Derbyshire (UK) was completely destroyed by a methane gas explosion from a nearby landfill site [142]. Similarly, an explosion took place at Skellingsted Landfill in Denmark which was reported to be a product of atmospheric pressure drops and saturated surface conditions [123]. Recently, in 2011, an underground fire erupted in Co. Kildare, Ireland, resulting in a recovery cost of approximately €30 million [126]. Other examples of environmental and health effects can be found in the following reviews [110, 106, 137, 117].

1.1.2 Water Systems

It has been well recognised that harmful substances exist within our water systems that are either directly harmful to water based life [454, 441, 130, 139] or can affect human health indirectly through the release of harmful substances into rivers, lakes, or oceans which can contaminate drinking water supplies [121, 145, 108]. A complete account of the effects of human activities in this area is beyond the scope of this thesis. However, due to the work presented in Chapter 3 there is a need to set a background for this area and highlight the need for the monitoring of water bodies.

One prime element is the disturbance of human activity upon water based life. For example, Orr *et al.* explores the acidification of oceans due to increasing carbon deposits in the atmosphere resulting in reduced ocean pH with carbonate ion concentrations and its impact on calcifying organisms [134]. In addition, the global warming effect has been attributed to the melting of ice in polar regions resulting in rising sea levels. One recent example of this was the degeneration of the Wilkins ice shelf in 2008 located in the Antarctic Peninsula [138].

Jackson *et al.* have reviewed human effects along coastal regions to include pollution, degeneration of water quality, and overfishing; eventually leading to local ecological extinction [119]. The consequence of such an effect have led the fishing industry to target areas within deeper waters. Further exploitation of the Earth's ocean life to meet the demands of our growing population may reach a negative climax. For instance, Worm *et al.* have studied the negative effects of human activities on oceanic ecosystems [143]. Their findings have suggested a collapse in the world's ocean ecology by 2048.

Ocean regions are not the only water based domain affected by the activities of humans. It has been well documented that river systems are also suffering from human influence. The result of this is negative consequences, directly to terrestrial

biological entities and indirectly to us. For example, Jobling *et al.* have documented high disruptions of river fish reproduction throughout the United Kingdom due to the presence of a number of chemicals [120]. Ternes *et al.* uncovered the residue of 32 drugs within the discharge of solid waste treatment plants in Germany [141]; which were being delivered into river and stream waters. Contamination of groundwater and drinking water of the Red River, Vietnam, for the city of Hanoi and surrounding population was documented by Berg *et al.* [105]. A change in the nutrient structure of a river dominated area, i.e. the northern Adriatic Sea and the northern Gulf of Mexico, over a 30 year period was studied by Justice *et al.* [122]. Their findings suggest that the change in the local ecosystem is a result of the nutrient imbalance.

1.1.3 Health

The two standing pillars determining one's health are essentially their physiological and psychological states at a given time. Both of which are in many ways interrelated and have a number of sources affecting/contributing to a person's health. The World Health Organisation (WHO) has defined health as:

> "*Health is a state of complete physical, mental and social well-being and not merely the absence of disease or infirmity*" [101].

Diabetes mellitus is a chronic illness for many individuals. It is essentially a metabolic disease where an individual has high blood sugar due to either the cells not responding to the insulin that is produced or that the pancreas does not produce enough insulin [92]. In 2010 an estimated 285 million people world wide were reported with this condition [102]. This figure rose to 371 million in 2012, with a reported 471 billion USD spenditure on healthcare for diabetes that year [96]. Management of this condition is centralised on keeping the blood sugars at normal levels through careful attention to medication, diet, and exercise [90].

Suicide is another major health issue facing modern society. It is the act of an individual intentionally causing their own death and it is attributed to mental disorders such as depression, alcoholism, drug abuse, or bipolar disorder [94]. According to a review by Bertolote *et al.* at least one million people are estimated to die annually from suicide worldwide [99], of which the young and middle-aged are reported to be the most at risk [100].

Obesity is a challenge facing the health of many countries. It is a medical condition where excess body fat has increased to such an extent as to adversely affect on an individual's health and can make an individual more prone to conditions such as heart disease, osteoarthritis, types of cancers, stroke, and type two diabetes [93]. One prime example of this is in the USA. According to the Centre for Disease Control and Prevention (CDC) more than one-third of U.S. adults (35.7%) are obese [98] and in 2008, medical costs associated with obesity were estimated at $147 billion

USD. The medical costs for people who were obese were 42% higher per capita than those of normal weight in 2006 [91]; with respect to 1998 figures, it is estimated that spendature on obesity had increased by 37% [91].

The increasing costs of health care sectors calls into question the sustainability of health systems for the future. For instance studies such as those by Mendelson *et al.* [97] and Heinrich *et al.* [95] have investigated a correlation between rising health care costs and increasing life expectancy for the elderly population alone. It has been shown that these factors impact spenditure in many areas such as the hospital, physician, and nursing home sectors. One answer to this issue may lie within the wearable sensor community with an ultimate aim for self or home care. As trends within the integrated circuit (IC) technology domain continue to progress - allowing for smaller, more efficient, cost effective, and lower power consumable devices [331] with increasing integrated capabilities [330] - it brings with it the opportunity to introduce newfound application areas such as those within the sensor research community. Wearable sensing technology has consequently emerged as a means for providing/gathering physiological information of a wearer. The concept of tele-health has emerged where medical professionals can monitor a patient without associated consultant and administrative costs for visitation [329].

1.1.4 Awareness and Information Access

Many scholars have been concerned with the consequences of industrialism with widespread awareness dating back to the works of Rachel Carson and before [148, 147, 146]. An awareness that challenged entities to re-evaluate their relationship to the natural world and eventually led to the establishment of legislative bodies and enforcement agencies to protect the environment and its inhabitants from harm. The information - or more specifically, the bio/chemical based information - with which environmental protection agencies base their decisions upon is critical to the effectiveness of maintenance/recovery processes, and similarly for medical professionals in diagnosing and treating illnesses. Lord Kelvin once wrote:

> *"If you can not measure it, you can not improve it."*

Without such information there is no support by which experts in the environmental and health sectors can base their decisions upon and ultimately reduce negative events from occurring (such as those reviewed previously). At the heart of this challenge is the ability to access such information with spatial and temporal requirements that reflect the dynamics of a system. How this information is gathered and delivered to relevant stakeholders, through the adoption of modern technology, is central to the work presented in this thesis. The novelty of this work lies in the exploration of methods/strategies for generating new knowledge related to previously unexplored areas of chemical sensing applications.

1.2 Chemical Sensing

There is no doubt that our natural sensing capabilities are limited and that substances/pollutants exist that can be harmful to human health or can affect us adversely through their negative effects on the environment. Examples of such substances in modern society can be seen from a multitude of sources such as household cleaning appliances, natural gas, asbestos, radiation, radon gas, and even bio/warfare agents. Moreover, some of these have been known to cause serious health issues including: cancer, birth defects, and even death [175, 174, 173]. Hence, the need to qualify the presence of, and quantify the concentration of these substances is self evident; chemical sensing has been identified as a means of achieving this. The world constantly looks to the molecular sensor research community to develop novel techniques capable of detecting key molecular targets. Today, chemical sensing is adopted into many application areas such as industry [172, 171], crime investigations [170, 169], and medicine [168]. Furthermore, the demand for such capabilities is on the increase and is expected to expand into many more areas. Two area of considerable importance that could substantially benefit from real-time chemical sensing is pollution measurement and control within the environment [167, 166] and wearable sensing devices for maintaining health [165].

It is well established that the condition of the environment and biological entities is dictated by its molecular state at any one time and that their relationship with industrialised societies can be negative [164]. The ever increasing population of the world has brought with it challenges in its sustainability in both the damages brought forth into the environment and monitoring the health of patients without the need for laboratory assistance - both considerable sustainability issues. With the ability to sense key molecular targets in both realms, and on a continuous basis, one can ultimately detect threats in real-time and respond in a timely fashion to reduce or even prevent their occurrence.

At present, monitoring of chemical species within both the environmental and health related domains is largely implemented on a manual basis [456]. The status of the environmental measurements are achieved by manually retrieving representative samples from a relatively small number of designated locations which are then transported to facilities equipped with sophisticated equipment and highly trained personnel capable of detecting the presence of many contaminants including concentrations of phosphate, nitrates, ammonia, pH, etc. [456, 162, 161]. A similar model is true for determining the health of patients. Drawing blood and analysis of patients through high end machines (e.g. MRI, CAT) has become standard. The commonality here is analysis of chemical species through a laboratory approach i.e. by means of sophisticated instrumentation and highly trained personnel. There are good reasons for employing this strategy, principally because of the high precision and accuracy of the measurements which are due to many factors including the

use of high quality reagents and appropriate implementation of quality assurances procedures. Moreover, these laboratories comply with regulations imposed by legislation such as the EPA Act of 1992 [160] and Health Act of 2007 [157]. As a result, the high quality and accuracy of this strategy is recognised; for court cases it is vital for obtaining legally binding decisions against polluters. For health issues the role of laboratories for the detection of health issues is paramount in the process of saving lives.

Arising from existing and forthcoming bodies of legislation, from both national and international institutions, a growing requirement for a higher spatial and selective monitoring of key chemical contaminants is underway. For instance, the Water Framework Directive [159] and the Kyoto Protocol [158] are noteworthy examples of the demand to monitor key molecular targets on a continuous basis. In addition, the ageing population will increase demands on health systems to a degree that they may become saturated. Although the current sensing model is highly precise and accurate, it is very expensive to manage these high-end analytical facilities and monitoring programmes. Consequently, it is inherently non scalable and measurements are therefore very restricted. To overcome this bottleneck and comply with future demands e.g. environmental legislation and quality of patient care, an alternative sensing model is currently under investigation by the research community which involves bringing the sensing technology to the location/patient to be analysed *in-situ/on-body*. The recent revolution in the electronics and information worlds coupled with sensing strategies from the chemical sensing community may allow for such a model to emerge.

1.3 Information Revolution

It has been well recognised that the end of the 20^{th} and the beginning of the 21^{st} centuries have heralded a new era of information gathering and exchange [179, 178, 177]. It is now possible to effectively and efficiently connect people, places and objects like never before through the emergence of technologies such as the internet, Global System for Mobile Communications (GSM), satellite transceivers and Wireless Sensor Networks (WSNs). By means of such technologies, we continuously exchange information in multiple forms including: social (GSM/GPRS/3G), domestic (broadband internet, satellite TV), and business (stock exchange, online banking/shopping). What is often missing from these newfound abilities is the means to gather information related to our personal health, the condition of our food, and the state of our environment in an efficient and timely manner.

Expanding research and commercial efforts continuously aim to use the existing infrastructure in new ways and/or to expand this field to communicate new sources of information. Only recently has the attention turned to the chemical/molecular

world which has the potential to grant us access to an almost limitless amount of sensory information of a person/place/object based on its molecular makeup. Therefore, the integration of inexpensive chemical sensors with digital communication devices within this information exchange infrastructure is intuitively an attractive proposition [448].

The pervasive nature of such technologies and its popularity have challenged commercial entities to create smaller, faster, and more power efficient devices for their next generation releases. Competition and increasing demand for computing power have played a significant role in the development of system-on-chip technology [180] and has given rise to small scale devices capable of significant computing power and at low cost. One noteworthy example of this is the Raspberry Pi capable of running a fully functional operating system, e.g. Linux, at a low cost of $25 [176]. Devices such as these enable program developers of all capabilities to aid in the creation of working prototypes without the need for specialised training in embedded software systems. The significance of this is that a number of sensing approaches may potentially benefit from the hidden sophistication of these devices i.e. opening new doors for researchers to develop novel approaches that may better suit some sensing applications.

1.4 Sensing Domains

According to Repko *et al.* the vast majority of research scholars are disciplinarians [183], however one must not lose sight of the potential to cross disciplinary barriers for the creation of newfound discoveries/capabilities. This does suggest, however, that a small minority of researchers are practising interdisciplinary science. Kuhn, amongst others, have argued that scientific understanding does not advance through the exclusive idea of aggregating 'bits' of understanding and eventually making the next logical progressive step. Instead he argued that 'normal science' (by disciplinarians) was periodically interrupted by times of 'revolutionary science' (by interdisciplinarians) which led to paradigm shifts in understanding [184, 183, 182, 181]. In this thesis the focus falls on traversing the molecular and digital divides for investigating a number of end applications. This section explores both of these domains or 'worlds' separately for introductory/background purposes before bringing them together to form a common context for future sections.

1.4.1 The Molecular World

1.4.1.1 Historical View

Chemical sensors are relatively new measurement devices and it is considered that the glass pH electrode was the only portable and reliable chemical sensor for dec-

ades since its foundation in 1922 [197]. Even though they needed to be calibrated on a daily basis, they are still used in modern laboratories as a frequently used and necessary piece of equipment. In addition, this ability to measure the concentration of hydronium (H_3O^+) and hydroxide (OH^-) ions in an aqueous solution via an instrument was a noteworthy event for the sensor research community and allowed for the emergence of other sensing technologies based on oxidation-reduction principles.

The next progressive step related to chemical sensing devices occurred during the 1950's with the ability to selectively detect key metallic ions within an aqueous environment. This gave rise to the aptly named electrochemical type sensor i.e. the *ion-selective electrode* (ISEs). Today it is possible to measure more than 60 ions [196] including sodium (Na^+), potassium (K^+), chloride (Cl^-), calcium (Ca^{2+}), magnesium (Mg^{2+}), and lithium (Li^+) [195]. Furthermore, they are very simple and yet very sensitive chemical sensors whose detection limits can be as low as parts-per-billion (ppb) in some cases [194]. They are robust, require virtually no power and can be easily miniaturised [193] which makes them excellent candidates for integration into WSNs for environmental monitoring. For their simplicity, low-cost, long history, limits of detection, selectivity, etc., ISEs have been recognised as novel analytical tools and continue to play a significant role in the sensor research community. Consequently, ISEs have provided us with new measurement capabilities and have provided the chemical research community with some of the first selective sensors. However, many problems still persist with this sensor type including, but are not limited to, cross-sensitivity, drift, limited lifetime, continuous calibration, etc. For these reasons, research and commercial entities have been looking for alternative methods capable of detecting key chemical species and sensing key elements more reliably for long term deployments.

The concept of a colorimetric indicator goes back as far as the age of alchemy. One may recognise a familiar concept i.e. the use of litmus paper to indicate the acidity or alkalinity of a given substance, giving rise to the common phrase *litmus test*. It wasn't until 1904 when the journal of electrochemistry (Zeitschrift fur Electrochemie) published an issue surrounding the works of Wilhelm Ostwald which held the first published summaries of modern colorimetric indicators [192, 191]. This work allowed a Swedish scientist Søren Sørensen (the pioneer of the pH scale) in 1909 to express the idea of hydrogen ion concentration on a logarithmic scale through the determination of pH using ca. 20 colour indicators [190, 198].

Optical pH indicators are based on reversible changes within their molecular structure which is induced by hydronium and/or hydroxide ions and translates to spectral phenomenon such as absorption, fluorescence, reflectance, luminescence, energy transfer, etc. [189]. Today, over 200 water-based and other solvent-based acid-base indicators have been reported [238]. It should be noted that colorimetric indicators are not confined to the detection of pH alone. Other analytes are reported

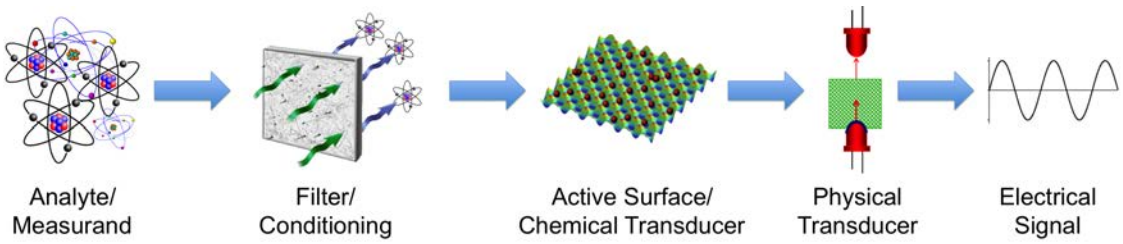

Figure 1.1: Arrangement of a typical chemical sensor for the detection of chemical targets (atoms/molecules/ions). The target analyte is first filtered and then reacts with an active surface. The change in the active surface molecular properties is then transformed into a measurable electrical signal.

from the commonly know blood and pregnancy test to published target analytes including personal alcohol levels [188], phosphate [187], nitrate [186], and CO_2 [185]. Finally, unlike contact based sensors, e.g. ISEs, optical sensors may offer some advantages including: insensitivity to electrical interference, possibility of being low-cost and disposable, no need for a reference element, etc. [189].

1.4.1.2 Chemical Sensor Composition

From the chemical sensors introduced previously, one can see common elements that exist between each sensor type i.e. indicator/reactive chemical, transducers, and the production of an electrical signal. Therefore it is possible to envisage a generic model that describes the high level workings of a chemical sensor. This can be depicted as a flow diagram shown in Figure 1.1 on page 10. Firstly, a filter is put in place to reduce any cross sensitive atoms, molecules, or ions that may interfere with the molecular target measurement of interest. This can be in the form of a polymer matrix that will allow exchange of ions and inhibit the transfer of larger molecules. Next, the response of the active surface to the presence of the analyte is expressed as change(s) in its molecular properties and may result as relative alterations in its impedance, light intensity, colour, fluorescence, weight, size, temperature, potential, resistance, etc. A common example of this is pH paper where, through the presence of hydronium and/or hydroxide ions, the optical absorbance characteristics of the pH dye within the paper will vary and result in a change of its apparent colour. After that, a physical transducer is used to transform the response of the active surface into an electrical signal for later measurement. For optical sensors this can be achieved via a photo-diode accompanied by an LED. Overall, this sensing model shows that any increase/decrease of the analyte concentration (input) will be proportional to changes in the electrical signal (output).

1.4.2 The Digital World

1.4.2.1 Definition

The digital world is the domain where information is represented digitally (in 1's and 0's) and is capable of being communicated through information exchanges to include the Internet, private networks, satellite telemetry, and via wireless devices. More specifically applicable to the context of this work is the ability to harvest information from an environment, digitise it, and communicate it wirelessly/remotely to central data centres capable of visualising the information to users via the Internet.

1.4.2.2 Historical Perspective

It wasn't until the invention of the transistor (John Bardeen, William Shockley and Walter Brattain at Bell Laboratories, 1947) that the world of high speed calculations sparked off into a domain of its own. It was so revolutionary that the three inventors received the 1956 Nobel Prize for Physics. The result of this work has formed the foundation of the modern computer revolution through subsequent inventions such as the micro-controller and the microprocessor. Since then, this new domain has taken profound strives forward including the ability to connect two previously unrelated technologies i.e. computers and communication which, like other technologies, have been driven by high impact events such as war.

Arising from the ashes of the second world war came a new drive towards research and development of key technologies capable of influencing the balance of power. It was clear that future technology played a tremendous part in war efforts and it was self evident in many ways including the application of radar, sonar, and the profound impact of nuclear technology on Hiroshima and Nagasaki [205]. After this, it was not surprising that technological breakthroughs kept tensions high. This was no truer than in the 1950's and 1960's during the height of the cold war where the potential casualty count would not be in the millions but in the hundreds of millions. Consequently, concerns were raised by the United States (US) over the speed of executing retaliatory strike(s) and the vulnerability of the communications method of the day. In the event of a nuclear detonation FM radio transmissions would be affected and if this was coupled with strategically placed ground strikes of AT&T's (the monopolising communications giant of the day) switching stations, it could take hours to react to such an attack and thus left the US exposed. As a result, a new more robust communications method was desirable.

It wasn't until later in 1960 when a researcher named Paul Baran - a member of a US think tank Research and Development (RAND) program - conceived of a revolutionary idea to ensure the delivery of vital communications during war periods and argued that the current communications model would not suffice [199]. Instead, Baran suggested a model based on neurological theories where the human

brain could synaptically relay information effectively even after a brain cell had died [200]. Contrary to the model at the time, which operated on a pure circuit switching basis, Baran's model adopted a non-central switching point where every node in the network could communicate to any/every other node. Messages sent across his theoretical network would be split up into chunks or *packets* each containing an additional *to* and *from* field and letting the nodes decide the optimum route through the network [201]. This would allow for the vital data/packets to be rerouted around destroyed/damaged areas by strategic attacks more reliably than the communications method of the time. This approach was eventually adopted and gave rise to what we know now as the Internet.

1.4.2.3 Wireless Sensor Networks

In August 1999, *Business Week* published a special double issue describing the 21 most important technologies for the 21^{st} century [274]. Of these, it was elected that electronic devices were getting smaller, faster, and cheaper insofar that they may accommodate multiple sensors, wirelessly connected through networks and the Internet, and also provide the opportunity for connecting homes, cities, and the environment [270]. At the time, the potential for low cost, wireless devices capable of operating unattended for long periods of time was already foreseen. In fact, early work by Hollar [273] has demonstrated the capabilities of autonomous sensing systems within a Wireless Sensor Network (WSN) equipped with a multitude of physical sensors including an accelerometer, a GMR magnetic sensor, humidity, light, pressure, and temperature sensors. Its longevity depended upon its use, however it was reported that it could operate continuously for five days and transmit data up to 30 m. Overall, Hollar's approach demonstrated the basic wireless sensor network setup successfully i.e. a single node communicating wirelessly to a gateway and eventually to a computer for harvesting/analysis. Additionally, the basic node-base station configuration can have multiple network topologies with scale up to include the most commonly employed type i.e. star configuration, and more complex systems e.g. tree and mesh setups; all of which are considered classical and reported in review articles [272]. Many examples of WSN implementations have already been reported in review articles such as by Yick *et at.* [271] and Chong *et al.* [270]. In subsequent sections, examples of WSNs will be reviewed when employing chemical sensing capabilities to realise a related version of WSNs i.e Wireless Chemical Sensor Networks (WCSNs). Specifically in Section 1.5 to set precedents and relevance to the work proposed in Chapter 2.

1.4.3 The Molecular-Digital Divide

Although elements within the chemical sensor research community (such as gas, water, and electrochemical sensing) are excelling within their own fields, a key question

that often goes unanswered is how to make practical use of, and how to implement, such newfound sensing capabilities. Previously, the world of multidisciplinary research was introduced along with its potential for detecting problems and ultimately allowing for one to focus efforts/resources in recovery. Reflecting on this, the two central research areas presented within this thesis were brought into the spotlight i.e. the molecular and the digital worlds, as discussed previously in Section 1.4.1 and Section 1.4.2, respectively.

1.4.3.1 Challenges

The literature, in the context of environmental monitoring, is rich with past and current studies with demonstrations of highly selective and sensitive chemical measurements, e.g. [211]. Correspondingly, studies within the technological domain describe how sensing platforms can easily incorporate chemical sensors [212, 219]. However, there are relatively few reports describing the application of chemical sensing capabilities outside the confines of the laboratory environment and even less so describing chemical sensor integration into autonomous wireless sensor networks for *in situ* deployments [449]; examples of these will be outlined within Section 1.5 for environmental sensing and Section 1.6 for wearable sensing. The realisation of such systems is not trivial and can be largely attributed to many underlying practical problems associated with chemical and biological sensors [235]. Understandably, the majority of deployments to date have been limited to physical sensors such as thermistors, flow meters, photodetectors, etc. [271]. Unlike chemical based sensors, which need to be in contact with its environment, physical sensors can be shielded by interferences. As a result, chemical sensors face a number of challenges including: biofouling, reduction of the indicator, drift, cross-sensitivity issues, selectivity, high temperature/humidity dependence, reproducibility, calibration, longer response times, etc. [235].

However, in order to expand chemical sensing within the environment/wearable applications and introduce deployments of chemical sensors, joint efforts from the sensor research and the technological communities will need to occur at an increasing rate than before in order to comply with current and future environmental and health care demands. In fact, this goal has been identified in a recent Analytical Chemistry Editorial as the the next "grand challenge" for analytical chemists [258].

> *"A 'Grand Challenge' posed for analytical chemistry is to develop a capability for sampling and monitoring air, water and soil much more extensively and frequently than is now possible [...] Such goals will require improvements in sampling methodology and in techniques for remote measurements, as well as approaches that greatly lower per-sample and per-measurement costs."* [258]

Furthermore, it has been widely recognised that many chemical parameters of interest vary broadly in the temporal and spatial domains and that the current manual based sampling methods employed by government agencies is inadequate for understanding the underlying principles of these changes within the environment [240, 207]. Therefore, there is a need for the creation and deployment of chemical sensing systems capable of performing complex analytical measurements *in situ* i.e. to join these two independent domains [225]; the molecular and digital worlds.

1.4.3.2 Lab-on-a-Chip

Perhaps one of the most active areas of multidisciplinary research - and relevant to the work in Chapter 4 and Chapter 5 - is within the µTAS/LOC realms. The term 'Micro Total Analysis Systems' or µTAS was introduced by Manz *et al.* over 20 years ago [203] and later became synonymous with Lab-on-a-Chip (LOC). This refers to the concept of miniaturised devices capable of performing laboratory functions that would have otherwise been confined to a traditional laboratory setting and operated by trained personnel. Moreover, such a device can involve the integration of a number of disciplines with fundamental challenges in the fields of: microfluidics, pumping technology, autonomous control, low power usage, detection techniques, communications, platform integration/packaging, and ultimately, automatic detection and analysis of events/anomalies. This vision has sparked a new area of research as the potential benefits are very attractive in a number of key areas including, amongst others: point of care patients, sporting activities, and sensing of pollutants within the environment [216, 215, 226, 214, 213, 222, 236, 249]. Consequently, this area has become a vast area of research since its conception.

One of the main advantages of LOC systems is the use of microfluidics with many researchers commenting on its potential [214, 213]. For example, Pennathur *et al.* summed this view up with:

> "*... microfluidics can potentially enable portability, reduced reagent consumption, reduced analysis time, and increased efficiency...*" [247].

One early and noteworthy example was in the development of the the inkjet printer [202]. However, microfluidics in turn promotes technical challenges in liquid handling/transport techniques at this scale (ca. 10-500 µm) and furthermore in collecting samples from the macro world and analysing them within the micro world [250].

The concept of LOC technology appears as revolutionary, however there are very few examples outside the laboratory realms. In a recent LOC editorial, George Whitesides (a leader in this area) reflected on this with:

> *"... Many people, myself included, expected that the ability to manipulate fluid streams, in micro-channels, easily, would result in a proliferation of commercial LoC systems, and that we would see applications of*

these devices proliferating throughout science. In fact, it has not (yet) happened... Microfluidics, to date, has been largely focused on the development of science and technology, and on scientific papers, rather than on the solution of problems." [472]

The challenge here may lie in the amalgamation of different disciplinary efforts which brings with it higher risk. This, coupled with the idea that a majority of commercial entities are most likely disciplinary in nature and are ill-equipped to support a number of disciplines.

Overall, the potential advantages of this approach can allow analytical systems to operate for long periods of time as an ideal LOC system will minimise operational costs i.e. use low power actuators (e.g. PPy actuators for instead of mechanical pumps [244]), power and cost efficient detectors (e.g. PEDDs [246]) with the added advantage of operating unattended. To fully understand this approach and others one must explore the processes involved in the sensing process; this discussion follows.

1.4.3.3 Sensing Process

This discussion now considers the process of applying chemical sensors to practical scenarios i.e. strategies on how to implement the measurement process for an effective system control. Technological instruments/devices have been identified to harvest objective information related to a system under investigation. However, there are many different sensing processes capable of achieving this goal i.e. from a fully manual to a fully autonomous model, or somewhere in between. Whatever model chosen for retrieving chemical information from a system, the sensing process can be viewed similarly, see Figure 1.2 on page 17.

Sample Collection. The process begins with the retrieval of an aliquot or a representative part of the system for analysis i.e. a sample. Manually, it requires a qualified operator to retrieve this and decide upon the best location. For example, environmental agencies physically traverse terrain (possibly in difficult conditions) to physically remove a sample from a system e.g. a river, marine environment, or a waste treatment site. Similarly, in a medical environment, a nurse/doctor removes interstitial fluid e.g. blood from a patient. Alternatively, autonomous devices may automatically retrieve samples through actuators e.g. pumps for environmental applications or micro-needles in medical scenarios. For many systems it is clear that circumstances require trained individuals for effective collection of samples. However, the autonomous model has scope for requiring highly trained personnel, sophisticated equipment, and possesses scope for increasing spatial and temporal sampling.

Conditioning. Once collected, the sample is to be transported to the analysis stage. For autonomous systems, the analysis process can begin almost immediately, however the manual approach requires storage and eventual transport to centralised facilities. The storage of certain samples can negatively effect the sample if specific conditions are not met. Conditioning in a positive manner can increase selectivity i.e. altering the sample to meet the circumstances needed for the analysis stage. One prime example of this is filtering. Unwanted components within the sample that may interfere with the analysis stage are removed (if possible, or through sophisticated techniques such as chromatography). Additionally, the analysis stage may require a specific temperature or perhaps allowed time for germination to occur for biological analysis.

Analysis. This process has been discussed to some degree during previous sections e.g. when discussing the technology behind sensing. However, for some applications this can be very involved depending upon what is to be detected. For example, consider a standard chemical measurement e.g. detection of pH using a glass electrode or optical instrument. Either way calibration solutions may need to be created and used as reference for the subsequent measurements. Furthermore, the instrumentation requirements can also vary and will be reviewed later in Section 1.5.

Interpolation. Instrumentation ultimately respond to physical stimuli based on the chosen transducer. In other words, the resulting data is proportional to the response from the stimuli and as a result the information is initially measured in arbitrary units. References are needed to support the data. For instance, consider calibration solutions for pH measurement as mentioned earlier. In this case, a mathematical model is created based on the generated response curve of discrete reference concentrations. This model is used to estimate unknowns and convert the data into meaningful information e.g. into standard units. Furthermore, the units may need conversion. This process is known as data interpolation and is required for all measurements.

Delivery. Finally, the sensed information is delivered to stakeholders e.g. environmental officials or medical specialists. Whether the method is through clip boards, email, or a login portal page, the information is communicated to the relevant authorities. Further processing may be required at this stage such as correlation between multiple sensor data sets. However, they then proceed to recommend or implement some action based on this information e.g. a change in medication or investigation of local industries for environmental concerns.

Figure 1.2: Sensing stages for gathering chemical information from a system.

1.4.3.4 Instrumentation Hierarchy

It is clear that instrumentation plays a significant part in the sensing process from the manual approach of laboratory based sensing, to in field analysis via portable instruments, or involved in low power autonomous devices capable of analytical measurements in situ. However, there are distinct differences in each approach in terms of cost, power requirements, autonomy, deployment density, etc. One study by Diamond [225] has compared and contrasted the instrumentation involved for each approach; this is depicted in Figure 1.3 on page 18. This study argued that analytical instruments can be arranged into a hierarchy based on three key criteria i.e. sophistication, operational costs, and degree of autonomy. The message in this case can be explained in two extreme cases. While laboratory settings have the capabilities, facilities, and trained personnel to analyse a collected sample with a high level of precision, the operational costs can be limiting. However, development of low power wireless sensor networks (LPWSN) capable of being manufactured and distributed easily and cost-effectively, can offer a number of advantages in terms of temporal and spatial measurements. Furthermore, with integrated communication devices, the information can be relayed in real time allowing for perpetrators involved in environmental pollution activities to be identified in a timely manner. Although it is clear that a compromise exists with both extreme approaches, a number of alternative options are available that may suit application needs, as shown within the figure.

Portable instruments have given users more flexibility than laboratory techniques e.g. allowing them to take in field/on body measurements without high costs. However, in certain circumstances this still may not suffice. The challenges/demands posed by current and forthcoming bodies of legislation may increase the need for deployable devices. Although many prototyping systems are under development within the research domain (explored later), the bottleneck for widespread use lies within the adoption of this technology by the commercial sector. Joint efforts by funding agencies, research domains, governing authorities, and commercial entities will need to take place more so than before for this goal to be reached.

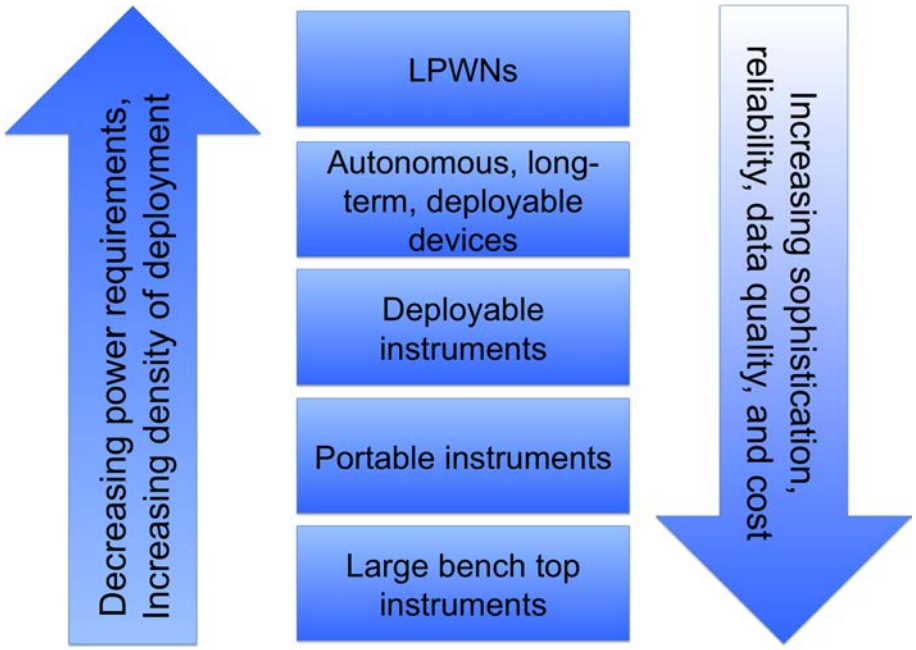

Figure 1.3: Instrumentation hierarchy for analytical devices. Diagram redrawn from [448].

1.4.3.5 Cloud Based Sensing

Up to this point the focus of discussions has been on harvesting chemical information i.e. the application of chemical transducers and digital hardware to control and route the data from the physical to the digital world. Another aspect of the digital world that can almost be considered as a separate domain within itself is information processing and handling. The emergence of continually growing processing power has given rise to capabilities for processing large amounts of data from a wide variety of sensory sources. Examples include metrological data [233, 245], satellite telemetry [254, 253, 237], chemical sensing of the environment [265, 257, 446, 262, 260], and bio/warfare protection [217, 241], CCTV systems [228, 259, 243], and life-logging [261]. It is important to realise that the dynamics of chemical information within a system may be associated with other factors and that such sources of information may offer important data related to the occurrences of events. Furthermore, an important question resides in how to weigh the importance of each source of information related to the state of the system at a give time. As a result, the discussion now shifts from how to harvest this information, to methods for the efficient processing of data sets consisting of millions of data points. Given that the diversity and scale of this information is growing at a huge rate, the ability to automatically extract summary information from these data repositories is essential. The importance of this space will come into focus in Chapter 2.

In order for a full description it is advantageous to initially reduce the argument to its basic form. For environmental or health applications authorities are often only interested in the dynamic nature of a system, i.e. events. In its gen-

eral form, an event is defined as something that happens at a given place and time (wordnetweb.princeton.edu/perl/webwn). Much of this interest comes in a number of forms e.g. defining and classifying such events, quantifying their frequency and extent, identifying patterns and ultimately, being able to predict future events. The area of *event computing* has emerged to address such requirements. According to Yan *et al.* [263] techniques generally employed for event detection include Dynamic Bayesian Networks [223, 234], TemporalBoosting [220], Bootstrapping [227], Continuous [209] and Finite [208] State Machines, Radial Reach Filter [210], Maximum Entropy [231], etc. Applications of these approaches have been reported in many areas such as surveillance [218, 239, 234], sports [206, 221, 230], networking [252, 256, 251], and social/indoor environments [229, 224, 232, 264].

It stands to reason that when a number of data sources, e.g. in the thousands, can consist of individual pieces of data in the millions as time progresses. When considering the system control model, it becomes very cumbersome to process this data on a manual basis. It is also important to realise that the more information related to a system, the better the chances that one can predict and prevent negative events. The above account is important for decision making and predictive modelling of system behaviours. With an abundant amount of sensory information related to a system and delivered in real time, data processing on the server end (or cloud based processing) possesses the possibility of triggering early warning signals and limit damages and loss of life e.g. environmental pollutants [204], earthquakes [268], medical conditions [269], or other negative occurrences [267, 266].

1.5 Environmental Monitoring

As the understanding of the molecular world developed during the 20^{th} century, the demands on technology to characterise chemical compounds increased to a point where most modern laboratories must now be equipped with the capabilities of detecting a vast range of chemical analytes. High reliability, precision, and confidence of these measurements is ultimately the responsibility of the technology employed. When considering environmental chemical sensing, analytical instruments can be arranged into a hierarchy which depends on a number of factors including: sophistication, capabilities, operational costs, and degree of autonomy [225]. Previously, Figure 1.3 on page 18 presented a hierarchy of instruments for chemical sensing. This is taken as a template and simplified into three principle categories that environmental instruments can be classified into; these are depicted in Figure 1.4 on page 20. This section focuses on each category and reviews the literature in the context of environmental chemical sensing.

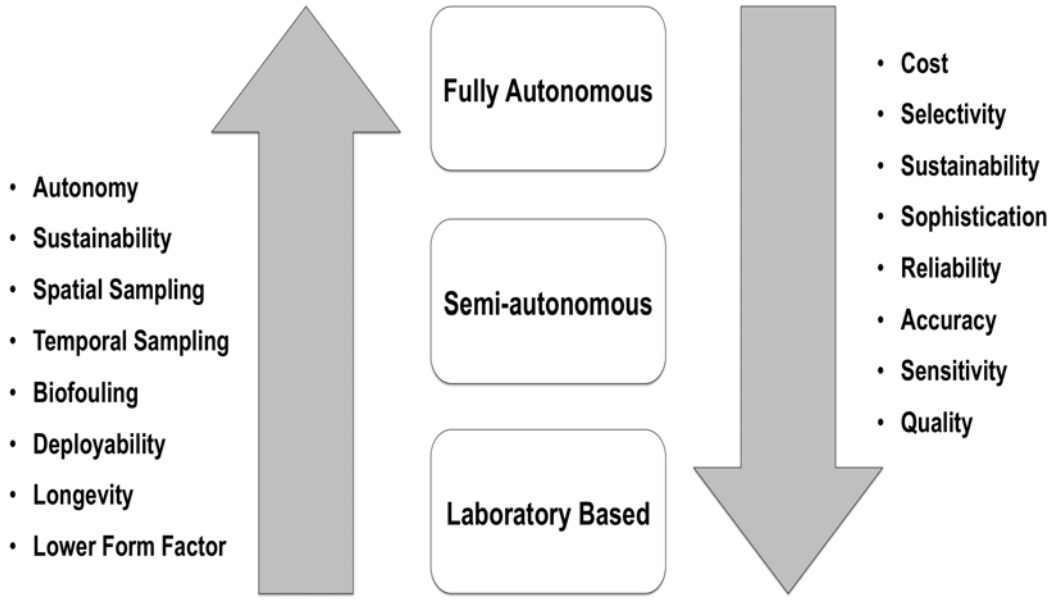

Figure 1.4: Environmental chemical sensing instrumentational hirearchy.

1.5.1 Laboratory Based Analysis

It is currently accepted that sophisticated bench top instrumentation are the gold standard for chemical sensing and also behave as reference for validating other measurement devices. As time progresses so too does the ability to study and characterise new and exciting substances constantly being discovered in the research domain through such emerging technologies. Bench top instrumentation has made it possible to characterise a substance and essentially determine its building blocks or makeup which is especially important in detecting key analytes within our environment [307, 306].

Through the advent of such technology, a bigger picture of the molecular world was opened to the sensing research community. These capabilities became very important for the detection of environmental contaminants that have been recognised as a serious problem in today's society. Environmental monitoring, at present, almost always takes place on a manual basis where agency personnel must travel to key locations - and at times face harsh terrain - acquire samples of solution/gas and/or soil from the area and then transport them to centralised laboratories for later analysis [307, 306]. There are well established reasons for adopting this approach, principally because of the high precision and accuracy that high-end bench-top instrumentation provide. Other advantages include strictly controlled measurement conditions, high-grade reagents, highly trained personnel, and broad range capabilities to measure a multitude of target analytes. For these reasons, amongst others, the confidence in each measurement is generally high which is a fundamental necessity in

court systems against perpetrators found illegally dumping hazardous materials in breach of legal emission limits and/or negligent in their disposal methods [305, 304].

Although this sensing model is considered very accurate and robust, the cost base associated with it is high; meaning that it is inherently non-scalable in terms of multiple sensing locations within the environment. Consequently, this model will be highly challenged to conform to the requirements of current and future bodies of legislation e.g. the Water Framework Directive (WFD) [275, 303] and therefore, maybe considered inadequate for understanding the underlying principles of these changes within the environment [240, 207]. Furthermore, this model can compromise the integrity of the sample at a number of stages in its sampling method i.e. collection, transport, storage, and/or analysis [302]. What is needed is a comparable sensing model that is capable of achieveing the same objective and minimising resources along with the risk of contamination by performing sampling at the target sensing location [301].

1.5.2 Semi-autonomous/Portable Monitoring

The advent of miniaturised devices made it possible to remove the technology from a laboratory environment and allow analytical measurements to be made at the sensing location. The realisation of such a model took place in the commercial and research domains. At first, the natural progression from a centralised laboratory environment was in the creation of field laboratories, e.g. a study by Drachev *et al.* [300], where it was either infeasible to transport samples to centralised facilities and/or the target area needed real-time continuous measurement. In such cases, a staffed static laboratory alongside a sensing area, e.g. a river, would be established and equipped with sophisticated instruments as those mentioned in the previous section. Although the measurements achieved through this method can be considered as more robust i.e. reducing the contamination affect [302], problems that persist include high cost, power access, trained personnel, and therefore the lifetime of the field laboratory.

A progression of this approach was to establish such sensing capabilities in a mobile lab. For instance, a study by Karellas *et al.* [299] monitored air pollution emissions from a fire started at a factory in Guelph, Ontario, who manufactured chemicals for use in swimming pools. The technology employed here was a mobile vehicle capable of monitoring hydrogen chloride and chlorine gas emissions from the factory in real time, again the cost base for such an approach is still a persistent problem for widespread measurements although it does add an easy mobility aspect for much needed cases. Other examples of this model can be seen with the US EPA's ESB Mobile Laboratory [298] and the National Environment Management Authority Laboratory [297]. Furthermore, this technology has become commonplace in so far that it is available from commercially available entities such as WAGTECH [296] and even serviced based entities that supply the personnel and mobile laboratory

for analytical measurements on site e.g. S & S Onsite Analytical [295].

Another option to harvest time series of bio/chemical information from sensing locations on a continuous basis without the enormous overhead of a mobile laboratory is through the use of auto-sampler devices where a unit is deployed within the environment, automatically takes samples at a set frequency and stores them for future analysis. This approach has become one standard and has appeared in the literature for many sensing targets. For example, Lundberg *et al.* [294] have applied the use of an auto-sampler for the determination of silver, bismuth, cadmium, and zinc within soils and analysed later in the laboratory using atomic absorption method. Yu-Chen Lin *et al.* [293] studied the impact of the semiconductor and electronics industries on down stream water quality by measuring perfluorinated chemical (PFC) contamination through the use of an auto-sampler. Boschera *et al.* [292] employed an auto-sampler to harvest samples from rivers in the North of Luxembourg in order to detect heavy metals and the affect on fish health. Finally, Ferguson [291] has compared manual with automatic sampling and store technique against an additional step using a refrigerated auto-sampler. The results of this study showed that there are significant differences in both approaches e.g. a lower pH and a higher conductivity was found for the manual method when compared to the automatic. However, the study concluded that these differences could be due to the storage time and therefore the time difference between sampling and analysis is critical for achieving a representative measurement of the environment.

An answer to this challenge came about in the form of portable devices which allowed a user to take samples and analyse them at the source. These devices have become standardised and are available as off the shelf analysers. For gas sensing there are many options such as GA90/GA2000/GEM500/GEM2000 (Landtec), G3 LMSxi (Ashtead), and Gas-Tec (AFC). Alternatively, for solution based analysis, available devices come in the form of colorimeters or portable spectrophotometers equipped reagent packs e.g. WPA CO7500 Colorwave Colorimeter (Biochrom), DR/890/820 (HACH), and SC-1919 (Omega), amongst many other available systems. These systems can be used by environmental enforcement officials when spot checks are needed. The advantage of this approach was in the minimisation of the time difference between sampling and analysis and resulted in a more representative measurement of the environment's state at that time. The disadvantages of this approach are that it still requires a large manual input, is not scalable and practical; in addition it cannot easily sample continuously over a long period of time. An ideal solution to these problems would be to encompass the whole sampling, analysis, and reporting processes into one single device.

1.5.3 Full Autonomous Monitoring

One strategy for minimising the problems associated with the previous sensing models is through the miniaturisation of analytical platforms to one based on low power electronic components and equipped with currently available communication devices for remotely relaying data to central servers [211, 290, 187]. The availability of low cost, low power detectors have opened the doorway for the creation and deployment of chemical sensing systems capable of performing *in situ* complex analytical measurements [289]. This relates to the emerging of Lab-on-Chip technologies - which was discussed earlier in Section 1.4.3.2 - where the manual element of sensing is, ideally, completely removed or practically minimised. Through such technology it is now more possible than ever to join the molecular and digital worlds through the vision of Internet Scale Sensing (ISS) [225] which involves, in this context, providing chemical information about one's environment to users/authorities, autonomously in real-time, via information exchanges such as the Internet. The advantages of such an approach can remove the manual efforts entirely, and with the availability of low cost digital electronics scalability increases for both temporal and spatial monitoring needs.

Environmental sensing often takes place without access to a wired/wireless communications network. It is also a good practise during development of a sensing platform to examine the sample and sensing elements before implementation of or addressing the most suitable communications elements. In either scenario where wireless comms is not possible or not implemented as yet, a number of platforms adopt this strategy. One example of this can be seen in [288, 287] where concentrations of carbon monoxide (CO) were monitored at the exit of an underground car park which employed an electrochemical sensor and logging system. Naughton *et al.* [308] deployed a number of Conductivity-Temperature-Depth (CTD) sensors in turloughs for long term data logging. Other examples can be seen in the deep sea data logging [309] where no communications is possible with the exception of satellite communications.

1.5.4 Robotic/Mobile Sensing

Challenges still exist when adopting previous models such as overall costs involved in spatial deployments and regular maintenance, which still requires a manual component. One answer to this has emerged in the form of autonomous sensing platforms capable of operating autonomously for long periods of time and report their findings wirelessly to central servers. This concept/approach is relevant to the work presented in Chapter 3.

As technological trends and capabilities continue, so too does the amalgamation of disciplines for the creation of new ideas to solve existing problems. Although

stand alone platforms at present are considered to be the state-of-the-art of chemical sensing within the environment, a persistent problem associated with this model is its maintenance in terms of its lifetime due to battery depletion, reagent volume, biofouling, and necessary calibrations. In ideal cases where a large number of these devices are deployed to increase spatial sensing capabilities, the inherent maintenance and costs thereof increases dramatically and in some cases may be in excess of the costs associated with manual monitoring. One strategy to overcome such issues may lie in the field of robotic systems by integrating chemical sensors into mobile autonomous sensing platforms. This concept is not non-trivial and investigation into the corresponding challenges have been a growing topic in robotics for the past 15 years [286].

For instance, Ishida *et al.* [285] have investigated the method a moth uses for detecting plumes of the chemical *bombyko*l and applied it to a mobile robot. Afterwards, they developed an *odor compass* [284, 283] to identify the odor source [282] using metal oxide gas sensors. Kuwana and Shimoyama [281] implemented a mobile robot with two antenna to detect pheromones. Kazadi *et al.* [280] used a similar method to track water vapour plumes using resistive polymer sensors. RoboLobster (a biomimetic robotic lobster) by Grasso *et al.* [279] have investigated how lobsters localise and track odour plumes using only left and right conductivity sensors. Song *et al.* [278] have developed an algorithm on a mobile robot to investigate how to fuse two different sensory sources for detection i.e. odour and sound and subsequently communicate with other mobile robots through a WSN setup. Other examples of mobile robots equipped with physical/chemical sensors for tracking/sensing have been reviewed by Lilienthal *et al.* [286]. It should be noted that many chemically equipped sensing robots are at a laboratory/research phase and few have made it to a practical/application point. A somewhat exception to this has been the EU FP7 SHOAL project (Search and monitoring of Harmful contaminants, other pollutants and leaks in vessels in port using a swarm of robotic fish) which aims to provide a detection system for pollutions in two forms i.e. surface based (oil) and dissolved based (e.g. nitrates) within a marine environment [277].

It is clear that many examples within the literature equip mobile robots with chemical sensors. There are good reasons for this i.e. in order to build up a spatial picture of an environment's state and therefore using this information to track the source of a target e.g. a pollutant. However, a major challenge faced by the wearable sensor research community is how to deal with movement artefacts and therefore the identification of what are known as 'false positives'. One could expect to face similar problems with the dynamic nature of water bodies. It is unclear at this point whether this is a substantial problem faced by robots within the environment without more examples of practical deployments.

1.5.5 Commercial Landfill Technology

One of the working chapters within this thesis (Chapter 2) investigates the possibility of a method to monitor the two major greenhouse gasses produced by landfill sites. With the advent of WSN technology over the last two decade and relatively recent emergence of WSN into the commercial domain, one area that has not fully availed of this technology is monitoring of emissions from landfill sites. The reasons for this can be the result of the declining use of landfills for more favourable disposal methods e.g. incineration [107], export [127], recycling [128], and also by means of landfilling [136]. It should be emphasised that even though there is a decline, sites needs to be monitored for decades or perhaps hundreds of years. As a result, monitoring instruments tend to be stationary fixed devices or portable in nature. This section reviews the technology from commercial and academic domains, see Figure 1.5 on page 26 for visual reference.

Rig Rat III from BW Technologies (http://www.emlinc.com/) is one example of a commercial product capable of measuring and relaying the data through short range radio transmissions. There are, however, a number of differences. The first is their advertised target gas sensors which do not include CO_2 or CH_4 according to its manual [276]. In addition, it is not equipped with a cellular communications unit i.e. only short range ISM bands which means that when placed in remote locations (e.g. landfill sites) with no receiver, the communications can be a limiting factor. In addition, the system has a 30 day lifetime and does not offer a cloud based data visualisation/access system. Finally, the costs of this system is approx. $7,500 USD which makes scalability another issue.

GasClam from Ion Science (http://www.ionscience.com/) offers an autonomous model for measuring the two target landfill gases. The basic model is approximately €13,000 EUR that logs data and operates for up to 1 month. Extras can include a GPRS feature for remote data access; note that GPRS may not be available for remote locations, only calls and texts. Furthermore, there is no offer of a comprehensive cloud based visualisation feature.

A slightly cost effective model is offered by Crowcon called Detective+ (http://www.crowcon.
at $5,500 USD, however it is less sophisticated. It has a battery life of 2.5 days with no communication facilities. As a result it is not equipped for remote monitoring scenarios, but may offer these features in the future.

Envirowatch's E-mote (http://www.envirowatch.ltd.uk/) does not provide the same target gases but the platform may be capable of incorporating other sensors. However, it does monitor other chemical species such as CO, NO, NO_2, SO_2, H_2S, and Cl. Communications is achieved through an ethernet port and/or through short range communications i.e. Zigbee or via GPRS (with an additional gateway platform). It is therefore not readily applicable for landfill monitoring but has demonstrated air quality monitoring via deployment of 250 devices in Medway Council

(a) Rig Rat III - BW Technologies.

(b) GasClam - Ion Science.

(c) Crowcon - Detective+.

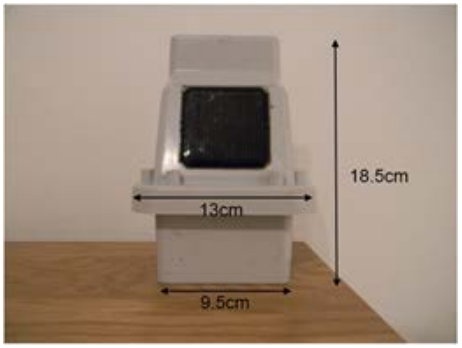

(d) E-Mote - Envirowatch.

Figure 1.5: Commercial products with features similar to the landfill device featured in Chapter 2.

and 70 motes in Liverpool Council. Remote monitoring is also available via a web portal page.

1.6 Wearable Technology

In many ways the technologies involved in environmental chemical sensing have existing parallels in wearable devices as the underlying sensing principles holds true for each domain. For instance, the fundamentals of bio/chemical sensing process still involves a number of stages of information gathering as discussed earlier in Section 1.4.1. Where they differ, however, can depend on the situation under consideration

or more specifically the challenges involved. Yang *et al.* have discussd some contrasts within WSNs and BSNs and tabulated the differences based on common sensing aspects [332], this is shown in Table 1.1 on page 28.

It can be seen that for environmental sensing (WSNs) there are certain freedoms in the technology, e.g. size, while for biosensing (BSNs) size can be crucial as a limited amout of space is available and can impede the wearer. The converse can be argued for battery maintenance in BSNs as being less challenging via charging availability/accessibility by the user than for remotely deployed systems within the environment. There are a number of other differences as well as commanilities which Table 1.1 on page 28 highlights. A full discussion will not take place however the primary differences can be reduced to temporal sampling, size, and biocompatibility. Therefore, it was advantageous to discuss the environmental aspect of chemical sensing first (see Section 1.5) in order to appreciate the diversity of chemical sensors within both application domains.

Wearable sensors can be broadly categorised into two major categories i.e. point-of-care and sporting activities. In may respects there are a number of overlapping concepts along with others that can be directly transferrable. This full discussion of which is larger than the needs of this thesis. However, what will be discussed in this section is how the technology enables chemical sensing and the challenges involved with realising such devices. The discussion begins with motivation of research in this area. Following this, the discussion moves to the technology of physical sensors, their implementations, and by extension it leads the discussion onto chemical sensing which is relevant to the work presented in Chapter 4.

1.6.1 Sensing Targets in BSNs

The most prevalent attention and potential demand for wearable sensors is currently coming from the health sector. As a result, there have been a number of methods elected to measure the various bio-signals emerging fsrom a user. Pantelopoulos *et al.* offers a comprehensive list of a number of bio-signals that can be incorporated into a wearable health monitoring system [328] and suggests the most common type of sensor for targeting the signal, see Table 1.2 on page 29. It can be seen that there are a number of bio-signals for target measurements and even more appropriate sensors. The potential for creating a system capable of monitoring all or a number these bio-signals on a continuous basis whilst addressing challenges shown in Table 1.1 on page 28 can result in a rich data set which can allow experts to detect the onset of disease and act accordingly. The potential for this technology is intuitaviely attractive and what is clear is that it will require a combination of physical and bio/chemical sensors to achieve maximum impact.

Table 1.1: Challenges in WSNs and BSNs. Information gathered from [332].

Challenges	**WSN**	**BSN**
Scale	As large as the environment being monitored (metres/kilometres)	As large as human body parts (millimetres/centimetres)
Node Number	Greater number of nodes required for accurate, wide area coverage	Fewer, more accurate sensors nodes required (limited by space)
Node Function	Multiple sensors, each perform dedicated tasks	Single sensors, each perform multiple tasks
Node Accuracy	Large node number compensates for accuracy and allows result validation	Limited node number with each required to be robust and accurate
Node Size	Small size preferable but not a major limitation in many cases	Pervasive monitoring and need for miniaturisation
Dynamics	Exposed to extremes in weather, noise, and asynchrony	Exposed to more predictable environment but motion artefacts is a challenge
Event Detection	Early adverse event detection desirable; failure often reversible	Early adverse events detection vital; human tissue failure irreversible
Variability	Much more likely to have a fixed or static structure	Biological variation and complexity means a more variable structure
Data Protection	Lower level wireless data transfer security required	High level wireless data transfer security required to protect patient information
Power Supply	Accessible and likely to be changed more easily and frequently	Inaccessible and difficult to replace in implantable setting
Power Demand	Likely to be greater as power is more easily supplied	Likely to be lower as energy is more difficult to supply
Energy Scavenging	Solar, and wind power are most likely candidates	Motion (vibration) and thermal (body heat) most likely candidates
Access	Sensors more easily replaceable or even disposable	Implantable sensor replacement difficult and requires biodegradability
Biocompatibility	Not a consideration in most applications	A must for implantable and some external sensors. Likely to increase cost
Context Awareness	Not so important with static sensors where environments are well defined	Vety important because body physiology is very sensitive to context change
Wireless Technology	Bluetooth, Zigbee, GPRS, and wireless LAN, and RF already offer solutions	Low power wireless required, with signal detection more challenging
Data Transfer	Loss of data during wireless transfer is likely to be compensated by number of sensors used	Loss of data more significant, and may require additional measures to ensure QoS and real-time data interrogation capabilities

Table 1.2: Biosensors and Biosignals. Information from [328].

Type of Bio-signal	**Type of Sensor**	**Description of Measured Data**
Electrocardiogram (ECG)	Skin/Chest electrodes	Electrical activity of the heart (continuous waveform showing the contraction and relaxation phases of the cardiac cycles)
Blood pressure (systolic & diastolic)	Arm cuff-based monitor	Refers to the force exerted by circulating blood on the walls of blood vessels, especially the arteries
Body and/or skin temperature	Temperature probe or skin patch	A measure of the body's ability to generate and get rid of heat
Respiration rate	Piezoelectric / piezoresistive sensor	Number of movements indicative of inspiration and expiration per unit time (breathing rate)
Oxygen saturation	Pulse Oximeter	Indicates the oxygenation or the amount of oxygen that is being "carried" in a patient's blood
Heart rate	Pulse Oximeter/skin electrodes	Frequency of the cardiac cycle
Perspiration (sweating) or skin conductivity	Galvanic Skin Response	Electrical conductance of the skin is associated with the activity of the sweat glands
Heart sounds	Phonocardiograph	A record of heart sounds, produced by a properly placed on the chest microphone (stethoscope)
Blood glucose	Strip-base glucose meters	Measurement of the amount of glucose (main type/source of sugar/energy) in blood
Electromyogram (EMG)	Skin electrodes	Electrical activity of the skeletal muscles (characterizes the neuromuscular system)
Electroencephalogram (EEG)	Scalp-placed electrodes	Measurement of electrical spontaneous brain activity and other brain potentials
Body Movements	Accelerometer	Measurement of acceleration forces in the 3D space

1.6.2 Physical Measurements in BSNs

What is clear from the literature is that the majority of efforts in this field focuses on applications involving the monitoring of physical movement which is apparent from a number of excellent reviews in the area [327, 328, 165, 326, 325, 324]. There are good reasons for addressing physical sensing targets before investigating the challenges that are inherent to bio/chemical sensing. The main reason is that physical sensors offer the road of least resistence in the sense that the sensing and communication infrastructure can be optimised while harvesting real data and producing a proven product. To expand on this, one need not tackle issues with cross disciplinary research to achieve certain wearable sensing goals. Another reason is that physical sensors are rich with information related to a user. Direct measurements can relate to a wearers' movement, however indirectly, this information could supply invaluable information. An example of this can be extracted from the way a wearer walks which may show signs of sever conditions such as muscular atrophy. Conditions such as this can be related to other forms of diseases e.g. cancer, AIDS, renal failure, arthritis, obesity, etc.

The use of wireless communications have offered a number of advantages to wearable sensing over the wired predecessor. This comparison has been studied by Townsend *et al.* and arguments for a wireless approac include ease of use, reduced risk of infection, reduced risk of failure, reduced user discomfort, enhanced mobiliy, and lower cost of care delivery [325]. Furthermore, with the curent and future trends of wirelesss options one can expect seamless connectivity to datacentres via 4G mobile communications [323], bluetooth [322], and zigbee (www.zigbee.org) standards. In this way measured data can be transmitted to datacentres for later analysis by medical experts and/or athletic coaches. There have been a number of studies reported within the literature that measure the physical parameters of a user and communicate the information to data repositories by wireless means; some of which will be reviewed here.

Sung *et al.* at the Medial Lab, MIT, have reported the development of a system (LiveNet) for detection and classification of a number of physical measurements [321]. These included accelerometers, ECG, conductiometric skin sensors, and an electromyogram (EMG) wich have been developed in conjunction with health care professionals for aiding in the detection of Parkinsons symptoms. Another health oriented system was reported by Ren *et al.* describiing a portable system capable of measuring phonocardiography (PCG - e.g. hart murmours), body temperature, and ECG [320]. Harvested data were communicated to a handheld PDA via Bluetooth. Mundt *et al.* describes a project entitled LifeGuard which was capable of measuring ECG, respiration rate, blood pressure, and body movement [319]. Their operating

conditions resulted in a 9 hour battery lifetime with data reported via Bluetooth.

These are just some of the many examples of wearable prototypes in the literature and are described here to give the reader insight into how far some scholars have progressed in the development of full systems capable of multiparameter measurements. For further reading the following review articles are recommended [327, 328, 165, 326, 325, 324]. Finally, it should be highlighted that many large companies are working towards harvesting wireless measurements through novel products. Some examples include Nike, Apple, Adidas, Foster-Miller, Philips, Fabric Works, Textronics Inc., etc.

1.6.3 Chemical Measurements in BSNs

In contrast to the vast number of studies for physical sensing, studies involving bio/chemical measurements are relatively few in comparison. The reasons for this can be attributed to challenges such as sampling, sample delivery to chemical transducer, filtration of the sample en route, wearability/compatibility, safety, longevity, along with inherent difficulties faced by bio/chemical reactive materials alone [449, 235].

Most measurements of bio/chemical samples are confined to the laboratory due to the same reasons discussed earlier for environmental monitoring (see Section 1.5.1 to avoid redundancies). However, wearable systems either purely based on chemical measurements or integrated systems incorporating a chemical sensing aspect have been reported. For instance, the ProeTEX project was a 6^{th} EU Framework program devoted to the development of smart textiles for use by firefighters in hazardous conditions [318, 317]. In addition to a number of physical measurements, the project incorporated chemical measurements i.e. CO and CO_2 concentration levels of the surrounding hazardous environment. However, more applicable to the workings of this thesis is measurements of an individual's internal state rather than the external environment.

It is clear that non-invasive measurement methods are the key to the success of bio/chemical wearable sensors. As a result, the spotlight has shifted from analysis of interal fluids such as blood towards measurement of target analytes within easily accessible bodily fluids. Body fluids contain all the information necessary to analyze the status of health of human beings and they are vital to monitor any change into the homeostatic conditions. The fluids of election have always been blood or urine, but the need for a non invasive monitoring is putting the attention on others media like saliva or sweat; giving the opportunity to realize point-of-care systems and improve the capabilities of athletic performances.

Monitoring of sweat is an excellent way for analysis of an individuals biochemical state as it is essentially filtered blood plasma which contains many biomarkers such as sodium, chloride, lactate, amongst others reviewed by Whitehouse [313]. Fur-

thermore, it is non-invasive and easily accessible. Despite this there has not been many examples reported in the literature possibly due to the difficulites in sample collection [311]. For example, Shirreffs *et al.* have reported a whole-body wash-down for sweat collect and electrolyte analysis [312] while Hayden *et al.* described a closed-pouch sweat collection technique [310].

Possibly the first attempt at analysing the pH of wearer's sweat in real time using a wireless device while exercising was reported by Coyle *et al.* as part of an EU FP6 project [311]. In this manner, a device was constructed consisting of a colorimetric pH patch, optical detectors, and a microcontroller-radio integrated device. One challenge was movement of the individual during exercise and as a result the exercise was restricted to an exercise bicycle. To address full movement for many other sporting activities the device integration will need to be address or an alternative. This discussion will continue in Chapter 4 to avoid repetition, which, coupled with previous discussions, sets the argument for an alternative to a dedicated device driven approach, and inlying restrictions, for pH sweat analysis.

1.6.4 Persistent Challenges

It is clear from the literature that the primary crucial constraints lies within the size of the wearable device and operational lifetime of the wearable system i.e. time between recharging cycles and/or if energy harvesting approaches can reflect the energy usage while in operation. Paradiso *et al.* has summed this view of power replenishment in a review article:

> "*Ubiquitous computing's dream of wireless sensors everywhere is accompanied by the nightmare of battery replacement and disposal.*" [316]

A result of this has been an emerging trend within the IC domain where electronic components are becoming more energy efficient and lower in form factor/footprint. One aspect of this has relied upon the ever increasing integrated devices and the chase for lower thermal emissions during operation [330].

Wireless security is another challenge. For instance, a popular wireless protocol for wearable devices is bluetooth [322]. However, it has been found that this framework is vulnerable to possible attacks/hacks [315, 314]. It stands to reason that devices with higher computing capability are capable of a more sophisticated level of data encryption and therefore data security. A consequence of using such a device for harvesting the sensor signals is the impact on the longevity of the device and/or the size of the overall device through adopting a larger capacity battery [328]. Clearly, a compromise exists here and the dependence/tolerations of the target application will come into play. In contrast to environmental sensing, unauthorised access to a person's health information can be a serious issue.

1.7 Parallel Measurement Strategies

1.7.1 Reproduction of Human Sensing

1.7.1.1 Electronic Sensing

Human sensing has the ability to identify a multitude of parameters based on various combinations of what is derived from a limited source of sensory input through what is known as *human perception* [386]. The concept of *electronic sensing* in this case refers to the reproduction of this capability through a multitude of sensors, parallel measurements, and pattern recognition approaches such as neural networks. Probably the first published work on this topic appeared in the 1960's by Moncrieff [385]. Since then, others have pushed this idea forward, for instance an article published in Nature by Persaud *et al.* [384] reported a reproducible approach for an *electronic nose* using semiconductor transducers that was capable of discriminating between a wide variety of odours. Moreover, this study showed that this discrimination was possible without the use of a great number of highly specific sensors. A published study by Gopel [387] describes the aims of electronic and bioelectronic noses:

- to develop highly sensitive sensors;
- to develop cheap and small online instruments for fast detection of specific chemicals, odours, or toxic substances with high spatial and time resolution;
- to develop new materials for odour detection based on molecular recognition principles which are similar to those in the human nose;
- to develop systems which produce signals that are related directly to human odour sensation;

Applications of such electronic detection techniques have been reported in the literature to include: classification of coffee types [383], discrimination between off-flavours in milk [382], the monitoring the flavours of beers [381], the prediction of bacteria type and culture growth [380], amongst others that have have been reviewed by Gardner *et al.* [379], Strike *et al.* [378], and Roeck *et al.* [377].

1.7.1.2 Optical Sensing

Less appreciated for chemical sensing applications is the use of an *electronic eye* or otherwise known as an *optoelectronic nose*. Studies of the human eye have concluded that the light receptors are classified into two categories i.e. rods (scotopic vision - for low light conditions) and cones (photopic vision - for colour vision in bright light conditions). There are three types of cones which respond mainly to different wavebands of the visible spectrum i.e. red, green, and blue [376, 375]. This model has given rise to the realisation of devices capable of detecting light in a very similar

manner which is widely known today as the digital colour camera. Further to this, an inherent ability of the human visual system is the capability of perceiving the same colour of an object under varying illumination conditions. This ability is known as colour constancy [374]. Furthermore, it has been found that not all mammals have four types of photoreceptors [373] where some only have two. This is a challenging concept in terms of light detection as a change of wavelength cannot be distinguished from a change in intensity which is a serious disadvantage from the single point electronic devices. If the capability of distinguishing between light intensity and wavelength could be replicated by an electronic device, e.g. a colour camera, one may conceptually achieve an extremely low cost colorimetric sensor that can detect a large number of colorimetric analytes in parallel while in uncontrolled lighting conditions.

1.7.2 Optical Responsive Materials

The fundamental aspect of optical sensors lies with the sensing element itself i.e. the material which changes in its optical properties when influenced by a target stimulii. This phenomenon is commonly known as chromism and is based on changes within the electron state of a molecue. Such materials that undergo a change in colour can be grouped into different categories which are often dependent upon the classification of the target stimulii. For example, thermochromatic materials change in colour with respect to a rise/fall in temperature [372, 371], or other materials that respond colorimetrically to e.g. mechanical strain [370, 369]. Other classifications along with their associated primary stimulus is shown in Table 1.3 on page 35.

It is clear that materials respond to a stimulus via a change in its optical properties e.g. its apparent colour. Others may respond to a number of stimuli [361]. However, the focus of this thesis is primarily on the analysis of chemoresponsive colorimetric materials capable of responding proportionally to target chemical species for detection/monitoring means. Chemochromic materials can include a number of chromatic categories such as halochromism or ionochromism present in Table 1.3 on page 35, but do not include physical stilumi such as temperature. A complete review of colorimetric chemical indicators/reagents are beyond the scope of this thesis, however some examples have already been mentioned somewhat in Section 1.4.1. Other examples can be gaind from the following excellent works in this area [360, 359, 358].

1.7.3 Colour Formation via pH Indicators

A significant part of this thesis is concerned with the detection of pH concentrations via colorimetric indicators - the phenomenon known as halochromism as listed in

Table 1.3: Categories of chromism, their associated stimulii, and example works for further reading.

Category	Stimulus	Example
Thermochromism	Temperature	[368]
Electrochromism	Electrical Current	[367]
Photochromism	Electromagnetic Radiation	[366]
Halochromism	pH	[365]
Ionochromism	Ions	[364]
Piezochromism	Mechanical Pressure	[363]
Solvatochromism	Solvent Polarity	[362]

Table 1.3 on page 35. Consequently, it is important to include the theory governing this process.

Water (H_2O) can undergo a process of self-ionization called autoprotolysis, under which it behaves as both an acid and base. These ions can occur when two water molecules interact, as depicted in Figure 1.6 on page 37, forming Hydronium (H_3O^+)[1] and Hydroxide (OH^-) ions.

$$H_2O + H_2O \rightleftharpoons H_3O^+ + OH^-$$

In an aqueous solution an acid is a subtance that can increase the concentration of H_3O^+ ions when added to water. Conversely, a base is a substance that decreases the concentration H_3O^+ ions or increases the concentration of OH^- ions. The product of the concentration of H^+ and OH^- ions within a solution yields an equilibrium constant denoted as K_W, i.e. the autoprotolysis of water. The system of measurement for this concentration is the pH scale, and defined as follows:

$$pH = -\log[H^+]$$

At $25°C$ the value of K_W is 1.01×10^{-14} [333] and it can be seen that the relationship between H^+ and OH^- ions can be expressed as:

$$K_W = [H^+][OH^-]$$

$$\log K_W = \log[H^+] + \log[OH^-]$$

$$-\log K_W = -\log[H^+] - \log[OH^-]$$

$$14.00 = pH + pOH \text{ (at } 25°C)$$

From the above equation it can be seen that if the concentrations of H^+ and OH^- ions are equal within a solution the pH is 7. Furthermore, when a weak acid (denoted as HA) reacts with water a proton is donated to the water molecule yielding:

[1]The term H^+ is used interchangably with H_3O^+.

$$HA + H_2O \overset{K_a}{\rightleftharpoons} H_3O^+ + A^-$$

The acid dissociation constant K_a is defined as follows where K_a is "small" for a weak acid:

$$K_a = \frac{[H^+][A^-]}{HA}$$

$$pK_a = -\log[K_a] = -\log\left[\frac{[H^+][A^-]}{HA}\right] \text{ (at lograthmic scale)}$$

One method of determining the pH of a solution is through the use of substances that change in colour with respect to the concentration of these ions, i.e. via aptly named pH indicators which are within themselves weak acids/bases. Bromocresol green is one example of a pH indicator, which appears yellow in its acidic state and blue in its conjugate base form, centred about a pK_a of 4.74 [571]. The extent of conjugation of the dye affects its spectral response resulting in a change in observable colour. Figure 1.7 on page 37 presents changes in the spectra of Bromocresol Green as the pH changes from ca. 6 to ca. 3.5, see Appendix B for more details. It can be seen that during protonation/deprotonation the spectral response changes, and consequently results in a change in apparent colour.

Measurement of this process can be in many forms. The standard technique is to plot changes of absorbance values at the wavelength of maximum change (i.e. λ_{max}), or for the case of Figure 1.7 on page 37 the arrow pointing up. This technique has been employed by others but using a single point light detector and a controlled light source about the wavelength of maximum absorbance, e.g. by O'Toole *et al.* [388]. The work within this thesis adopts a different approach, instead it uses digital imagery which detects the visible spectrum, i.e. from ca. 400 - 700 nm. Appendix B outlines a comparison between using a standard camera and the reference instrument (spectrophotometer). The results of this study showed the camera was capable of detecting changes in pH via apparent colour and that when compared to the reference instrument a high correlation resulted ($R^2 = 0.98835$), yielding high confidence that the camera behave as a colorimetric chemical detector for the working chapters.

1.7.4 Chemical Sensing via Imaging Techniques

Studies within the literature attempting to reproduce the capability of the human visual system in terms of chemical measurements have been reported. Barnard and Walt [357] have reported the use of a CCD colour camera for the determination of the pH of blood using three individual indicators. Later, Sawada *et al.* [356] have

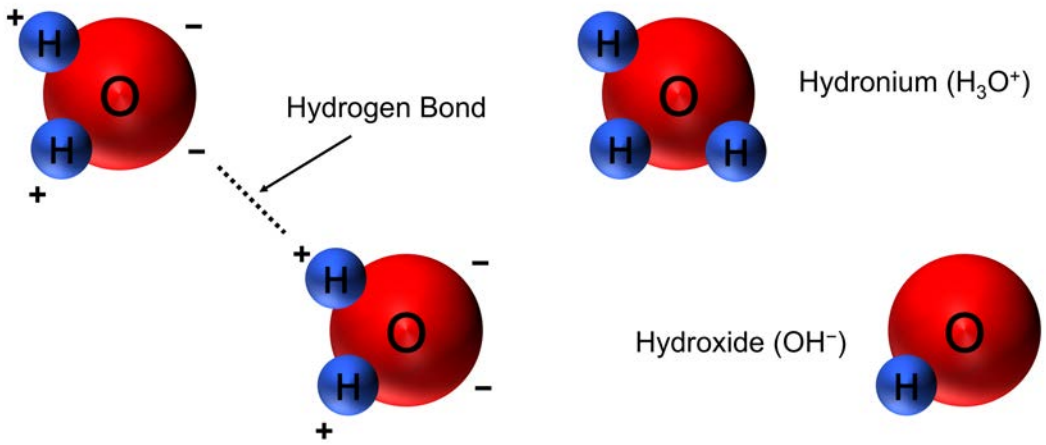

(a) Hydrogen bond forming between two water molecules.

(b) Two ions form: Hydronium (H_3O^+) and Hydroxide (OH^-).

Figure 1.6: Formation of Hydronium and Hydroxide ions.

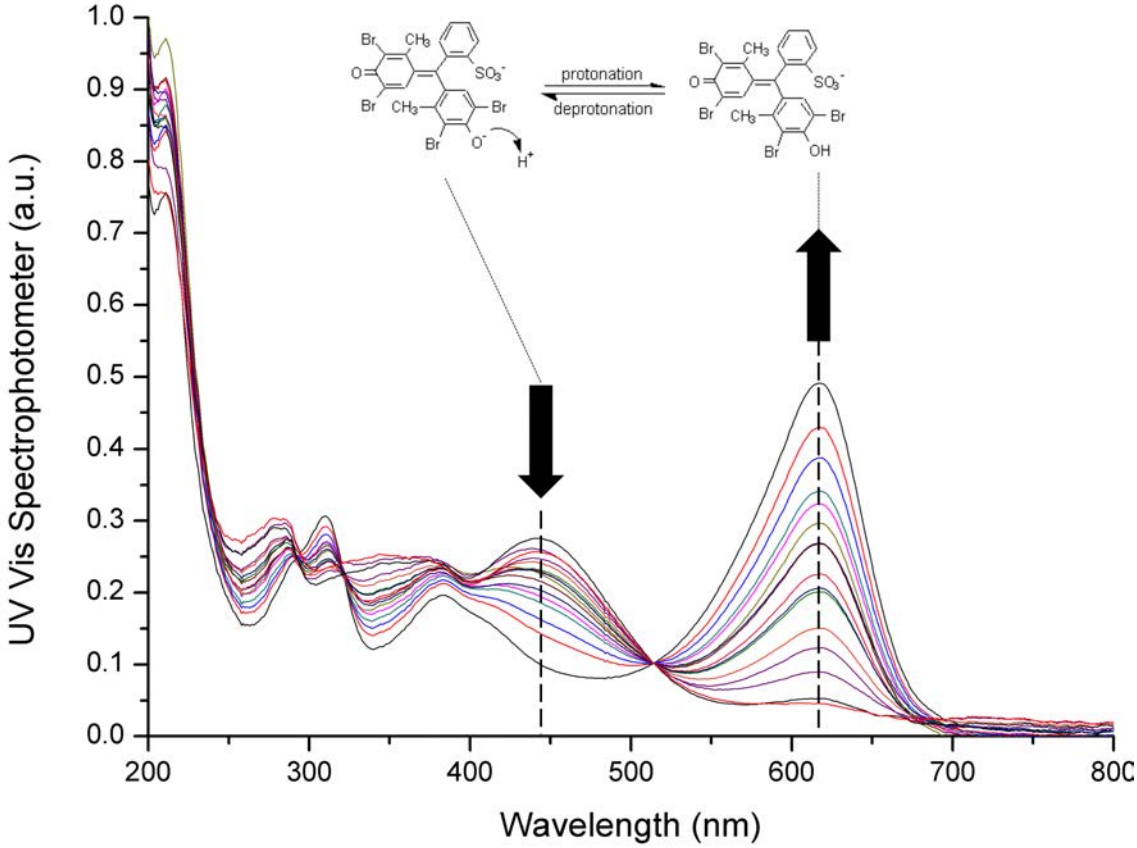

Figure 1.7: Spectral response of indicator Bromocresol Green as the pH is lowered from ca. 6 to ca. 3.5.

applied this approach to the development of a full range pH sensor i.e. 0-14. In the same way, Alexandre *et al.* [496] proposed a colorimetric detection of DNA. The work by Byrne *et al.* [504, 505] have applied the use of a camera to the determination of fish spoilage using a single colorimetric indicator for ammonia levels. Safavi *et al.* [465] have demonstrated a full range pH sensor using multiple pH indicators coupled with a pattern recognition approach i.e. Artificial Neural Networks (ANNs). A similar study was conducted by Stich *et al.* [351] who demonstrated the novelty of this approach by applying the technique to more than one sensing target i.e. CO_2 and temperature. Similarly, a sensor array for a variety of analytes based on colour and fluorescence changes within the indicator structure was quantified using a CCD colour camera by Goodey *et al.* [350]. Furthermore, He *et al.* [349] have applied this technique (CCD and ANNs) towards the identification of pH (1-12) along with 6 types of heavymetals (Cu^{2+}, Fe^{2+}, Fe^{3+}, Ca^{2+}, Zn^{2+}, and Mg^{2+}) in waters. Other works based in imaging techniques have been reported in the literature to include the use of hand held scanners [348, 347, 346], flatbed scanners [345, 344], web cams [343] and camera phones [342]. All of these studies have been conducted in controlled lighting conditions and using either the Grey or RGB colour space. There are good reasons for adopting the RGB colour space for analysis, principally because one can achieve absorptions via the raw tri-optical sensors within a camera i.e. within a fixed waveband e.g. red, green, or blue. This is an excellent strategy for a direct correlation with reference instruments, however what has previously been unexplored is the use of colour models other than RGB. One question that all of the above studies raises is the specific choice of colour space adopted. With many available (a review can be found by Pacale [334]), it can be difficult to reproduce their results without exploring all possible RGB colour space instances.

This review would not be complete without including the works by the group of L.F. Capitán-Vallvey. Although much of their camera work was based along the same lines of others in the field, i.e. through the use of the RGB colour space [341, 340, 339], it wasn't until very recent work where another colour space (HSV) was considered for analytical measurements of chemical species [338, 506, 336]. The HSV colour space transforms the raw RGB values into one more akin to human perception [583] where the colour (Hue - H), colour intensity (Saturation - S), and light intensity (Value - V) are divided into separate components. The key point about this approach is that by separating the colour from the light intensity, one can achieve a more robust representation of the colour and allow for the use of this approach outside the confinds of controlled lighting conditions where previous studies have been conducted. In addition, more studies are needed to explore the robustness of a camera measuring chemical analytes outside controlled lighting conditions and achieve what humans perceive as *colour constancy*. Finally, it should be mentioned that although the HSV colour space offers advantages over RGB for

colorimetric analysis, there are many other colour spaces as yet to be explored in this context.

1.8 Thesis Overview

1.8.1 Theme

The overarching theme of this thesis resides in the investigation of novel techniques for generating chemical information through the application of technology. This premise is examined through the use of optical chemical sensors and explores their use in the applied rather than theoretical research domain. Often, as one progresses from a controlled environment (e.g. a laboratory) towards practical environments (e.g. the natural world), studies become focused to account for influencing factors. As a result, four studies are considered within this thesis that fall under the construct of either two approaches for optical chemical sensing, i.e. a customised approach (dedicated devices) and later investigates a more general approach (digital imaging) under different scenarios. The following sections delves deeper into the working of this thesis.

1.8.2 Research Space and Argument

A complete account of the contributions by the student during this research program is not presented as part of this thesis; a list is provided on page viii in place of this. Where they differ depends upon the specific circumstance of the sensing environment in question (e.g. a laboratory, river system, or biological entity, etc.) and the chemical sensor of choice. However, what they have in common lies within the research space of interfacing with chemical transducers, the challenges associated with extracting chemical based information from an environment, delivery of this information to end users/devices, and interpretation of the results. The method by which this information is harvested is the direct theme of this thesis. The work in its entirety can be viewed as resting on two pillars, each relating to a different approach by which the aforementioned process occurs.

In the first instance the sensing approach follows from an established mote-based method adopted by many studies within the literature. This is best explained with reference to Figure 1.8 on page 41, which presents a number of common processes involved in the operation of wireless chemical sensing devices. As the information from the measurand/analyte of interest tracks through to data stored on the cloud (or to end users), the information can ultimately be presented in a generic format i.e. a time stamp with a corresponding sensed value. However, the implementation of such a device tends to be specific to local circumstances and the nature of the chemical transducer. This approach has been adopted as standard within the

literature and throughout this program in the investigation of a number of areas, e.g. from miniaturised portable instruments [8, 10, 7, ?], wearable devices [9, 13], towards deployable environmental sensing platforms [4, 5, 14]. Often, the findings that such systems generate are emphasised over the sensing implementation, which is understandable as they continue to follow this model and the novelty is mostly in its application.

There are good reasons for adopting the above sensing approach, principally because it is established, widely accepted, and many devices are available off-the-shelf for development. However, there are a number of challenges that this approach continues to face. The first is in the creation of the sensing infrastructure i.e. its design, development, testing, and deployment. This challenge becomes more profound when considering a large number of nodes. Related to this is the maintenance costs e.g. battery changes per node. Wireless connectivity and data/traffic handling is another point to consider. Expanding the platform to incorporate other sensing targets may require additional components as discussed earlier, see Figure 1.8 on page 41. A final consideration here must include the aspect of upgradability. Dedicated devices such as these are dependant upon a number of IC components and the possibility therefore exists that one or more components maybe discontinued or the next generation is not backward compatible. Consequences of this may range from as little as rerouting the PCB to accommodate secondary components, or perhaps a complete redesign for primary components (e.g. new toolchains, programming languages, for micro-controller/microprocessor).

The second *pillar* or approach to chemical sensing investigated during the course of this program considers a different model, one which may offer an ability to address some of the issues outlined above. This refers to the use of digital imagery for the detection of key sensing targets. There are many arguments for advocating this approach to chemical sensing given the recent advent and widespread use of imaging technology. For instance, the availability of optical responsive materials to various stimuli have been discussed earlier in Section 1.7.2 in addition to studies within the literature reporting chemical sensing via digital imaging techniques (Section 1.7.4). The potential for using an existing sensing infrastructure already in place without the need to design, develop, and deploy such hardware is intuitively attractive. Furthermore, many systems such as CCTV or SMART devices most likely possess the means for internet connectivity and processor requirements; meaning that the specific implementations necessary for dedicated devices (Figure 1.8 on page 41) may no longer be necessary. Furthermore, with the standardisation of colour profiles, such as sRGB [391], one can reduce compatibility issues from camera to camera. In addition to this, imaging may address issues related to upgradability i.e. digital scenes have become increasingly standardised with possible future differences lying mainly in the image's resolution. In other words, processing and analytical techniques of

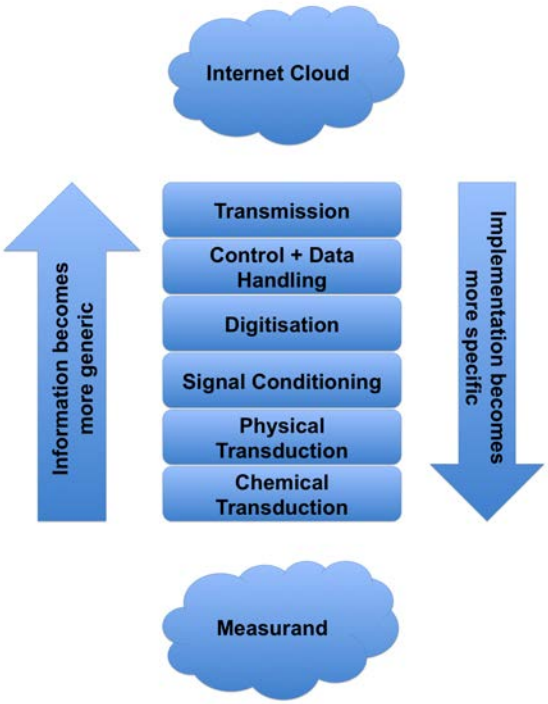

Figure 1.8: Common processes involved in a wireless-based device for chemical sensing.

such images can remain largely the same if the standard continues.

Consider the deployment of a chemical sensing system network by the US department of transport and energy entitled PROTECT (Program for Response Options and Technology Enhancements for Chemical/Biological Terrorism) [390]. A sensing network consisting of a number of nodes for the detection of harmful chemical species. The production costs of each sensing unit (following the device dependent model discussed earlier) was up to $25,000 USD with multiple deployments in over two dozen railway sites [389]. Conversely, consider that such sites already possesses CCTV surveillance equipment (digital imagery) that has the potential to monitor colorimetric changes in chemical indicators which can be placed in the camera's field of view. In this scenario, the costs have conceptually been reduced significantly along with the complexity of deploying and maintaining dedicated devices for harvesting chemical information within this area.

It is clear from the literature explored in Section 1.7.4 that this method for chemical sensing is in its infancy where most of the studies have taken place under laboratory settings. Although this stage of its research is important, successive studies focus on the ability to detect other sensing targets, or expand the study to sensing multiple analytes. Rather than demonstrating the ability to detect colorimetric chemical changes to the detection of another analyte, the work presented in this thesis takes a more pragmatic role in investigating the place of digital imagery in much needed areas of chemical sensing.

1.8.3 Objectives

It is important to understand that any sensing approach is largely influenced by the application scenario and therefore one of the only ways of exploring sensing approaches is under specific circumstances. As a result a number of secondary objectives have emerged with respect to the primary objective. The main focus of this thesis lies in the exploration of strategies and methods for harvesting chemical based information from practical scenarios/applications. Two distinct methods of investigating this has been adopted and applied to numerous scenarios. The first adopts a device-dependent driven model (discussed earlier), while the second investigates similar concepts but through the use of digital imagery that may offer some advantages over the first model.

The device dependent approach has been applied in numerous novel scenarios during this program (see page viii), however including all of them as part of this thesis is cumbersome and unnecessary. One objective of this thesis is to explore the efforts that must go into the design, development, deployment, and maintenance of a sensing device under this model. As a result, one of these studies is selected and presented that encompasses the end-to-end aspects of this model. In doing so it addresses important issues related to the treatment and monitoring of our waste through the process of landfilling and the work involved in addressing scalability issues in terms of multiple sampling locations i.e. three devices in this case.

A number of challenges facing the device dependent approach have been discussed earlier. The objectives explored as part of the remaining working chapters explores some of these issues through an approach based on digital imagery. The first continues on the environmental theme whereby a mobile sensing platform with an onboard camera interrogrates three sensor stations placed at separate locations. Investigations into the advantages that this method may have on monitoring a spatial area, scalability issues, and the detection of events is explored. The sensing scenario is then changed to investigate the possibility of quantitatively measuring the pH concentration of an athlete's sweat during exercise without the need to equip the wearer with electronic circuitry. The final question/objective relates to the inherent two-dimensional spatial nature of cameras. This is explored in the detection of chemical gradients along a microfluidic channel.

Tackling these issues is challenging and given that each sensing scenario is heavily influenced by its sensing environment, it becomes difficult to direcly compare each approach in practical terms. An important part of comparing two approaches is in the exploration of each approach individually, which can then lead onto methods for direct comparison. The importance of the working chapters based on the digital imaging model comes into focus under this concept. Through the use of these

works, and drawing from the literature, the final objective is to offer a conceptual comparison of both approaches and to discuss future work for a direct comparison.

1.8.4 Structure

A second way of viewing the work in this thesis is in the exploration of novel techniques for optical chemical sensing. Figure 1.9 on page 44 shows the structure of this thesis under the construct of optical chemical sensing with the work categorised into two detection spaces (discussed earlier). The figure also shows works by the student (represented in grey) that will not, explicitly, be presented as part of this thesis; instead these will be drawn upon later to aid in a comparison of the detector spaces.

Representing the dedicated device is the work monitoring greenhouse gas emissions from landfill sites. This was not only chosen to explore the efforts necessary for the dedicated device approach, but it also helps to tie the thesis together under a common construct of chemical sensing via optical means. In this case IR absorption is used as the detection method where information about the local chemistry of the target environment is generated. In a similar way, the chapters exploring novel avenues relating to the generation of chemical information from an environment via imaging techniques is also based on optical techniques. However, in these cases the novel concept worth exploring is in the possibility of reducing costs and efforts associated with the dedicated-device approach. Aspects of this is investigated by considering three application scenarios and studying the underlying challenges and potential benefits of digital imaging in each case.

This method of exploring a novel detection technique for chemical sensing through application scenarios is not new. A thesis by O'Toole made contributions to this space by using a PEDD detector and exploring its detection capabilities in pH detection, phosphate, HPLC, and the detection of transition metals: manganese and cobalt [388]. This thesis follows the same approach but also offers a conceptual comparison drawing from additional studies by the student.

The following account takes the discussion into the specifics of each study. It should be noted at this point that in each study the chemical transduction element is either purchased as an off-the-shef component (Chapters 2 and 3), or the work of another researcher (Chapters 4 and 5). For each working chapter a preamble is presented that brings the work into the context of this thesis, outlines additional necessary information, in addition to outlining the contributions to the field, by the author of this thesis, and recognising the work by other contributors. Finally, the discussion shifts to reviewing the overall significance of this thesis and what the next possible phase of work will focused on (Chapter 6). A brief summary of the entire thesis takes place followed by each paper being discussed separately. The adopted model will give a synopsis of each paper, discuss its significance, and finally

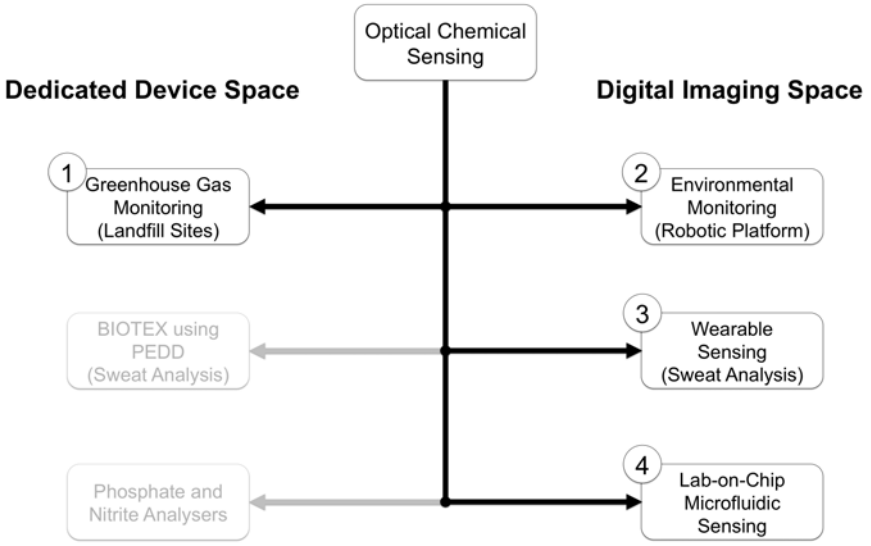

Figure 1.9: The structure of this thesis and the classification of the work in either the dedicated device or digital imaging space. Numbers represent the working chapters: 1 (Chapter 2), 2 (Chapter 3), 3 (Chapter 4), and 4 (Chapter 5). Grey boxes show pieces of work not appearing in this thesis but represent reflections in the detection space.

explore future work/stages of the study. Finally, the discussion takes a wider view of the thesis and proposed hypothesis i.e. a conceptual comparison of both sensing approaches is presented from the findings of the working chapters, which relates to proposed future work for direct comparison(s).

1.9 References

[89] A. Sorensen and J. Okata. *Megacities: Urban Form, Governance, and Sustainability ; [International Workshop on World Megacities Held 7 - 8 March 2008 by the Center for Sustainable Urban Regeneration (cSUR) at the University of Tokyo]*. Csurut Series: Library for Sustainable Urban Regeneration. Authors, 2011.

[90] Diabetes Control and Complications. **The effect of intensive treatment of diabetes on the development and progression of long-term complications in insulin-dependent diabetes mellitus. the diabetes control and complications trial research group.** *N Engl J Med.*, **30**(329(14)):977–86, 1993.

[91] Eric A. Finkelstein and Justin G. Trogdon and Joel W. Cohen and William Dietz. **Annual medical spending attributable to**

obesity: payer-and service-specific estimates. *Health Affairs*, **28**(5):822–831, 2009.

[92] D. Gardner and D. Shoback. *Greenspan's Basic and Clinical Endocrinology, Ninth Edition*. McGraw-Hill Education, 2011.

[93] David W Haslam and W Philip T James. **Obesity**. *The Lancet*, **366**(9492):1197 – 1209, 2005.

[94] Hawton K, Van Heeringen K. **Suicide**. *Lancet*, **18**(373(9672)):1372–81, 2009.

[95] Heinrich, Sven and Luppa, Melanie and Matschinger, Herbert and Angermeyer, Matthias C. and Riedel-heller, Steffi G. and Koenig, Hans-helmut. **Service utilization and health-care costs in the advanced elderly**. *Value in Health*, **11**(4):611–620, Jul-aug 2008.

[96] International Diabetes Federation. **Annual report 2012**. *International Diabetes Federation Online (`http://www.idf.org/sites/default/files/IDF_Annual_Report_2012-EN-web.pdf`)*, 2012.

[97] Mendelson, D N and Schwartz, W B. **The effects of aging and population growth on health care costs**. *Health Affairs*, **12**(1):119–125, 1993.

[98] Cynthia L. Ogden and Margaret D. Carroll and Brian K. Kit and Katherine M. Flegal. **Prevalence of obesity in the united states, 2009–2010**. *Nchs*, (82), 2012.

[99] Raj Persaud. **Suicide: an unnecessary death**. *British Medical Journal*, **323 (7304)**(114), 2001.

[100] Danuta Wasserman and Qi Cheng and Guo-xin Jiang. **Global suicide rates among young people aged 15-19**. *World Psychiatry*, **4**(2), 2005.

[101] World Health Organisation. **The preamble of the constitution of the world health organization**. *Public Health Classics*, **80**(12), 2002.

[102] R.H. Williams, J.D. Wilson, and D.W. Foster. *Williams Textbook of endocrinology*. Saunders, 1985.

[103] S. N. Al-bahry and I. Y. Mahmoud and K. I. A. Al-belushi and A. E. Elshafie and A. Al-harthy and C. K. Bakheit. **Coastal sewage discharge and its impact on fish with reference to antibiotic resistant enteric bacteria and enteric pathogens as bio-indicators of pollution**. *Chemosphere*, **77**(11):1534–1539, Dec 2009.

[104] Andrews, William J. and Masoner, Jason R. and Cozzarelli, Isabelle M. **Emerging contaminants at a closed and an operating landfill in oklahoma**. *Ground Water Monitoring and Remediation*, **32**(1):120–130, Win 2012.

[105] Berg, M and Tran, Hc and Nguyen, Tc and Pham, Hv and Schertenleib, R and Giger, W. **Arsenic contamination of groundwater and drinking water in vietnam: a human health threat**. *Environmental Science & Technology*, **35**(13):2621–2626, Jul 1 2001.

[106] Brown, Charlotte and Milke, Mark and Seville, Erica. **Disaster waste management: a review article**. *Waste Management*, **31**(6):1085–1098, Jun 2011.

[107] Denison, Ra and Silbergeld, Ek. **Risks of municipal solid-waste incineration - an environmental perspective**. *Risk Analysis*, **8**(3):343–355, Sep 1988.

[108] I. Dési and G. Somosi. **Toxicological investigation and evaluation of drinking-water pollution caused by chemical wastes**. *Ecotoxicology and Environmental Safety*, **8**(4):315 – 327, 1984.

[109] L. Drouin. In *Proc. of the 17th Canadian Waste Management Conference*, Ottawa, Quebec, Ontario, Canada, September 1995. Association Canadienne des Industries de l'Environment, National Research Council of Canada.

[110] University of Birmingham Enviros Consulting Ltd. **Review of Environmental and Health Effects of Waste Management: Municipal Solid Waste and Similar Wastes**. Online (http://www.defra.gov.uk/publications/2011/03/26/health-report-pb9052a/), March 26 2011. Department for Environment Food and Rural Affairs (DEFRA).

[111] The European Parliament. **EU Waste Legislation: Waste Framework Directive**. Online (http://ec.europa.eu/environment/waste/legislation/a.htm), November 2008.

[112] Office for Official Publications of the European Communities. **Waste generated and treated in Europe - Eurostat**. Online (`http://epp.eurostat.ec.europa.eu/statistics_explained/index.php/Waste_statistics`), 2009. Luxembourg.

[113] The European Commission. **Europe in figures - Eurostat Yearbook 2011**. Online (http://epp.eurostat.ec.europa.eu/portal/page/portal/publications/eurostat_yearbook_2011), 2011.

[114] The European Commission. **The EU Environmental Waste Homepage**. Online (http://ec.europa.eu/environment/waste/index.htm), 2013.

[115] Peter Flyhammar. *Heavy metals in municipal solid waste deposits*. Department of Water Resources Engineering, Lund University, Box 118, S-221 00 Lund, Sweden,, 1997.

[116] Franzidis, Jean-pierre and Heroux, Martin and Nastev, Miroslav and Guy, Christophe. **Lateral migration and offsite surface emission of landfill gas at city of montreal landfill site**. *Waste Management and Research*, **26**(2):121–131, Apr 2008.

[117] Anthony Staines, Claire Collins, John Bracken, Michael Bruen, John Fry, Victor Hrymak, Dermot Malone, Bill Magette, Michael Ryan, and Colin Thunhurst. **Health and Environmental Effects of Landfilling and Incineration of Waste - A Literature Review**. Online (http://www.hrb.ie/publications/hrb-publication/publications/162/), 20 February 2003. Health Research Board Publication.

[118] Mark V. Hoyer and D. L. Watson and D. J. Wills and D. E. Canfield Jr. **Fish kills in florida's canals, creeks/rivers, and ponds/lakes**. *Journal of Aquatic Plant Management*, **47**:53–56, 2009.

[119] Jackson, Jbc and Kirby, Mx and Berger, Wh and Bjorndal, Ka and Botsford, Lw and Bourque, Bj and Bradbury, Rh and Cooke, R and Erlandson, J and Estes, Ja and Hughes, Tp and Kidwell, S and Lange, Cb and Lenihan, Hs and Pandolfi, Jm and Peterson, Ch and Steneck, Rs and Tegner, Mj and Warner, Rr. **Historical overfishing and the recent collapse of coastal ecosystems**. *Science*, **293**(5530):629–638, Jul 27 2001.

[120] Jobling, S and Nolan, M and Tyler, Cr and Brighty, G and Sumpter, Jp. **Widespread sexual disruption in wild fish**. *Environmental Science & Technology*, **32**(17):2498–2506, Sep 1 1998.

[121] L. T. A. Joosten and S. T. Buijze and D. M. Jansen. **Nitrate in sources of drinking water? dutch drinking water companies aim at prevention**. *Environmental Pollution*, **102**(1, Supplement 1):487 – 492, 1998. Nitrogen, the Confer-N-s First International Nitrogen Conference 1998.

[122] Justic, D and Rabalais, Nn and Turner, Re and Dortch, Q. **Changes in nutrient structure of river-dominated coastal waters - stoichiometric nutrient balance and its consequences**. *Estuarine Coastal and Shelf Science*, **40**(3):339–356, Mar 1995.

[123] Kjeldsen, P and Fischer, Ev. **Landfill gas migration - field investigations at skellingsted landfill, denmark**. *Waste Management and Research*, **13**(5):467–484, Oct 1995.

[124] Kollikkathara, Naushad and Feng, Huan and Stern, Eric. **A purview of waste management evolution: special emphasis on usa**. *Waste Management*, **29**(2):974–985, Feb 2009. 5th Asian-Pacific Landfill Symposium, Sapporo, JAPAN, OCT 22-24, 2008.

[125] X.f. Lou and J. Nair. **The impact of landfilling and composting on greenhouse gas emissions - a review**. *Bioresource Technology*, **100**(16):3792 – 3798, 2009. Selected papers from the International Conference on Technologies and Strategic Management of Sustainable Biosystems.

[126] FRANK McDONALD. **Underground Fire Rages on**, Jan 27 2011. Copyright - Copyright The Irish Times Ltd. Jan 27, 2011; Language of summary - English; ProQuest ID - 1015294773; Last updated - 2012-05-23; Place of publication - Dublin, Ireland; Corporate institution author - McDONALD, FRANK; DOI - 2266569792; 26145573; 81199.

[127] Menkes, Db. **Exporting hazards to developing countries**. *World Health Forum*, **19**(4):412–416, 1998.

[128] E Metin and A Eröztürk and C Neyim. **Solid waste management practices and review of recovery and recycling operations in turkey**. *Waste Management*, **23**(5):425 – 432, 2003. <ce:title>Appropriate Solid Waste Management and Technologies for Developing Countries</ce:title>.

[129] Mor, Suman and Ravindra, Khaiwal and De Visscher, Alex and Dahiya, R. P. and Chandra, A. **Municipal solid waste characterization and its assessment for potential methane generation: a case study**. *Science of The Total Environment*, **371**(1-3):1–10, Dec 1 2006.

[130] Brian Austin. *The involvement of pollution with fish health*, pages 13–30. Multiple Stressors: A Challenge for the Future. Springer, The Netherlands, 2007.

[131] Nikolaou, K. **Environmental management and landfill fire accidents**. *Journal of Environmental Protection and Ecology*, **9**(4):830–834, 2008.

[132] Nozhevnikova, An and Lifshitz, Ab and Lebedev, Vs and Zavarzin, Ga. **Emission of methane into the atmosphere from landfills in the former ussr**. *Chemosphere*, **26**(1-4):401–417, Jan-feb 1993. Nato Advanced Research Workshop On Atmospheric Methane : Sources, Sinks And Role In Global Change, Mt Hood, Or, Oct 07-11, 1991.

[133] Nyns, Ej and Gendebien, A. **Landfill gas - from environment to energy**. *Water Science and Technology*, **27**(2):253–259, 1993.

[134] Orr, Jc and Fabry, Vj and Aumont, O and Bopp, L and Doney, Sc and Feely, Ra and Gnanadesikan, A and Gruber, N and Ishida, A and Joos, F and Key, Rm and Lindsay, K and Maier-reimer, E and Matear, R and Monfray, P and Mouchet, A and Najjar, Rg and Plattner, Gk and Rodgers, Kb and Sabine, Cl and Sarmiento, Jl and Schlitzer, R and Slater, Rd and Totterdell, Ij and Weirig, Mf and Yamanaka, Y and Yool, A. **Anthropogenic ocean acidification over the twenty-first century and its impact on calcifying organisms**. *Nature*, **437**(7059):681–686, Sep 29 2005.

[135] Park, Soyoung and Brown, K. W. and Thomas, J. C. and Lee, Incheol and Sung, Kijune. **Comparison study of methane emissions from landfills with different landfill covers**. *Environmental Earth Sciences*, **60**(5):933–941, May 2010.

[136] Pipatti, Riitta and Wihersaari, Margareta. **Cost-effectiveness of alternative strategies in mitigating the greenhouse impact of waste management in three communities of different size**. *Mitigation and Adaptation Strategies for Global Change*, **2**(4):337–358, 1997.

[137] Reinhart, Dr. **A review of recent studies on the sources of hazardous compounds emitted from solid-waste landfills - a united-states experience**. *Waste Management and Research*, **11**(3):257–268, Jun 1993.

[138] Scambos, Ted and Fricker, Helen Amanda and Liu, Cheng-chien and Bohlander, Jennifer and Fastook, James and Sargent, Aitbala and Massom, Robert and Wu, An-ming. **Ice shelf disintegration by plate bending and hydro-fracture: satellite observations and model results of the 2008 wilkins ice shelf break-ups**. *Earth and Planetary Science Letters*, **280**(1-4):51–60, Apr 15 2009.

[139] Walter Schüssler and Lutz Nitschke. **Death of fish due to surface water pollution by liquid manure or untreated wastewater: analytical preservation of evidence by hplc**. *Water Research*, **33**(12):2884 – 2887, 1999.

[140] Sormunen, Kai and Ettala, Matti and Rintala, Jukka. **Detailed internal characterisation of two finnish landfills by waste sampling**. *Waste Management*, **28**(1):151–163, 2008.

[141] Ternes, Ta. **Occurrence of drugs in german sewage treatment plants and rivers**. *Water Research*, **32**(11):3245–3260, Nov 1998.

[142] Williams, Gm and Aitkenhead, N. **Lessons from loscoe - the uncontrolled migration of landfill gas**. *Quarterly Journal of Engineering Geology*, **24**(2):191–207, 1991.

[143] Worm, Boris and Barbier, Edward B. and Beaumont, Nicola and Duffy, J. Emmett and Folke, Carl and Halpern, Benjamin S. and Jackson, Jeremy B. C. and Lotze, Heike K. and Micheli, Fiorenza and Palumbi, Stephen R. and Sala, Enric and Selkoe, Kimberley A. and Stachowicz, John J. and Watson, Reg. **Impacts of biodiversity loss on ocean ecosystem services**. *Science*, **314**(5800):787–790, Nov 3 2006.

[144] Zhao, Youcai and Song, Liyan and Huang, Renhua and Song, Lijie and Li, Xiong. **Recycling of aged refuse from a closed landfill**. *Waste Management and Research*, **25**(2):130–138, Apr 2007.

[145] Bjorn P. Zietz and Hermann H. Dieter and Max Lakomek and Heide Schneider and Barabara Kebler-gaedtke and Hartmut Dunkelberg. **Epidemiological investigation on chronic copper toxicity to children exposed via the public drinking water supply**. *The Science of The Total Environment*, **302**(1-3):127 – 144, 2003.

[146] Walker, Kenny and Walsh, Lynda. **"no one yet knows what the ultimate consequences may be": how rachel carson transformed scientific uncertainty into a site for public participation in silent spring**. *Journal of Business and Technical Communication*, **26**(1):3–34, Jan 2012.

[147] Kroll, G. **The "silent springs" of rachel carson: mass media and the origins of modern environmentalism**. *Public Understanding of Science*, **10**(4):403–420, Oct 2001.

[148] R. Carson, E.O. Wilson, and L. Lear. *Silent Spring*. Houghton Mifflin Harcourt, 1962.

[149] Meehl, Ga and Tebaldi, C. **More intense, more frequent, and longer lasting heat waves in the 21st century**. *Science*, **305**(5686):994–997, Aug 13 2004.

[150] Scambos, Ted and Fricker, Helen Amanda and Liu, Cheng-chien and Bohlander, Jennifer and Fastook, James and Sargent, Aitbala and Massom, Robert and Wu, An-ming. **Ice shelf disintegration by plate bending and hydro-fracture: satellite observations and model results of the 2008 wilkins ice shelf break-ups**. *Earth and Planetary Science Letters*, **280**(1-4):51–60, Apr 15 2009.

[151] Foley, Ja and Defries, R and Asner, Gp and Barford, C and Bonan, G and Carpenter, Sr and Chapin, Fs and Coe, Mt and Daily, Gc and Gibbs, Hk and Helkowski, Jh and Holloway, T and Howard, Ea and Kucharik, Cj and Monfreda, C and Patz, Ja and Prentice, Ic and Ramankutty, N and Snyder, Pk. **Global consequences of land use**. *Science*, **309**(5734):570–574, Jul 22 2005.

[152] Thomas, Cd and Cameron, A and Green, Re and Bakkenes, M and Beaumont, Lj and Collingham, Yc and Erasmus, Bfn and De Siqueira, Mf and Grainger, A and Hannah, L and Hughes, L and Huntley, B and Van Jaarsveld, As and Midgley, Gf and Miles, L and Ortega-huerta, Ma and Peterson, At and Phillips, Ol and Williams, Se. **Extinction risk from climate change**. *Nature*, **427**(6970):145–148, Jan 8 2004.

[153] Hooper, Du and Chapin, Fs and Ewel, Jj and Hector, A and Inchausti, P and Lavorel, S and Lawton, Jh and Lodge, Dm and Loreau, M and Naeem, S and Schmid, B and Setala, H and Symstad, Aj and Vandermeer, J and Wardle, Da. **Effects of biodiversity on ecosystem functioning: a consensus of current knowledge**. *Ecological Monographs*, **75**(1):3–35, Feb 2005.

[154] Orr, Jc and Fabry, Vj and Aumont, O and Bopp, L and Doney, Sc and Feely, Ra and Gnanadesikan, A and Gruber, N and Ishida, A and Joos, F and Key, Rm and Lindsay, K and Maier-reimer, E and Matear, R and Monfray, P and Mouchet, A and Najjar, Rg and Plattner, Gk and Rodgers, Kb and Sabine, Cl and Sarmiento, Jl and Schlitzer, R and Slater, Rd and Totterdell, Ij and Weirig, Mf and Yamanaka, Y and Yool, A. **Anthropogenic ocean acidification over the twenty-first century and its impact on calcifying organisms**. *Nature*, **437**(7059):681–686, Sep 29 2005.

[155] Keeling, Cd. **The concentration and isotopic abundances of carbon dioxide in the atmosphere**. *Tellus*, **12**(2):200–203, 1960.

[156] Diamond, D. **Internet-scale sensing**. *Analytical Chemistry*, **76**(15):278A–286A, Aug 1 2004.

[157] Irish Government: Dept. Health. **Health act 2007**. *Irish Statute Book*, 2007.

[158] United Nations Framework Convention on Climate Change. **Kyoto Protocol**.

[159] The European Commission for the Environment. **The EU Water Framework Directive**.

[160] Irish Government. **Environmental Protection Agency Act, 1992**. Online `http://www.irishstatutebook.ie/1992/en/act/pub/0007/index.html`, 1992.

[161] EPA. **EPA List of Approved Laboratories 2009**. Online `http://www.epa.ie/downloads/pubs/water/other/name,30285,en.html`, 2010.

[162] Mr. Darragh Page Conor Clenaghan, Niamh ONeill. **Dangerous Substances Regulations National Implementation Report 2005**. Online, 2005. ISBN 1-84095-204-0.

[163] John Lucey. **Water Quality in Ireland 2007-2008:Key Indicators of the Aquatic Environment**. Online `http://www.epa.ie/downloads/pubs/water/waterqua/name,27541,en.html`, 2009. ISBN 978-1-84095-319-0.

[164] Committee On Challenges For The Chemical Sciences In The 21st Century. **The environment: the environment: challenges for the chemical sciences in the 21st century**. *The National Research Council*, 2003.

[165] Allet, Lara and Knols, Ruud H. and Shirato, Kei and Bruin, Eling D. De. **Wearable systems for monitoring mobility-related activities in chronic disease: a systematic review**. *Sensors*, **10**(10):9026–9052, 2010.

[166] Weschler, C. J. **Chemistry in indoor environments: 20 years of research**. *Indoor Air*, **21**(3):205–218, Jun 2011.

[167] Aboulkassim, Ta and Simoneit, Brt. **Detergents - a review of the nature, chemistry, and behavior in the aquatic environment .1. chemical-composition and analytical techniques**. *Critical Reviews in Environmental Science and Technology*, **23**(4):325–376, 1993.

[168] Ran, Xia and Ma, Li and Peng, Cheng and Zhang, Hong and Qin, Lu-ping. **Ligusticum chuanxiong hort: a review of chemistry and pharmacology**. *Pharmaceutical Biology*, **49**(11):1180–1189, Nov 2011.

[169] Hyde, Robyn M. and Hooker, Paul D. **Chemistry of crime scene investigation: laboratory exercises introducing fundamental principles and instrumentation**. *Abstracts of Papers of The American Chemical Society*, **237**:1, Mar 22 2009.

[170] Manjunath, B. C. and Chandrashekar, B. R. and Mahesh, Melkundi and Rani, R. M. Vatchala. **Dna profiling and forensic dentistry - a review of the recent concepts and trends**. *Journal of Forensic and Legal Medicine*, **18**(5):191–197, Jul 2011.

[171] Chelton, Cf and Glowatz, M and Mosovsky, Ja. **Chemical hazards in the semiconductor industry**. *IEEE Transactions on Education*, **34**(3):269–288, Aug 1991.

[172] Bogue, Robert. **Optical chemical sensors for industrial applications**. *Sensor Review*, **27**(2):86–90, 2007.

[173] Vs Kazakov and Ep Demidchik and Ln Astakhova. **Thyroid cancer after chernobyl**. *Nature*, **359**(6390):21, Sep 3 1992.

[174] Vini G. Khurana and Lennart Hardell and Joris Everaert and Alicja Bortkiewicz and Michael Carlberg and Mikko Ahonen. **Epidemiological evidence for a health risk from mobile phone base stations**. *International Journal of Occupational and Environmental Health*, **16**(3):263–267, Jul-sep 2010. Article.

[175] Manabu Yasuda and Takeshi Hanagiri and Yoshiki Shigematsu and Takamitsu Onitsuka and Kouji Kuroda and Tetsurou Baba and Makiko Mizukami and Yoshinobu Ichiki and Hidetaka Uramoto and Mitsuhiro Takenoyama and Kosei Yasumoto. **Identification of a tumour associated antigen in lung cancer patients with asbestos exposure**. *Anticancer Research*, **30**(7):2631–2639, Jul 2010. Article.

[176] E. Upton and G. Halfacree. *Meet the Raspberry Pi*. Wiley, 2012.

[177] Cliff Wymbs. **Telecommunications, an instrument of radical change for both the 20th and 21st centuries**. *Technological Forecasting and Social Change*, **71**(7):685 – 703, 2004.

[178] Judit Bar-ilan. **Informetrics at the beginning of the 21st century–a review**. *Journal of Informetrics*, **2**(1):1 – 52, 2008.

[179] L. P. Rai and K. Lal. **Indicators of the information revolution**. *Technology in Society*, **22**(2):221 – 235, 2000.

[180] Brand, O. **Microsensor integration into systems-on-chip**. *Proceedings of The IEEE*, **94**(6):1160 –1176, June 2006.

[181] Daniel Stokols, Shalini Misra, Richard P. Moser, Kara L. Hall, and Brandie K. Taylor. **The ecology of team science - Understanding contextual influences on transdisciplinary collaboration**. *American Journal of Preventive Medicine*, **35**(2, S):S96–S115, AUG 2008. NCI Conference on the Science of Team Science - Assessing the Value of Transdiciplinary Resarch, Bethesda, MD, OCT 30-31, 2006.

[182] R.S. Root-Bernstein. *Discovering*. Replica Books, 1997.

[183] A.F. Repko, W.H. Newell, and R. Szostak. *Case Studies in Interdisciplinary Research*. SAGE Publications, 2011.

[184] T.S. Kuhn. *The Structure of Scientific Revolutions*. International encyclopedia of unified science. University of Chicago Press, 1996.

[185] M.a. Carvajal, I.m. Perez De Vargas-sansalvador, A.j. Palma, M.d. Fernandez-ramos, and L.f. Capitan-vallvey. **Hand-held optical instrument for co2 in gas phase based on sensing film coating optoelectronic elements**. *Sensors and Actuators B: Chemical*, **144**(1):232 – 238, 2010.

[186] Samuel C. Hooker. **A rapid colorimetric method for the estimation of nitrates in natural waters**. *Journal of The Franklin Institute*, **127**(1):61 – 62, 1889.

[187] M. Bowden and D. Diamond. **The determination of phosphorus in a microfluidic manifold demonstrating long-term reagent lifetime and chemical stability utilising a colorimetric method**. *Sensors and Actuators B: Chemical*, **90**(1-3):170 – 174, 2003. Proceedings of the 6th European Conference on Optical Chemical Sensors and Biosensors EUROPT(R)ODE VI.

[188] Richard H Schwartz, Regina M O'donnell, Mary Margaret Thorne, Pamela R Getson, and Jocelyn M Hicks. **Evaluation of colorimetric dipstick test to detect alcohol in saliva: a pilot study**. *Annals of Emergency Medicine*, **18**(9):1001 – 1003, 1989.

[189] S. Capel-cuevas, M.P. Cuellar, I. de Orbe-Paya, M.C. Pegalajar, and L.F. Capitan-Vallvey. **Full-range optical ph sensor based on imaging techniques**. *Analytica Chimica Acta*, **681**(1-2):71 – 81, 2010.

[190] Soren Sorensen. **Enzymstudien. ii mitteilung. uber die messung und die bedeutung der wasserstoffionenkoncentration bei enzymatischen prozessen**. *Biochemische Zeitschrift*, **21**:131 – 304, 1909.

[191] I. M. Kolthoff. **Acid-base indicators**. *Macmillan Company: New York*, **1**:106, 1937.

[192] Rollie J. Myers. **One-hundred years of ph**. *Journal of Chemical Education*, **87**(1):30–32, 2010.

[193] Erno Lindner and Robert E. Gyurcsanyi. **Quality control criteria for solid-contact, solvent polymeric membrane ion-selective electrodes**. *Journal of Solid State Electrochemistry*, **13**:51–68, 2009.

[194] Aleksandar Radu, Shane Peper, Eric Bakker, and Dermot Diamond. **Guidelines for improving the lower detection limit of ion-selective electrodes: a systematic approach**. *Electroanalysis*, **19**(2-3):144–154, 2007.

[195] Goce Dimeski, Tony Badrick, and Andrew St John. **Ion selective electrodes (ISEs) and interferences–a review**. *Clinica Chimica Acta*, **411**(5-6):309 – 317, 2010.

[196] Erno Pretsch. **The new wave of ion-selective electrodes**. *Trac Trends in Analytical Chemistry*, **26**(1):46 – 51, 2007.

[197] Walter S. Hughes. **The potential difference between glass and electrolytes in contact with the glass**. *Journal of The American Chemical Society*, **44**(12):2860–2867, 1922.

[198] Wolfgang Gopel and Jay N. Zemel. *Sensors: A Comprehensive Survey*, **1**. Wiley, 2008.

[199] Paul Baran. **On a Distributed Command and Control System Configuration**. *RAND Corporation*, **1**:1, December 1960.

[200] Stewart Brand. **Paul Baran conceived the Internet's architecture at the height of the Cold War.** Online `http://www.wired.com/wired/archive/9.03/baran.html`, 1961.

[201] P Baran. **On Distributed Communications Networks**. *IEEE Transactions On Communications Systems*, **CS12**(1):1, 1964.

[202] E Bassous, HH Taub, and L Kuhn. **Ink Jet Printing Nozzle Arrays Etched In Silicon**. *Applied Physics Letters*, **31**(2):135–137, 1977.

[203] A Manz, N Graber, and HM Widmer. **Miniaturized Total Chemical-analysis Systems - A Novel Concept For Chemical Sensing**. *Sensors and Actuators B-Chemical*, **1**(1-6):244–248, Jan 1990. 5th International Conf On Solid-state Sensors and Actuators and Eurosensors 3 (Transducers 89), Montreux, Switzerland, Jun 25-30, 1989.

[204] DW Dockery, CA Pope, XP Xu, JD Spengler, JH Ware, ME Fay, BG Ferris, and FE Speizer. **An Association Between Air-Pollution and Mortality In 6 United-States Cities**. *New England Journal Of Medicine*, **329**(24):1753–1759, DEC 9 1993.

[205] J. Hakim. *A History of US: Book 9: War, Peace, and All that Jazz*. History of the United States Series. Oxford University Press, 1995.

[206] N. Babaguchi, S. Sasamori, T. Kitahashi, and R. Jains. **Detecting events from continuous media by intermodal collaboration and knowledge use**. In *Multimedia Computing and Systems, 1999. IEEE International Conference on*, **1**, pages 782 –786 vol.1, jul 1999.

[207] K. L. Daly. **Meeting explores sensor technology for remote, interactive aquatic experiments**. *EOS Transactions*, **81**:580–580, 2000.

[208] A. Bonzanini, R. Leonardi, and P. Migliorati. **Event recognition in sport programs using low-level motion indices**. In *Multimedia and Expo, 2001. ICME 2001. IEEE International Conference on*, pages 1005 –1008, aug. 2001.

[209] H. Kawashima and T. Matsuyama. **Integrated event recognition from multiple sources**. In *Pattern Recognition, 2002. Proceedings. 16th International Conference on*, **2**, pages 785 – 789 vol.2, 2002.

[210] Y. Satoh, H. Tanahashi, Caihua Wang, S. Kaneko, Y. Niwa, and K. Yamamoto. **Robust event detection by radial reach filter (RRF)**. In *Pattern Recognition, 2002. Proceedings. 16th International Conference on*, **2**, pages 623 – 626 vol.2, 2002.

[211] Margaret Sequeira, Michaela Bowden, Edel Minogue, and Dermot Diamond. **Towards autonomous environmental monitoring systems**. *Talanta*, **56**(2):355 – 363, 2002.

[212] Xiping Yang, Keat G. Ong, William R. Dreschel, Kefeng Zeng, Casey S. Mungle, and Craig A. Grimes. **Design of a Wireless Sensor Network for Long-term, In-Situ Monitoring of an Aqueous Environment**. *Sensors*, **2**(11):455–472, 2002.

[213] PA Auroux, D Iossifidis, DR Reyes, and A Manz. **Micro total analysis systems. 2. Analytical standard operations and applications**. *Analytical Chemistry*, **74**(12):2637–2652, Jun 15 2002.

[214] DR Reyes, D Iossifidis, PA Auroux, and A Manz. **Micro total analysis systems. 1. Introduction, theory, and technology**. *Analytical Chemistry*, **74**(12):2623–2636, Jun 15 2002.

[215] A Terray, J Oakey, and DWM Marr. **Microfluidic control using colloidal devices**. *Science*, **296**(5574):1841–1844, Jun 7 2002.

[216] P Paik, VK Pamula, MG Pollack, and RB Fair. **Electrowetting-based droplet mixers for microfluidic systems**. *Lab On A Chip*, **3**(1):28–33, 2003.

[217] Jonathan Kiell. **Program for Response Options and Technology Enhancements for Chemical-Biological Terrorism**. Online `http://www.nti.org/e_research/source_docs/us/department_defense/reports/27.pdf`, April 2003.

[218] Somboon Hongeng and Ramakant Nevatia. **Large-scale event detection using semi-hidden Markov models**. In *Computer Vision, 2003. Proceedings. Ninth IEEE International Conference on*, pages 1455 –1462 vol.2, oct. 2003.

[219] Keat G. Ong, Xiping Yang, Niloy Mukherjee, Haidong Wang, Shrawan Surender, and Craig A. Grimes. **A Wireless Sensor Network for Long-term Monitoring of Aquatic Environments: Design and Implementation**. *Sensor Letters*, **2**(1):48–57, 2004.

[220] Haisong Gu and Qiang Ji. **Facial event classification with task oriented dynamic Bayesian network**. In *Computer Vision and Pattern Recognition, 2004. CVPR 2004. Proceedings of the 2004 IEEE Computer Society Conference on*, **2**, pages II–870 – II–875 Vol.2, june-2 july 2004.

[221] Xiao-Feng Tong, Han-Qing Lu, and Qing-Shan Liu. **A three-layer event detection framework and its application in soccer video**. In *Multimedia and Expo, 2004. ICME '04. 2004 IEEE International Conference on*, **3**, pages 1551 –1554 Vol.3, june 2004.

[222] T Vilkner, D Janasek, and A Manz. **Micro total analysis systems. Recent developments**. *Analytical Chemistry*, **76**(12):3373–3385, Jun 15 2004.

[223] M.T. Chan, A. Hoogs, J. Schmiederer, and M. Petersen. **Detecting rare events in video using semantic primitives with HMM**. In *Pattern Recognition, 2004. ICPR 2004. Proceedings of the 17th International Conference on*, **4**, pages 150 – 154 Vol.4, aug. 2004.

[224] S. Reiter and G. Rigoll. **Segmentation and classification of meeting events using multiple classifier fusion and dynamic programming**. In *Pattern Recognition, 2004. ICPR 2004. Proceedings of the 17th International Conference on*, **3**, pages 434 – 437 Vol.3, aug. 2004.

[225] D Diamond. **Internet-scale sensing**. *Analytical Chemistry*, **76**(15):278A–286A, Aug 1 2004.

[226] T Vestad, DWM Marr, and J Oakey. **Flow control for capillary-pumped microfluidic systems**. *Journal Of Micromechanics and Microengineering*, **14**(11):1503–1506, Nov 2004.

[227] Brett Adams and Svetha Venkatesh. **Situated event bootstrapping and capture guidance for automated home movie authoring**. In *Proceedings of the 13th annual ACM international conference on Multimedia*, MULTIMEDIA '05, pages 754–763, New York, NY, USA, 2005. ACM.

[228] Rita Cucchiara. **Multimedia surveillance systems**. In *Proceedings of the third ACM international workshop on Video surveillance & sensor networks*, VSSN '05, pages 3–10, New York, NY, USA, 2005. ACM.

[229] S.N. Sinha and M. Pollefeys. **Synchronization and calibration of a camera network for 3D event reconstruction from live video**. In *Computer Vision and Pattern Recognition, 2005. CVPR 2005. IEEE Computer Society Conference on*, **2**, page 1196 vol. 2, june 2005.

[230] Wen-Nung Lie and Sheng-Hsiung Shia. **Combining Caption and Visual Features for Semantic Event Classification of Baseball Video**. In *Multimedia and Expo, 2005. ICME 2005. IEEE International Conference on*, pages 1254 –1257, july 2005.

[231] C.G.M. Snoek and M. Worring. **Multimedia event-based video indexing using time intervals**. *Multimedia, IEEE Transactions on*, **7**(4):638 – 647, aug. 2005.

[232] P. Smith, N. da Vitoria Lobo, and M. Shah. **TemporalBoost for event recognition**. In *Computer Vision, 2005. ICCV 2005. Tenth IEEE International Conference on*, **1**, pages 733 – 740 Vol. 1, oct. 2005.

[233] SM Uppala, PW Kallberg, AJ Simmons, U Andrae, VD Bechtold, M Fiorino, JK Gibson, J Haseler, A Hernandez, GA Kelly, X Li, K Onogi, S Saarinen, N Sokka, RP Allan, E Andersson, K Arpe, MA Balmaseda, ACM Beljaars, L Van De Berg, J Bidlot, N Bormann, S Caires, F Chevallier, A Dethof, M Dragosavac, M Fisher, M Fuentes, S Hagemann, E Holm, BJ Hoskins, L Isaksen, PAEM Janssen, R Jenne, AP McNally, JF Mahfouf, JJ Morcrette, NA Rayner, RW Saunders, P Simon, A Sterl, KE Trenberth, A Untch, D Vasiljevic, P Viterbo, and J Woollen. **The ERA-40 reanalysis**. *Quarterly Journal of The Royal Meteorological Society*, **131**(612, Part b):2961–3012, OCT 2005.

[234] M.T. Chan, A. Hoogs, Zhaohui Sun, J. Schmiederer, R. Bhotika, and G. Doretto. **Event Recognition with Fragmented Object Tracks**. In *Pattern Recognition, 2006. ICPR 2006. 18th International Conference on*, **1**, pages 412 –416, 0-0 2006.

[235] R Byrne and D Diamond. **Chemo/bio-sensor networks**. *Nature Materials*, **5**(6):421–424, JUN 2006.

[236] PS Dittrich, K Tachikawa, and A Manz. **Micro total analysis systems. Latest advancements and trends**. *Analytical Chemistry*, **78**(12):3887–3907, Jun 15 2006.

[237] A. Fawcett, S. Bernard, G. C. Pitcher, T. A. Probyn, and A. du Randt. **Real-time monitoring of harmful algal blooms in the southern Benguela**. *African Journal of Marine Science*, **28**(2):257–260, SEP 2006. 11th International Conference on Harmful Algae, Cape Town, SOUTH AFRICA, NOV 15-19, 2004.

[238] R. W. Sabnis; S. Sanders; LLP. Dempsey. *Handbook of Acid-Base Indicators*. CRC Press, 2007.

[239] Peng Cui, Li-Feng Sun, Zhi-Qiang Liu, and Shi-Qiang Yang. **A Sequential Monte Carlo Approach to Anomaly Detection in Tracking Visual Events**. In *Computer Vision and Pattern Recognition, 2007. CVPR '07. IEEE Conference on*, pages 1 –8, june 2007.

[240] Ralf D. Prien. **The future of chemical in situ sensors**. *Marine Chemistry*, **107**(3, SI):422–432, DEC 1 2007. 9th International Estuarine Biogeochemistry Symposium, Warnemunde, GERMANY, MAY 07-11, 2006.

[241] Phillip N. Price, Ashok J. Gadgil, and Michael D. Sohn. **Trade-offs between moving and stationary particle collectors for detecting a bio-agent plume**. *Atmospheric Environment*, **41**(38):8818–8824, DEC 2007.

[242] Dermot Diamond, Shirley Coyle, Silvia Scarmagnani, and Jer Hayes. **Wireless Sensor Networks and Chemo-/Biosensing**. *Chemical Reviews*, **108**(2):652–679, 2008. PMID: 18215076.

[243] Guanling Chen, Prabhu Govindaswamy, Nan Li, and Jie Wang. **Continuous camera-based monitoring for assistive environments**. In *Proceedings of the 1st international conference on PErvasive Technologies Related to Assistive Environments*, PETRA '08, pages 31:1–31:8, New York, NY, USA, 2008. ACM.

[244] Jung Ho Kim, K.-T. Lau, C. Fay, and D. Diamond. **Development of optical sensing system for detection of Fe ions using conductive polymer actuator based microfluidic pump**. In *Sensors, 2008 IEEE*, pages 1155–1158, 2008.

[245] Luca Lombroso, Salvatore Quattrocchi, and Giulia Silvestri. **Meteorlogical data fro 2008, 182nd year of meteorlogical measurement in Modena**. *Atti della Societa dei Naturalisti e Matematici di Modena*, **139**:7–44, 2008.

[246] Martina OToole and Dermot Diamond. **Absorbance Based Light Emitting Diode Optical Sensors and Sensing Devices**. *Sensors*, **8**(4):2453–2479, 2008.

[247] S. Pennathur, C. D. Meinhart, and H. T. Soh. **How to exploit the features of microfluidics technology**. *Lab On A Chip*, **8**(1):20–22, 2008.

[248] John Cleary, Conor Slater, Christina McGraw, and Dermot Diamond. **An autonomous microfluidic sensor for phosphate: On-site analysis of treated wastewater**. *IEEE Sensors Journal*, **8**(5-6):508–515, MAY-JUN 2008.

[249] Jonathan West, Marco Becker, Sven Tombrink, and Andreas Manz. **Micro total analysis systems: Latest achievements**. *Analytical Chemistry*, **80**(12):4403–4419, Jun 15 2008.

[250] Raymond Mariella, Jr. **Sample preparation: the weak link in microfluidics-based biodetection**. *Biomedical Microdevices*, **10**(6):777–784, Dec 2008.

[251] Carlos M. S. Figueiredo, Eduardo F. Nakamura, and Antonio A. F. Loureiro. **A Hybrid Adaptive Routing Algorithm for Event-Driven Wireless Sensor Networks**. *Sensors*, **9**(9):7287–7307, 2009.

[252] Vinh Hao Nguyen and Young Soo Suh. **Networked Estimation for Event-Based Sampling Systems with Packet Dropouts**. *Sensors*, **9**(4):3078–3089, 2009.

[253] B. Kumari, M. Raman, and K. Mali. **Locating tuna forage ground through satellite remote sensing**. *International Journal of Remote Sensing*, **30**(22):5977–5988, 2009.

[254] Luis Cadahia, Pascual Lopez-Lopez, Vicente Urios, Alvaro Soutullo, and Juan J. Negro. **Natal dispersal and recruitment of two Bonelli's Eagles Aquila fasciata: a four-year satellite tracking study**. *Acta Ornithologica*, **44**(2):193–198, WIN 2009.

[255] George M. Whitesides. **Solving problems**. *Lab Chip*, **10**:2317–2318, 2010.

[256] Sung-Jib Yim and Yoon-Hwa Choi. **An Adaptive Fault-Tolerant Event Detection Scheme for Wireless Sensor Networks**. *Sensors*, **10**(3):2332–2347, 2010.

[257] C. Slater, J. Cleary, K. T. Lau, D. Snakenborg, B. Corcoran, J. P. Kutter, and D. Diamond. **Validation of a fully autonomous phosphate analyser based on a microfluidic lab-on-a-chip**. *Water Science and Technology*, **61**(7):1811–1818, 2010.

[258] R. W. Murray. **Challenges in Environmental Analytical Chemistry**. *Analytical Chemistry*, **82**(5):1569–1569, Mar 2010.

[259] Nan Li, Bo Yan, Guanling Chen, Prabhu Govindaswamy, and Jie Wang. **Design and implementation of a sensor-based wireless camera system for continuous monitoring in assistive environments**. *Personal Ubiquitous Comput.*, **14**(6):499–510, September 2010.

[260] B. O'Flynn, F. Regan, A. Lawlor, J. Wallace, J. Torres, and C. O'Mathuna. **Experiences and recommendations in deploying a real-time, water quality monitoring system**. *Measurement Science & Technology*, **21**(12):12–1, DEC 2010.

[261] Aiden R. Doherty, Chris J. A. Moulin, and Alan F. Smeaton. **Automatically assisting human memory: A SenseCam browser**. *Memory*, **19**(7):785–795, 2011.

[262] Cormac Fay, Aiden R. Doherty, Stephen Beirne, Fiachra Collins, Colum Foley, John Healy, Breda M. Kiernan, Hyowon Lee, Damien Maher, Dylan Orpen, Thomas Phelan, Zhengwei Qiu,

Kirk Zhang, Cathal Gurrin, Brian Corcoran, Noel E. O'Connor, Alan F. Smeaton, and Dermot Diamond. **Remote Real-Time Monitoring of Subsurface Landfill Gas Migration**. *Sensors*, **11**(7):6603–6628, 2011.

[263] Weiqi Yan, Declan F. Kieran, Setareh Rafatirad, and Ramesh Jain. **A comprehensive study of visual event computing**. *Multimedia Tools Appl.*, **55**(3):443–481, December 2011.

[264] Young-Sook Lee and Wan-Young Chung. **Visual Sensor Based Abnormal Event Detection with Moving Shadow Removal in Home Healthcare Applications**. *Sensors*, **12**(1):573–584, 2012.

[265] Colin S. Reynolds, Stephen C. Maberly, Julie E. Parker, and Mitzi M. De Ville. **Forty years of monitoring water quality in Grasmere (English Lake District): separating the effects of enrichment by treated sewage and hydraulic flushing on phytoplankton ecology**. *Freshwater Biology*, **57**(2):384–399, FEB 2012.

[266] Tetsuya Matsubayashi, Yasuyuki Sawada, and Michiko Ueda. **Natural disasters and suicide: evidence from Japan**. *Social science and medicine*, **82**:126–33, 2013.

[267] Kairi Kolves, Keili E. Kolves, and Diego De Leo. **Natural disasters and suicidal behaviours: A systematic literature review**. *Journal Of Affective Disorders*, **146**(1):1–14, MAR 20 2013.

[268] Sang-Eun Park, Yoshio Yamaguchi, and Duk-jin Kim. **Polarimetric SAR remote sensing of the 2011 Tohoku earthquake using ALOS/PALSAR**. *Remote Sensing of Environment*, **132**:212–220, MAY 15 2013.

[269] Xingzheng Wang, Bob Zhang, Zhenhua Guo, and David Zhang. **Facial image medical analysis system using quantitative chromatic feature**. *Expert Systems With Applications*, **40**(9):3738–3746, JUL 2013.

[270] Kumar S.P. Chong, C.-Y. **Sensor networks: Evolution, opportunities, and challenges**. *Proceedings of the IEEE*, **91**(8):1247–1256, 2003. cited By (since 1996) 932.

[271] Jennifer Yick, Biswanath Mukherjee, and Dipak Ghosal. **Wireless sensor network survey**. *Computer Networks*, **52**(12):2292 – 2330, 2008.

[272] Paolo Baronti, Prashant Pillai, Vince W.C. Chook, Stefano Chessa, Alberto Gotta, and Y. Fun Hu. **Wireless sensor networks:**

A survey on the state of the art and the 802.15.4 and ZigBee standards. *Computer Communications*, **30**(7):1655 – 1695, 2007. Wired/Wireless Internet Communications.

[273] Seth Edward-Austin Hollar. *COTS Dust*. PhD thesis, Massachusetts Institute of Technology, University of California, Berkeley, 2000.

[274] Peter Coy and Neil Gross. **21 Ideas for the 21st Century**. *Business Week*, **Aug 30**:1, 1999.

[275] Johannes Grath, Rob Ward, Andreas Scheidleder, and Philippe Quevauviller. **Report on eu guidance on groundwater monitoring developed under the common implementation strategy of the water framework directive**. *J. Environ. Monit.*, **9**:1162–1175, 2007.

[276] Bw Technologies. **Rig rat iii manual**. *Electronic Measurement Labs Website*, 2013.

[277] **SHOAL Robotic Fish Homepage**. Online (`http://www.roboshoal.com/`), 02 2011.

[278] Kai Song, Qi Liu, and Qi Wang. **Olfaction and hearing based mobile robot navigation for odor/sound source search**. *Sensors*, **11**(2):2129–2154, 2011.

[279] Fw Grasso, Tr Consi, Dc Mountain, and J Atema. **Biomimetic robot lobster performs chemo-orientation in turbulence using a pair of spatially separated sensors: progress and challenges**. *Robotics and Autonomous Systems*, **30**(1-2):115–131, Jan 31 2000.

[280] S Kazadi, R Goodman, D Tsikata, D Green, and H Lin. **An autonomous water vapor plume tracking robot using passive resistive polymer sensors**. *Autonomous Robots*, **9**(2):175–188, Sep 2000.

[281] Y Kuwana and I Shimoyama. **A pheromone-guided mobile robot that behaves like a silkworm moth with living antennae as pheromone sensors**. *International Journal of Robotics Research*, **17**(9):924–933, Sep 1998.

[282] Hiroshi Ishida, Takamichi Nakamoto, and Toyosaka Moriizumi. **Remote sensing of gas/odor source location and concentration distribution using mobile system**. *Sensors and Actuators B: Chemical*, **49**(1-2):52 – 57, 1998.

[283] H. Ishida, A. Kobayashi, T. Nakamoto, and T. Moriizumi. **Three-dimensional odor compass**. *Robotics and Automation, IEEE Transactions On*, **15**(2):251 –257, Apr 1999.

[284] H. Ishida, T. Nakamoto, and T. Moriizumi. **Study of odor compass**. In *Multisensor Fusion and Integration for Intelligent Systems, 1996. IEEE/SICE/RSJ International Conference on*, pages 222 –226, dec 1996.

[285] H Ishida, K Suetsugu, T Nakamoto, and T Moriizumi. **Study of autonomous mobile sensing system for localization of odor source using gas sensors and anemometric sensors**. *Sensors and Actuators A-physical*, **45**(2):153–157, Nov 1994.

[286] Achim J. Lilienthal, Amy Loutfi, and Tom Duckett. **Airborne chemical sensing with mobile robots**. *Sensors*, **6**(11):1616–1678, 2006.

[287] Dermot Diamond, Fiachra Collins, John Cleary, Claudio Zuliani, and Cormac Fay. **Distributed Environmental Monitoring**. In Daniel Filippini, editor, *Autonomous Sensor Networks*, **13** of *Springer Series on Chemical Sensors and Biosensors*, pages 321–363. Springer Berlin Heidelberg, 2013.

[288] Breda M. Kiernan, Stephen Beirne, Cormac Fay, and Dermot Diamond. **Monitoring of gas emissions at landfill sites using autonomous gas sensors**. *Environmental Protection Agency*, **2005-AIC-MS-43-M4**:1–35, 2010.

[289] M Sequeira and D Diamond. **Progress in the realisation of an autonomous environmental monitoring device for ammonia**. *Tractrends in Analytical Chemistry*, **21**(12):816–827, Dec 2002.

[290] Ma Schwarz and Pc Hauser. **Recent developments in detection methods for microfabricated analytical devices**. *Lab on a Chip*, **1**(1):1–6, 2001.

[291] C.m. and Ferguson. **Refrigerated autosampling for the assessment of bacteriological water quality**. *Water Research*, **28**(4):841 – 847, 1994.

[292] Aurore Boscher, Sylvie Gobert, Cédric Guignard, Johanna Ziebel, Lionel L'hoste, Arno C. Gutleb, Henry michel Cauchie, Lucien Hoffmann, and Gérard Schmidt. **Chemical contaminants in fish species from rivers in the north of luxembourg: potential impact on the eurasian otter (lutra lutra)**. *Chemosphere*, **78**(7):785 – 792, 2010.

[293] Angela Yu chen Lin, Sri Chandana Panchangam, and Chao chun Lo. **The impact of semiconductor, electronics and optoelectronic industries on downstream perfluorinated chemical contamination in taiwanese rivers**. *Environmental Pollution*, **157**(4):1365 – 1372,

2009. <ce:title>The Behaviour and Effects of Nanoparticles in the Environment</ce:title>.

[294] Erik Lundberg and Wolfgang Frech. **Direct determination of trace metajls in solid samples by atomic absorption spectrometry with electrothermal atomizers: part 3. application of an autosampler to the determination of silver, bismuth, cadmium and zinc in steels**. *Analytica Chimica Acta*, **108**(0):75 – 85, 1979.

[295] **S & S Onsite Analytical: Mobile Environmental Laboratory**. Online (`http://www.snsonsite.com/`).

[296] WAGTECH. **Customisable Project Vehicles for Environmental Surveys**. Online (`http://www.wagtechprojects.com/mobile-laboratories`).

[297] **The National Environment Management Authority Laboratory**. Online (`http://www.nemaug.org/`).

[298] United States Environmental Protection Agency. **EPA Mobile Laboratory**. Online (`http://www.epa.gov/region6/6lab/mobilelab.htm`).

[299] N. S. Karellas, Q. F. Chen, G. B. De Brou, and R. K. Milburn. **Real time air monitoring of hydrogen chloride and chlorine gas during a chemical fire**. *Journal of Hazardous Materials*, **102**(1):105 – 120, 2003. On-site Analysis.

[300] S M Drachev and S D Zamyslova. **Portable laboratory for water analysis**. *Gigiena I Sanitariia*, **7**:45–8, 1950.

[301] Leanne Marle and Gillian M. Greenway. **Microfluidic devices for environmental monitoring**. *Trac Trends in Analytical Chemistry*, **24**(9):795 – 802, 2005.

[302] Clifford K. Ho, Alex Robinson, David R. Miller, and Mary J. Davis. **Overview of sensors and needs for environmental monitoring**. *Sensors*, **5**(1):4–37, 2005.

[303] Ian J. Allan, Graham A. Mills, Branislav Vrana, Jesper Knutsson, Arne Holmberg, Nathalie Guigues, Serena Laschi, Anne-marie Fouillac, and Richard Greenwood. **Strategic monitoring for the european water framework directive**. *Trac-trends in Analytical Chemistry*, **25**(7):704–715, Jul-aug 2006.

[304] Waikato Regional Council. **Mangakino awarded $30,000 after restorative justice process**. *Info News (Online http://www.infonews.co.nz/news.cfm?id=59727)*, October 2010.

[305] Environment Agency. **Â£74,250 in fines for massive illegal dumping operation**. *EPA UK (Online http://www.environment-agency.gov.uk/news/119506.aspx)*, May 2010.

[306] John Lucey. **Water quality in ireland 2007-2008:key indicators of the aquatic environment**. *Environmental Protection Agency Website*, 2009. ISBN 978-1-84095-319-0.

[307] Epa. **Epa list of approved laboratories 2009**. *Environmental Protection Agency Website (online)*, 2010.

[308] O. Naughton, P.m. Johnston, and L.w. Gill. **Groundwater flooding in irish karst: the hydrological characterisation of ephemeral lakes (turloughs)**. *Journal of Hydrology*, **470 - 471**(0):82 – 97, 2012.

[309] J Dunn, Cd Hall, Mr Heath, Rb Mitchell, and Bj Ritchie. **Aries - a system for concurrent physical, biological and chemical-sampling at sea**. *Deep-sea Research Part I-oceanographic Research Papers*, **40**(4):867–878, Apr 1993.

[310] G Hayden, Hc Milne, Mj Patterson, and Ma Nimmo. **The reproducibility of closed-pouch sweat collection and thermoregulatory responses to exercise-heat stress**. *European Journal of Applied Physiology*, **91**(5-6):748–751, May 2004.

[311] S. Coyle, K.-t. Lau, N. Moyna, D. O'gorman, D. Diamond, F. Di Francesco, D. Costanzo, P. Salvo, M.g. Trivella, D.e. De Rossi, N. Taccini, R. Paradiso, J.-a. Porchet, A. Ridolfi, J. Luprano, C. Chuzel, T. Lanier, F. Revol-cavalier, S. Schoumacker, V. Mourier, I. Chartier, R. Convert, H. De-moncuit, and C. Bini. **Biotex biosensing textiles for personalised healthcare management**. *Information Technology in Biomedicine, IEEE Transactions On*, **14**(2):364–370, 2010.

[312] Sm Shirreffs and Rj Maughan. **Whole body sweat collection in humans: an improved method with preliminary data on electrolyte content**. *Journal of Applied Physiology*, **82**(1):336–341, Jan 1997.

[313] A. G. R. Whitehouse. **The dissolved constituents of human sweat**. *Proceedings of The Royal Society of London. Series B - Biological Sciences*, **117**(803):139–154, 1935.

[314] C.T. Hager and S.F. Midkiff. **An analysis of Bluetooth security vulnerabilities**. In *Wireless Communications and Networking, 2003. WCNC 2003. 2003 IEEE*, **3**, pages 1825–1831 vol.3, 2003.

[315] R. Bouhenguel, I. Mahgoub, and M. Ilyas. **Bluetooth Security in Wearable Computing Applications**. In *High Capacity Optical Networks and Enabling Technologies, 2008. HONET 2008. International Symposium on*, pages 182–186, 2008.

[316] J.a. Paradiso and T. Starner. **Energy scavenging for mobile and wireless electronics**. *Pervasive Computing, IEEE*, **4**(1):18–27, 2005.

[317] G. Magenes, D. Curone, L. Caldani, and E.L. Secco. **Fire fighters and rescuers monitoring through wearable sensors: The ProeTEX project**. In *Engineering in Medicine and Biology Society (EMBC), 2010 Annual International Conference of the IEEE*, pages 3594–3597, 2010.

[318] D. Curone, E.l. Secco, A. Tognetti, G. Loriga, G. Dudnik, M. Risatti, R. Whyte, A. Bonfiglio, and G. Magenes. **Smart garments for emergency operators: the proetex project**. *Information Technology in Biomedicine, IEEE Transactions On*, **14**(3):694–701, 2010.

[319] C.w. Mundt, K.n. Montgomery, U.e. Udoh, V.n. Barker, G.c. Thonier, A.m. Tellier, R.d. Ricks, B.b. Darling, Y.d. Cagle, N.a. Cabrol, S.j. Ruoss, J.l. Swain, J.w. Hines, and G.t.a. Kovacs. **A multiparameter wearable physiologic monitoring system for space and terrestrial applications**. *Information Technology in Biomedicine, IEEE Transactions On*, **9**(3):382–391, 2005.

[320] Jia-Ren Chang Chien and Cheng-Chi Tai. **A New Wireless-Type Physiological Signal Measuring System Using a PDA and the Bluetooth Technology**. In *Industrial Technology, 2006. ICIT 2006. IEEE International Conference on*, pages 3026–3031, 2006.

[321] Michael Sung, Carl Marci, and Alex Pentland. **Wearable feedback systems for rehabilitation**. *Journal of Neuroengineering and Rehabilitation*, **2**(17), 2005.

[322] G. Troster. **2005 the agenda of wearable healthcare, g tröster - imia_yearbook_05**. January 2005.

[323] J. Govil and J. Govil. **4G Mobile Communication Systems: Turns, Trends and Transition**. In *Convergence Information Technology, 2007. International Conference on*, pages 13–18, 2007.

[324] Alexandros Pantelopoulos and Nikolaos Bourbakis. **A survey on wearable biosensor systems for health monitoring**. In *Engineering in Medicine and Biology Society, 2008. EMBS 2008. 30th Annual International Conference of the IEEE*, pages 4887 –4890, aug. 2008.

[325] Yang Hao and Robert Foster. **Wireless body sensor networks for health-monitoring applications**. *Physiological Measurement*, **29**(11):R27–R56, Nov 2008.

[326] Paul Yager, Gonzalo J. Domingo, and John Gerdes. **Point-of-care diagnostics for global health**. *Annual Review of Biomedical Engineering*, **10**:107–144, 2008.

[327] Shyamal Patel, Hyung Park, Paolo Bonato, Leighton Chan, and Mary Rodgers. **A review of wearable sensors and systems with application in rehabilitation**. *Journal of Neuroengineering and Rehabilitation*, **9**:1–12, Apr 20 2012.

[328] A. Pantelopoulos and N.g. Bourbakis. **A survey on wearable sensor-based systems for health monitoring and prognosis**. *Systems, Man, and Cybernetics, Part C: Applications and Reviews, IEEE Transactions On*, **40**(1):1–12, 2010.

[329] Sabine Koch. **Home telehealth - current state and future trends**. *International Journal of Medical Informatics*, **75**(8):565–576, Aug 2006.

[330] O. Brand. **Microsensor integration into systems-on-chip**. *Proceedings of The IEEE*, **94**(6):1160 –1176, June 2006.

[331] International Solid State Circuits (ISSC). **ISSCC 2011 Trends Report**. Technical report, Solid State Circuits Society, 2011.

[332] G. Yang. *Body sensor networks*. Springer-Verlag London Limited, 2006.

[333] William L. Marshall and E. U. Franck. **Ion product of water substance, 0–1000 [degree]c, 1–10,000 bars new international formulation and its background**. *Journal of Physical and Chemical Reference Data*, **10**(2):295–304, 1981.

[334] Danny Pascale. **A reveiw of rgb color spaces**. *The Babelcolor Company*, 2003.

[335] Alvy Ray Smith. **Color gamut transform pairs**. In *SIGGRAPH '78: Proceedings of the 5th annual conference on Computer graphics and interactive techniques*, pages 12–19, New York, NY, USA, 1978. ACM.

[336] A. Lapresta-fernandez, R. Huertas, M. Melgosa, and L. Capitan-vallvey. **Colourimetric characterisation of disposable optical sensors from spectroradiometric measurements**. *Analytical and Bioanalytical Chemistry*, **393**:1361–1366, 2009. 10.1007/s00216-008-2552-4.

[337] Erenas M.m.a De Orbe-paya I.b Capitan-vallvey L.f.b Cantrell, K.a. **Use of the hue parameter of the hue, saturation, value color space as a quantitative analytical parameter for bitonal optical sensors**. *Analytical Chemistry*, **82**(2):531–542, 2010. cited By (since 1996) 11.

[338] S. Capel-Cuevas, MP Cuellar, I. de Orbe-Paya, MC Pegalajar, and LF. Capitan-Vallvey. **Full-range optical ph sensor based on imaging techniques**. *Analytica Chimica Acta*, **681**(1-2):71 – 81, 2010.

[339] Capitan-vallvey L.f. Lapresta-fernandez, A. **Multi-ion detection by one-shot optical sensors using a colour digital photographic camera**. *Analyst*, **136**(19):3917–3926, 2011. cited By (since 1996) 0.

[340] Capitan-vallvey L.f. Lapresta-fernandez, A. **Environmental monitoring using a conventional photographic digital camera for multianalyte disposable optical sensors**. *Analytica Chimica Acta*, **706**:328–37, 2011. cited By (since 1996) 0; Article in Press.

[341] Erenas M.m.b Marinetto E.d.a Abad C.a.a De Orbe-paya I.b Palma A.j.a Capitan-vallvey L.f.b Garcia, A. **Mobile phone platform as portable chemical analyzer**. *Sensors and Actuators B: Chemical*, **156**(1):350–359, 2011. cited By (since 1996) 0.

[342] Phillips S.t.a Carrilho E.a B Thomas Iii S.w.a Sindi H.a Whitesides G.m.a Martinez, A.w.a. **Simple telemedicine for developing regions: camera phones and paper-based microfluidic devices for real-time, off-site diagnosis**. *Analytical Chemistry*, **80**(10):3699–3707, 2008. cited By (since 1996) 130.

[343] Lundstrom I. Filippini, D. **Measurement strategy and instrumental performance of a computer screen photo-assisted technique for the evaluation of a multi-parameter colorimetric test strip**. *Analyst*, **131**(1):111–117, 2006. cited By (since 1996) 14.

[344] Capitan-vallvey L.f. Lapresta-fernandez, A. **Scanometric potassium determination with ionophore-based disposable sensors**. *Sensors and Actuators B: Chemical*, **134**(2):694–701, 2008. cited By (since 1996) 8.

[345] Hart M.b Jarelov A.a Kuhn I.a Mckenzie D.c Mollby R.a Gabrielson, J.a. **Evaluation of redox indicators and the use of digital scanners and spectrophotometer for quantification of microbial growth in microplates**. *Journal of Microbiological Methods*, **50**(1):63–73, 2002. cited By (since 1996) 43.

[346] Ponder J.b. Bailey D.p. Ingison C.k. Suslick K.s. Janzen, M.c. **Colorimetric sensor arrays for volatile organic compounds**. *Analytical Chemistry*, **78**(11):3591–3600, 2006. cited By (since 1996) 86.

[347] Suslick K.s. Zhang, C. **A colorimetric sensor array for organics in water**. *Journal of The American Chemical Society*, **127**(33):11548–11549, 2005. cited By (since 1996) 98.

[348] Mansourian M.b Ravaee F.b Kompany-zareh, M.a. **Simple method for colorimetric spot-test quantitative analysis of fe(iii) using a computer controlled hand-scanner**. *Analytica Chimica Acta*, **471**(1):97–104, 2002. cited By (since 1996) 21.

[349] Hq He, Gx Xu, Xs Ye, and P Wang. **A novel chemical image sensor consisting of integrated microsensor array chips and pattern recognition**. *Measurement Science & Technology*, **14**(7):1040–1046, Jul 2003.

[350] Adrian Goodey, John J. Lavigne, Steve M. Savoy, Marc D. Rodriguez, Theodore Curey, Andrew Tsao, Glen Simmons, John Wright, Seung-jin Yoo, Youngsoo Sohn, Eric V. Anslyn, Jason B. Shear, Dean P. Neikirk, and John T. Mcdevitt. **Development of multianalyte sensor arrays composed of chemically derivatized polymeric microspheres localized in micromachined cavities**. *Journal of The American Chemical Society*, **123**(11):2559–2570, 2001.

[351] Matthias I. J. Stich, Sergey M. Borisov, Ulrich Henne, and Michael Schaeferling. **Read-out of multiple optical chemical sensors by means of digital color cameras**. *Sensors and Actuators B: Chemical*, **139**(1):204–207, May 20 2009. Pt: J; Nr: 25; Tc: 0; J9: Sensor Actuator B-Chem; Si: Sp. Iss. Si; Pg: 4; Ga: 450Vo; Ut: Isi:000266429400033.

[352] A. Safavi, N. Maleki, A. Rostamzadeh, and S. Maesum. **Ccd camera full range ph sensor array**. *Talanta*, **71**(1):498–501, Jan 15 2007.

[353] L Byrne, Kt Lau, and D Diamond. **Development of ph sensitive films for monitoring spoilage volatiles released into packaged fish headspace**. *Irish Journal of Agricultural and Food Research*, **42**(1):119–129, Jun 2003.

[354] L Byrne, J Barker, G Pennarun-thomas, D Diamond, and S Edwards. **Digital imaging as a detector for generic analytical measurements**. *Trac-trends in Analytical Chemistry*, **19**(8):517–522, Aug 2000.

[355] Hamels S.a Dufour S.a Collet J.a Zammatteo N.a De Longueville F.a Gala J.-l.b Remacle J.b Alexandre, I.a. **Colorimetric silver detection of dna microarrays**. *Analytical Biochemistry*, **295**(1):1–8, 2001. cited By (since 1996) 111.

[356] K Sawada, S Mimura, K Tomita, T Nakanishi, H Tanabe, M Ishida, and T Ando. **Novel ccd-based ph imaging sensor**. *IEEE Transactions on Electron Devices*, **46**(9):1846–1849, Sep 1999.

[357] Steven M. Barnard and David R. Walt. **A fibre-optic chemical sensor with discrete sensing sites**. *Nature*, **353**(6342):338–340, September 1991.

[358] Paul V Lambeck. **Integrated optical sensors for the chemical domain**. *Measurement Science and Technology*, **17**(8):R93, 2006.

[359] Jie Lin. **Recent development and applications of optical and fiber-optic ph sensors**. *Trac Trends in Analytical Chemistry*, **19**(9):541 – 552, 2000.

[360] Colette Mcdonagh, Conor S. Burke, and Brian D. Maccraith. **Optical chemical sensors**. *Chemical Reviews*, **108**(2):400–422, 2008. PMID: 18229950.

[361] C. Reichardt. **Solvatochromism, thermochromism, piezochromism, halochromism, and chiro-solvatochromism of pyridinium n-phenoxide betaine dyes**. *Chem. Soc. Rev.*, **21**:147–153, 1992.

[362] C. Reichardt. *Solvents and Solvent Effects in Organic Chemistry*. Wiley, 2006.

[363] Kazuo Hosokawa, Kotaro Hanada, and Ryutaro Maeda. **A polydimethylsiloxane (pdms) deformable diffraction grating for monitoring of local pressure in microfluidic devices**. *Journal of Micromechanics and Microengineering*, **12**(1):1, 2002.

[364] L. Holzer, F. P. Wenzl, S. Tasch, G. Leising, B. Winkler, L. Dai, and A. W. H. Mau. **Ionochromism in a light-emitting electrochemical cell with low response time based on an ionic conductive polyphenylene vinylene**. *Applied Physics Letters*, **75**(14):2014–2016, 1999.

[365] Sandra P. Zanotto, Marivania Scremin, Clodoaldo Machado, and Marcos Caroli Rezende. **Cationic and anionic halochromism**. *Journal of Physical Organic Chemistry*, **6**(11):637–641, 1993.

[366] M. Irie. **Photochromism memories and switches - introduction**. *Chemical Reviews*, **100**(5):1683–1684, 2000.

[367] Roger J. Mortimer. **Electrochromic materials**. *Annual Review of Materials Research*, **41**(241-268), 2011.

[368] A. Seebotn, D. Lötzsch, and Rapra Technology Limited. *Thermochromic phenomena in polymers*. Smithers Rapra Updates Series. iSmithers Rapra Publishing, 2008.

[369] Stephen W James, Ralph P Tatam, Stephen R Fuller, and Colin Crompton. **Monitoring transient strains on a gun barrel using fibre bragg-grating sensors**. *Measurement Science and Technology*, **10**(2):63, 1999.

[370] M J O'dwyer, G M Maistros, S W James, R P Tatam, and I K Partridge. **Relating the state of cure to the real-time internal strain development in a curing composite using in-fibre bragg gratings and dielectric sensors**. *Measurement Science and Technology*, **9**(8):1153, 1998.

[371] C. C. Ye, S. W. James, and R. P. Tatam. **Simultaneous temperature and bend sensing with long-period fiber gratings**. *Opt. Lett.*, **25**(14):1007–1009, Jul 2000.

[372] S.w. James, M.l. Dockney, and R.p. Tatam. **Simultaneous independent temperature and strain measurement using in-fibre bragg grating sensors**. *Electronics Letters*, **32**(12):1133–1134, 1996.

[373] Martin J. Tovée. *An Introduction to the Visual System*. Cambridge University Press, 1996.

[374] Semir Zeki. *A Vision of the Brain*. Blackwell Scientific Publications, 1993.

[375] Wb Marks, Ef Macnichol, and Wh Dobelle. **Visual pigments of single primate cones**. *Science*, **143**(361):1181–&, 1964.

[376] Pk Brown and G Wald. **Visual pigments in single rods + cones of human retina - direct measurements reveal mechanisms of human night + color vision**. *Science*, **144**(361):45–&, 1964.

[377] Frank Roeck, Nicolae Barsan, and Udo Weimar. **Electronic nose: current status and future trends**. *Chemical Reviews*, **108**(2):705–725, Feb 2008.

[378] Dj Strike, Mgh Meijerink, and M Koudelka-hep. **Electronic noses - a mini-review**. *Fresenius Journal of Analytical Chemistry*, **364**(6):499–505, Jul 1999.

[379] JW Gardner and PN Bartlett. **A brief-history of electronic noses**. *Sensors and Actuators B: Chemical*, **18**(1-3):211–220, Mar 1994. Eurosensors VII, Budapest, Hungary, Sep 26-29, 1993.

[380] Jw Gardner, M Craven, C Dow, and El Hines. **The prediction of bacteria type and culture growth phase by an electronic nose with a multi-layer perceptron network**. *Measurement Science & Technology*, **9**(1):120–127, Jan 1998.

[381] Tc Pearce, Jw Gardner, S Friel, Pn Bartlett, and N Blair. **Electronic nose for monitoring the flavor of beers**. *Analyst*, **118**(4):371–377, Apr 1993. Symp on Sensors and Signals, At The 1992 Autumn Meeting Of The Royal Soc of Chemistry, Trinity Coll, Dublin, Ireland, Sep 16-18, 1992.

[382] S Ampuero and Jo Bosset. **The electronic nose applied to dairy products: a review**. *Sensors and Actuators B: Chemical*, **94**(1):1–12, Aug 15 2003.

[383] Jw Gardner, Hv Shurmer, and Tt Tan. **Application of an electronic nose to the discrimination of coffees**. *Sensors and Actuators B: Chemical*, **6**(1-3):71–75, Jan 1992. Eurosensors 5 Conf, Rome, Italy, Sep 30-Oct 01, 1991.

[384] K Persaud and G Dodd. **Analysis of discrimination mechanisms in the mammalian olfactory system using a model nose**. *Nature*, **299**(5881):352–355, 1982.

[385] R. W. Moncrieff. **An instrument for measuring and classifying odors**. *Journal of Applied Physiology*, **16**(4):742–749, 1961.

[386] D.A. Bernstein, Houghton Mifflin College Division, P.W. Nash, A. Clarke-Stewart, L.A. Penner, and E.J. Roy. *Essentials Of Psychology*. Houghton Mifflin, 2007.

[387] Wolfgang Gopel. **Chemical imaging: i. concepts and visions for electronic and bioelectronic noses**. *Sensors and Actuators B: Chemical*, **52**(1-2):125 – 142, 1998.

[388] Martina O'Toole. *Novel integrated paired emitter-detector diode flow analysis system*. PhD thesis, School of Chemical Sciences, Dublin City University, Ireland., August 2007.

[389] Frances Kernodle Associates. **Synopsis: Chemical and Biological Agent Detection Systems —- Pilot Programs in Washington, D.C. and Boston Transit**. Online (http://www.fkassociates.com/Chemical

[390] Anthony J. Policastro and Susanna P. Gordon. **The Use Of Technology In Preparing Subway Systems For Chemical/Biological Terrorism**. *American Public Transport Association*, pages 1–9, 1999.

[391] Michael Stokes, Matthew Anderson, Srinivasan Chandrasekar, and Ricardo Motta. **A Standard Default Color Space for the Internet - sRGB**. *W3*, 1996.

2

Remote Real-Time Monitoring of Subsurface Landfill Gas Migration

"The packaging for a microwavable 'microwave' dinner is programmed for a shelf life of maybe six months, a cook time of two minutes and a landfill dead-time of centuries."

— David Wann, Buzzworm, November 1990

THE COST OF MONITORING greenhouse gas emissions from landfill sites is of major concern for regulatory authorities. The current monitoring procedure is recognised as labour intensive, requiring agency inspectors to physically travel to perimeter borehole wells in rough terrain, and manually measure gas concentration levels with expensive hand-held instrumentation. In this article we present a cost-effective and efficient system for remotely monitoring landfill subsurface migration of methane and carbon dioxide concentration levels. Based purely on an autonomous sensing architecture, the proposed sensing platform was capable of performing complex analytical measurements *in situ* and successfully communicating the data remotely to a cloud database. A web tool was developed to present the sensed data to relevant stakeholders. We report our experiences in deploying such an approach in the field over a period of approximately 16 months.

Preamble

This study investigates the design, development, and deployment of an autonomous device[1] capable of analysing the major constituents of landfill gas (CO_2 and CH_4) emissions from landfill sites. The first hypothesis examined within this study is in the application of a non-invasive optical sensing method for environmental gas monitoring. While other chemical detector types are difficult/troublesome - e.g. reagent-based (requiring replemensihment and disposal of solutions), pellistor (explosive with the LEL of methane), or electrochemical (prone to drift and has a low shelf life) - IR absorption is better suited to the conditions of landfill sites. This is examined in a practical scenario with the information related to the local chemistry harvested, transmitted, and displayed in an end-to-end fashion. This sudy also serves as an example for examining the underlying requirements for developing such a chemcial sensing system. It will provide a grounds for comparing this model with the model based on digital imagery explored in subsequent chapters. Thus examining the second hypothesis within this thesis. Supporing information to this study is presented in Appendix A and will be referenced explicity for the remainder of this preamble.

Sampling Frequency

A number of facors ultimately impact the chosen sampling frequency of a deployed battery-powered autonomous sensing system. In this case a 12 hour sampling period was chosen for three main reasons. The first was to initially investigate the system's main function, i.e. to perform autonomous measurements at a problematic borehole (location A). Daily measurements were necessary at the time and were being taken manually by the site manager; the desire was to automate this process. However, a higher sampling frequency of twice per day was possible due to data analysis when understanding the relationship between sampling frequency and operational lifetime, see Section A.7. The findings were that a 12-hour sampling period allowed for a comprimise between maximissing the sampling frequency while minimising the efforts/costs involved in maintaining the system (battery changes); this predicted a lifetime of ca. 4.5 weeks. It also for teh possibility for measurements to be taken periodically at night, which have never been investigated previously. Furthermore, this time period allowed site personnell to traverse the landfill on their regular monthly visits to each borehole well and change the battery *en route*. Subsequent to this, and as the data were being gathered, variation between the noon and night measurements were observed within the data. Possible reasons for this were site activity, temperature, weather, etc. To investigate this further the sampling frequency was

[1]Please note that the device described in this paper is a progression of two previously developed prototypes, of which publications describing these and related studies can be found in [66, 64] for background information.

increased to measure every 6 hours. Overall, based on the data gathered during this study, it is unclear if a single governing sampling frequency is sufficient for monitoring all landfill sites as there are vast number of factors effecting the rate of landfill gas migration. However, the data has allowed for this question to be raised over the current sampling frequency of once per month. This is one reason for exploring an adaptive sampling regeime, which is discuseed in 2.4.7.2.

System Validation

Validation of the system has followed well established protocols for landfill monitoring technology by the governing authorities. For instance, it is recommended that smilar technology to the device presented in this chapter be recalibrated every 6 months [392]. For this reason, the deployments listed in this chapter never exceeded that duration, i.e. with an aim to check/verify the calibration of each system before subsequent redeployment. Section A.8 in Appendix A provides a discussion realted to recalibration and/or calibration checks of each of the 3 systems. The findings show that the calibration parameters are similar when considering each system, indicating that there is high reliability in the data for long term deployments.

Contributions

- To the Field
  - Novel technology for remote measurements of landfill gas constituients;
  - New information generated - in the spatial and temporal domains, and across multiple sites;
  - Findings show that events are missed using the current sensing model and indicates that a change in the practise is needed;
- By Candidate
  - Design - Sourcing of components, conceptual design, early bread-board/proto-board based implementation;
  - Development - System integration: electrical, electronic, mechanical, embedded programming, control regeime;
  - Deployment(s) - Initial system preparation, troubleshooting on site (esp. non-standard borehole wells);
  - Sampling Methodology - Recycling method for reducing emissions;
  - Communications - Packet structure, transmission, reception (basestation program design/development);

  - Maintenance - Ongoing system repair, data management, integration to online visualisation page;

- By Others
  - Doherty, A. - Online visualisations development and optimisation of sampling times;
  - Beirne, S. - System construction support;
  - Kiernan, B. - Administration and chemical sensor calibration;

2.1 Introduction

2.1.1 Global Environment

Global warming is recognised as a serious worldwide challenge. The Intergovernmental Panel on Climate Change (IPCC) fourth report (IPCC WG1 AR4 Report) states that the warming of our climate is evident and that human activities are very likely the cause through the emission of substantial amounts of greenhouse gases into the atmosphere [409]. It is predicted that the global mean temperature will show an increasing trend and result in rising sea levels, extreme weather conditions and have a negative impact on ecosystems. Consequently, governing bodies have established international (IPCC) and national systems to deal with this situation including the Office of Climate Change (UK), Heritage Council, Climate Control (Ireland), Department of Climate Change (Australia), etc.

One of the most commonly referred to elements within this discussion is the role of carbon emissions, and in particular the role of Carbon Dioxide (CO_2) i.e. one of the major contributing greenhouse gases. Many governments have produced policy documents and targets related to reducing CO_2 emissions over the coming years with one of the most ambitious targets set by the European Union's "20-20-20" target where the aim is to reduce the 2020 CO_2 emissions by 20% from the 1990 levels, through a 20% reduction of energy consumption and a 20% increase in renewable energy sources [406]. The environment is not, any more, just a backdrop in our society but a bedrock of our future so its important that new technologies have a strong awareness of their potential to help us better manage it.

Greenhouse gas emissions are caused by human activities including burning of fossil fuels such as coal. Ultimately these are controlled by large macro-societal organisations including governments, local authorities, and large corporations, and cover activities such as city street lighting, large factories, power generation stations, landfill waste sites, etc.

There are three main sources of energy that generate high quantities of gases such as CO_2 to the environment, namely electricity, thermal, and transport. The form of energy we immediately think of is electricity which was responsible for approximately 31% of CO_2 emissions in Ireland in 2008, however thermal forms of energy in that country were responsible for approximately 33% of CO_2 emissions. Of most concern is the fact that the largest contributor to energy-related CO_2 emissions was from the transport domain, with 36% of CO_2 emissions, representing a growth of 177% over the period of 1990-2008 in Ireland [408].

2.1.2 Landfill Emissions and the Current Monitoring Standard

Waste activities accounts for approximately 5% of the global greenhouse gas (GHG) emissions and of all the waste management methods in use, land-filling is by far the most common [417, 421]. The major components of landfill gas (LFG) are typically methane (CH_4: 40-60%) from the decomposition of biodegradable waste and carbon dioxide (CO_2: 40-60%) from waste water decomposition [410, 397].

Following decomposition of the waste, landfill gas generation can begin as early as 6-12 months after capping and typically continues for a further 20-50 years [393] and even as long as several hundred years in some cases [396]. The waste license to landfill sites, from the U.K. and Ireland Environmental Protection Agencies, state that concentration levels (measured from perimeter borehole wells) must not exceed 1% for methane and 1.5% for carbon dioxide [424].

Arising from legislative enforcement, emission levels from landfill sites require continuous monitoring [426]. Monitoring is required to take place at an average frequency of once per month - and can even be as infrequent as 4 times per year - by extracting from the top of perimeter borehole wells, for a duration of approximately one minute, using a hand-held gas analyser. Subsequently, these levels are manually reported to national environmental protection agencies by the license holders via email/phone. If in breach of permitted gas concentration limits, fines are levied. However, a real threat exists whereby reported emissions to regulating authorities can easily be manipulated to show a more favorable result to avoid non compliance penalties. Furthermore, governing inspectors perform sporadic monitoring of landfill sites if reported results are in doubt. Again, this process is vulnerable to manipulation because inspectors must announce their visits beforehand, allowing for the possibility of high concentration gasses to be vented to atmosphere prior to inspection.

2.1.3 Chemical Sensing and Information Retrieval from the Environment

It is well established that hazardous substances have a negative effect on human/animal health as well as on our environment. Substances such as concentrated pH levels, high phosphate levels, asbestos, radiation, bio/warfare agents, etc., have been known to cause crop failures, affect drinking waters, respiratory diseases, cancer, etc. [394, 432, 411, 412]. Our natural sensing capabilities are limited and only allows us to observe the after effects of what these substances ultimately cause. Before the prevention of such matters, one must first ascertain identification. With the ability to harvest chemical information from our environment one can effectively provide the means to enforce preventative measures and/or to provide early warn-

ing systems. Hence, chemical sensing is on the increase and encouraged by local and global governmental legislation such as: the Water Framework Directive [427], Kyoto protocol [429], Climate Change Act [401], and the Global Warming Solutions Act (California) [398].

However, this requirement of effectively deploying target specific chemical sensing methods is not trivial due to the many problems of integrating chemical sensors into practical, long term sensing platforms [395]. For instance, to realise a fully functional chemical sensing system, the designers must face a multitude of multidisciplinary issues such as: reduction of the sensing surface, drift, cross sensitivity, bio-fouling, chemo-electronic transducer, power consumption, elemental robustness, security, vandalism/damage, autonomous control, successful and secure delivery of data to stakeholders/authorities, etc.

The concept of Internet Scale Sensing (ISS) for chemical sensing was first introduced by Diamond [402] where he explained that although new and emerging technologies from the digital and physical worlds continue to progress, a critical missing element is 'the gateway' linking these two realms. One of our aims has been to progress chemical sensing from its fundamental levels to autonomous information retrieval via the world-wide-web by addressing key integration issues and providing suitable, reliable, and robust gateways for a variety of target chemical species. In light of increased environmental awareness of late, coupled with the necessity for reducing carbon emissions to our atmosphere, we have recently focused our attention on hazardous chemical sensing in gas phase [423] and techniques for reducing one's carbon footprint [403].

In addition, an ultimate goal for autonomous environmental monitoring is in providing the ability to easily access that data. The advent of the "cloud computing" vision is quite apt nowadays, where data should be stored on a server which is always available via the Internet. This data should then be available across a wide variety of computing/software platforms e.g. Internet browsers, iPhones, iPads, smartphones, etc.

The final vital ingredient behind our vision was in turning the masses of raw sensor data into meaningful information. We believed that this process will be achieved via intelligent signal processing with event detection models (e.g. by Doherty *et al.* [404]). After those events have been identified, software outlier detection algorithms should then be employed to identify the events of most interest to be alerted to the relevant stakeholder(s).

2.1.4 Chemical Sensing of Greenhouse Gases from Landfill Sites

It is clear that the current landfill emission monitoring standard is labour intensive, time consuming, requires users to work in harsh environments, and data that are re-

layed back to enforcement agencies are not fully reliable. In addition, serious health issues have been linked to landfill site proximity [430, 418, 431, 405]. Consequently, an automated monitoring technique is essential for reducing the manual costs, diminish the cumbersome task, improve the reliability of the gas concentration levels reported to governing authorities, and ultimately provide a means to end excessive GHG emissions to our atmosphere as well as reducing health issues.

Our research centre ethos involves the implementation of a close collaborative, multidisciplinary environment where expertise from the chemical, engineering and computer science worlds are applied to successfully solving real worlds problems. In recent years we have made breakthroughs in new sensing techniques [407, 420, 428, 422] with the development of autonomous systems capable of performing complex, *in-situ*, chemo-analytical measurements of our environment [425, 400, 413].

In this paper we apply the template of internet scale sensing and offer a proof of principle, realised, end-to-end sensing model for landfill emission monitoring. Specifically, we describe the gateway platform (Section 2.2), show approximately one year of harvested data from an extended *in-situ* trial on an active landfill site (Section 2.4.3) and finally, we describe potential improvements which can be implemented from this development phase to reduce cost, improve efficiency, increase in-situ lifetime, etc. (Section 2.4.6).

2.2 Internet Scale Sensing for Landfill Emission Monitoring

2.2.1 Sensing Model

To achieve the goal of a long term deployment based on an autonomous sensing model, the concept of internet scale sensing (ISS) was employed and expanded to suit a realised sensing model for real-time landfill migration monitoring via a live web-site.

Figure 2.1 on page 83 provides a visual representation of our end-to-end sensing model. Firstly, the physical/chemical gas sensors are exposed to the sample landfill gas and generate an electrical signal that can be related to the concentration of the target gases in the sample. These signal lines are conditioned by the gateway platform and digitised by the system's micro-controller. At this point, the sensor data are stored on-board and transmitted via the GSM network to a base station where the data are then forwarded to a web-enabled sensor network server. After storage on a relational database, the data are visually presented to web users and governing authorities by means of an easy to interpret web page. The following sections gives a more detailed explanation of these processes.

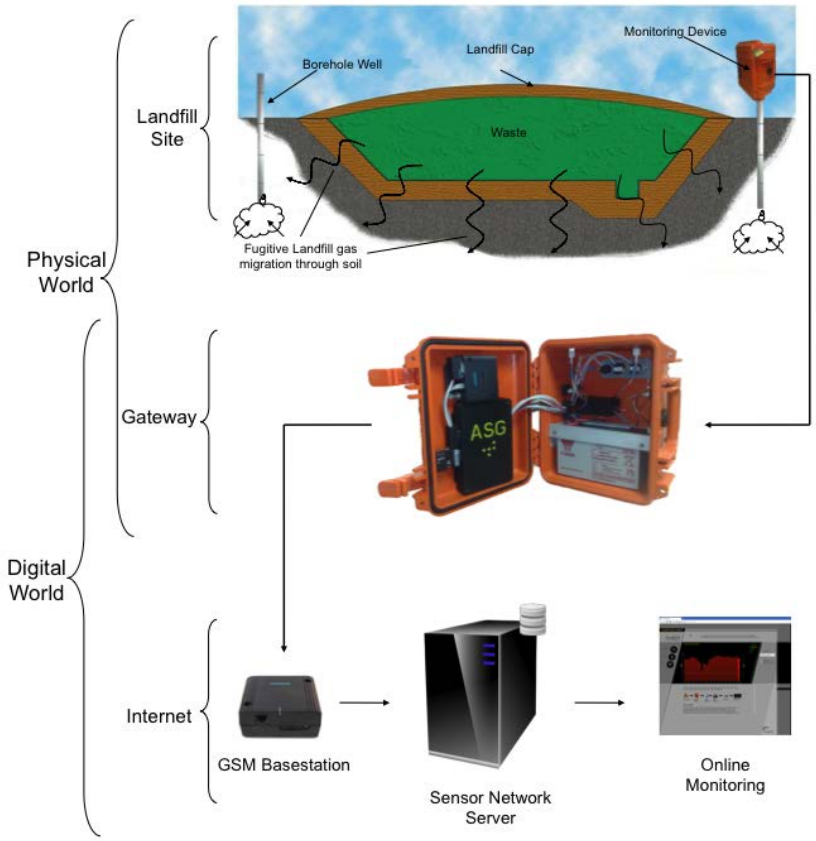

Figure 2.1: Visual representation of the landfill gas sensing model from the device placed in the field to a web-based visualisation user interface. The model shows the progression of chemical sensed data from the physical world to the digital world by means of a gateway platform.

2.2.2 Gas Sensors

The system was equipped with a humidity sensor (Honeywell HIH-4000-001); linear range 0 to 100% RH and a temperature sensor (a 10 kΩ thermistor - Thermometrics DKF103N5) with an operational response range of $-40\,^{\circ}\mathrm{C}$ to $+250\,^{\circ}\mathrm{C}$. Both temperature and humidity measurements are critical for providing background information when analysing gas samples, especially during developmental stages and for correlation with environmental artefacts that may give rise to erroneous signals from the chemical sensors.

More importantly, the system was also equipped with two chemical gas sensors; for CH_4 and CO_2 detection. As discussed earlier, landfill gas is composed mainly (greater than 95% - [397]) of CH_4 and CO_2, thus these are the principle sensing targets. Although the permitted concentration limits of both gases are low, it was found through previous developmental phases and field validation trials that measured readings were up to 10 times that of the allowed regulated range [414]. As a result, both sensors (NDIR based) were sourced from Dynament Ltd. with a custom range of 0-20% to suit problematic landfill sites.

2.2.3 Gateway Platform

2.2.3.1 System Components

All system components were housed within a robust case (Peli Case 1300). An internal volume of 25.1 (L) × 17.8 (W) × 15.5 (H) cm allowed sufficient space for all system elements to be securely packaged and for a systematic layout of components. The case's lid held the most accessible and frequently used system elements employed by users during system development and deployment i.e. control and communications. Conversely, the sensors and actuators were positioned within the case's base for secure and fixed positioning while allowing sufficient room for gas tubing and electrical connections. Figure 2.2 on page 86 shows the layout views of the system's components for control/communications and sensors/actuators, respectively.

1. Micro-controller board
   A custom, in-house designed and assembled PCB (Printed Circuit Board manufactured by Beta LAYOUT Ltd.) was developed to suit the requirements of this project. At its core lay an MSP430F449 (Texas Instruments) which controlled component power switching, timing, signal conversion, data handling, storage, communications, etc., i.e. all processes necessary to achieve full autonomy of the system.
   The board was equipped with ten switchable power ports (8xPFETs and 2xNFETs). Each port's power supply was capable of being manually selected (via on board jumper pins) from 3 separate voltage supplies i.e. 3V3 regulator (Texas Instruments - LP2985A), 5V regulator (National Semiconductor -

LP2992IM5), and 12V (main battery).

2. Short range communications
   A miniature bluetooth module (LM Technologies LM048) was included for local (short range) communications. This feature allowed users to interface with the system without exposing the electrical components/connections such as the microcontroller to external conditions, such as rain. The module communicated to the microcontroller through a DE9 connection, via an RS232 transceiver (Maxim - MAX3232CSE) and finally to one of its UART channels. Power to the bluetooth module was applied by means of an external, weatherproof (IP67 rated) switch and power supplied via the 5V power regulator.

3. Long range communications
   Remote reporting of landfill gas concentrations to a local base station was achieved by means of a GSM module (Siemens MC35iT). This allowed standalone developmental systems to be deployed in very remote locations while still being able to communicate data back to stakeholders. Power was supplied via three PFET power switches. Communications were achieved in a similar fashion as with the bluetooth module with the exception of using the microcontrollers secondary UART channel.

4. Signal and actuation control lines
   Wiring for switching power to components was of single core and insulated (RS 140420). Sensor signal lines were connected using shielded wiring (RS 1643740).

5. Power source
   A low cost, rechargeable and high capacity 12V battery supplied power to the entire system (YUASA - NP712). Note: a 2xAAA battery pack supplied power to the microcontroller (behind a diode) for an uninterrupted power supply to the microcontroller which allowed the main battery to be changed with no loss of RAM e.g. the real time clock.

6. Extraction pump
   An air pump (SKC Grab Air 222-2301) with closed circuit input/output ports allowed sample gas to flow through the sample chamber at a rate of 0.6 L/min. This was actuated by a single microcontroller I/O port and one NFET with power from a 5V regulator.

7. Gas chamber
   A custom designed gas chamber accommodated all sensors and two port connections. It was fabricated using a Dimension SST 768 rapid prototyper and uniformly sealed using a combination of MEK and silicon coupled with O-rings for sensor access.

Figure 2.2: Component layout of the gateway platform. (1) control system, (2) bluetooth module, (3) GSM module, (4) signal and actuation control lines, (5) power source, (6) extraction air pump, (7) gas chamber, (8) flow selection valves.

8. Flow selection valves
   In order to select the supply source and target exhaust flows (Section 2.2.3.3) the system was equipped with two 3/2 way latching pneumatic control valves (Lee Products Ltd. LHLA0531211H).

2.2.3.2 Sampling Procedure

As discussed earlier, the existing legislative monitoring procedure (for determining landfill gas emissions from perimeter borehole wells) calls for a sampling frequency of once per month, extracting gas for ca. 1 minute using a hand-held instrument and venting to atmosphere. In this study, the sampling frequency was increased 60 fold. However, this immediately meant that much more greenhouse gases would be emitted to atmosphere when following the existing sampling procedure; a contamination that this device was ultimately expected to reduce. To address this issue, a previous study was conducted to investigate a recycling technique whereby the sampled gas was exhausted back into the borehole well (at a different depth) instead of venting to atmosphere [414]. The findings of the study showed that this recycling technique (of landfill gas recycling back to the borehole well) did not affect the gas composition measurements when compared with venting to atmosphere. Moreover, the same study discovered that when multiple borehole wells of various head space depths were sampled, the longest time to achieve a steady state measurement was ca. 2 minutes. To allow for appropriate settling time, a 3 minute monitoring duration was chosen. As a result, the automated monitoring time was divided into 3 separate procedures (*baseline*, *sample,* and *purge*) where each was monitored for

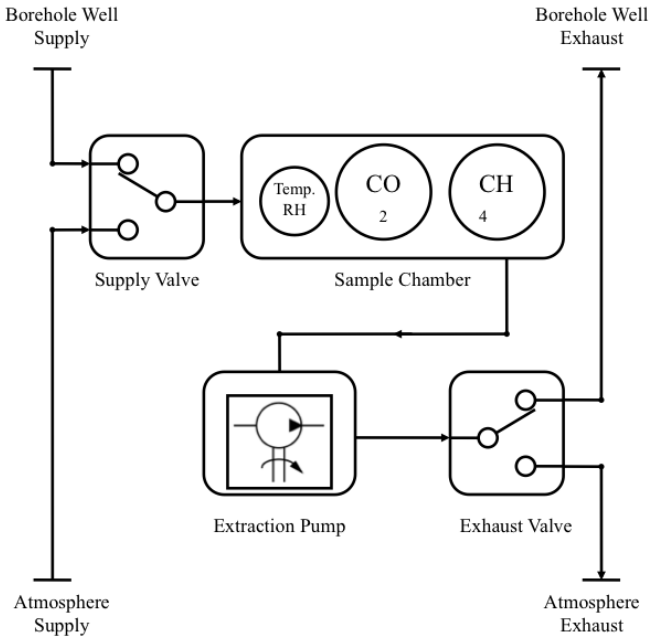

Figure 2.3: Schematic flow diagram illustrating the gas flow control system. The flow control valves allow the system to be switched between sampling mode (from 'Borehole Well Supply Supply' to the 'Borehole Well Exhaust') and baseline and purge modes (from 'Atmosphere Supply' to the 'Atmosphere Exhaust').

a duration of 3 minutes and sampled at 3 second intervals. The device's air flow control system is illustrated in Figure 2.3 on page 87.

Firstly, for the *baseline* procedure, the 'Supply Valve' was switched to the 'Atmosphere Supply', and the 'Exhaust Valve' to the 'Atmosphere Exhaust' settings. The motivation for this step was three fold. The primary reason was to check that the sensors were in fact powered up, i.e. a valid measurement gave a value of no less than the sensors standard offset of 0.4 V at 0% v/v (if unpowered the sensors report an electrical potential of 0 V). Coupled with this, it allowed sufficient time for the IR sensors to warm up and stabilize; a necessary step for accurate measurements. Furthermore, it was also ensured that no residual landfill gas was present in the chamber from previous measurement cycles. Subsequently, the *sample* procedure took place whereby both valves were toggled from the *baseline* step so that landfill gas was extracted from the 'Borehole Well Supply' and exhausted to the 'Borehole Well Exhaust'. Finally, the valves were again toggled to the state used for the *baseline* procedure. The following *purge* procedure was used to remove the landfill gas from the gas chamber.

2.2.3.3 Signal and Data Flow

A total of five signal lines were connected to the microcontroller's analogue to digital converter (ADC) channels. As a rule, the ADC channels may only digitise voltage levels between 0V and 3.3V. The dynamic range of each analogue signal line was first conditioned to lie within the ADC measurement range by means of appropriate signal conditioning circuitry. Once conditioned, the sensor outputs were digitised (via the ADC channels) at 3 second intervals over the full 9 minute sampling procedure. Along with the sensor data, a single battery reading was saved as part of the data set, along with a timestamp according to the on board real time clock (set to GMT). The full data set was retained in RAM before storage or reporting back to the stakeholder. Following this, the data was saved as raw ADC values on two separate 2 Mbit flash chips (Numonyx M25P20-VMN6P) allowing a total of 131.072 Kbytes to be stored over 8 separate sectors. The data were arranged in a structured format to utilise all data bits in each byte. The first, second, and third sectors on each chip were assigned to store the data harvested during the baseline, sample, and purge procedures respectively. By the same token, the fourth sectors were kept in reserve for additional sensor data overflow or system specific settings. As a result, the system was able to save up to two years of separate trial data assuming a sampling frequency of twice per day.

2.2.3.4 Communications

As environmental devices are often placed in remote locations, one of the only readily available methods of wirelessly transmitting sensed data to stakeholders is to take advantage of the GSM networks' national coverage. The system's GSM module was powered via three of the eight positive switching power channels for mains power, wake up, and shut down triggering. After harvesting and storing landfill gas data from a monitoring cycle, a statistical representation was compiled (average, max, and min) and sent to the Sensor Network Server (SNS). SMS messaging is used at present with optional use of the module's GPRS feature; however it was found to be more effective to use SMS for maintenance and continuous power costs. For complete dataset retrieval, one must interface with the device and download stored data from the on-board flash memory chips. Initially, this was achieved in the same manner as in a laboratory setting, i.e. a direct wired connection to a laptop PC. However, this method is highly undesirable (i.e. to open the system in situ) as it left the system vulnerable to such conditions as rain, wind, and biofouling; potentially causing damage such as electrical shorting. As a result, the system was equipped with an external power control switch (IP67 rated) for the Bluetooth module. Thus, full system control was accessible for diagnosis of individual components, setting the system clock, and retrieval of data without breaching the system's environmental seal.

2.2.4 Sensor Network Server

2.2.4.1 Base Station and Database Interface

The GSM base station (Siemens MC35iT) was connected to a server PC via an RS232 interface (Rotronic UC232A) and powered by a standard 12V power adapter (Masterplug MVA1200-MP). Written in the Java programming language and using the Javax.comm package, a custom written application, denoted here as the GSM Database Interface (GDI), provided the functionality to progress data from new Landfill SMS texts to a secure MySQL database. Figure 2.4 on page 90 depicts the overall process of advancing the data from the GSM base station to the primary environmental database.

At first, the base station was placed into 'SMS Alert Mode' where, upon receipt of a new SMS, a string of characters was sent to the server indicating which slot the new text was stored within the GSM's memory. Once the GDI was alerted to a new packet, it automatically parsed the alert string and extracted the SMS memory storage address on the base station. Next, the GDI requested and received the full SMS text located the appropriate memory address. After parsing the new text header, the sender's phone number was used as the unit identification factor. At this point the GDI connected to a 'registry database' where it received all relevant information related to the remote device such as type, unit number, and calibration settings based on the sender's phone number. Next, the text body was parsed. All reported measurements were extracted and automatically placed on the database using standard SQL statements. Also, inline conversions of ADC CO_2, CH_4, and battery levels occurred at this point using previously acquired calibration data (Section 2.3.1) in the lab. Finally, the text was deleted from the base station as the storage capacity of the SIM card was limited.

2.2.4.2 Data Organization

Once data were transmitted via the GSM network to a central base-station, the data was stored in a relational database which can manage data from multiple landfill locations. This relational database was constantly available on the Internet which thus fulfils our mission of data accessibility, and also it was stored in a replicated database setup; meaning that there was multiple copies of the data, thus ensuring data redundancy. Figure 2.5 on page 90 provides an overview of our end-to-end system, from sensing our environment through to informing users of the relevant levels of CO_2 and CH_4 in their local landfill site.

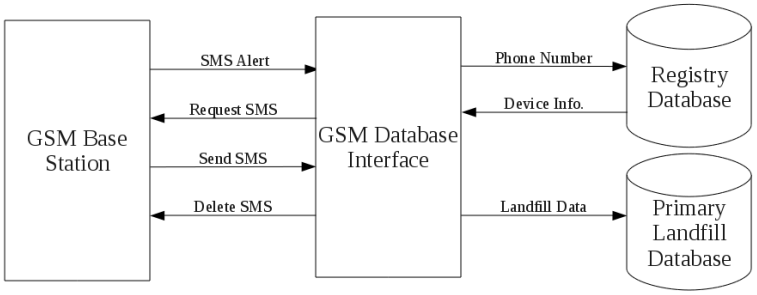

Figure 2.4: Block diagram showing the interactions between the GSM base station, the GSM database interface and the relational databases. The remotly reported data is received by the GSM base station where, through a number of programming stages, the data is stored on the primary landfill database.

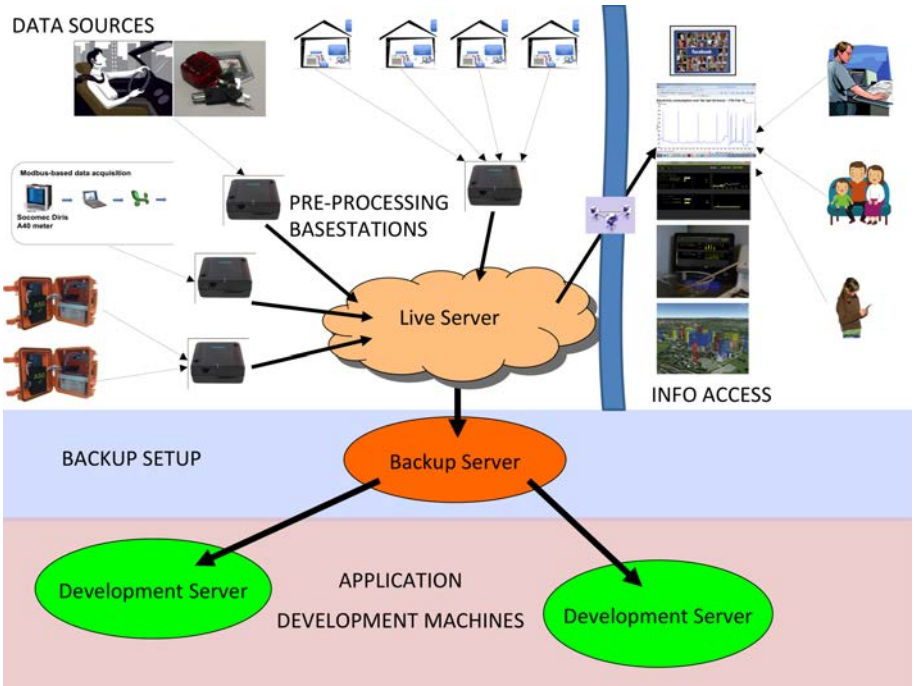

Figure 2.5: Overview of Data Storage, Backup and Presentation. Multiple landfill sensors can upload data to a single cell base-station. Thereafter these base-stations upload data to a central server, which is also backed up. Finally this data is available via the Internet to for end users to access.

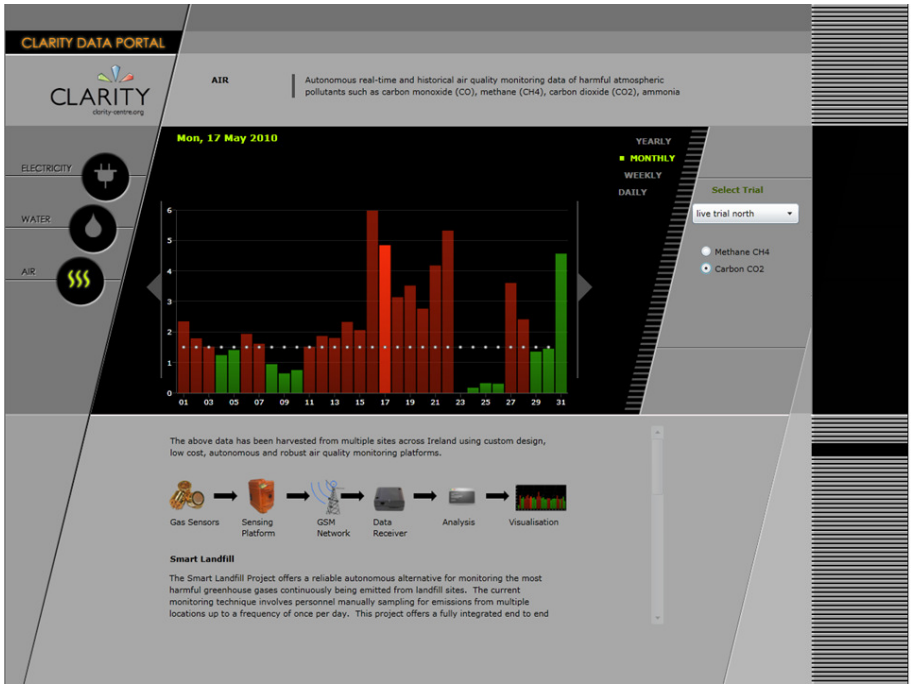

Figure 2.6: Sensor Data Portal: Our web application which allows relevant stakeholders to easily view in real-time the air quality (CO_2 & CH_4) data from landfill sites. The website can be viewed at http://clarityapp.ucd.ie/~sensorportal/

2.2.4.3 Data Presentation

The data were accessible by relevant stakeholders via an intuitive web interface in which the data were displayed graphically. Figure 2.6 on page 91 shows the designed Silverlight web interface. Initially the user is presented with a list of trials (both live and historical) via a combo box on the right hand side of the screen. After selection of a relevant trial the user can click on the relevant radio button on the right hand side to view either the CO_2 or CH_4 values, which are displayed as a bar chart, with yellow-green bars indicating values within recommended limits and orange bars indicating that the limits have been exceeded. The user can change the visualisation unit to daily, monthly, and yearly by clicking on the option buttons, and arrow buttons are provided to slide the time period to previous or next equal time span. Finally, below the main display area a brief description of how the information is collected is illustrated.

2.3 Methodology

In this section, the various procedures and experimental setups that were utilised to evaluate the system are described. Firstly, it was necessary to thoroughly calibrate the relevant sensors in a lab environment. Most importantly, the protocol for field deployment for a period of over one year is then described. Finally, a review of the

protocol to carry out post-analysis software optimisation simulations is carredied out on the array of data gathered in the field from the previous year.

2.3.1 Calibration of the Chemical Sensors

Before any deployment of the system could take place it was first essential to calibrate the chemical sensors. At first, the system was setup in the same configuration for field trials i.e. when sampling and exhausting to/from a borehole well (Section 2.2.3.2), except that the supply was connected to source gases and the exhaust to a fume hood extraction system. Next, the microcontroller executed a pre-programmed calibration routine where all the sensors were powered on and the digitised ADC values were continually output (in an endless loop at a frequency of 0.33 Hz) to a laptop computer via a serial port and captured using Microsoft Hyperterminal (a command line interface communications utility).

Each sensor was calibrated against source gases (CO_2/CH_4 supplied by Scott Specialty Gases) at concentrations of 0% to 50% with a nitrogen balance. Coupled with a dilution of ambient air, sourced using an air compressor (Werther International 42040 100/50), and managed with mass flow controllers (Cole Parmer YO-32708-26), various gas concentrations were achieved for calibration of the CO_2 and CH_4 sensors. A flow rate of 0.6 L/min (matching the flow rate of the system's air pump[2]) was ensured using a standard flow meter. Furthermore, a GA2000 Plus device (the current landfill gas monitoring standard hand-held gas analyser) was used as reference and verification of both gas concentrations and flow rate. A ten point calibration plot for each IR sensor (CO_2 and CH_4), was achieved (Section 2.4.1).

2.3.2 Power Usage

The system was programmed to autonomously wake up from a low power mode every 12 hours (changed to every 6 hours subsequently), perform a monitoring (analyse gas composition and report) cycle, and subsequently return to its low power state. As this system was placed at a remote location, it was desirable to establish how long the system would remain operational using the existing power source (7 Ah lead acid battery). Consequently, a current consumption analysis was performed using a high end multi meter (Keithly 2700), which was capable of sampling at a frequency of 60 Hz with a resolution of 9 decimal places. The landfill system's power source was connected in series with the multi meter and configured for a typical monitoring cycle - see Section 2.4.2 for analysis.

[2]This was to ensure a constant flow rate across the calibration, standard reference instrument (GA2000), and proposed system.

2.3.3 System Deployments

While the overall sensing model was in the final stages of development, including the implementation of 3 deployable platforms, a parallel effort was undertaken to find a suitable location for the first deployment. It was desirable to locate a site that would allow subsequent access, be safe from possible vandalism, and have an eventful borehole well to monitor. As many landfill sites in Ireland are privately owned, the first criteria was not easily met. After much evaluation, a site was located (closed to public access) where the personnel were very accommodating and enthusiastic, as they had a problematic well that needed continuous monitoring (*location A*) therefore providing rich dynamic data for this study. After the site personnel experienced the remote sampling advantages of the system, the site manager asked for another well on the same site to be monitored (*location B*). Sometime afterwards, our national environmental enforcement agency requested that another system be deployed to a problematic site that they were dealing with at the time (a borehole well with high concentrations of CO_2) - (*location C*). Stakeholder involvement is time-consuming in building up a working relationship, but critical to the success of research efforts like this.

After calibrating the sensors, 3 landfill systems were ready to be deployed into the physical environment. From previous developmental models [414, 416, 415], it was believed that the systems were sufficiently robust to withstand long term deployments in the environment. Initially, one landfill unit was deployed at *location A* on the 28^{th} of May 2009, which sampled twice per day (11am + 11pm) until the 8^{th} of October 2009. From the 13^{th} of August 2009 a second landfill unit was deployed at *location B* to concurrently sample twice per day (11am + 11pm). After these two trials, the units were recalled to carry out some maintenance work after discovering that insects had breached the system during a regular battery change. At this point, the systems were thoroughly examined, cleaned and the PCB boards were protected by a layer of spray silicone (Electrolube ERDCA200H). Between November and December one landfill unit was deployed at *location A*. After further maintenance, from early March 2010 the system was sampling at 4 times per day (12am, 6am, 12pm, and 6pm) in both *location A* and *location B*. From May 24^{th} a third location was added (*location C*) meaning that three locations were being sampled 4 times per day at 12am, 6am, 12pm, and 6pm.

2.3.4 Deployment Data Processing

As described earlier, each monitoring cycle consisted of a 3 minute *baseline* (60 samples taken at 0.33 Hz), a 3 minute *sample* (60 samples taken at 0.33 Hz), and a 3 minute *purge* (60 samples taken at 0.33 Hz), with a statistical representation of each of the 3 stages being automatically compiled and reported to the central base-

station via SMS. Meanwhile the fully recorded dataset was stored in on-board flash memory within the landfill system, and then downloaded at a later date for further analysis. This data was subsequently downloaded during battery changes to carry out post-event analysis and determine what the optimum sampling rate should be for future deployments of the landfill systems. The objective of this exercise was to improve battery lifetime, and to reduce transmission and processing costs.

To carry out the computational analysis data from *location A* between the 29^{th} of July 2009 and the 9^{th} of October 2009 were considered. This equated to 143 9-minute monitoring cycles (baseline + sample + purge) taken over this period of time. In this exercise, the raw sensor data (recorded every 3 seconds) which equated to 25,740 readings were considered. A software processing algorithm was then used to go through 95 scenarios on all 143 $\times$ 60 baseline/sample/purge readings, thus representing optimisation investigations on 2,445,300 simulated data readings. The results section will report the findings as to the optimal sampling rate.

As noted in Table 2.1 there was a period of time during *location C's* deployment where there was a 9 minute sampling period to/from the borehole well (with no baseline extraction beforehand or purge extraction afterwards). These 93 instances (16,020 raw data samples) allowed for the opportunity to investigate whether the nature of the sample stage remains similar without baseline and purge stages. This could potentially allow for many savings in terms of shorter sampling times (power, memory, and communications loads) and being able to disregard valves (component cost, complexity).

2.4 Results and Discussion

2.4.1 Chemical Sensor Calibration

The calibration routine of the chemical sensors was described earlier (Section 2.3.1). At each of the 10 calibration steps the data when each sensor arrived at a steady state response were extracted. Once this was achieved, the respective gas concentration levels from our reference instrument (GA2000 Plus) was noted. A 10 point calibration plot for each IR sensor, CO_2 and CH_4, is presented in Figure 2.7 on page 96 and Figure 2.8 on page 97, respectively. Excellent correlation between the reference system and landfill sensors was obtained for CO_2 ($R^2 = 0.9966$, $n = 10$), and for CH_4 ($R^2 = 0.9994$, $n = 10$). It is clear that the system's detection performance was on par with the currently used reference instrument when detecting these two chemical targets. Finally, the linear correlation equations generated by these calibration plots were used as inline conversions from reported ADC measurements by the remote systems for presenting real concentration values online.

Table 2.1: Field deployment data gathered over a 16 month period. For *location C* a 9 minute *sample only* approach was taken, as opposed to *baseline + sample + purge.*

Location	Start Date	End Date	Number of Data Readings	Sampling Rate	CO_2 Avgerage (% v/v)	CH_4 Average (% v/v)	CO_2 Limit Breaches	CH_4 Limit Breaches	CO_2 and CH_4 Breaches
A	28-May-09	08-Oct-09	255	2× /day	7.71	13.70	185	133	133
B	13-Aug-09	08-Oct-09	113	2× /day	3.23	0.13	77	0	0
A	20-Nov-09	28-Dec-09	77	2× /day	5.99	0.85	58	10	10
C*	03-Mar-10	07-Sep-10	764	4× / day	3.78	0.09	738	0	0
A	10-Mar-10	07-Sep-10	768	4× / day	1.52	0.30	243	47	47
B	24-May-10	07-Sep-10	446	4× / day	1.48	0.02	189	0	0
SUM			2,403				1,490	190	190

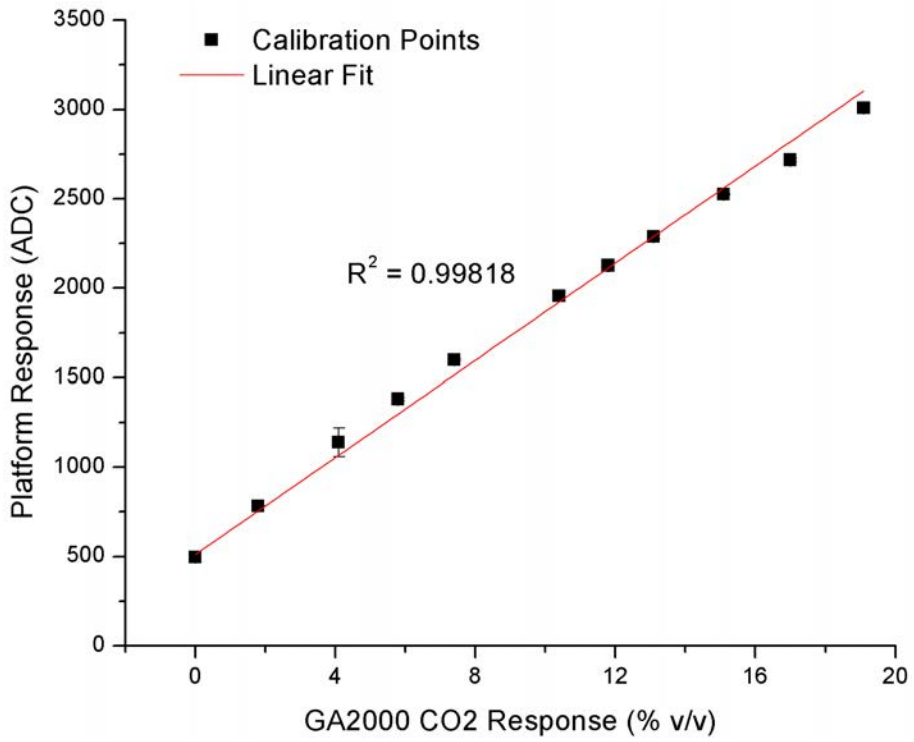

Figure 2.7: Calibration of the system's CO_2 infrared gas sensor. Points represent the average of the steady state response over circa 2 minutes. Error bars (present but difficult to see due to the high sensor accuracy) represent the standard deviation.

2.4.2 Power Consumption Analysis

Figure 2.9 on page 97 shows the current consumption analysis during an aforementioned monitoring and reporting routine (Section 2.3.2). One can see identifiable trends relating to the four procedures (baseline, sample, purge and communications), and also the times when the extraction and exhaust valves were toggled. The average current consumption during this time was found to be circa 230.1 mA over a duration of 9 minutes and 45 seconds (585 seconds in total). By the same analysis method, when in its inactive state, the multimeter reported an average current draw of 6.13 mA for 42,615 seconds before the next sampling routine. This was calculated to be an average continuous current draw of 9.16 mA from the 12V battery source. Assuming an ideal power source with these characteristics, the system (with its present power source and sampling routine) can autonomously monitor landfill gas concentrations for an estimated 4.5 weeks which was a sufficient deployment time (without requiring a battery change) to explore this proof of principle study.

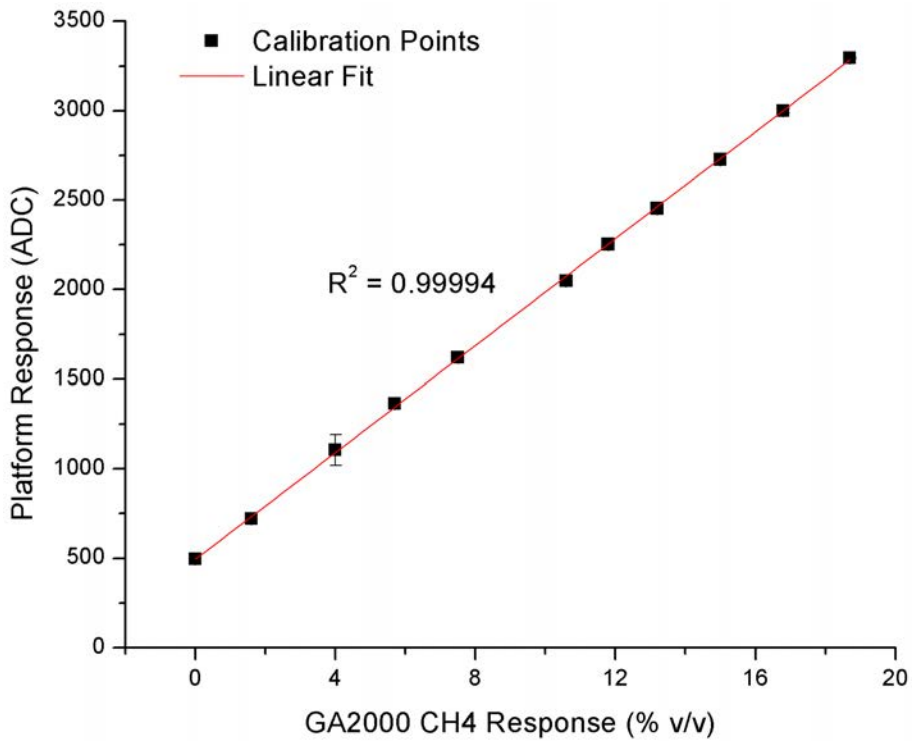

Figure 2.8: Calibration of the system's CH_4 infrared gas sensor. Points represent the average of the steady state response over circa 2 minutes. Error bars (present but difficult to see due to the high sensor accuracy) represent the standard deviation.

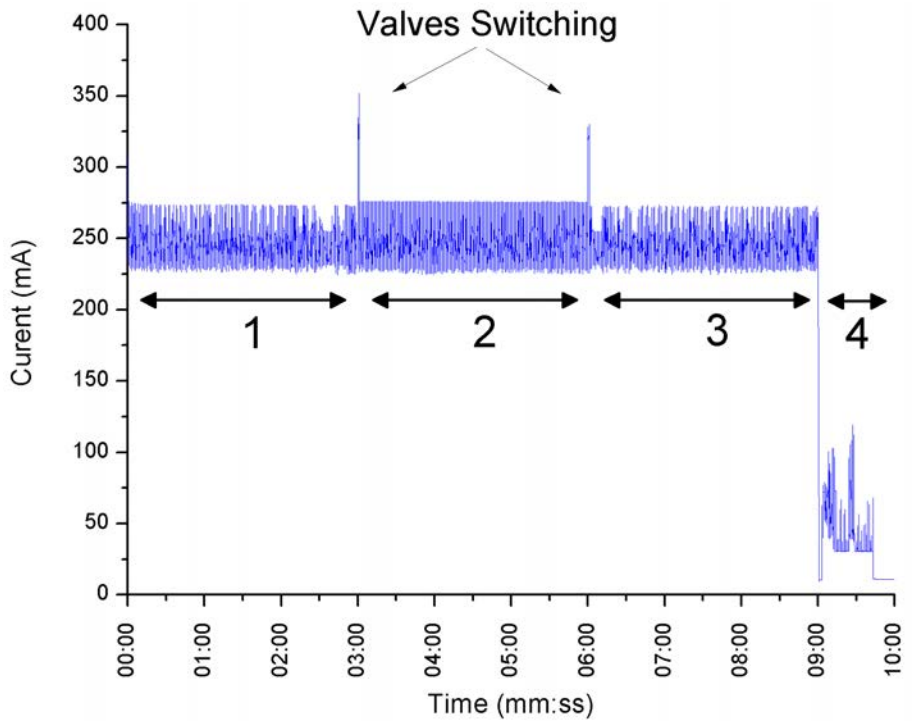

Figure 2.9: Current analysis of landfill system during a full monitoring routine (1) baseline procedure, (2) sampling procedure, (3) purge procedure, (4) communications and storage procedure.

2.4.3 Deployment Data

Table 2.1 summarises the collection of data over a 16 month period as described in Section 2.3.3. Overall, it can be observed that 2,403 samples were sent to the central server, in which the CO_2 limit was exceeded in 1,490 (62%) samples! The CH_4 limit was exceeded on 190 (8%) occasions, while both CO_2 and CH_4 were exceeded together on 190 (8%) occasions. To consider an individual deployment, all the sampled readings from the *location C* field deployment are displayed in Figure 2.10 on page 99. In this case, the CO_2 component exceeded the recommended limit [424] in 96.6% of the samples, while CH_4 never exceeded the recommended limit [424] i.e. 0% of the time. The average recorded CO_2 value was 3.78% v/v, which is 2.52 times above the regulatory limit of 1.5% v/v. The average CH_4 value was 0.01% which is within the regulation limit of 1% v/v. It is worthwhile to note that, CO_2 levels in soil / sub soil layer can naturally exceed 1.5% due to a number of external processes e.g. aerobic degradation of organic matter in soil, dissolution of CO_2 from groundwater high in carbonate, or microbial methane oxidation. Thus CO_2 levels above 1.5% v/v do not necessarily indicate landfill gas migration, however our methology follows well established procedures and pre-existing monitoring routines by the EPA. An ideal solution would be to investivate typical background levels in the area being monitored, which are unaffected by the landfill.

Even considering this, observing the 7 month trend of sampled data, significant CO_2 events were recorded around the 17^{th} of March, 28^{th} April, and 25^{th} of September. Greenhouse gas emissions from landfills are inherently dynamic (especially during their initial phase) and events such as these can be attributed to a number of factors including: borehole proximity to the landfill, time of year, seal of the borehole well cap, water table, head-space, sample depth as well as human activities, and extraction system failures/blockages. It is difficult to pinpoint the exact cause(s) of these events at this early stage in our investigations, but clearly, the availability of this type of information will open the way to gaining a fuller understanding of the dynamics of greenhouse gas generation in, and therefore more effective management of, landfill sites. This only strengthens the need for this type of real time monitoring technology. Finally, one important question that arises from this data series is: how many of these events are missed by the current manual monitoring frequency of once per month? The next section explores this question.

2.4.4 Human Operator Error Simulation

Considering Figure 2.11 on page 100, in which a human operator taking a reading on a particular first day of each given month is simulated, it can be clearly seen that many dynamic events would not be noticed particularly for the middle of March-

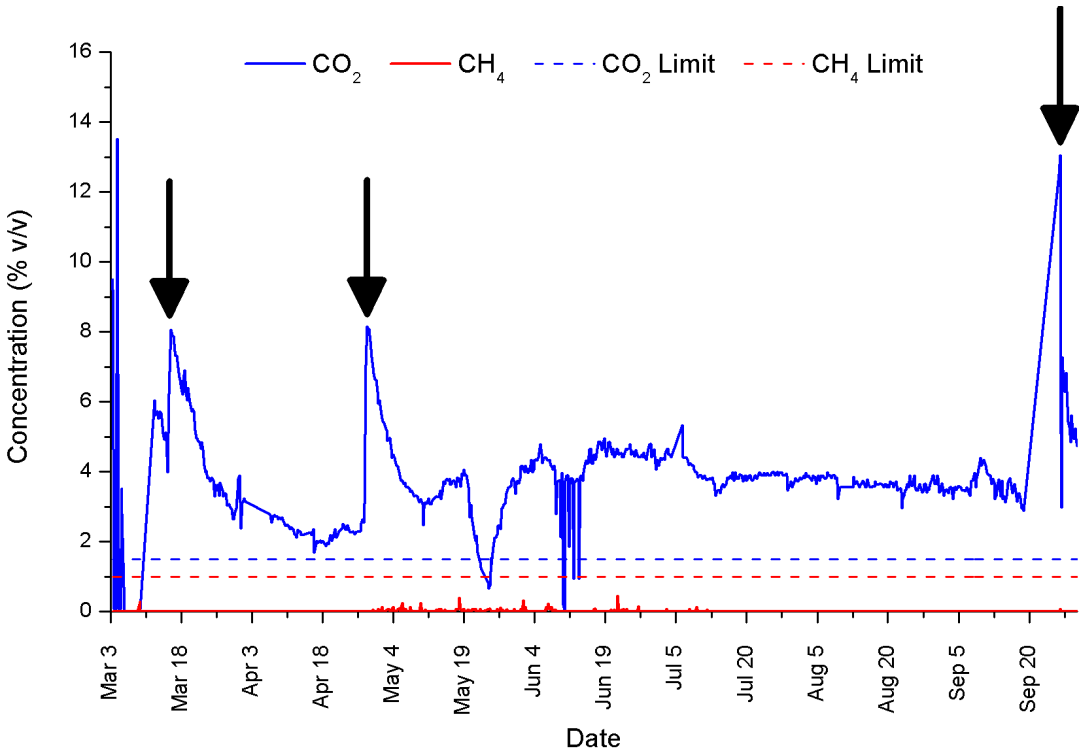

Figure 2.10: CO_2 and CH_4 readings from a 7 month field deployment at *location C* between March 2010 and October 2010. Note that CO_2 exceeds the recommended limit 96.6% of the time, while CH_4 never exceeds the recommended limit. The arrows on the graph illustrate significant CO_2 events that were recorded around the 17^{th} of March, 28^{th} April, and the 25^{th} of September. There were no CH_4 events.

2010, the end of April-2010, and the middle of September. For example, if a human operator noted a reading on the first Monday of every month (at 12 noon), then there would be an average error of 7% (4.05% for CO_2 vs. actual average reading of 3.78% from all sampled data points over 7 months). The first Tuesdays in the dataset would have yielded an average error of 11%, Wednesdays an error of 35%, Thursdays 33%, and Fridays an average error 0%. From these 5 scenarios alone (plus a visual inspection of Figure 2.11 on page 100), it can be seen that there is a wide degree of error in selecting a manual rota for human operators to monitor overall landfill emissions.

2.4.5 Sampling Procedure Analysis

To carry out our computational analysis data from *location A* between the 29^{th} of July 2009 and the 9^{th} of October 2009 were considered. As described, the system firstly carried out a 3 minute *baseline* stage, followed by an actual 3 minute *sample* stage, and finally a 3 minute *purge* stage (see Figure 2.12 on page 102). The CO_2 and CH_4 profiles associated with each of those stages are now considered. Note: all data presented here is from the full dataset downloaded from the field-deployed

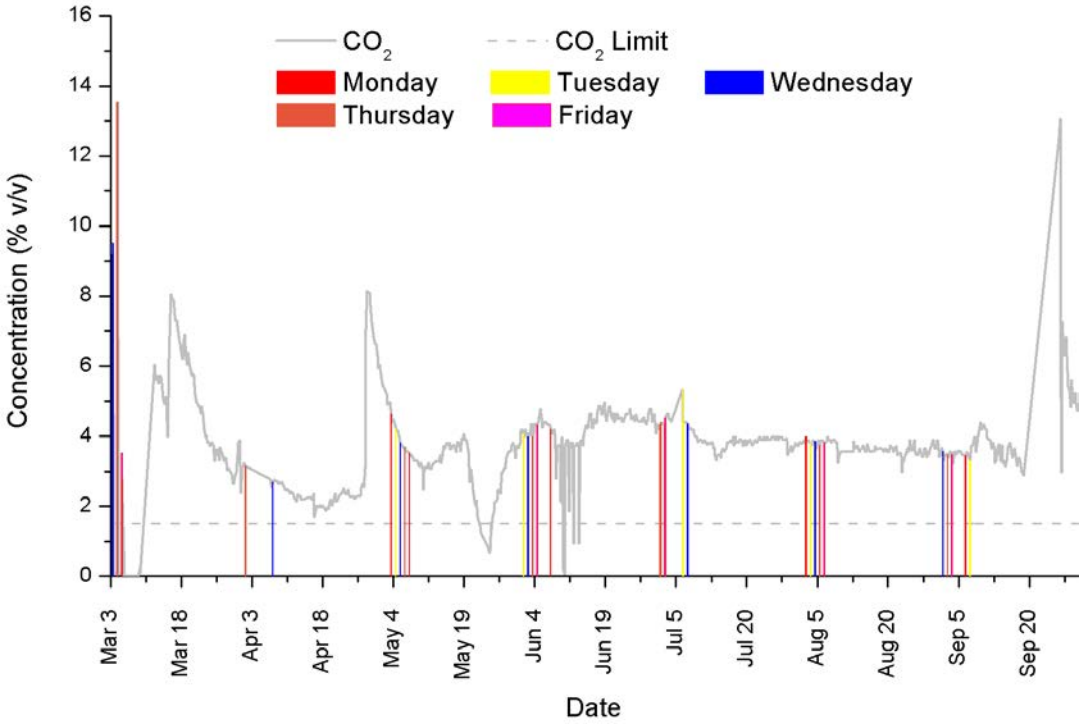

Figure 2.11: CO_2 readings over a 7 month field deployment at *location C* between March 2010 and October 2010. Note that a simulated human operator sampling the landfill emissions on a particular first day of each month would miss a lot of events of interest e.g. the middle of March-2010, the end of April-2010, and the middle of September. The average error across each of the 5 days (Mon-Fri) would have been 17% in our field deployment at *location C*.

landfill units.

2.4.5.1 Baseline Stage

The average *baseline* profile (across the entire 143 recorded readings) is illustrated in Figure 2.12a on page 102. Throughout the field deployment, the transmitted CO_2 and CH_4 *baseline* readings were calculated by taking the last 11 readings (33 seconds) of the full dataset (i.e. after the sensors had time to warm up and just before the sampling stage), and calculating the average, however on post-analysis inspection of the baseline within the figure it appeared that one could get near that average by taking fewer samples. A software simulation program was compiled which went through 95 variations on all 143 $\times$ 60 *baseline* readings. The finding was that after 20 readings, and taking the average of the last 5 samples, a very low average reading error of 0.17% for CO_2 and 0.62% for CH_4 was acheieved, with an individual outlier worst case of 2.51% (CO_2) and 2.57% (CH_4) error in ADC reading, compared to the field-deployment implementation. This means that the point at which the sensors achieve a steady state response after a necessary and unavoidable warm up period was identified. Overall, this represents a realtive battery saving of over 60% for the *baseline* sampling stage alone (within the context of the baseline stage).

2.4.5.2 Sample Stage

Next, the average *sample* profile (across the entire 143 recorded readings) is illustrated in Figure 2.12b on page 102, for the chemical and physical sensors, respectively. Throughout the field deployments, the CO_2 and CH_4 composition levels were calculated by taking the maximum CO_2, CH_4, Humidity, and Temperature readings (60 $\times$ 3-second samples taken in total). However, on inspection of the sample stage within the figure it appeared that one could achieve those maximum values through taking less samples by visual inspection of the trends alone. A software simulation program was then comiled which went through 95 variations, on all 143 x 60 *sample* readings. The finding was that after 30 readings, and taking the average of the maximum sampled values, an average error of 0.72% (CO_2), 0.34% (CH_4), 0.07% (Humidity), and 0.007% (Temperature) is obtained, with an individual outlier worst case of 2.88% (CO_2), 2.55% (CH_4), 1.04% (Humidity), and 0.17% (Temperature) error in ADC reading, compared to the field-deployment implementation. This represents a potential battery reduction of 50% for the *sample* stage.

2.4.5.3 Purge Stage

Lastly, the average *purge* profile (across the entire 143 recorded readings) is illustrated in Figure 2.12c on page 102. Throughout our field deployment, CO_2 and CH_4

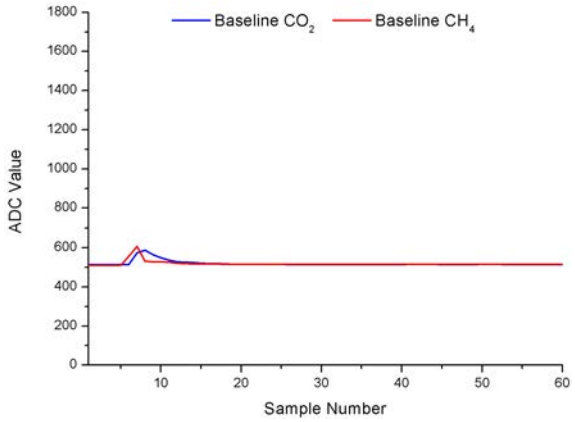

(a) Averaged Baselines.

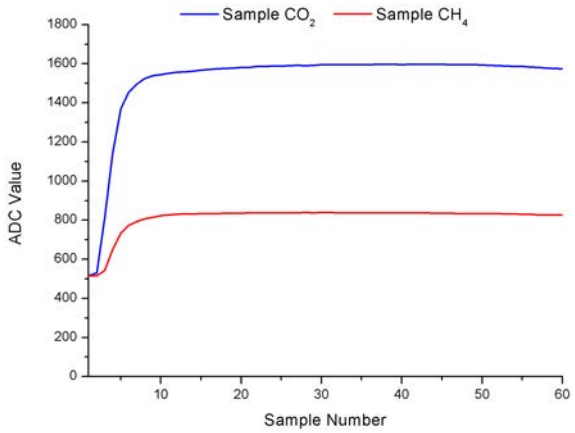

(b) Averaged Samples.

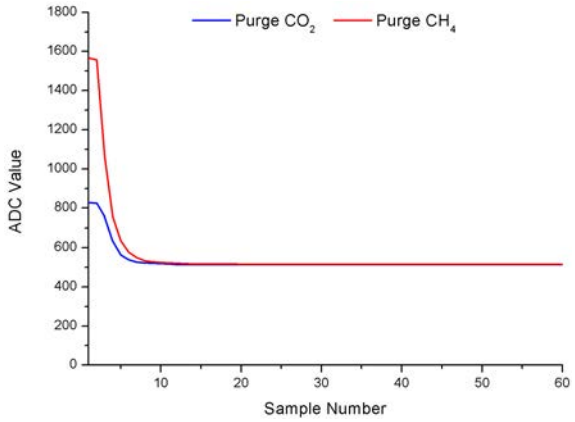

(c) Averaged Purges.

Figure 2.12: Profile of a typical 9 minute *baseline, sample, & purge* sampling stage, which comprises of 180 CO_2 & CH_4 samples recorded every 3 seconds. This occurs in the order of 60 × *baseline*, 60 × *sample*, and 60 × *purge* samples. Initially all 180 items were sampled, however after a close analysis of 10+ weeks of data, it is capable to minimise the length of this sampling procedure. This has a positive effect on battery power consumption.

levels were calculated by taking the minimum recorded readings (60 × 3-second samples taken in total), however on post-analysis inspection of the purge stage within the figure it appeared that one could achieve such a representative value through taking many less samples. A software simulation program was compiled which went through 95 variations, on all 143 × 60 *purge* readings. The finding was that after 20 readings, and taking the minimum recorded value, one could achieve an average reading error of only 0.28% for CO_2 and 0.12% for CH_4, with an individual outlier worst case of 2.74% (CO_2) and 0.78% (CH_4) error in ADC reading, compared to the field-deployment implementation. This represents a battery saving of over 60% for the *purge* sampling stage.

So in summary, if one was to consider using a system as follows: 1 minute baseline; 1.5 minute sample; and 1 minute purge, it would be within an average sample stage error of 0.72% (CO_2), 0.34% (CH_4), 0.07% (Humidity), and 0.007% (Temperature), with a worst case of 2.88% (CO_2) in ADC readings. This would mean that the total field trial samples could be reduced from 10,010, as opposed to 25,740 which would represent a potential extension of battery life by 2.57 times.

2.4.5.4 Investigation into Removal of Baseline and Purge Stages

As noted in Table 2.1 there was a period of time in the *location C* deployment where there was a 9 minute monitoring period (with no baseline extraction beforehand or purge extraction afterwards). Comparing the very similar signatures of the sample stage in **??** (*baseline + sample + purge*) and Figure 2.12 on page 102 (*sample only*), there is an indication that only the sample stage is needed. Carrying out a software optimisation of a *sample only* system, it was found that just 30 (× 3 second) readings are required. The first 10 readings (i.e. 30 seconds) are required for the sensors to heat up to a steady state.

2.4.6 Lessons Learned

The evaluation procedure in Section 2.4.5.4 is not sufficiently comprehensive at this stage to make a definite case to drop the baseline and purge stages. The most effective way to do this would be to run the 2 systems in parallel and verify that both are analysing the same landfill gas. However, from all the data and experience available, it is felt that a *sample only* system is the best approach to take in future deployments. A sampling stage as follows (at least 4 times per day) is recommended:

1. Allow 30 seconds for sensors to warm up (no sampling required);
2. Sample every 3 seconds for the next 90 seconds (CO_2, CH_4, Humidity, Temperature);

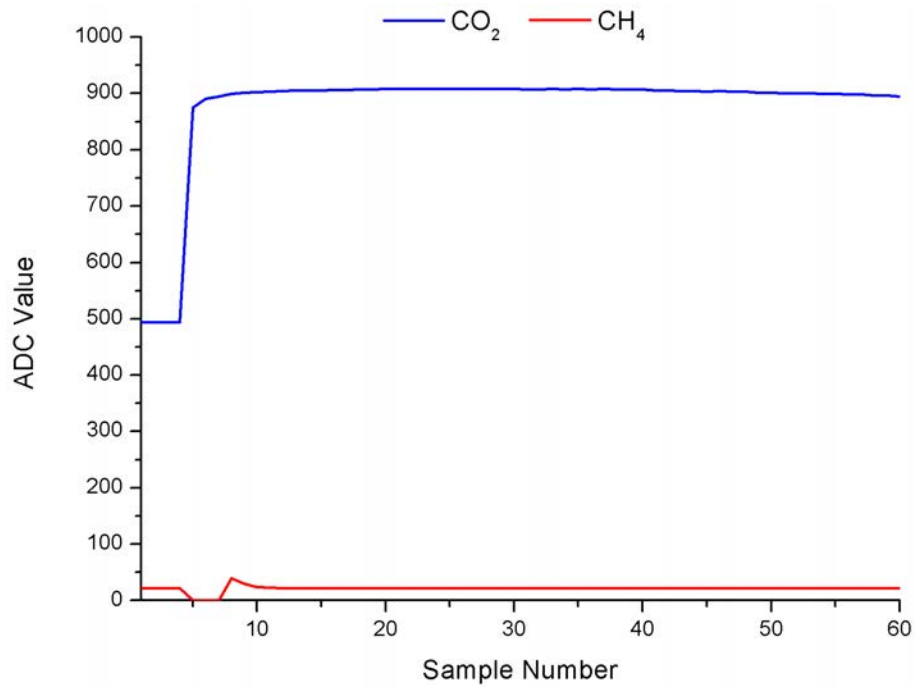

Figure 2.13: Profile of our *"sample only"* system, note the same signature as in Figure 2.12 on page 102, which possibly indicates that only the *sample* stage is needed to measure the air emissions at a given landfill site.

3. Stop if 5 consecutive readings report the same values;

4. Record the maximum reported values from step 2 for CO_2, CH_4, Temperature, and Humidity;

Such a system, compared to that deployed to the field trials (9 minute samples with *baseline, sample,* and *purge* stages), would offer a number of advantages:

- No valves required, so less mechanical complexity and cost, and increased reliability and longer battery life;
- Total sample time reduced from 9 minutes to 1 minute 45 seconds. A saving of 80% in active power consumption, and potentially increasing battery field lifetime from 6 weeks to approximately 12 weeks (this figure does not factor in power savings achieved through not having to actuate valves);
- Reduced manufacturing costs and increased battery life and reliability, as switching valves are no longer required;

2.4.7 Future Work

2.4.7.1 Communications

Remote data retrieval has been achieved through compiling a statistical representation of the data and transmission to the base station by means of SMS. The SMS

text structure was formed so that it could be readily interpreted by a human observer. Although this option was beneficial at early stages of this work, it has since progressed to a complete data orientated formulation where human observations are now at the visualisation end (see Figure 2.6 on page 91). As a result, one can retrieve a richer sensor data-set by introducing encoding schemes (such as Huffman or Arithmetic) to compress the data and ultimately retrieve more information per transmission. This will reduce transmission frequency resulting in lower cost and power use. Furthermore, this can potentially result in retrieval of fully recorded datasets via SMS without the user physically being present.

Alternatively, when multiple units are deployed on a site an additional communications layer should be considered, whereby the units will be equipped with low power, short range radio transceivers (such as Zigbee). Then each sensor would report all its findings to a central communications gateway over a star/mesh/bus wireless sensor network as outlined by a recent survey [433]. Scope has been left to allow for a communications gateway to relay all data to the base-station via GPRS/3G on sites without any local access points. On the other hand, many active sites have a nearby workplace with internet capability where one can potentially take advantage of new generation technologies such as WiMAX [419]. This strategy will give a new layer of scalability to the sensing structure and allow many other plug and play sensing nodes to be added (such as more sensed locations, wider range of gases e.g. H_2S, gas pressure monitoring, etc.).

Ultimately, the chosen communications method will depend on the layout of the site and also on the number of nodes needed. At this stage in our deployments, SMS communications has been found to be sufficient to explore this application principle.

2.4.7.2 Adaptive Sampling

Borehole measurements typically involve monitoring the sensor output until a steady state signal is achieved for a representative gas sample. Many factors have been found to affect this and have been listed earlier in Section 2.4.3. A subset of these has already been explored by [414], and to accommodate these factors, it has been chosen to sample for a period of 3 minutes. However, there are disadvantages to this approach with the primary drawback being unnecessary power usage on wells that generate a steady state signal relatively quickly. This ultimately reduces the lifetime of the device in the field.

Although this issue was addressed earlier (Section 2.4.5), it is foreseen that a further extension of an overall adaptive sampling technique including a varied sampling cycle frequency i.e. a fixed frequency of 2 times per day may be too high for some sites and too low for others. It is foreseen that the application of computer classification techniques to adaptively select the optimum sampling frequency, based on previous reported gas concentrations and battery capacity at the time.

2.4.7.3 Energy Reduction/Harvesting

It has been determined earlier (Section 2.4.2) that the system can function autonomously for circa 4.5 weeks using the current power source. Although this was acceptable for our purposes, it is desirable to maximise the functional lifetime of the system (where possible) in the environment. The principle reason for this is that the cost of maintenance alone (for battery changes and the human resources required to change them) can be substantial, especially with multiple sites. A future option to explore is harvesting energy through devices such as solar panels in the first instance. This is a crucial limiting factor, as scalability depends on sensors being able to meet their operational energy requirements from integrated energy generation capabilities.

2.4.7.4 Integration of Other Sensors

Conceptually, our setup can accommodate many more sensor types (with minimum alterations to the gateway platform) and also many more gateway platforms. Also, individual components such as the communications module can be swapped out very easily to accommodate other standards.

Recently, the landfill platform has been equipped with other chemical gas sensors to monitor levels of ammonia (NH_3) and hydrogen sulphide (H_2S) by introducing simple signal conditioning circuitry to the system, and the work is ready to interface the system to the portal page once a suitable location has been found. In addition, we have already expanded the sensor server and web visualisation interface to include real-time monitoring of phosphate (PO_4^{3-}) in river waters, carbon monoxide (CO) in car parks[3], domestic carbon emissions, and pressure of extraction systems on landfill sites [399].

2.5 Conclusions

This work has successfully realised and validated a platform for real the time monitoring of landfill subsurface migration gases. The system incorporated the sensing of carbon dioxide and methane emissions at landfill sites, GSM communications to a "cloud database" and an on-line visualisation element to deliver near real time data to users in an easy to interpret format. This system has been successfully deployed in field-tests over a 16 month period, with 3 separate devices running concurrently across multiple locations towards the end of the trial generating 2,445,300 *in-situ* measurements of gas concentrations during this time.

Overall, in the context of this report, this work has explored the design, development, and long term deployment of an autonomous chemical sensing model.

[3]Available to view on our web portal under air quality monitoring section, http://clarityapp.ucd.ie/~sensorportal/

The efforts involved in the realisation of such a system for the detection of chemical pollutants *in situ* in a real practical scenario have been document in this work and will be used as a basis for comparison to a novel sensing model in future works.

2.6 References

[392] Regina Campbell, Brian Donlon, Peter Webster, Dara Lynott, and Gerry Carty. **Landfill Manuals - Landfill Monitoring 2nd Edition**. *Environmental Protection Agency*, 2003.

[393] Aitchison E. **Methane generation from UK landfill sites and its use as an energy resource**. *Energy Conversion and Management*, **37**(6):1111–1116, 1996.

[394] Brian Austin. *The involvement of pollution with fish health*, chapter 1, pages 13–30. Multiple Stressors: A Challenge for the Future. Springer, The Netherlands, 2007.

[395] R. Byrne and D. Diamond. **Chemo/bio-sensor networks**. *Nature Materials*, **5**(6):421–424, June 2006.

[396] Gunnar Borjesson, Ingvar Sundh, and Bo Svensson. **Microbial oxidation of CH_4 at different temperatures in landfill cover soils**. *FEMS Microbiology Ecology*, **48**(3):305 – 312, 2004.

[397] E. A. C.Crouch, L. C. Green, and S.G. Zemba. **Estimation of Health Risk from Landfill Gas Emissions**. In *Proceedings of the GRCDA 13th Annual International Landfill Gas Symposium.*, Lincolnshire, Illinois., 1990. GRCDA - The Association of Soil Waste Management Professionals.

[398] California Environmental Protection Agency. **Assembly Bill 32: Global Warming Solutions Act 2006**. Online (http://www.arb.ca.gov/cc/ab32/ab32.htm). Last accessed July 1 2013.

[399] CLARITY. **CLARITY Environmental Sensor Portal Page**. Online (http://clarityapp.ucd.ie/∼sensorportal/). Last accessed July 1 2013.

[400] John Cleary, Conor Slater, Christina McGraw, and Dermot Diamond. **An autonomous microfluidic sensor for phosphate: On-site analysis of treated wastewater**. *Sensors Journal, IEEE*, **8**(5-6):508–515, May 2008.

[401] Department for Environment Food and Rural Affairs. **Implementing the Climate Change Act (UK)**. Online

(http://www.defra.gov.uk/environment/climate/legislation/), 2008. Last accessed July 1 2013.

[402] D. Diamond. **Internet-scale sensing**. *Analytical Chemistry*, **76**(15):278A–286A, August 2004.

[403] Aiden R. Doherty, Zhengwei Qiu, Colum Foley, Hyowon Lee, Cathal Gurrin, and Alan F. Smeaton. **Green Multimedia: Informing People of their Carbon Footprint through Two Simple Sensors**. In *ACM Multimedia*, Firenze, Italy, October 2010.

[404] Aiden R. Doherty and Alan F. Smeaton. **Automatically Segmenting Lifelog Data Into Events**. In *WIAMIS: 9th International Workshop on Image Analysis for Multimedia Interactive Services*, pages 20–23, Washington, DC, USA, 2008. IEEE Computer Society.

[405] H Dolk, M Vrijheid, B Armstrong, L Abramsky, F Bianchi, E Garne, V Nelen, E Robert, JES Scott, D Stone, and R Tenconi. **Risk of congenital anomalies near hazardous-waste landfill sites in Europe: the EUROHAZCON study**. *Lancet*, **352**(9126):423–427, AUG 8 1998.

[406] European Commission. **EU Action against climate change. Leading global action to 2020 and beyond**. Online (http://ec.europa.eu/europeaid/infopoint/publications/communication/15g_en.htm), 2007. Last accessed July 1 2013.

[407] Cormac Fay, King-Tong Lau, Stephen Beirne, Ciaran O' Conaire, Kevin McGuinness, Brian Corcoran, Noel E. O'Connor, Dermot Diamond, Scott McGovern, Greg Coleman, Rod Shepherd, Gursel Alici, Geoff Spinks, and Gordon Wallace. **Wireless aquatic navigator for detection and analysis (WANDA)**. *Sensors and Actuators B: Chemical*, **150**(1):425 – 435, 2010.

[408] Martin Howley, Brian O Gallachoir, and Emer Dennehy. **Energy in Ireland 1990-2008: The 2011 Report.** Online (http://www.seai.ie/Publications/Statistics_Publications/Archived_Reports/), 2011.

[409] Susan Solomon, Dahe Qin, Martin Manning, Melinda Marquis, Kristen Averyt, Melinda M.B. Tignor, Henry LeRoy Miller Jr., and Zhenlin Chen. **Contribution of Working Group I to the Fourth Assessment Report of the Intergovernmental Panel on Climate Change, 2007**. Online

(http://www.ipcc.ch/publications_and_data/ar4/wg1/en/contents.html), 2007. Last accessed July 1 2013.

[410] IPCC. **2006 IPCC Guidelines for National Greenhouse Gas Inventories: Vol. 5 Waste**. Online (http://www.ipcc-nggip.iges.or.jp/public/2006gl/), 2006. Last accessed July 1 2013.

[411] Vasili S. Kazakov, Evgeni P. Demidchik, and Larisa N. Astakhova. **Thyroid cancer after Chernobyl**. *Nature*, **359**(6390):21, SEP 3 1992. Letter.

[412] Vini G. Khurana, Lennart Hardell, Joris Everaert, Alicja Bortkiewicz, Michael Carlberg, and Mikko Ahonen. **Epidemiological Evidence for a Health Risk from Mobile Phone Base Stations**. *International Journal of Occupational and Environmental Health*, **16**(3):263–267, JUL-SEP 2010. Article.

[413] Beirne S. Diamond D Kiernan B., Fay C. **Monitoring of gas emissions at landfill sites using autonomous gas sensors**. Project report, Environmental Protection Agency, 2010.

[414] Breda Kiernan, Stephen Beirne, Cormac Fay, and Dermot Diamond. **Measurement of Representative Landfill Gas Migration Samples at Landfill Perimeters: A Case Study**. In *24th International Conference on Solid Waste Technology and Management*, **24**, 2009.

[415] Breda Kiernan, Stephen Beirne, Cormac Fay, and Dermot Diamond. **Landfill Gas Monitoring at Borehole Wells using an Autonomous Environmental Monitoring System**. In *The 5th International Conference on Climate Change and Global Warming 2008*, **33**, pages 166–171, Heidelberg, Germany, September 2008.

[416] Breda Kiernan, Cormac Fay, Stephen Beirne, and Dermot Diamond. **Development of an Autonomous Greenhouse Gas Monitoring System**. In *World Congress on Science, Engineering and Technology 2008*, **34**, pages 153–157, Venice, Italy, 2008. WCSET 2008.

[417] X.F. Lou and J. Nair. **The Impact of Landfilling And Composting On Greenhouse Gas Emissions - A Review**. *Bioresource Technology*, **100**(16):3792 – 3798, 2009. Selected papers from the International Conference on Technologies and Strategic Management of Sustainable Biosystems.

[418] Marco Martuzzi, Francesco Mitis, and Francesco Forastiere. **Inequalities, inequities, environmental justice in waste management and health**. *European Journal of Public Health*, **20**(1):21–26, FEB 2010.

[419] Tuomas Nissila, Kostas Pentikousis, Ilkka Harjula, Jyrki Huusko, and Mika Rautio. **WiMAX backhaul for environmental monitoring**. In *MUM '08: Proceedings of the 7th International Conference on Mobile and Ubiquitous Multimedia*, pages 185–188, New York, NY, USA, 2008. ACM.

[420] Martina O'Toole, Roderick Shepherd, Gordon G. Wallace, and Dermot Diamond. **Inkjet printed LED based pH chemical sensor for gas sensing**. *Analytica Chimica Acta*, **652**(1-2, Sp. Iss. SI):308–314, October 2009.

[421] Riitta Pipatti and Margareta Wihersaari. **Cost-effectiveness of alternative strategies in mitigating the greenhouse impact of waste management in three communities of different size**. *Mitigation and Adaptation Strategies for Global Change*, **2**:337–358, 1997. 10.1007/BF02437050.

[422] Aleksandar Radu, Salzitsa Anastasova-Ivanova, Beata Paczosa-Bator, Marek Danielewski, Johan Bobacka, Andrzej Lewenstam, and Dermot Diamond. **Diagnostic of functionality of polymer membrane - based ion selective electrodes by impedance spectroscopy**. *Analytical Methods*, **2**(10):1490–1498, 2010.

[423] Tanja Radu, Cormac Fay, King-Tong Lau, and Dermot Diamond. **Wearable gas sensors**. In *International Workshop on Wearable Micro and Nano Technologies for the Personalised Health*, Oslo, Norway., June 2009.

[424] Alan Rosevear, Chris Deed, Jan Gronow, John Keenlyside, Richard Smith, and Peter Braithwaite. **Guidance on monitoring landfill gas surface emissions**. Technical report, Environmental Agency, U.K., 2004.

[425] C. Slater, J. Cleary, K. T. Lau, D. Snakenborg, B. Corcoran, J. P. Kutter, and D. Diamond. **Validation of a Fully Autonomous Phosphate Analyser Based on A Microfluidic Lab-on-a-chip**. *Water Science and Technology*, **61**(7):1811–1818, 2010. Article.

[426] The European Council. **1993/31/EC**. Technical report, The EC Council Directive, 1993.

[427] The European Parliament. **The EU Water Framework Directive**. Online (http://ec.europa.eu/environment/water/water-framework), 2010. Last accessed July 1 2013.

[428] Martina O' Toole, Leon Barron, Roderick Shepherd, Brett Paull, Pavel Nesterenko, and Dermot Diamond. **Paired emitter-detector diode detection with dual wavelength monitoring for enhanced sensitivity to transition metals in ion chromatography with post-column reaction**. *Analyst*, **134**(1):124–130, 2009.

[429] United Nations. **Kyoto Protocol**. Online (http://www.unfccc.int), 2010. Last accessed July 1 2013.

[430] M Vrijheid, B Armstrong, H Dolk, and EUROHAZCON Collaborative Grp. **Hazard scoring of landfill sites in relation to risk of congenital anomalies near hazardous waste landfill sites in Europe.** *American Journal of Epidemiology*, **147**(11, Suppl. S):297, JUN 1 1998.

[431] M Vrijheid, H Dolk, B Armstrong, L Abramsky, F Bianchi, I Fazarinc, E Garne, R Ide, V Nelen, E Robert, JES Scott, D Stone, and R Tenconi. **Chromosomal congenital anomalies and residence near hazardous waste landfill sites**. *LANCET*, **359**(9303):320–322, JAN 26 2002.

[432] Manabu Yasuda, Takeshi Hanagiri, Yoshiki Shigematsu, Takamitsu Onitsuka, Kouji Kuroda, Tetsurou Baba, Makiko Mizukami, Yoshinobu Ichiki, Hidetaka Uramoto, Mitsuhiro Takenoyama, and Kosei Yasumoto. **Identification of a Tumour Associated Antigen in Lung Cancer Patients with Asbestos Exposure**. *Anticancer Research*, **30**(7):2631–2639, JUL 2010. Article.

[433] Jennifer Yick, Biswanath Mukherjee, and Dipak Ghosal. **Wireless sensor network survey**. *Computer Networks*, **52**(12):2292 – 2330, 2008.

3

Wireless Aquatic Navigator for Detection and Analysis (WANDA)

"... Innovation is hard because it means doing something that people don't find very easy, for the most part. It means challenging what we take for granted, things that we think are obvious. The great problem for reform or transformation is the tyranny of common sense; things that people think, 'Well, it can't be done any other way because that's the way it's done'..."

— Sir Ken Robinson, TED, February 2010.

THE COST OF MONITORING and detecting pollutants in natural waters is of major concern. Current and forthcoming bodies of legislation will continue to drive the demand for spatial and selective monitoring of our environment, as the focus increasingly moves towards effective enforcement of legislation through detection of events, and unambiguous identification of perpetrators. However, these monitoring demands are not being met due to the infrastructure and maintenance costs of conventional sensing models. Advanced autonomous platforms capable of performing complex analytical measurements at remote locations still require individual power, wireless communication, processor and electronic transducer units, along with regular maintenance visits. Hence the cost base for these systems is prohibitively high, and the spatial density and frequency of measurements are insufficient to meet requirements. In this paper we present a more cost effective approach for water quality monitoring using a low cost mobile sensing/communications platform together with very low cost stand-alone 'satellite' indicator stations that have an integrated colorimetric sensing material. The mobile platform is equipped with a wireless video camera that is used to interrogate each station to harvest information about the water quality. In simulation experiments, the first cycle of measurements is carried out to identify a 'normal' condition followed by a second cycle during which the platform successfully detected and communicated the presence of a chemical contaminant that had been localised at one of the satellite stations.

Preamble

Paper 2 is based on another aspect of environmental chemical sensing/monitoring by optical means. The concept postulates the use of a different model for the monitoring of chemical contaminants within a water area without the need for repeating sensing components per sensing device in a network. In other words, a principle based on reduction of components is considered; a question that was raised due to the underlying costs involved in the traditional *dedicated device* approach e.g. Paper 1. In the first instance, i.e. proof of principle study, the possibility of this is examined. It is investigated through the use of a number of satellite stations (equipped with a colorimetric chemical transducer) in conjunction with a mobile robotic fish platform (equipped with a digital colour camera). The platform patrols a water body within a laboratory setting where it is investigated if the digital images can detect a localised chemical event induced through the introduction of a concentrated chemical *contaminant*. Overall, this study examines aspects of the digital imagery hypothesis i.e. repetition of electronic hardware within a sensing network, its capability to detect local events, and the dual use of a camera (i.e. additionally for navigation - albeit on a manual basis). Supporting information for the work within this chapter is present in Appendix B.

Sensing Approach

The proposed approach of using stationary sensor stations possess a number of conceptual advantages over equipping the mobile fish with sensors. The first is related to accuracy of the sensing location. By anchoring sensing stations to specific locations, one can ensure that the set location (in terms of latitude/longitude) is more accurate than a mobile platform that can be affected by strong currents or require additional circuitry (e.g. GPS, in which signals may not penetrate large depths). In addition, traditional WSNs must take into consideration the attenuation of standard radio signals by water (at 2.1 GHz, e.g. Zigbeem or Bluetooth), with necessary maintenance to power such devices. The approach proposed in this chapter harvests chemical information on an alternate basis without the need for wireless signals. Furthermore, reaction times for chemical sensors may also have an impact on the chosen approach, e.g. Nitrite detection by Griess approach can take up to 20 minutes for colour to form [559]. With sensors integrated on a sensing platform, a sample is traditionally harvested and stored within the device to allow for such reactions to occurr. Otherwise if the sensor is exposed to the surrounding environment, the location must be fully ensured; for mobile platforms this maybe difficult. However, for stationary stations, this is not an issue. Other rational advocating this approach will appear and be discussed within this chapter. As this work is in its proof of concept phase, additional arguments for this sensing approach will be discussed in

the future work section, i.e. in 6.3.2

Contributions

- To the Field
  - Investigation of a novel water quality sensing network;
  - Concept offers significant cost reduction method of infrastructure and maintenance;
  - Qualatitative or proof of principle stage explored through event detection of a chemical plume;
- By Candidate
  - Network - Concept, implementation, experimentation;
  - Robotic Fish - Design of electronic control circuitry and integration to PPy actuators;
  - Vision System - Image processing and analysis;
  - Control Program - Full design and implementation of base station control program;
- By Others
  - McGovern, S. - Polypyrrole actuators fabrication;
  - Lau, K.T. - Coating of the indicator strip with ethyl cellulose;

3.1 Introduction

It has been long recognised that the interaction between industrialised societies and the environment can be negative, in that concentrations of people in urbanised areas, with co-located industries will have a negative impact on the overall quality of the environment. An important aspect of this interaction is the release of pollutants into local water bodies, such as rivers and lakes, which can adversely affect the health of people and cause devastating fish kills [454, 441, 443, 459, 451, 463]. Consequently, environmental protection is a priority in modern society, and an extensive, and growing, body of legislation exists that specifies the limits of key chemical and biological pollutants in various types of water (potable, drinking, ground, etc.) [447, 440, 442].

Arising from the enforcement of this body of legislation is a growing need to police these pollutant limits, through analytical measurements that are used to determine the water quality [456]. However, these measurements are almost always achieved by taking samples from a relatively small number of designated locations, and analysing the composition at a centralised laboratory facility equipped with sophisticated state-of-the-art equipment. There are good reasons for employing this strategy, principally because of the high precision and accuracy of the measurements, which are vital for obtaining legally binding decisions against polluters. However, because of the expense involved to manage the analytical facilities and monitoring programmes, this model is inherently not scalable, and measurements are very restricted in terms of the number of locations and sampling frequency [448, 449].

In recent years, we have developed autonomous analyser platforms that can perform complex analytical measurements at remote locations, and make the resulting data globally available via websites. However, the cost base for these devices is still relatively high as it includes pumps, valves, microfluidics, optical detection, reagents, standards, electronics, power, and wireless communications, all housed within a robust enclosure [458, 452, 446]. In this paper, we present a radically different approach to remote water quality monitoring based on a low cost, biomimetic robotic fish, known as WANDA (wireless aquatic navigator for detection and analysis). The WANDA platform is capable of movement via a polymer actuator based tailfin [457], and can report what it 'sees' via an integrated low-power wireless video camera. The biomimetic fish can be used in conjunction with very low cost, dispersed, colorimetric 'satellite' sensors integrated into an easily recognised 3D form that enable very effective shape-identification algorithms [464] to be employed to distinguish the sensor from its surroundings. Once the sensor has been located, the camera is used to interrogate its condition and make the resulting data available via a wireless link. In this manner, a single, low-power robotic platform can harvest analytical information about the local chemical and/or biological environment at multiple locations using very low cost sensors.

In this paper, we demonstrate the principle of this approach using dispersed colorimetric sensors to probe changes in the local pH at several locations. Specifically, a water container of sufficient size (to allow for manoeuvrability) is setup within a laboratory setting. Several colorimetric sensors are then dispersed within the water container whereby an initial sensing patrol by WANDA allows for reference measurements of the sensors in uncontaminated conditions. A subsequent sensing patrol takes place whereby the water surrounding one station is acidified, resulting in a colorimetric change that is sensed by the camera. The results of the two patrols are compared showing that a change in pH has occurred in the water surrounding the station.

3.2 Robotic Fish Platform

The mobile wireless sensor platform used combines many disciplines into one practical device including materials science, wireless communications, vision systems, chemistry, systems control, biomimetics, and robotics. However, in this paper, we will focus on three of these:

- the biomimetic novel propulsion method;
- the ability to navigate and sense chemical events;
- system construction and control.

3.2.1 Propulsion Method

Conducting polymer actuators (or artificial muscles) based on polypyrrole (PPy) [461] have been utilised within the propulsive element of the tailfin of WANDA. With the application of an oscillating voltage (e.g. a low voltage square wave, ± 1 V 1 Hz), a bi-directional bending movement is derived from the actuators as one side becomes oxidised, and the other side is reduced. This oxidation/reduction process is accompanied by swelling/contraction of the respective polymer layers, due to movement of anions and water of hydration associated with the maintenance of overall charge neutrality, see Figure 3.1a. In such a system, the direction of bending is controlled by the polarity of the applied voltage. If a rigid tail fin is attached to a pair of actuators (Figure 3.1b) the force generated can enable a transfer of energy from the bending motion of the actuator to the water.

3.2.2 Navigation and Sensing

The WANDA platform was equipped with a wireless video camera for two main purposes. The first was for navigation as, through the video images, one can estimate

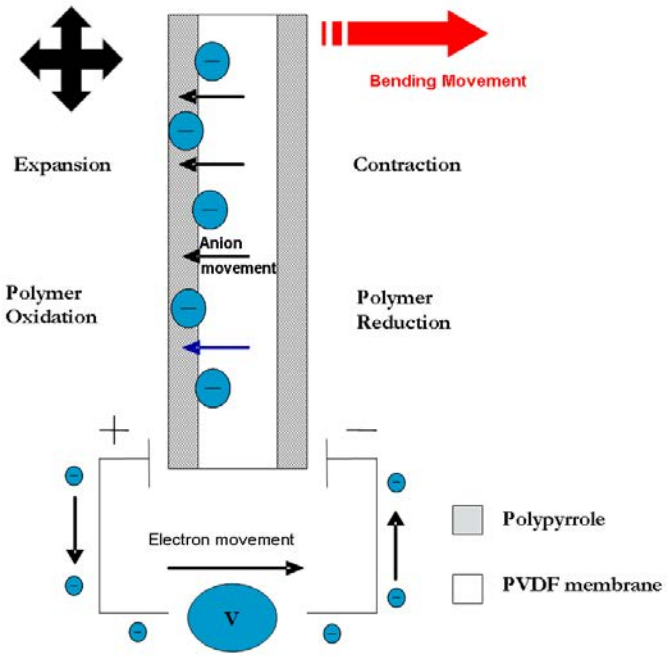

(a) Cross-sectional diagram showing bending principle of the tri-layer conducting polymer actuators. Applying a low electrical potential 'V' causes oxidation of one polypyrrole layer and reduction of the other resulting in a bending movement.

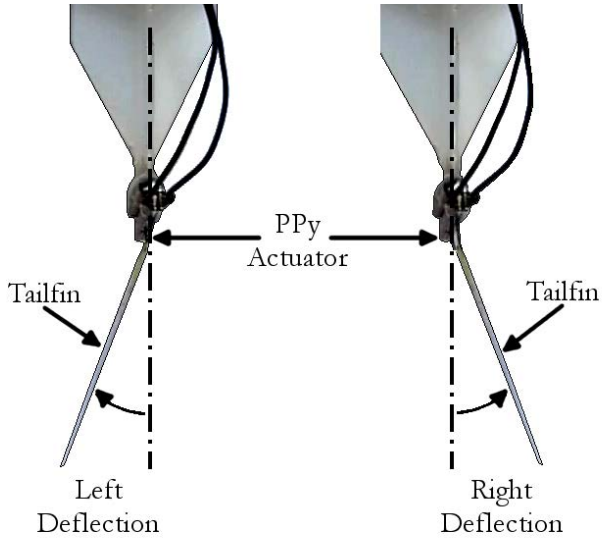

(b) Images showing the resulting bending movement of WANDA's polymer actuators when a rigid tailfin is attached.

Figure 3.1: Conducting polymer actuators used to propel the fish.

the location of the device while building a map of the environment. This technique, known as simultaneous localisation and mapping (SLAM), has received continuous attention for the last two decades [450, 444]. The second purpose of the onboard camera was to harvest information about the chemistry of the water body WANDA moves through. In this study, we achieve this through the use of a number of sensing stations fitted with a chemo-responsive dye which responds colorimetrically to changes in the chemistry of the local environment. By using the onboard camera, a mobile device can easily detect differences in colour and, in turn, this can be related to the levels of certain chemicals in that region of the water body. Previous works [493, 534, 465, 462, 453] have shown that it is possible to monitor changes of pH in a laboratory using a colour camera, and we have therefore selected this measurement as the proof of principle test for the platform.

3.2.3 System Construction and Control

A primary goal for the research was to control the movement of WANDA using a biomimetic polymer actuator. Figure 3.2 shows the assembly of the WANDA fish platform presented in schematic (Figure 3.2a) and photographic (Figure 3.2b) formats for clarity. The main components, i.e. wireless camera and control circuitry, were housed within a waterproof container (a truncated 50 ml syringe). Connected to the casing's bung are the PPy actuators to which the tailfin (cut from a thin plastic sheet) was attached. The range of the WANDA device was dictated by the wireless camera allowing for a transmission length of 100 m. The control circuitry was powered from the wireless camera's battery allowing for a continuous operation (PPy bi-directional actuation of 1 Hz with wireless video transmission) of WANDA for a period of ca. 3.5 h in its current configuration.

By coupling the propulsion method with machine vision techniques, autonomous control was achievable. Further, by interpreting the scene with data captured by the onboard camera using a combination of image processing algorithms, WANDA can avoid obstacles, track towards objects of interest, and/or perform chemical analysis. To achieve this, commands were sent from the base station to the tailfin control circuitry on board WANDA (Figure 3.3) and, in turn, alter the tailfin's state, resulting in motion.

In this study, WANDA moves through a fixed patrol route in a water container under remote control from the base station. When a chemical indicator station appears within the camera's field of view, colorimetric analysis is performed on the pixels representing the chemically responsive dye. This returns a quantitative estimation of the pH of the immediate environment surrounding the chemical indicator station.

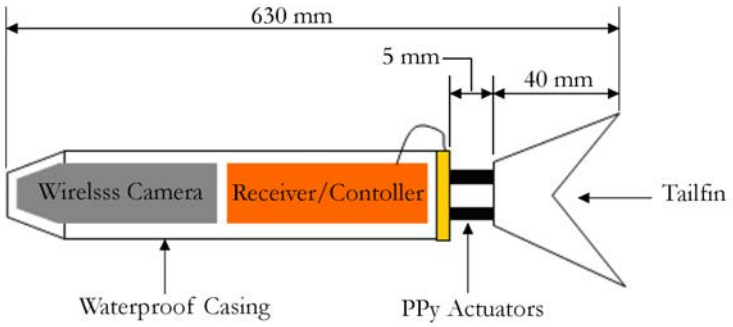

(a) Diagram showing the wireless camera, controller, casing, PPy actuators, and tailfin arrangement on the WANDA device. Dimensions added for size reference.

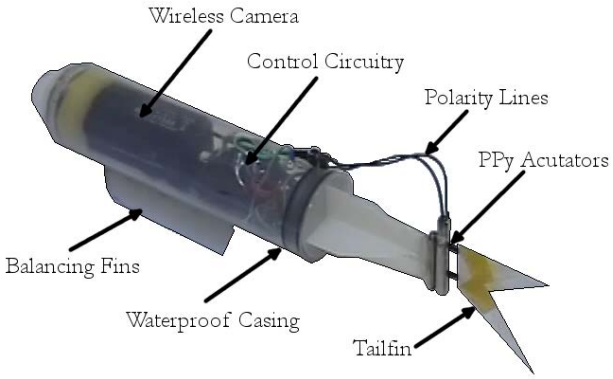

(b) Image of WANDA assembly for visual reference. Major components labelled including left balancing fin (right balancing fin obscured from view).

Figure 3.2: Assembly of the WANDA platform.

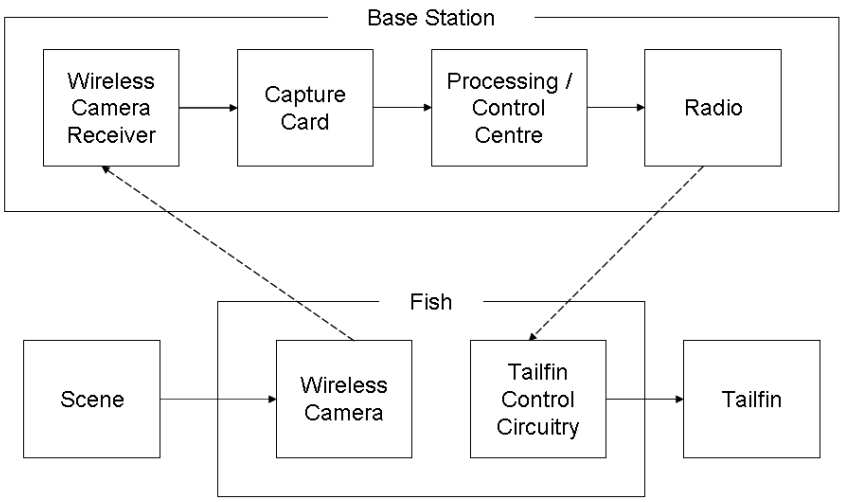

Figure 3.3: Block diagram illustrating the full closed loop control system of WANDA and sub unit interactions thereof. A captured 'scene' is relayed via the 'wireless camera' on the 'fish' to the 'wireless camera receiver' on the 'base station'. The 'capture card' forwards the image to a pc or 'processing/control centre' where it extracts and analyses data. Decisions are made based on this data and forwarded via the 'radio' to the 'tailfin control circuitry' on board the 'fish' where it alters the 'tailfin' state resulting in controlled directional movement.

3.3 Experimental

3.3.1 Materials and Equipment

A standard colour reference chart (X-Rite Colour Checker Passport) was used as reference for colorimetric analysis. The wireless camera (ZTV ZT830T) transmits a video stream from WANDA to the receiver (AEE AR101 placed ca. 4 m from the water container), which forwards it to the video capture card (Avermedia C038). The main processor (Dell Latitude D630) interrogates the signal and sends a direction command via radio (EZ Radio ER900TRS 250 m possible range) to the microcontroller (PIC16F683) on WANDA which, in turn, controls the tailfin (polypyrrole) movement.

The water container (Intex 59416NP) used for experimentation, was cylindrically shaped with a diameter of 114 cm, a height of 25 cm and filled 8 cm with water allowing sufficient room for WANDA to manoeuvre. One molar HCl solution was made from 37% HCl (Scharlau AC0741) and ultra pure water (Millipore Milli-Q), and this was used to change the local pH near one of the pH sensing stations. Three identical pH sensing stations were constructed as shown in Figure 3.4. The stations consisted of a standard 20 ml vial affixed (Loctite 3430) to a heavy metallic base with a strip of Universal Indicator (Johnson Universal pH Indicator) attached around the centre of the vial. The strip was modified with ethyl cellulose (Sigma–Aldrich 28244) to reduce leaching effects. This was achieved by dissolving 100 mg of ethyl cellulose in 10 ml of solvent (ethanol). After manually coating the strip, a thin layer of porous ethyl cellulose resulted, allowing efficient exchange of H^+ ions but inhibits loss of the much larger dye molecules.

Software components used as part of overall system integration include:

- Java runtime edition (JRE) — standard java programming package;
- Javax.comm — serial port communications;
- Direct show java (DSJ) — video capture;
- Java advanced imaging (JAI) — video processing and analysis;

3.3.2 Image Processing

The video stream was captured from the capture card at a standard size of 640 × 480 pixels, 15 frames per second (fps), 24-bit colour depth (8 × 8 × 8), and

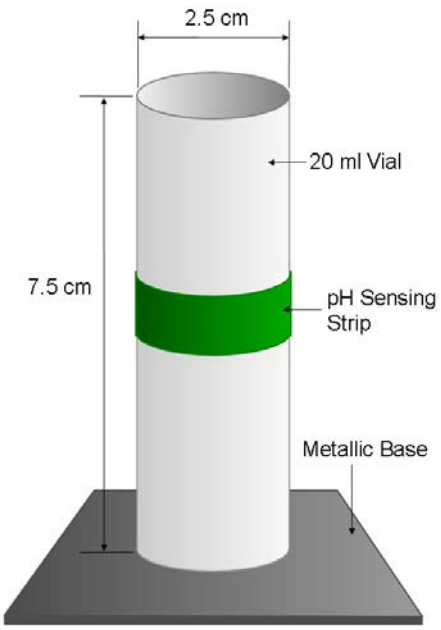

Figure 3.4: Diagram showing the construction of a pH sensing station used during patrols. A standard 20 ml cylindrical vial is affixed to a heavy metallic base used as an anchor. One strip of universal pH indicator coated with ethyl cellulose is attached around the centre of the vial. Dimensions added for size reference.

in raw RGB format as any artefacts arising from compression algorithms (such as the MPEG family) may distort the estimated values. Figure 3.5a shows a captured image of a submerged sensor station. For colorimetric analysis, it was necessary to extract the image region representing the pH sensing strip (see Figure 3.4). To achieve this (Figure 3.5cb) a number of image processing steps were combined to segment the region of interest (i.e. to identify all pixels that represent the pH chemo-responsive material of the sensor station). Firstly, a region of interest is selected containing the indicator material and background. After that, to aid in the segmentation process, noise reduction techniques were applied; a median filter [439] followed by a standard 3×3 grey level morphological dilation [438]. Subsequently, a transformation from the sRGB colour space to the HSI colour space [567] was performed to assist colorimetric analysis, i.e. to investigate if a more robust model to variable lighting intensities can be used, see Section 3.4.1. Since the pH material will only change colour between green and red when acid is introduced (Figure 3.6), a band pass filter was applied to the Hue channel (from 0 to 2.09 rad, see Figure 3.7 for quantitative values in relation to colours [436]). Next, a standard region labelling algorithm was applied to the Hue channel. This gave a grey level image whereby neighbouring pixels of similar colour/hue were connected together into one region. These regions were then ranked in order of their total number of pixels. The second largest region was taken to represent the indicator material as the largest

(a) Single captured image of a pH sensing station from the wireless camera.

(b) Generated binary mask image after applying region segmentation image processing algorithms. White pixels representing the pH sensing strip region.

(c) Resulting image of the extracted pH indicator region after applying the binary mask image to the original captured image.

Figure 3.5: Segmentation process to selectively extract the pH indicator region of the test station in the water container.

Figure 3.6: Image showing the reference chart accompanying the pH indicator (Johnson Universal pH Indicator).

represented the background. A binary mask image was created with white pixels set as the indicator region, see Figure 3.5b. Following this, a binary morphological erosion process [435] was applied to remove edge pixels that may belong to the background and thus interfere with analysis. Figure 3.5c shows the final step of the segmentation process once the mask was applied to the original image. The average of every identified pixel's hue component was taken to represent the pH at a given station.

3.3.3 Experimental Procedure

First, a comparison was drawn between using the sRGB and HSI colour spaces to investigate which model was more robust to light variation. To achieve this, the camera was maintained at a fixed location in an area of variable lighting intensities with the colour checker chart in view for reference (Figure 3.8a), and a number

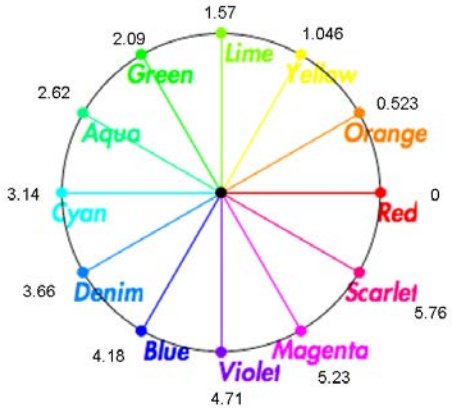

Figure 3.7: Hue channel of the HSI colour space [436] normalised between 0 and 2π. Image shows quantitative values in relation to common colours at 30 degree (0.523 rad) intervals.

of changes in the lighting were applied to investigate the robustness of the colour determination, see Section 3.4.1 and Figure 3.8d.

Next it was necessary to investigate the camera's response to pH induced colour changes. WANDA was kept stationary in the water container allowing for a continuous view of one pH station, see Figure 3.9 for setup. Next, ca. 5 ml of the HCl solution was injected using a standard 5 ml pipette around the sensing station causing a colorimetric change of the pH sensor. After that, the indicator was encouraged to return to its original state i.e. prior to the addition of the acid solution by manually mixing the water in the vicinity of the station to disperse the acid plume. The resulting video stream was processed and analysed as explained previously in Section 3.3.2 and a plot of the changing state of the colorimetric sensor from a neutral (green) to an acidic (yellow) state was generated, see Section 4.2 and Figure 3.10. This process was repeated three times to investigate reproducibility.

To determine if WANDA can detect a chemical event during a patrol, three pH indicator stations, designated as L1, L2 and L3, were placed at three different locations within the water container as shown in Figure 3.11. Software was implemented to achieve an autonomous circular patrol route within the water container with a diameter of ca. 0.7 m. The starting point 'S' was defined to be the starting point and the finishing point WANDA reaches on its circular patrol route when viewed from above. Each station was positioned to be in the camera's field of view as WANDA swims past. Next, a pH plume was injected at station L2 causing a colorimetric change in the pH sensor. Three images of each pH station were processed and analysed as explained in Section 3.2. Finally, the hue value of each sensor station against time was plotted, see Section 4.3, Figure 3.12, and Figure 3.13.

(a) Single captured image of the X-Rite colour reference chart from the wireless camera.

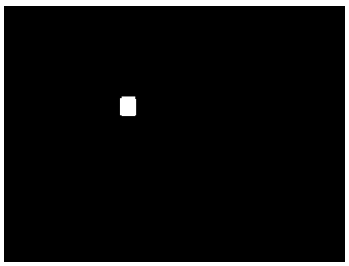

(b) Generated binary mask image after applying region segmentation image processing algorithms.

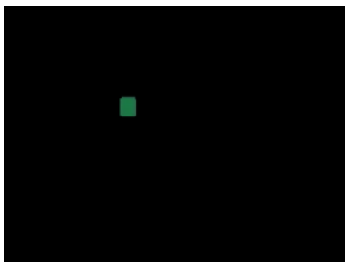

(c) Resulting image of the extracted green patch region after applying the binary mask image to the original captured image.

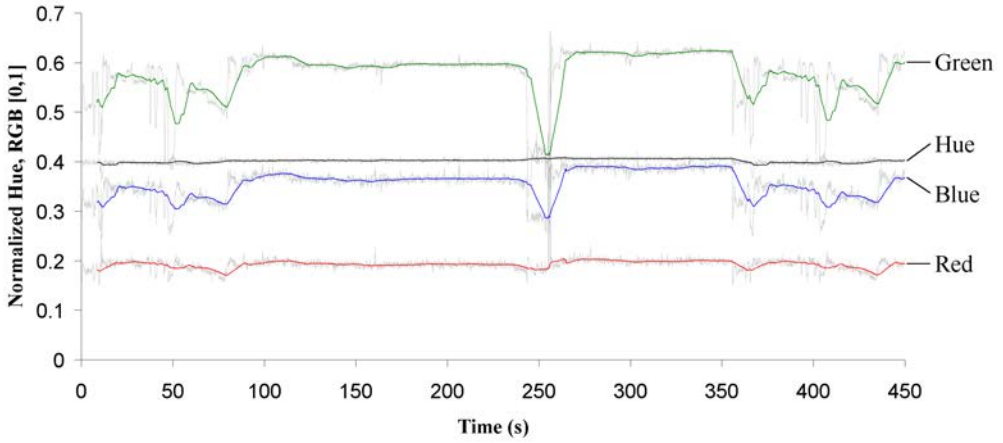

(d) Real-time plot of the colour reference chart's green patch over a period of 450 s, showing the response of the red, green, blue, and hue components. Smoothing (heavy lines) applied to raw captured data (grey lines) for visualisation purposes.

Figure 3.8: Segmentation and evaluation process to selectively extract a reference colour patch, analyse it under induced light intensity variations and compare the RGB and HSI colour spaces.

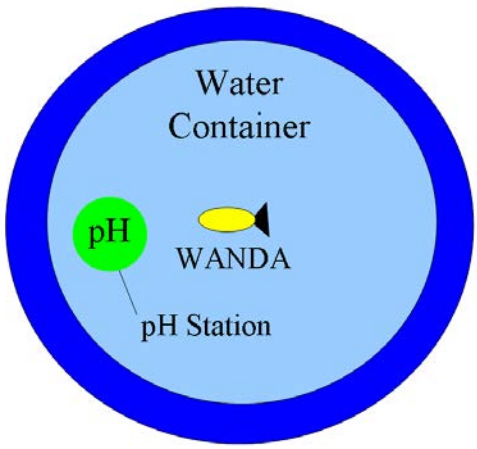

Figure 3.9: Layout of pH station and WANDA within the water container for profiling the response of the camera to induced pH changes of the water surrounding a sensing station. See Figure 3.5a for a similar captured view of the sensing station.

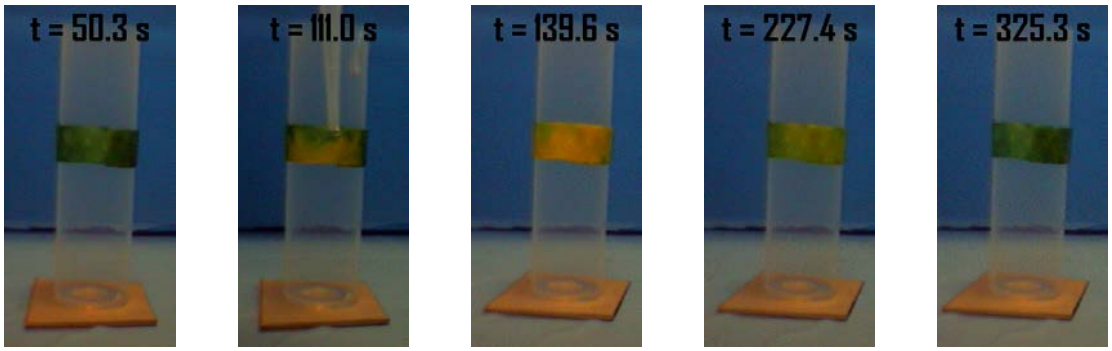

(a) Before acidification. (b) During acidification. (c) Acidified. (d) Recovering. (e) Recovered.

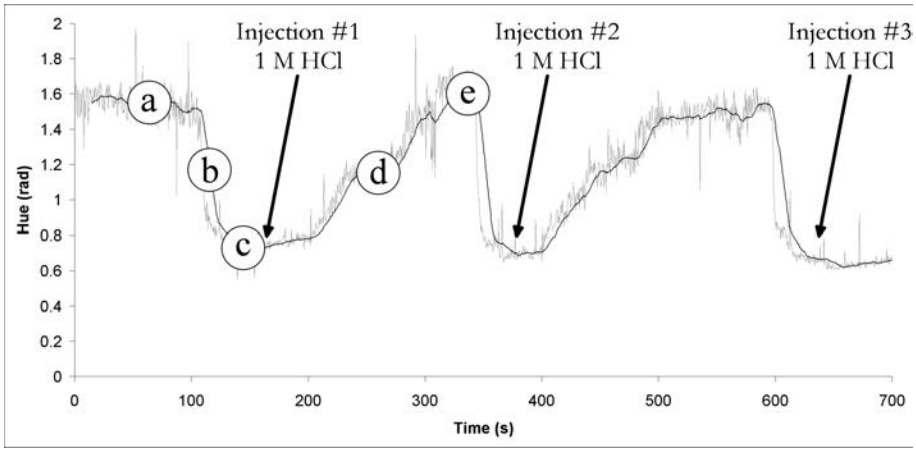

(f) Real-time response plot of the camera's hue analysis of the sensing station to 3 induced pH changes over time. Labels 'a'–'e' correspond to sub figures 'a–e', respectively. Smoothing (black line) applied to raw captured data (grey line) for visualisation purposes.

Figure 3.10: Image sequence and response plot showing reaction to addition of acid near a sensor station.

3.4 Results and Discussion

3.4.1 Using a Video Camera as a Chemical Detector

Previous studies, as mentioned in Section 2.2, have successfully used a video camera as a pH colorimetric detector. However, these studies have been performed under controlled lighting conditions and using the RGB colour model. A key requirement

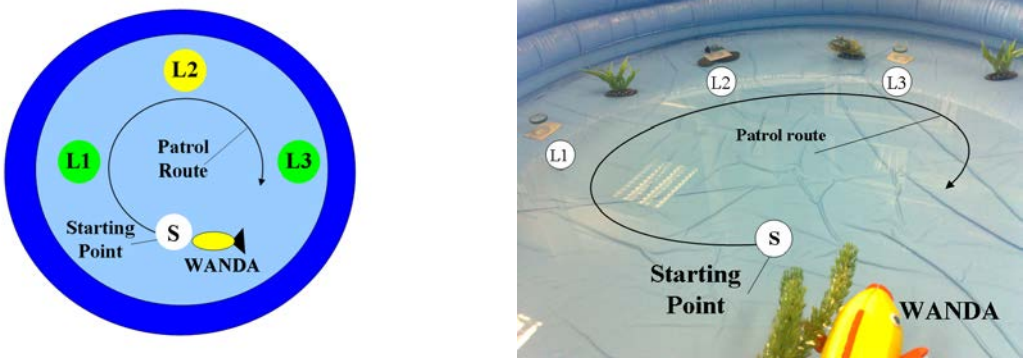

(a) Plan view diagram of patrol route of sensing platform.

(b) Corresponding photographic image for reference.

Figure 3.11: Layout of pH stations and patrol route within the water container. 'S' starting and ending point of the patrol route, 'L1' pH station 1, 'L2' pH station 2, 'L3' pH station 3.

in this study was for the system to be capable of performing under variable ambient lighting conditions. The RGB colour space is inherently sensitive to variations in lighting, and cannot meet this requirement; thus a more robust method was needed. For this reason the HSI colour space technique was adopted. The transformation from RGB to HSI separates the light intensity 'I' (intensity), colour intensity 'S' (saturation) and colour 'H' (hue) into separate components. By separating the light intensity from the colour, the Hue component is more robust than RGB to variable lighting conditions. To illustrate this, Figure 3.8a–c shows segmentation steps of the colour chart's green patch (chosen as it was the nearest colour to the neutral state of the pH indicator, seen in Figure 3.5a).

Figure 3.8d shows the real-time plot of the colour reference chart's green path over a period of 450 s. During this time deliberate light variation effects were implemented such as shadows at the beginning (0 – 100 s) and end (350 – 450 s) and switching on and off the laboratory light at ca. 250 s. This figure (where all component values are normalised between 0 and 1) shows the effects of light intensity variations on the individual green, blue, red and hue components, ordered from most to least effected. It can be seen that the RGB components do not respond uniformly to the induced lighting effects. The non-uniformity results from a combination of two factors; the light source and the response of the red, green and blue photo sensors within the camera. However, the hue component remains less sensitive to the camera calibration and light source and, as such, is our preferred choice for our analysis during subsequent patrols, see Section 3.4.3.

3.4.2 Camera Evaluation

For proving the overall concept hypothesised in this paper we are only interested in two clearly detectable states; neutral 'pH 7' and an identifiable acidic 'pH < 5' while

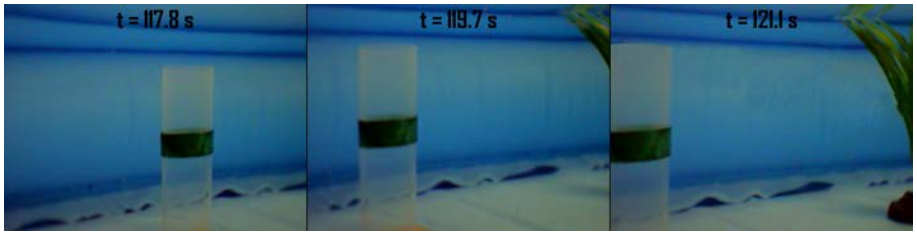

(a) Three captured video frames of pH station L1 as WANDA swims past.

(b) Three captured video frames of pH station L2 as WANDA swims past.

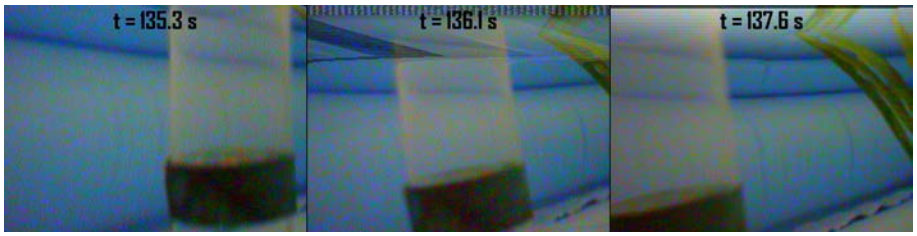

(c) Three captured video frames of pH station L3 as WANDA swims past.

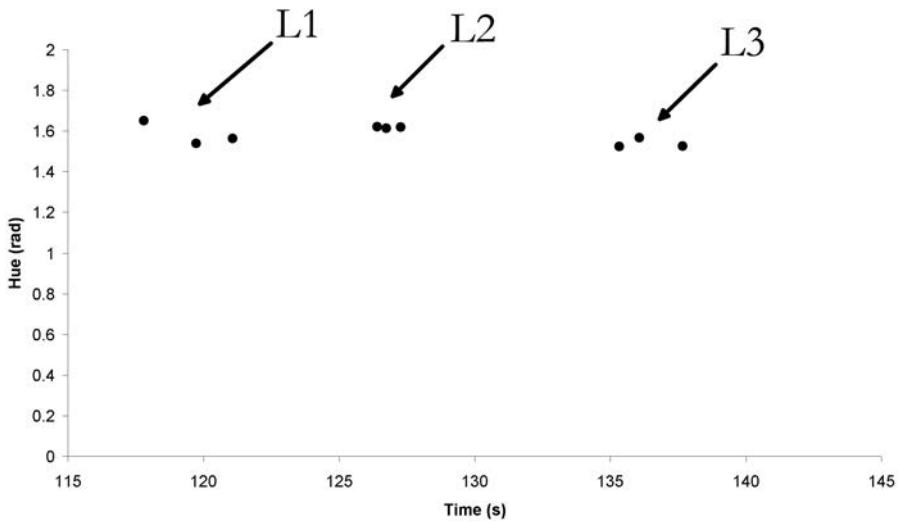

(d)

(d) Response plot of the camera's hue analysis of sensing stations L1, L2, and L3 corresponding to sub figures (a)–(c).

Figure 3.12: Image sequence and response plot showing the response of the camera to all three pH sensing stations during Patrol # 1 'normal conditions' in the water container.

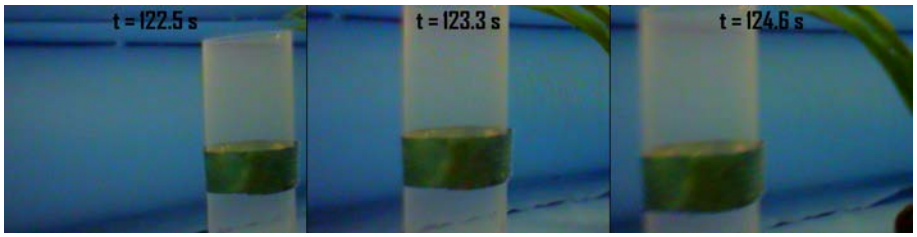

(a) Three captured video frames of pH station L1 as WANDA swims past.

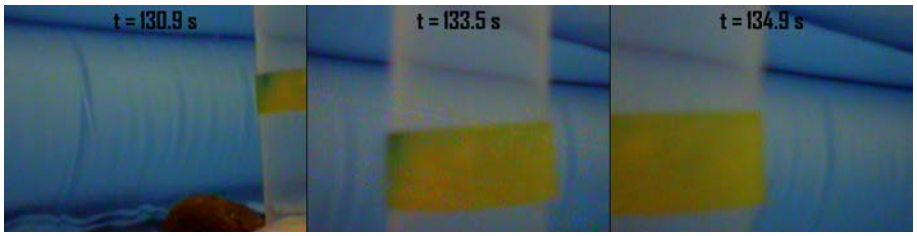

(b) Three captured video frames of pH station L2 as WANDA swims past.

(c) Three captured video frames of pH station L3 as WANDA swims past.

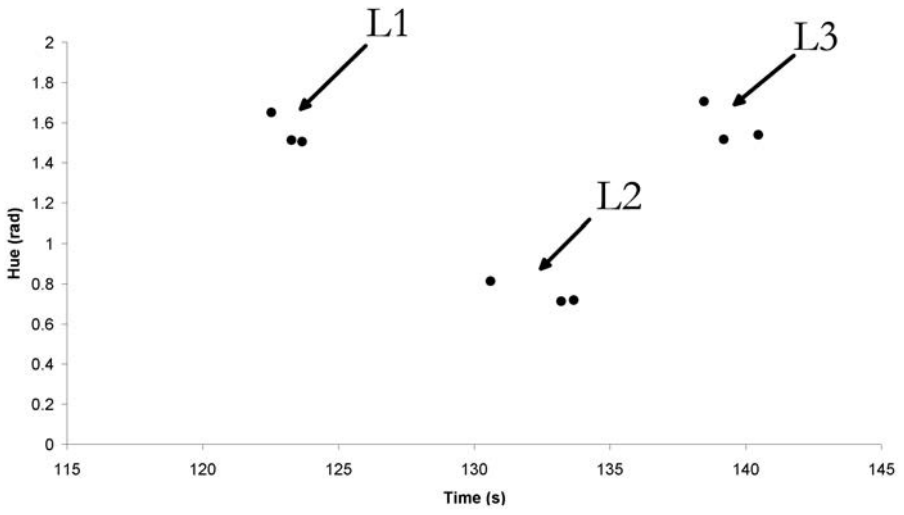

(d) Response plot of the camera's hue analysis of sensing stations L1, L2 and L3 corresponding to sub figures (a)–(c).

Figure 3.13: Image sequence and response plot showing the response of camera to all three pH sensing stations during Patrol # 2 'change in local pH conditions' in the water container.

keeping the detection system robust to variations in lighting. Figure 3.6 shows the reference chart accompanying the pH indicator. In its neutral state, i.e. pH 7, the indicator is green in colour, however, when an acid is introduced the colour will shift towards a colour between green and red depending on the concentration of acid and its dispersion in the water.

The camera's response was profiled by analysing the pH strip in its neutral and acidic states. WANDA was kept stationary in the water container with a pH station directly in the camera's field of view (Figure 3.9). An acidic plume was introduced near the pH station by injecting ca. 5 ml 1 M hydrochloric acid, triggering a colour change of the pH indicator material. The indicator pixels in the captured image were extracted using the image processing approach outlined previously and the colour change was represented numerically according to the hue angle. Figure 3.10 shows the analysis of the dominant Hue colour value of the pH station in the two identifiable states; green in neutral state and yellow when the acidic plume was introduced (a pH change from 7 to ca. 5, see Figure 3.6 and Figure 3.7). Figure 3.10f shows a plot of this change occurring three times. Labels a–e in Figure 3.10f show a correlation to Figure 3.10 sub-figures (a)–(e), numerically and visually, of the change and recovery at specified times. From Figure 3.10f it can be seen that this process is clearly reproducible and that the colour/Hue is proportional to the level of chemical contaminant. The response is sufficiently clear to enable the two states to be identified. For more accurate analysis we could consider employing noise reduction algorithms such as dropping frames with identifiable noise during image processing.

3.4.3 Environmental Monitoring—WANDA on Patrol

Once it had been established that the camera can be used to detect the presence of an acid plume in the immediate environment surrounding the pH sensor station, the approach was extended to the use of WANDA in a 'patrol' mode, where WANDA would follow a set path to check the pH status of the water container by monitoring the colour of several land mark stations.

The three pH stations, labelled (L1, L2, and L3), were placed in different areas of the water container and a fixed patrol route was defined; starting from point S, passing station 1, 2, and 3 *en route* and finishing up back at the starting point. Video images were recorded and transmitted wirelessly in real-time to a PC. Image analysis was performed off-line for these experiments, but it was our intention to develop a fully autonomous procedure that will be implemented on the WANDA platform. Three video frames per station were manually selected to investigate reproducibility. These frames were chosen to offer the best quality for analysis, i.e. those without any noise obscuring the colorimetric sensor pixel area.

Two separate patrol operations were performed to demonstrate the principle.

- Patrol # 1: Normal condition; all landmark stations were green in colour;
- Patrol # 2: Event occurred; the environment surrounding station L2 was acidified and the station indicated a yellow colour. The other two stations (L1 and L3) remained unchanged to simulate a locally occurring event;

The results from Patrol # 1 were analysed and used as reference for normal conditions. Any change in colour on each of the landmark station would therefore be indicative of a change in their respective local chemical environment.

During operation, the individual landmark identity was signified by its specific shape and feature (cylindrical with colour strip) from its surroundings and the time taken to reach it. A specifically shaped colour code could be used for each location if preferred; here we adopted the simplest format to reduce the amount of image analysis for site recognition in this first trial.

Figure 3.12(a–c) displays an extracted image sequence from the video stream showing that the three indicator stations are green for visual reference. The result of the image analysis (Figure 3.12d) indicates that the three stations gave a similar green hue output with values of ca. 1.6 rad, in agreement with the initial camera response experiments (see Figure 3.10f). This data has shown that WANDA – in conjunction with the image analysis technique – was successful in determining the correct status of the colorimetric sensors, i.e. that the environmental status of all sensor stations was 'normal'. This information was stored and used as reference for future monitoring operations.

By comparing the colour/hue state of the indicator stations in future patrols with the reference data; one can therefore provide information about changes in the local pH. This is demonstrated here in the case of Patrol # 2. The exact same method for Patrol # 1 was employed to produce video images and colour information for Patrol # 2, shown in Figure 3.12 and Figure 3.13, respectively. The captured images (Figure 3.12 and Figure 3.13) show that stations L1 and L3 remain unchanged, whereas station L2 (Figure 3.12 and Figure 3.13) has changed from green to yellow, visually indicating that the sensor has responded to a change in pH of the environment immediately surrounding station L2 and that this contaminant was localised because it did not affect stations L1 or L3. The results of the image analysis (Figure 3.12 and Figure 3.13) indicates that the two stations L1 and L3 gave similar green hue outputs (ca. 1.6 rad) as previously recorded, whereas L2 has changed its reported hue output from ca. 1.6 rad to ca. 0.7 rad. Hence the change in sensor colour was successfully captured by WANDA.

A more robust and simple technique has also been developed to determine if an event has occurred. It is based on comparing the hue value of each respective sensor stations between different patrols through the comparison of the ratio of the sensor hue values between runs. For comparison, a single hue value is taken to represent each sensing station; i.e. the hue average of the 3 captured images of a single sensing

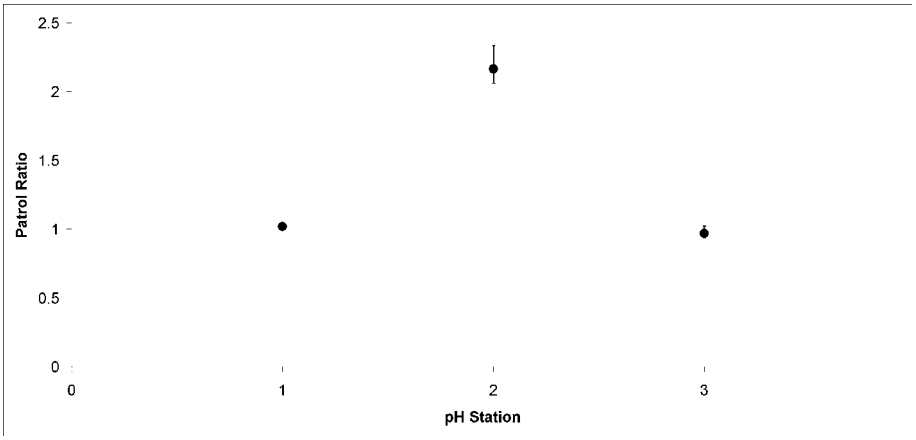

Figure 3.14: Comparison of Patrol # 1 and Patrol # 2. A single hue value is taken to represent each sensing station. Points represent the average hue ratio of station's L1, L2 and L3. Upper and lower error bars represent the max and min hue ratio, respectively.

station is calculated and is representative of the station's pH state. Next, the hue ratio of each respective sensing station is calculated, e.g. ratio of L1 (Patrol # 1) to that of L1 (Patrol # 2). Figure 3.14 shows the plot of the hue ratio of respective sensors between Patrol # 1 and Patrol # 2. The results clearly show that when there was no change in the pH environment, the colour ratio of the sensor stations (L1 and L3) were very close to 1. Meanwhile a ratio value of >2 was obtained for L2 when a pH change in the surrounding environment was induced. This demonstrates that WANDA has successfully reported a chemical change in the local environment.

This simple analysis technique can be made useful for detecting minor changes in a pH environment by setting a threshold value of how far the ratio deviates from normal conditions (e.g. 5% deviation from ratio = 1), resulting in a semi quantitative mobile warning system for detecting localised events in target areas.

3.4.4 Significance and Future Developments

The significance of the approach demonstrated in this paper to the realisation of water quality monitoring sensing networks is that it potentially allows for a significant cost reduction of infrastructure and maintenance. The need for power, communications, and processing units is no longer necessary for individual sensor stations. As a result, this model is inherently more scalable than traditional techniques and as such allows for wider areas to be sensed meeting the needs of future legislation. Other areas where this type of technology may be useful include; port monitoring for oil spillages, air quality in hazardous workplaces, food preparation surroundings, detection of threats (e.g. detection of release of chem/bio-warfare agents) using mobile or fixed cameras. For example, low cost colorimetric sensors could be deployed within water catchments areas or aquariums where ammonia levels increases

with biological waste. If the continuously operating filtration system breaks down without a monitoring technique in place, such as the approach offered in this paper, it can result in heavy cost and loss of fish life. As this concept is in its early stage, numerous improvements can be introduced. Since the patrol route was fixed; the order/time at which the stations were encountered was used for identification purposes. Although it is not required for the simplified conditions in this lab experiment, deployments in real situations will rely more significantly on a shape and/or a colour coded pattern design as a discriminating factor. The chemical indicator stations can be designed with a unique 3D shape/colour id with a high contrast to anything in its environment for location/identification purposes.

Noise is an unavoidable problem for any analytical measurement. For the approach used in this study, i.e. using a wireless camera for chemical analysis, image quality is paramount. Limitations of using wireless cameras have been outlined by Byrne et al. [434], where one faces challenges such as range, chromatic noise, horizontal scan line noise, and visible vertical blanking due to vertical sync loss. Such challenges have been encountered in this study, i.e. visible in plots Figure 3.8 and Figure 3.10 shown as grey lines. Methods to overcome these problems can include noise identification in video frames (mentioned in Section 3.4.2) and/or to perform image and video processing on the device itself (mentioned in Section 3.4.3) whereby an autonomous regime can be implemented on WANDA allowing for flexibility towards true autonomy without range limitations.

Improvements to the platform itself are also foreseen. At present, WANDA is limited to low flow rate areas in its current implementation. Enhancements may include; the development of a more streamlined casing to accommodate higher flow rates, investigation into new PPy arrangements for greater efficiency, or even replacement of the propulsion method with a more conventional system. However, replacing the propulsion may impact on deployment life-time due to a higher power draw, e.g. a motor with directional control. Multiple dye-based sensors immobilised on a single station will enable the status of multiple components and numerous locations to be monitored. Establishing colour references on stations in conjunction with adaptive training techniques may help with any potential biological fouling or medium discolouration encountered in long term real deployments. Further research into how this detector will behave with drastically changing lighting conditions in a real environment, e.g. night time, is clearly necessary. In addition, generating more robust quantitative data will be necessary before one can expect real deployments to be productive.

3.5 Conclusions

This work reports the successful demonstration of a novel approach to chemical sensing networks. A low cost, biomimetic robotic fish was used to patrol a water container in a laboratory and inspect static chemical sensor stations *en route*. A first patrol was used as a reference for normal conditions. During a second patrol, a contaminant was added in the vicinity of one of the stations. By applying a sequence of image processing techniques to the captured video stream, the presence of the pH plume was successfully identified. While this study comprised of three stations, each with one colorimetric sensor, the approach is potentially scalable to numerous stations fitted with multiple sensors for a range of possible contaminants. Moreover with evolving CCD technology, power efficiency and processing power; it is feasible that the entire detection-processing algorithm will be integrated onto the autonomous vehicle in the near future.

3.6 References

[434] J. Byrne and R. Mehra. **Wireless Video Noise Classification for Micro Air Vehicles**. In *Proceedings of the 2008 Association for Unmanned Vehicle Systems International (AUVSI) Conference*. AUVSI, June 10-12, 2008 2008.

[435] Rafael C. Gonzalez and Richard E. Woods. *Digital image processing*. Prentice Hall, Upper Saddle River, NJ, 2002.

[436] Brand Fortner and Theodore E. Meyer. *Number by colors : a guide to using color to understand technical data*. TELOS, Electronic Library of Science, Santa Clara, Calif, 1997.

[437] Alvy Ray Smith. **Color gamut transform pairs**. In *SIGGRAPH '78: Proceedings of the 5th annual conference on Computer graphics and interactive techniques*, pages 12–19, New York, NY, USA, 1978. ACM.

[438] SUN Microsystems. *Programming in Java Advanced Imaging*. SUN Microsystems, 1999.

[439] J.J. BARDYN et al. **Une architecture VLSI pour un operateur de filtrage median**. In *Congres Reconnaissance des Formes et Intelligence Artificielle*, **1**, pages 557–566, Paris, 25th - 27th January 1984 1984.

[440] United States Environmental Protection Agency. **Office of Ground Water and Drinking Water**. Online (`http://water.epa.gov/drink/index.cfm`), January 2013.

[441] S. N. Al-Bahry, I. Y. Mahmoud, K. I. A. Al-Belushi, A. E. Elshafie, A. Al-Harthy, and C. K. Bakheit. **Coastal sewage discharge and its impact on fish with reference to antibiotic resistant enteric bacteria and enteric pathogens as bio-indicators of pollution**. *Chemosphere*, **77**(11):1534–1539, DEC 2009.

[442] The United States Water Quality Association. **Water Quality Association**. Online (`http://www.wqa.org/`), January 2013.

[443] Brian Austin. **The Involvement of Pollution with Fish Health**. In Carmel Mothersill, Irma Mosse, and Colin Seymour, editors, *Multiple Stressors: A Challenge for the Future*, NATO Science for Peace and Security Series, pages 13–30. Springer Netherlands, 2007.

[444] Tim Bailey and Hugh Durrant-Whyte. **Simultaneous localization and mapping (SLAM): Part II**. *IEEE Robotics & Automation Magazine*, **13**(3):108–117, SEP 2006.

[445] Liam Byrne, Kim Lau, Steve Edwards, and Dermot Diamond. **Digital imaging as a detector for quantitative colorimetric analyses**. In SPIE, editor, *Proc. SPIE 4205, Advanced Environmental and Chemical Sensing Technology*, **267**, pages 267–277. SPIE, February 2001.

[446] John Cleary, Conor Slater, Christina McGraw, and Dermot Diamond. **An autonomous microfluidic sensor for phosphate: On-site analysis of treated wastewater**. *IEEE Sensors Journal*, **8**(5-6):508–515, MAY-JUN 2008.

[447] The European Commission. **The EU Water Framework Directive - integrated river basin management for Europe**. Online (`http://ec.europa.eu/environment/water/water-framework/index_en.html`), October 2000.

[448] D Diamond. **Internet-scale sensing**. *Analytical Chemistry*, **76**(15):278A–286A, AUG 1 2004.

[449] Dermot Diamond, King Tong Lau, Sarah Brady, and John Cleary. **Integration of analytical measurements and wireless communications - Current issues and future strategies**. *Talanta*, **75**(3):606–612, May 15 2008.

[450] H Durrant-Whyte and T Bailey. **Simultaneous localization and mapping: Part I**. *IEEE Robotics & Automation Magazine*, **13**(2):99–108, Jun 2006.

[451] James Hayden. **Fisheries officials investigate Tipperary fish kill**. Online (`http://search.proquest.com/docview/529531204?accountid=15753`), Jul 02 2009. Copyright - Copyright The Irish Times Ltd. Jul 2, 2009; Language of summary - English; ProQuest ID - 529531204; Last updated - 2010-07-17; Place of publication - Dublin, Ireland; Corporate institution author - Hayden, James; DOI - 1889735562; 24025008; 81199.

[452] Jer Hayes, John Cleary, Conor Slater, King Tong Lau, and Dermot Diamond. **Intelligent Environmental Sensing with a Phosphate Monitoring System and Online Resources**. *AIP Conference Proceedings*, **963**(2):1216–1219, 2007.

[453] J. Hayes, A. Pacquit, K. Crowley, Kim Lau, and D. Diamond. **Web-based colorimetric sensing for food quality monitoring**. In *Sensors, 2006. 5th IEEE Conference on*, pages 855 –858, oct. 2006.

[454] Mark V. Hoyer, D. L. Watson, D. J. Wills, and D. E. Canfield, Jr. **Fish Kills in Florida's Canals, Creeks/Rivers, and Ponds/Lakes**. *Journal of Aquatic Plant Management*, **47**:53–56, Jan 2009.

[455] KT Lau, S Edwards, and D Diamond. **Solid-state ammonia sensor based on Berthelot's reaction**. *Sensors and Actuators B-Chemical*, **98**(1):12–17, MAR 1 2004.

[456] John Lucey. **Water Quality In Ireland 2007-2008 : Key Indicators of the Aquatic Environment**. Technical Report 978-1-84095-319-0, Environmental Protection Agency, Johnstown Castle, Wexford, Ireland, 2009.

[457] Scott McGovern, Gursel Alici, Van-Tan Truong, and Geoffrey Spinks. **Finding NEMO (novel electromaterial muscle oscillator): a polypyrrole powered robotic fish with real-time wireless speed and directional control**. *Smart Materials & Structures*, **18**(9):1, SEP 2009.

[458] Christina M. McGraw, Shannon E. Stitzel, John Cleary, Conor Slater, and Dermot Diamond. **Autonomous microfluidic system for phosphate detection**. *Talanta*, **71**(3):1180–1185, FEB 28 2007.

[459] VOA News. **Fish Kills Linked to Water Pollutants**. Online (`http://www.voanews.com/content/a-13-2009-10-19-voa1/414776.html`), November 2009.

[460] A. Safavi, N. Maleki, A. Rostamzadeh, and S. Maesum. **CCD camera full range pH sensor array**. *Talanta*, **71**(1):498–501, JAN 15 2007.

[461] E Smela, O Inganas, and I Lundstrom. **Conducting polymers as artificial muscles: challenges and possibilities**. *Journal of Micromechanics and Microengineering*, **3**(4):203, 1993.

[462] Matthias I. J. Stich, Sergey M. Borisov, Ulrich Henne, and Michael Schaeferling. **Read-out of multiple optical chemical sensors by means of digital color cameras**. *Sensors and Actuators B-Chemical*, **139**(1, SI):204–207, May 20 2009. 9th European Conference on Optical Chemical Sensors and Biosensors (EUROPT(R) ODE 9), Dublin, IRELAND, MAR 30-APR 02, 2008.

[463] Martin Wainwright. **Pollution kills fish in waterways**. Online (`http://www.guardian.co.uk/environment/2003/jun/04/food.conservationandendangeredspecies`), June 2003.

[464] DS Zhang and GJ Lu. **Review of shape representation and description techniques**. *Pattern Recognition*, **37**(1):1–19, Jan 2004.

4

Real-time Sweat pH Monitoring Based on a Wearable Chemical Barcode Micro-fluidic Platform Incorporating Ionic Liquids

"... We thought we could build it, so we built it. [Long Applause] But, but it didn't work. [Laughter] So we built it again. And we did this 32 times. [Laughter] But I'm very excited to tell you that last year we did build it – it works..." (On the development of a simple, portable, low-cost, point-of-care device to test for anemia)

— Dr. Myshkin Ingawale, TED, February 2012.

THIS WORK PRESENTS the fabrication, characterisation and the performance of a wearable, robust, flexible and disposable chemical barcode device based on a micro-fluidic platform that incorporates ionic liquid polymer gels (ionogels). The device has been applied to the monitoring of the pH of sweat in real time during an exercise period. The device is an ideal wearable sensor for measuring the pH of sweat since it does not contain any electronic parts for fluidic handle or pH detection and because it can be directly incorporated into clothing, head or wristbands, which are in continuous contact with the skin. In addition, due to the micro-fluidic structure, fresh sweat is continuously passing through the sensing area providing the capability to perform continuous real time analysis. The approach presented here ensures immediate feedback regarding sweat composition. Sweat analysis is attractive for monitoring purposes as it can provide physiological information directly relevant to the health and performance of the wearer without the need for an invasive sampling approach.

Preamble

One of the main challenges of wearable sensors is the impact that it can have on the wearer. Carrying additional electronics, as with the dedicated device approach, can impede the wearer in many ways e.g. size, weight, battery changes, straps to hold the device in place, etc. This is profoundly significant for sporting activities where a sensing device should not, ideally, impede an athlete's movement or alter their performance in any way; which additionally holds true for health applications. To this end, the application of the underlying hypothesis in this thesis may have the ability to address this i.e. by digital imaging. For instance, by considering each individual element of an optical chemical sensor, it is clear that for bio/chemical sensors an element of the sensor must be in full contact with the wearer i.e. to collect a sample and also to react with the chemical transducer. In addition to this, the remaining elements relates to the electronic hardware, power element, casing, and support for the entire device. As with many systems, some variables/features/implementations must be compromised as a result of optimising others. For example, the inherent non-planar, dynamic, and variable surfaces of skin can make it difficult to connect to devices that are ridged in nature or perhaps the working lifetime as a result of optimising the weight/size. Based on this, and the implications of the sensing approach explored in the previous paper for chemical sensing, a concept was put forward that may address the wear-ability issue for wearers, allow for the separation of detector and transducer, and by extension may demonstrate the diversity of chemical sensing through readily available technology via devices equipped with an image capturing feature e.g. cameras.

To this end, an experiment was conceived to investigate the development of a flexible microfluidic structure capable of passively gathering a bodily fluid, i.e. sweat, and react colorimetrically with respect to the presence of a target chemical species, pH in this case. The other side of this conceptual system was its optical detection mechanism. By taking snapshots/photos of the optical indicators while a wearer is exercising and producing sweat, generation of information related to the bio/chemistry of a wearer maybe possible. This paper explores this concept through the realisation of such a microfluidic device, establishment of calibration models, employment of an athlete for sweat trials, capturing of digital images at a discrete frequency, offline processing of images, and comparison of the results to a reference instrument.

Contributions

- To the Field
  - A novel, functional, non-invasive, chemical detection approach for sweat analysis (pH);

  - Accuracy of ± 0.49 pH Unit;
  - Colour space sRGB explored;
  - Freedom from traditional device artifacts;
  - Flexible approach for various body shapes

- By Candidate
  - Sensing Approach - Concept, implementation, sweat trials;
  - Amendments to patch design to include reference colour patches;
  - Image processing and analysis;
  - Data processing;

- By Others
  - Curto, V. - Development of barcode from previous work for [489], calibration, sweat trials;

4.1 Introduction

Wearable sensors such as heart rate monitors and pedometers are in common use by people involved in sports and exercise activities. This area is growing exponentially, and while it is mainly driven by interest from health/sports enthusiasts, it will increasingly expand into health monitoring, as the economics of healthcare will force trends towards remote (home based) monitoring of patient status, rather than the current hospital focused model. In particular, the true potential of wearable chemical sensors for the real-time ambulatory monitoring of bodily fluids such as tears, sweat, urine, and blood has not been realised due to difficulties associated with sample generation, collection and delivery, sensor calibration and reliability, wearability and safety issues [449].

Sweat is naturally generated during exercise, thus the possibility of monitoring its contents provides very rich information about the physiological condition of the individual [490]. Sweat analysis is known to be used to identify pathological disorders such as cystic fibrosis [482]. Moreover, real-time sweat analysis, particularly during exercise [471], potentially opens a route to gathering valuable information on dehydration and the detection of conditions related to changes in the concentrations of important biomolecules and ions, such as hyponatremia (low sodium concentration). This information can be used to optimise approaches to rehydration and re-mineralisation [483] which can enhance athletic performance and general health.

There are several factors that correlate the pH of sweat with health. Changes in the pH of the skin are reported to play a role in the pathogenesis of skin diseases like irritant contact dermatitis and acne, among others [466]. Patterson *et al.* showed that inducing metabolic alkalosis through the ingestion of sodium bicarbonate led to increased blood and sweat pH [479]. Furthermore, it has been reported that sweat pH will rise in response to an increased sweat rate [487]. A relationship was also observed between pH and sodium (Na^+) levels in isolated sweat glands in that the greater the concentration of Na^+, the higher the sweat pH will be [478]. As exercising in a dehydrated condition has been shown to lead to increased levels of Na^+, it can be seen that such changes can be measured directly (using a Na^+ selective sensor) or indirectly by monitoring the pH of sweat [485].

Micro-Total-Analysis (TAS) or Lab-on-a-Chip (LOC) is an important concept for the development of personalised health care and point of care diagnostic devices, and it will improve the performance and capabilities of many commercial products that are already available in the market [472]. Important technological barriers such as miniaturisation, low cost production, reusability or disposability, robustness, flexibility, and adaptability are continuously being overcome using this approach. However, sweat, which is easily accessible using non-invasive means, remains largely unexplored as a sample medium for tracking personal health status using the LOC approach [491].

The use of optical pH sensors offer several advantages such as freedom from electrical noise, possibility of miniaturisation, ability to monitor status without physical contact, and flexibility in interrogation approaches (human eye, LED sensors, cameras, spectrometers) [448]. Also, optical pH sensors are suitable for applications where conventional electrodes cannot be used because of their size or because of the risk of electric shock, such as during in vivo measurements. In order to provide optical pH sensors with good sensitivity, selectivity, and stability, various support materials, methods and reagents, and immobilisation techniques for pH indicator dyes have been employed [477, 468]. In particular, ionic liquids (ILs) have been rarely employed in optical sensors despite their excellent chemical and thermal stabilities, low vapour pressure, high ionic conductivity properties, and tuneable hydrophobic and hydrophilic nature [465, 467, 495, 494, 488, 481, 473]. The incorporation of ILs into polymer gels to form so-called 'ionogels' is a particularly attractive strategy as it may generate materials that maintain the inherent advantages of ILs within a solid or semi-solid gel-type structure [492, 475, 470, 474].

Here we show how a simple, autonomous, wearable, robust, flexible and disposable micro-fluidic platform based on ionogels can be used for monitoring the pH of sweat generated during an exercise period in real-time. Accurate pH values can be obtained by simply observing the barcode colour variation in comparison to a standard colour chart or through more sophisticated methods such as photo or video analysis of the colour changes. A significant advantage of these approaches is that the on-body sensor consumes no power, does not require any electronics for signal acquisition or communication, and therefore does not need a battery. On the other hand, remote interrogation by eye or by camera requires direct line of sight of the sensor status by the observer or camera. However, the colourimetric response can also be monitored on-line using simple opto-electronic components integrated into the device, along with wearable communications electronics (mote, dedicated platforms, mobile phones, etc.), providing continuous feedback of the sweat composition to remote locations via a local base-station [491, 474, 489].

4.2 Experimental

4.2.1 Materials

N-Isopropylacrylamide (NIPAAm, Wako) was purified by recrystallisation in a mixed solution of hexane and toluene and dried under a vacuum. N,N-Methylene-bis(acrylamide) (MBAAm, Sigma–Aldrich), 2,2-dimethoxy-2-phenyl acetophenone (DMPA, Sigma–Aldrich, St. Louis, USA), methyl red (MR), bromophenol blue (BPB), bromocresol green (BCG), bromocresol purple (BCP), and bromothymol blue (BTB) (Sigma–Aldrich, St. Louis, USA), were used without further purification. Trihexyltetradecyl- phosphonium dicyanoamide [P6,6,6,14][dca] was obtained with compliments of Cytec

Industries. The IL was purified thoroughly by column chromatography [476], dried under vacuum at $40\,^{\circ}C$ for 48 hours, and stored under argon at $20^{\circ}C$. Artificial sweat was prepared according to the standard ISO 3160-2 (20 g/L NaCl, 17.5 g/L NH4OH, 5 g/L acetic acid and 15 g/L lactic acid) (Sigma–Aldrich, St. Louis, USA). Super-absorbent non-woven textiles (Absortex) were purchased from Texsus SpA, Italy. Hansaplast commercially available plasters were used to encapsulate the micro-fluidic platforms.

Devices were fabricated using multilayer lamination. A CO_2 laser (Laser Micromachining Light Deck, Optec, Belgium) system was used to cut the various polymer layers. Connecting holes and micro-fluidic channels were cut from an 80 m thick layer of pressure-sensitive adhesive (PSA-AR9808, Adhesives Research, Ireland) and laminated onto a 125 m poly(methylmethacrylate), PMMA, support layer (Good-Fellow, UK) using a thermal roller laminator (Titan-110, GBC Films, USA).

Photographs were taken using a Canon PowerShot G7 camera. The skin pH sensor was purchased from Hanna Instruments, India. The UV light source used for photo-polymerisation was a BOND- wand UV-365 nm obtained from Electrolyte Corporation, USA. UV light intensity was measured with a Lutron (Taiwan) UV-340A UV light meter. The pictures were processed and analysed using the Open Computer Vision (OpenCV) image processing libraries.

4.2.2 Micro-fluidic Platform Fabrication

The micro-fluidic platform ($20\,mm \times 17\,mm$), Figure 4.1a, consists of four independent reservoirs and channels, fabricated in six layers of poly(methyl methacrylate) and PSA using CO_2 ablation laser and lamination. Figure 4.1b shows the fabrication protocol that starts with a $125\,\mu m$ thick PMMA base layer followed by two layers of PSA ($160\,\mu m$), containing the micro-channels ($5\,mm \times 1\,mm$ and $160\,\mu m$ in depth), four rectangular ionogel reservoirs and an absorbent reservoir. Then an additional layer of PMMA ($125\,\mu m$), which contains only the four rectangular reservoirs ($2\,mm \times 6\,mm$) and the absorbent reservoir, was laminated over the PSA layers. The incorporation of the four ionogels inside of the micro-fluidic was performed as describe in Section 4.2.3. To seal the system, a lid con- sisting of two more layers, PSA and PMMA ($205\,\mu m$), was laminated over the previous four layers. The lid contains four rectangular holes ($1\,mm \times 5\,mm$) fabricated using the CO_2 laser. The holes were carefully arranged to site directly over the polymerised iono- gels. The micro-channels connect the four rectangular independent ionogel/dyes reservoirs with a common reservoir ($15\,mm \times 5\,mm$ and $285\,\mu m$ depth), where an absorbent fibre drives the sweat from the sensing area through the channels by capillary action. This ensured that fresh sweat from the skin is continuously drawn into contact with the ionogel/dyes sensors.

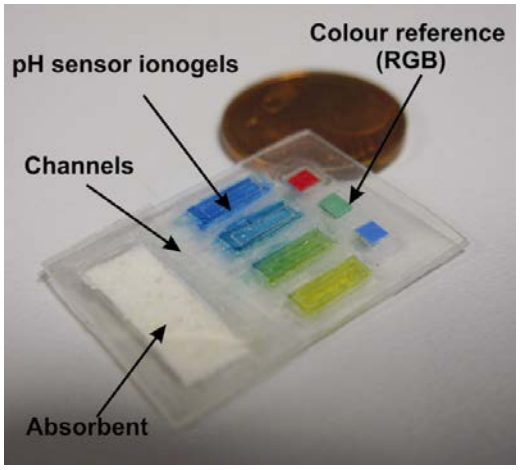

(a) Picture of the micro-fluidic platform.

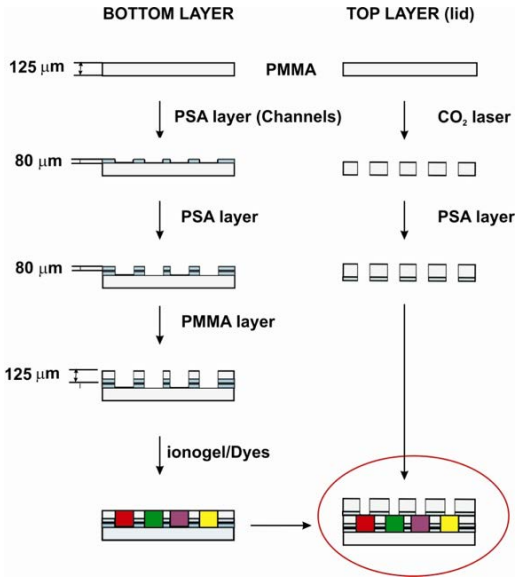

(b) Microfluidic platform fabrication process.

Figure 4.1: Microfluidic platform.

4.2.3 Preparation of the Phosphonium Based Ionogel with Integrated pH Sensitive Dyes

The ionogel consisted of two monomeric units: N- isopropylacrylamide and N,N - methylene-bis(acrylamide) in the ratio 100:5, respectively. The reaction mixture was prepared by dissolving the NIPAAm monomer (4.0 mmol), the MBAAm (0.2 mmol) and the photo-initiator 2,2-dimethoxy-2-phenylacetophenone DMPA (0.11 mmol) into 1.5 mL of [P6,6,6,14][dca] ionic liquid, shown in Figure 4.2b on page 145. 7 L of the reaction mixture was placed in each of the reservoirs after mixing at $45\,^{\circ}C$ for 10 min. The monomers were then photo-polymerised within the ionic liquid matrix using a UV irradiation source (365 nm) placed 5 cm from the monomers for 30 min (UV intensity $\sim 630\,\mu W\,cm^{-2}$). 365 nm UV irradiation source is necessary to have the correct radical polymerisation process and obtain the desired ionogel structure and physical consistence. When the polymerisation was complete, the ionogels were washed with deionised water and subsequently with ethanol for 1 min each, and the procedure was repeated three times to remove any unpolymerised monomer and any excess of ionic liquid. Finally the ionogels were left to fully dry for 5 hours at room temperature. 5 L ethanol solution of each of the dyes ($10^{-3}\,M$) was pipetted over the ionogel and left until dry. This process was repeated three times. Then, the barcode system was washed in ethanol and in water several times until no leaching of the dyes was observed. The lid was placed on top of the barcode and laminated to form the final structure. Finally the device was dried at room temperature for 5 h. The stability of the micro-fluidic barcode against pH was carried out following the same protocol than that in Benito-Lopez *et al.*, and similar results were obtained [474].

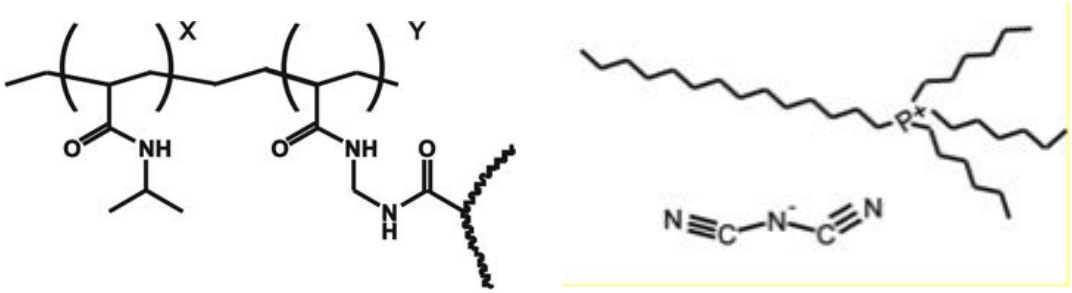

(a) N-Isopropylacrylamide and N,N-methylene-bis(acrylamide) crosslinked polymer in the ratio 100(x):5(y).

(b) The ionic liquid trihexyltetradecylphosphonium dicyanoamide [P6,6,6,14][dca] structure.

Figure 4.2: The molecular structure of the two components that make up the ionogel material.

4.2.4 pH Sensor and Optical Detection

A colorimetric approach was employed to quantitatively deter-mine the concentration of pH of sweat by means of a digital colour camera (Canon PowerShot G7). The approach involved the use of four pH sensitive dyes (methyl red, bromocresol green, bromocresol purple and bromothymol blue), which change in colour over a pH range defined by their respective pK_as. Figure 4.3 on page 146 visually shows colour changes in the dyes in a pH range from 4.5 to 8, which covers the typical pH range of a human's sweat during exercise [487], i.e. from 5 to 7. Although this range was sufficiently covered, it was important to ascertain how the dyes respond over the full pH scale for later analysis. Therefore a calibration routine was carried out, where the platform was exposed to artificial sweat at different pHs, from ca. 1 to ca. 14, within 0.5 pH unit steps. A photograph of each event was captured with the parameters of the camera set to manual, 1/16 and at optimum resolution. For each capture, the camera was fixed at a distance of 5 cm from the barcode's planar surface along with ensuring that the barcode platform was captured in its entirety within the camera's field of view. In addition, a light source (60 W, Philips, 30°*8L, Sportline R63, 240 V, Holland) was placed at a 45° angle for illumination and minimisation of background visual effects. Later, each captured image was processed by employing a standard set of algorithms using OpenCV. Firstly, each image region of interest (4 dyes and 3 reference patches) was identified through the creation of a binary mask image. This involved creating a copy of the original image, applying noise reduction filtering techniques (Gaussian blurring, median and erosion/dilation morphological algorithms) to aid in the segmentation step and then applying a connected component algorithm to the image. This resulted in a binary image with neighbouring pixels of similar colour being grouped together and identified as separate image regions. Next, the regions representing the 4 dyes and 3

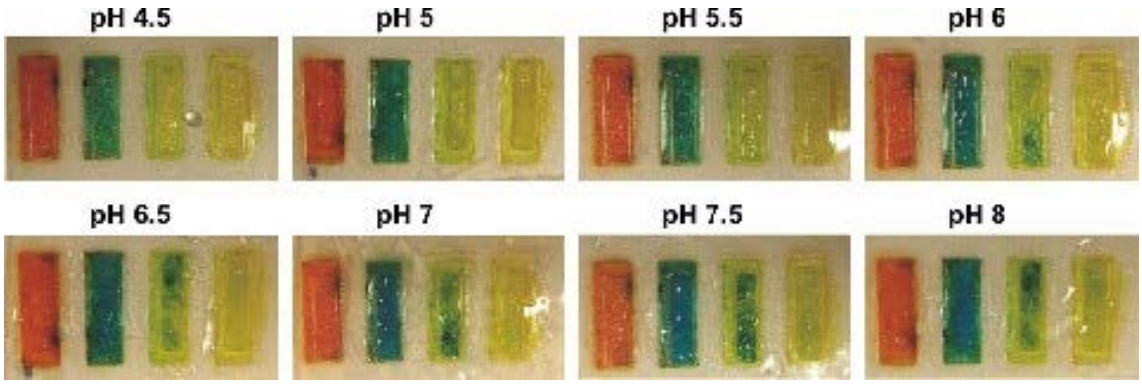

Figure 4.3: Photographs of the micro-fluidic system at different pHs tested with artificial sweat (ISO 3160-2). (For interpretation of the references to colour in the text, the reader is referred to the web version of the article).

reference patches were identified based on their location within the original image and stored in memory while the rest (misclassified regions) were omitted. After this, the resulting binary image was applied to the original image, removing the background (unwanted pixels) and leaving only pixel regions representing the ionogel/dye regions and reference patches. Subsequently, each region was considered in turn where the dominant colour component was calculated (i.e. the mean value) on each of the region's colour channel components (RGB). Next, the colour components of the dyes regions were normalised with respect to the reference patches to account for potential ambient lighting effects. A calibration plot for each dye was ascertained and the camera response (R') was calculated by: $R' = {}^{R}/_{(R+G+B)}$ using the normalised response of the RGB channels. Finally, a sigmoidal regression analysis (Boltzmann) was applied to achieve a calibration model.

4.2.5 On-body Trials

The micro-fluidic system was incorporated into an adhesive plaster to avoid direct contact of the ionogels with the skin, see Figure 4.4a on page 147. The plaster was placed in the lower back region of the body where the sweat rate is approximately $0.85 \pm 0.41\, mg\, min^{-1}\, cm^{-2}$ [478]. Reference measurements were taken manually at fixed time intervals (10 min) using a commercial pH probe. At the same time three pictures of the barcode were taken in order to measure the pH of the sweat and for comparison with the reference values as explained above. The exercise protocol involved indoor cycling (room temperature $18\,°C$) using a bicycle ergometer. Elite athletes participated in the study, who cycled for 1 hour at a self-selected pace.

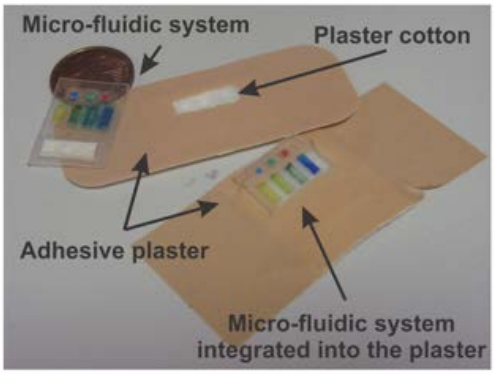

(a) Microfluidic system integrated into a plaster.

(b) Microfluidic system integrated into a wristband and worn by subject.

Figure 4.4: Picture of the microfluidic system during trials.

4.3 Results and Discussion

4.3.1 Why a Barcode pH Sensor Micro-fluidic Platform?

Several methods for measuring the pH of sweat are already established, which are based mainly on glass electrodes and ion-sensitive field-effect transistors (ISFETs). The most popular are planar-tipped conventional pH-probes, which can be placed directly in contact with the skin in order to measure the pH. The drawback to this approach is that it is physically difficult to maintain contact between the probe and the skin over a prolonged period of time as it tends to suffer from drift and motion artefacts. Moreover, they are typically planar glass electrodes, which can cause skin damage when broken. The micro-fluidic platform is more fit-for-purpose as a wearable pH sensor since it can be directly incorporated into clothing or attached as an adhesive strip in continuous contact with the skin. Furthermore, due to the micro-fluidic structure, fresh sweat is continuously passing through the sensing area providing a real-time monitoring capability.

The ionogel matrix provides an ideal platform for the pH indicators dyes. This is because of, firstly, ion-pair interactions between the different pH indicators and the ionic liquid that forms the ionogel structure, and secondly, there is no leaching of the pH dyes during the experiments [476]. Furthermore, it was observed that the ionogel material is impressively robust under harsh conditions (pH ranges from 0 to 14) [474].

4.3.2 Micro-fluidic Platform Fabrication and Performance

The micro-fluidic system was fabricated using six thin PMMA and PSA layers ($615\,\mu m$, total thickness). This ensures that the whole device is flexible and can easily adapt to the body contours. In addition, it is comfortable to wear providing an unobtrusive and non-invasive method for the analysis of sweat during exercise.

The micro-fluidic system can be encapsulated into an adhesive plaster, Figure 4.4a on page 147, integrated in the sport clothes or into a sweat band worn on the head or the wrist, in order to directly obtain pH information of sweat during an exercise period, see Figure 4.4b on page 147.

The micro-fluidic structure ensures that fresh sweat is continuously sampled from the skin and flows pass the ionogels during the entire training period. The performance of the micro-fluidic platform is presented schematically in Figure 4.5 on page 149. Sweat is absorbed by the fabric of the clothes/adhesive plaster cotton and comes in contact with the barcode sensor. The dyes react with the sweat and change colour according to their respective pK_a values. Sweat is continuously drawn through the micro-fluidic device by the super-absorbant material, which acts as a passive pump.

In order to test the performance of the micro-fluidic platform, artificial sweat was used to calculate the flow rate in the channels generated by the device. Snap-shot pictures of the channels were taken over time (see Figure 4.5 on page 149) and then analysed. The flow rate of the device was found to be initially ca. $6.4 \pm 2\,L min^{-1}$ (n = 12) but once the micro-fluidic channel was filled up by the artificial sweat, the flow rate decreased gradually to $1.1 \pm 0.8\,L\,min^{-1}$ ($n = 12$) in the steady state. At this point, the flow rate remains constant until the absorbent reaches its maximum loading capacity, $148 \pm 2\,L$ ($n = 20$). This gives the device an operational lifetime of ca. 135 min, in the current manifestation. However, since the device is easy to fabricate, and multiple replicates can be prepared in a single batch, the design can be easily modified for applications involving longer exercise periods. For example, the amount of absorbent material can be increased, or the channel dimensions varied to reduce the device flow rate, both of which would extend the useful operational time.

In addition, due to the inherent micro-sampling capability of the platform the area of the skin that is sampled is much smaller than commercially available sweat collection systems, i.e. patches. Considering the total exposed sensing areas, equal to the four lid holes (4 cm × 0.05 cm), the flow rate per unit area of the whole device is determined by the average steady state flow rate per unit area of each channel, $22\,L\,min^{-1}cm^{-2}$, times four. This gives a total device flow rate of $88\,L\,min^{-1}cm^{-2}$. This value is much smaller than typical skin sweat flow rates, e.g. lower back $850 \pm 410\,L\,min^{-1}cm^{-2}$ (assuming sweat density equal to $1\,mg\,mL^{-1}$) [478]. This ensures that sufficient fresh sweat is always passing through the device.

The response of the four immobilised dyes in the ionogel matrixes was evaluated through a calibration routine using buffer solutions, as explained in detail in Section 4.2.4. The results show that the dyes exhibited a colour change depending on the pH and are shown in Figure 4.6 on page 150. The change in colour intensity of each of the pH indicators was plotted against the pH value. A sigmoidal regression analysis

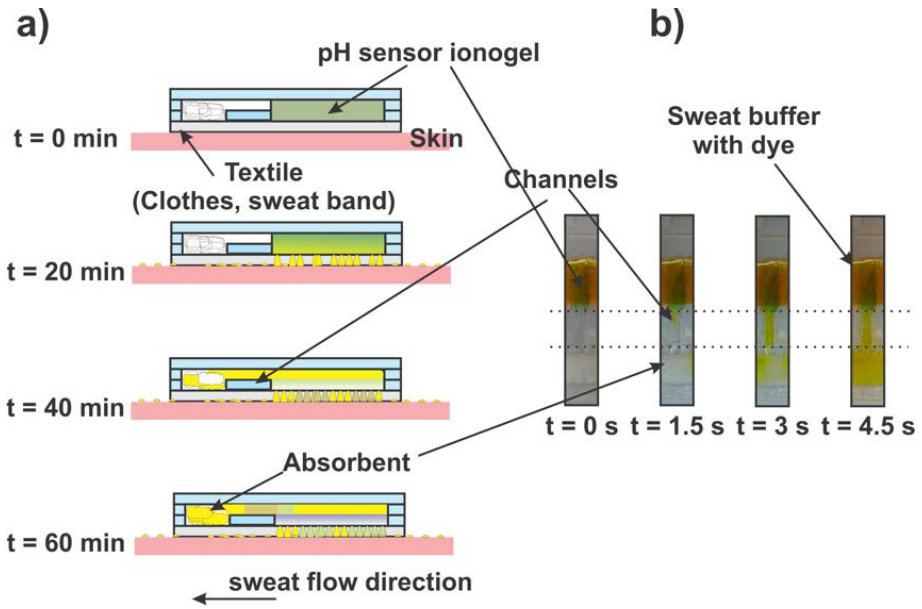

Figure 4.5: (a) Schematic representation of the micro-fluidic system's performance over time and (b) series of pictures showing the channel performance in the micro-fluidic system (artificial sweat with dye). Pictures like these were used to estimate the sweat flow rate through the device. (For interpretation of the references to colour in the text, the reader is referred to the web version of the article).

(Boltzmann technique) was then applied to the calibration points and resulted in a calibration model for each dye.

Figure 4.6 on page 150 shows the calibration curves for the indicators BCG and BCP and as an example. The pK_a of MR was not determined since its colour did not vary over the experimental pH range conditions. This could be due to the fact that the anion of the ionic liquid [dca]−, that is known to show characteristics of Lewis base [484], and this could interfere with the acid/base chemistry of the methyl red dye. For the other ionogel/dyes the experimental values for the pK_a values were estimated to be: bromocresol green BCG: 3.43; bromocresol purple BCP: 7.61 and bromothymol blue BTB: 8.82, which slightly varied with respect to the literature values (BCG: 4.6, BCP: 6.4 and BTB: 7.1). The variations are not surprising, as it has been shown that immobilisation of acidochromic dyes leads to variations in pK_a due to a change of local micro-environment [469].

Moreover, the stability of the barcode was demonstrated by performing three calibrations using three different barcode platforms. The calibration showed good repeatability with relative standard deviation (R.S.D.) typically within 4% (n = 3). This indicated that the pH indicator dyes are fully reversible to pH changes and that no significant dye leaching occurred during the experiments. Signal intensity is reproducible after three calibrations using the same barcode with relative standard deviation (R.S.D.) typically within 6% (n = 3) [474].

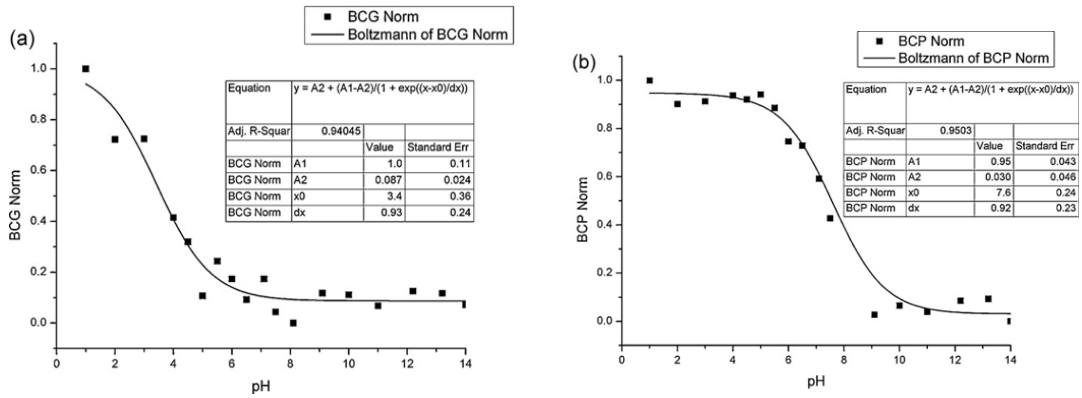

(a) Bromocresol green. (b) Bromocresol purple.

Figure 4.6: Calibration curves showing pH vs. $R' = {}^{R}/_{(R+G+B)}$ normalised [0,1].

4.3.3 On-body Trials

Sweat flow rate and fluid losses vary for individuals and are generally dependent on body size, gender, exercise intensity, environmental conditions, and individual metabolism [480]. For on-body trials, the subject was equipped with a micro-fluidic platform on the low back region. The micro-fluidic platform was activated before with a hydrochloric acid solution at pH 2 for 5 min. After a period of 20 min, following the approach used by Morris *et al.* where it was shown that it takes approximately 10 – 15 min to produce an appreciable amount of sweat during exercise [486], sweat reached the sensors and it was possible to begin monitoring the pH of the sweat. This delay arises firstly from the fact that sweat does not commence immediately upon exercise and that the device has a small but finite dead volume that must be filled before the sample reaches the sensors and a colour change is gained. Then a picture of the micro-fluidic platform was taken every 10 min along with parallel manual reference measurements using a pH electrode for specific use (Hanna instruments HI-1413B/50). The results are presented in Figure 4.7a on page 152. In the micro-fluidic platform, continuous fresh sweat is passed through the ionogel matrix, and the conditioning of the activation solution is quickly flushed away from the sensing area. After 20 min of a training period, no activation solution is observed in bromocresol green and bromocresol purple doped ionogels. For instance, the bromocresol green ionogel is yellow at times from 0 to 10 corresponding to pH 2 (i.e. that of the conditioning solution), after a 20 min training period, the ionogel is blue in colour (pH 6) and it varies from dark to light blue, i.e. pH 5.5 – 6.5, during the rest of the experiment. Therefore, the pH of the two ionogels compared reasonably well with the commercial pH probe reference measurements.

As previously described, the ionogel incorporating the methyl red indicator did not perceptibly change over the whole pH range of study even though it has a pK_a of 5 (red to yellow). Therefore the dye was replaced by bromophenol blue that has a similar pK_a (ca. 4) and it changes colour during the calibration process.

Unfortunately, since the pH range of the dye is 3 – 4.6 (yellow to blue) a colour change gradient was not observed during trials. Moreover, no colour changes were also observed for the ionogel doped with bromothymol blue since the estimated pK_a of 8.82 is over the range of the pH measurements carried out during the on-body trial shown in Figure 4.7a on page 152. Nevertheless, these two dyes (BPB, BTB) are potentially useful for picking up anomalous variations of the pH in the sweat during real-time analysis.

A more sophisticated approach to quantify the colour variations within the sweat's pH can be achieved using wearable device such as SMD-LED technology as previously reported [474]. However, a colourimetric electronic-free device can be easily read by the individual during the physical activity, considerably decreasing the complexity of the detection system (electronic part of the device) but improving the wearability and the read-out approach. Furthermore, the micro-fluidic platform has a major advantage in performance with respect to commercially available systems since they measure the pH of sweat from where it emerges and within an almost enclosed package therefore it minimises the interaction with carbon dioxide of the atmosphere, which can cause a lowering of the pH values.

In the presented system, a particular colour pattern of the barcode corresponds to a defined pH of the sweat where the captured images were analysed as explained earlier in 4.2.4 using OpenCV. Here, each pH prediction of each dye is calculated by normalisation with respect to the reference patches and then applied to the calibration model ascertained earlier. To achieve a single pH prediction from the barcode sensor, each dye was considered equally with a weight of 1 and cumulative pH prediction was determined via their average value; this is shown in Figure 4.7b on page 152 and values are presented in Table 4.1[1]. It can be seen that by combining the two dyes a low relative percentage error was achieved with the exception of the first measurement (7.68%) where the dye's pH values might differ slightly from the ones of the pH meter due to residual conditioning of the activation solution in the ionogel. In addition, Figure 4.7b on page 152 does show a similar trend by both measurement methods. It should be noted however that the accuracy of 0.49 of a pH unit ascertained in this study may need further investigation. For instance, a study may be needed to determine the correct weights when combining the dyes predictions to increase accuracy. However, to the best of our knowledge, the micro-fluidic device described in this work is the only wearable electronic-free sensor capable of performing real-time measurements during active exercise periods, with non-standardised light conditions. Similar work in the literature by Byrne *et al.* have reported an accuracy of ± 0.5 pH units [493] when using a digital colour camera but under controlled lighting conditions.

[1]The percentage relative error (%RE) is defined as $((|A - B|)/A) \times 100$, where A and B are the values obtained using the pH-meter and the combined predictive values of the dyes, respectively.

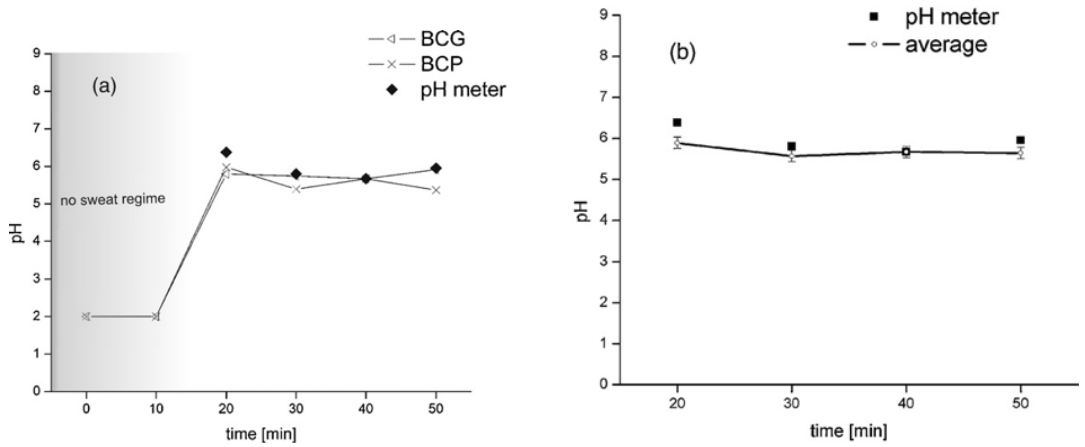

(a) Plot showing the reference instrument in conjunction with the individual predictions of each dye when normalised with respect to the reference patches and predicted using the calibration model.

(b) Plot of the reference measurement and the average of all the dye predictions when weighted equally.

Figure 4.7: pH determination of sweat using the micro-fluidic system during a 50 min training period.

Time [min]	pH meter	Dyes prediction (pH)	%RE
20	6.38	5.89	7.68
30	6.38	5.56	4.14
40	5.67	5.67	0.00
50	5.95	5.63	5.38

Table 4.1: Time series measurements of pH from the reference instrument (pH meter) and the predictions of the dyes when combined and weighted equally.

4.4 Conclusions

In this work, the fabrication, characterisation and the performance of a wearable, electronic-free and flexible micro-fluidic system based on ionic liquid polymer gels (ionogels) for monitoring (in real-time) the pH of the sweat generated during an exercise period has been presented.

As proven before, the ionogel matrix is very robust even at harsh pH conditions and that the pH indicators bromophenol blue, bromocresol green, bromocresol purple, and bromothymol blue retained their pH indicator properties on the ionogel. The ionogel–dye interactions ensure no leaching of the dyes during experiments, providing long durability of the device and accuracy on the pH of sweat measurements over time. The approach presented here provides immediate feedback regarding sweat composition, i.e. pH, to individuals during exercise period. A

particular colour pattern of the barcode corresponds to a defined pH of the sweat with an accuracy of 0.49 pH units after applying standard image processing and analysis techniques to the pictures, which were captured during exercise trials when the sensor was applied on the skin.

Future work will focus on the development of a more robust code for image processing, aiming a better resolution and accuracy in the pH prediction. Moreover, through a systematic comparison and correlation of the pH of sweat with pH and lactate from blood, it will provide an easy, non-invasive and cheap tool to perform pH sweat analysis, improving sport performance and health.

4.5 References

[465] Afsaneh Safavi, Norouz Maleki, and Mozhgan Bagheri. **Modification of chemical performance of dopants in xerogel films with entrapped ionic liquid**. *Journal of Materials Chemistry*, **17**(17):1674–1681, 2007.

[466] M. H. Schmid-Wendtner and H. C. Korting. **The pH of the skin surface and its impact on the barrier function**. *Skin Pharmacology and Physiology*, **19**(6):296–302, 2006.

[467] K Seddon. **Ionic liquids: designer solvents for green synthesis**. *Institution of Chemical Engineers*, **730**(730):33–35, APR 2002.

[468] Ciaran Smyth, King Tong Lau, Roderick L. Shepherd, Dermot Diamond, Yanzhe Wu, Geoffrey M. Spinks, and Gordon G. Wallace. **Self-maintained colorimetric acid/base sensor using polypyrrole actuator**. *Sensors and Actuators B-Chemical*, **129**(2):518–524, FEB 22 2008.

[469] B.R. Soller. **Design of intravascular fiber optic blood gas sensors**. *Engineering in Medicine and Biology Magazine, IEEE*, **13**(3):327 –335, june-july 1994.

[470] Masahiro Tamada, Toshiyuki Watanabe, Kazuyuki Horie, and Hiroyuki Ohno. **Control of ionic conductivity of ionic liquid/photoresponsive poly(amide acid) gels by photoirradiation**. *Chemical Communications*, **39**(39):4050–4052, 2007.

[471] Jessica Weber, Arun Kumar, Ashok Kumar, and Shekhar Bhansali. **Novel lactate and pH biosensor for skin and sweat analysis based on single walled carbon nanotubes**. *Sensors and Actuators B-Chemical*, **117**(1):308–313, SEP 12 2006.

[472] George Whitesides. **Solving problems**. *Lab on a Chip*, **10**(18):2317–2318, 2010.

[473] Peter Wasserscheid. *Recent Developments in Using Ionic Liquids as Solvents and Catalysts for Organic Synthesis*, chapter 11, pages 105–117. Wiley-VCH Verlag GmbH, 2008.

[474] F. Benito-Lopez, S. Coyle, R. Byrne, C. O'Toole, C. Barry, and D. Diamond. **Simple Barcode System Based on Inonogels for Real Time pH-Sweat Monitoring**. In *Body Sensor Networks (BSN), 2010 International Conference on*, pages 291 –296, june 2010.

[475] Marie-Alexandra Neouze, Jean Le Bideau, Philippe Gaveau, Severine Bellayer, and Andre Vioux. **Ionogels, new materials arising from the confinement of ionic liquids within silica-derived networks**. *Chemistry of Materials*, **18**(17):3931–3936, AUG 22 2006.

[476] S O'Neill, S Conway, J Twellmeyer, O Egan, K Nolan, and D Diamond. **Ion-selective optode membranes using 9-(4-diethylamino-2-octadecanoatestyryl)-acridine acidochromic dye**. *Analytica Chimica Acta*, **398**(1):1–11, OCT 11 1999.

[477] Martina O'Toole, Roderick Shepherd, Gordon G. Wallace, and Dermot Diamond. **Inkjet printed LED based pH chemical sensor for gas sensing**. *Analytica Chimica Acta*, **652**(1-2):308–314, OCT 12 2009.

[478] MJ Patterson, SDR Galloway, and MA Nimmo. **Variations in regional sweat composition in normal human males**. *Experimental Physiology*, **85**(6):869–875, NOV 2000.

[479] MJ Patterson, SDR Galloway, and MA Nimmo. **Effect of induced metabolic alkalosis on sweat composition in men**. *Acta Physiologica Scandinavica*, **174**(1):41–46, JAN 2002.

[480] N.J. Rehrer and L.M. Burke. **Sweat losses during various sports**. *Australian Journal of Nutrition and Dietetics*, **53**:13–16, 1996.

[481] Robin D. Rogers and Kenneth R. Seddon. **Ionic Liquids: Industrial Applications to Green Chemistry**. *Journal of the American Chemical Society*, **125**(24):7480–7480, 2003.

[482] Brynja Jonsdottir, Horour Bergsteinsson, and Olafur Baldursson. **Cystic Fibrosis - Review**. *Laeknabladid*, **94**(12):831–837, DEC 2008.

[483] Robert D. Kersey, Diane L. Elliot, Linn Goldberg, Gen Kanayama, James E. Leone, Mike Pavlovich, and Harrison G. Pope, Jr. **National Athletic Trainers' Association Position Statement: Anabolic-Androgenic Steroids**. *Journal of Athletic Training*, **47**(5):567–588, SEP-OCT 2012.

[484] Douglas R. MacFarlane, Jennifer M. Pringle, Katarina M. Johansson, Stewart A. Forsyth, and Maria Forsyth. **Lewis base ionic liquids**. *Chem. Commun.*, **0**:1905–1917, 2006.

[485] RM Morgan, MJ Patterson, and MA Nimmo. **Acute effects of dehydration on sweat composition in men during prolonged exercise in the heat**. *Acta Physiologica Scandinavica*, **182**(1):37–43, SEP 2004.

[486] Deirdre Morris, Shirley Coyle, Yanzhe Wu, King Tong Lau, Gordon Wallace, and Dermot Diamond. **Bio-sensing textile based patch with integrated optical detection system for sweat monitoring**. *Sensors and Actuators B-Chemical*, **139**(1):231–236, MAY 20 2009. 9th European Conference on Optical Chemical Sensors and Biosensors (EUROPT(R) ODE 9), Dublin, IRELAND, MAR 30-APR 02, 2008.

[487] D Granger, M Marsolais, J Burry, and R Laprade. **Na+/H+ exchangers in the human eccrine sweat duct**. *American Journal of Physiology-Cell Physiology*, **285**(5):C1047–C1058, Nov 1 2003. 40th Annual Meeting of the American-Society-of-Cell-Biology, SAN FRANCISCO, CALIFORNIA, DEC 09-13, 2000.

[488] Simon Coleman, Robert Byrne, Stela Minkovska, and Dermot Diamond. **Investigating Nanostructuring within Imidazolium Ionic Liquids: A Thermodynamic Study Using Photochromic Molecular Probes**. *Journal Of Physical Chemistry B*, **113**(47):15589–15596, Nov 26 2009.

[489] Vincenzo F. Curto, S. Coyle, R. Byrne, N. Angelov, D. Diamond, and F. Benito-Lopez. **Concept and development of an autonomous wearable micro-fluidic platform for real time pH sweat analysis**. *Sensors and Actuators B: Chemical*, **175**(0):263 – 270, 2012. <ce:title>Selected Papers presented at Eurosensors XXV</ce:title>.

[490] M Beauchamp and LC Lands. **Sweat-testing: A review of current technical requirements**. *Pediatric Pulmonology*, **39**(6):507–511, Jun 2005.

[491] F. Benito-Lopez, S. Coyle, R. Byrne, Alan Smeaton, Noel E. O'Connor, and D. Diamond. **Pump Less Wearable Microfluidic**

Device for Real Time pH Sweat Monitoring. *Procedia Chemistry*, **1**(1):1103 – 1106, 2009. <ce:title>Proceedings of the Eurosensors XXIII conference</ce:title>.

[492] Fernando Benito-Lopez, Robert Byrne, Ana Maria Raduta, Nihal Engin Vrana, Garrett McGuinness, and Dermot Diamond. **Ionogel-based light-actuated valves for controlling liquid flow in micro-fluidic manifolds**. *Lab Chip*, **10**:195–201, 2010.

[493] Liam Byrne, Kim Lau, Steve Edwards, and Dermot Diamond. **Digital imaging as a detector for quantitative colorimetric analyses**. *Advanced Environmental and Chemical Sensing Technology*, **4205**:267–277, 2001.

[494] Robert Byrne, Kevin J. Fraser, Ekaterina Izgorodina, Douglas R. MacFarlane, Maria Forsyth, and Dermot Diamond. **Photo- and solvatochromic properties of nitrobenzospiropyran in ionic liquids containing the [NTf(2)](-) anion**. *Physical Chemistry Chemical Physics*, **10**(38):5919–5924, 2008.

[495] Robert Byrne, Simon Coleman, Kevin J. Fraser, Ana Raduta, Douglas R. MacFarlane, and Dermot Diamond. **Photochromism of nitrobenzospiropyran in phosphonium based ionic liquids**. *Physical Chemistry Chemical Physics*, **11**(33):7286–7291, 2009.

5

Dynamic pH Mapping in Microfluidic Devices by Integrating Adaptive Coatings Based on Polyaniline with Colorimetric Imaging Techniques

"...Many people, myself included, expected that the ability to manipulate fluid streams, in microchannels, easily, would result in a proliferation of commercial LoC systems, and that we would see applications of these devices proliferating throughout science. In fact, it has not (yet) happened...Microfluidics, to date, has been largely focused on the development of science and technology, and on scientific papers, rather than on the solution of problems."

— George Whitesides, Lab on a Chip, Editorial, 2010

IN THIS PAPER we present a microfluidic device that has integrated pH optical sensing capabilities based on polyaniline. The optical properties of polyaniline coatings change in response to the pH of the solution that is flushed inside the microchannel offering the possibility of monitoring pH in continuous flow over a wide pH range throughout the entire channel length. This work also features an innovative detection system for spatial localisation of chemical pH gradients along microfluidic channels through the use of a low cost optical device. Specifically, the use of a microfluidic channel coated with polyaniline is shown to respond colorimetrically to pH and that effect is detected by the detection system, even when pH gradients are induced within the channel. This study explores the capability of detecting this gradient by means of imaging techniques and the mapping of the camera's response to its corresponding pH after a successful calibration process. The provision of an inherently responsive channel means that changes in the pH of a sample moving through the system can be detected dynamically using digital imaging along the entire channel length in real time, without the need to add reagents to the sample. This approach is generic and can be applied to other chemically responsive coatings immobilised on microchannels.

Preamble

Lab-on-a-Chip (LOC) technology aims to integrate several functions into one miniaturised device that would have otherwise been confined to laboratory settings. Many scholars have theorised on the potential of LOC devices, one of which is the health care domain where diagnosis of diseases can take place without support of a classic laboratory [**?**]. Often, this involves transportation of minute levels of liquids (i.e. microfluidics) for mixing purposes. A particular aspect of this is in time critical reactions when reagents are introduced to samples. During sample harvestation, filtration, transportation stages, and general environmental conditions, a number of challenges can arise along micro-channels to include unwanted bubble formation, measurements at a number of locations along the channel, timing, and cost, amongst others.

In the previous two papers appearing in Chapter 3 and Chapter 4, the potential of digital imaging to analytical chemical analysis will be seen. This work explored in this paper extends that of previous papers and investigates some advantages that digital imagery can bring to sensing within microfluidic structures. Specifically, the investigation takes place by functionalising the walls of a microfludic channel with a chemo-responsive material (polyaniline - PAni) which changes in colour with respect to concentrations of pH. By means of this coating and through digital imaging, the detection of spatial localisation of chemical pH gradients along the entire length of the channel is investigated. Supporing information to this study is presented in Appendix C.

Contributions

- To the Field
  - First time to quantify pH via spactral changes of PANi using digital imaging;
  - Generation of chemical information along the full length of a microfluidic channel;
  - Digital imaging analysis under ambient lighting conditions;
  - Demonstration of chemical detection without the need for a special measurement window;
  - Detection of the point of chemical gradients along the a microfluidic channel;
- By Candidate
  - Calibration - Image processing and analysis, addressing ambient lighting effects;

  - Data Analysis - Correlation with reference instrument;
  - Gradient Detection - Concept, implementation, detection;

- By Others
  - Florea, L. - Construction of microfluidic channel, functionalisation with PANi, spectral measurements;
  - Phelan, T. - Chip holder for spectral measurements;

5.1 Introduction

Conventional glass-type electrodes have been widely used for pH measurements for many years in both industry and academic areas. However, in terms of specific applications (e.g. in vivo, food industry, or for clinical applications), they posses several disadvantages due to their size constraints, rigidity, and the inflexibility of the glass electrode. In recent years, a wide number of pH sensors have been developed to overcome these limitations, including ion sensitive field-effect transistor (iSFET) pH sensors [536, 529, 542, 510], optical pH sensors based on pH responsive dyes [507, 521, 530, 518], hydrogel film pH sensors [546, 553], and solid-state metal oxides pH sensors [508, 554, 526]. In particular, optical pH sensors present several advantages over the traditional pH electrodes such as their low costs, immunity from electromagnetic field, absence of electric contacts, possibility of reference electrode removal, and a high degree of miniaturisation [536]. Optical fiber-based pH sensors have been particularly popular, as the fibre allows the optical signal to be transported over long distances, which can facilitate applications in remote sensing [**?**]. Usually, these optical pH sensors (or optrodes) employ a dye or an indicator that requires immobilisation onto a solid support material. There are several critical issues related to this approach: firstly, the dye should retain its optical properties after the immobilisation process [**?**] and secondly, it should not leach into the solution [531]. A third issue of practical importance is their inherently narrow dynamic response range which is usually around 3-4 pH-units centred on the dye's pK_a [547].

Therefore, the further improvement of such sensors focuses on the search for new materials that can overcome these issues. An alternative approach is to use the inherent optical response of certain polymers like the conducting polymer polyaniline (PAni) rather than a conventional pH-sensitive dye. PAni displays striking changes in the visible/NIR spectrum upon proton-mediated doping-dedoping of the polymer backbone, thus offering the possibility of developing optical sensors with extended pH ranges. The polymer itself, therefore, acts as both the matrix support and the indicator dye. In this way, leaching is prevented, thereby enhancing the long-term stability and reproducibility.

PAni is an excellent candidate for the fabrication of optical sensors in the visible-near IR detection since it is an intrinsically pH-sensitive polymer with good environmental stability [519, 497]. Furthermore, by focusing on PAni nanofibres we can dramatically increase the surface area of the material [525], which in turn can manifest in improved response times and sensitivity.

A relatively new and promising approach to produce sensors of this kind involves optofluidics wherein optical and fluidic functionalities are integrated at the micro- and nano-scale to leverage their combined advantages by functionalising the inner walls of a microchannel with a responsive material [517, 516]. For example, functionalisation with antibodies for flow-through cell separation have been reported

[541], as have florescent dyes for optical sensing of acidity [540] and monolayers that exhibit metal ion sensing properties [500, 501].

Nowadays, a wide variety of detectors can be employed to transduce the colorimetric analytical signal, such as light dependent resistors [535, 538], photodiodes [549, 511, 522], phototransistors [528, 503, 515] and even reverse-biased LEDs [534, 533, ?]. More specific to this study is the use of digital imaging cameras for the detection of colorimetric reactions. Up to now, almost all of the studies carried out have been based on the RGB colour model, probably because this is readily accessible via a number of popular image processing packages [498, 496, 504, 505, 532]. The major challenge with this approach is that the RGB colour space is inherently sensitive to changes in ambient lighting, and measurements therefore have to be made under strictly controlled light conditions. Recently, studies such as those by Fay *et al.* [514] (qualitatively) and Cantrell *et al.* [506] (quantitatively) explored the use of a different colour model (Hue) for colorimetric chemical analysis which has shown to be more tolerant of ambient light variations [551].

Based on this concept, we present an innovative, robust, simple, and fast method to measure pH simultaneously at all locations across an entire microfluidic system using polyaniline nanofibres modified microchannel coupled with HSV-based digital image color analysis.

5.2 Experimental

5.2.1 Microfluidic Device Fabrication

The fabrication of the master mold was carried out using a laser ablation system-excimer/CO_2 laser (Optec Laser Micromachining Systems, Belgium) by cutting the microfluidic structures in a $50\,\mu m$ double-sided pressure sensitive adhesive film, PSA, (AR8890, Adhesives Research, Ireland) and pasting one of the PSA sides to a petri dish [550].

For PDMS casting, the precursor was prepared by mixing PDMS elastomer with the curing agent from Sylgard 184 kit at a weight ratio of 10 : 1, poured onto a master mould, and cured in an oven at $80\,^{\circ}C$ for 2 hours. Following curing, the PDMS layer is peeled from the master. The inlets and outlets ($800\,\mu m$ in diameter) were made using a manual puncher (Technical Innovations, Inc., Brazoria, TX). The PDMS replica ($\sim 1\,mm$ in height) was thoroughly washed with isopropanol and exposed to oxygen plasma to seal the chip to a clean glass slide ($35\,mm \times 64\,mm$, Agar Scientific Limited, England) or another flat PDMS layer ($\sim 2\,mm$ height). Silicon tubes were employed to further connect the main inlets with a syringe pump (PHD 2000 Syringe, Harvard Apparatus) for sample delivery and washing.

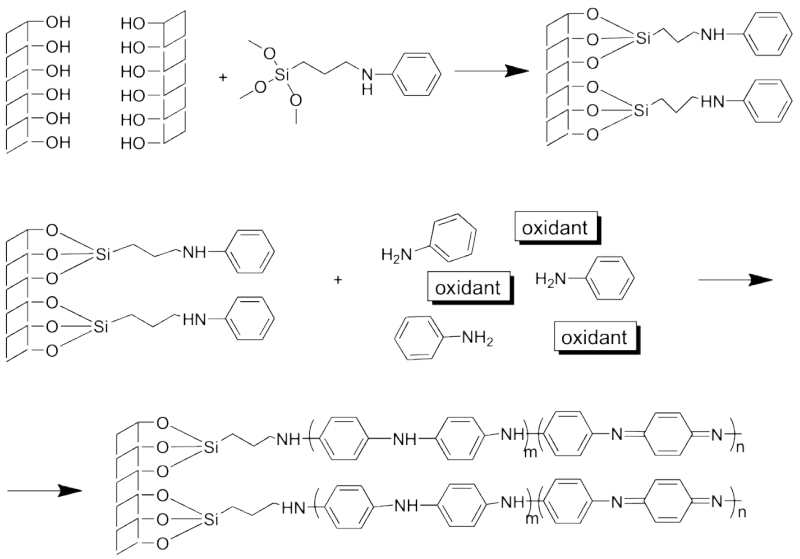

Figure 5.1: Chemical functionalisation of microchannel surface with polyaniline chains.

5.2.2 Microfluidic Device Functionalisation

The functionalisation of the inner walls of the microfluidic channel with PAni nanofibres was achieved using the procedure described in Figure 5.1 on page 162. The detailed microchannel functionalisation process and the corresponding characterisation of the coating are listed in Appendix C. Briefly, immediately after exposure of the PDMS chips to oxygen plasma for $60\,s$ (Harrick Plasma) and sealing to the glass slide/PDMS layer, the activated channels ($1000 \times 100\,\mu m$) were flushed with a 20% wt solution of N-[3- (trimethoxylsilyl) propyl]aniline in ethanol for $60\,min$ at a flow rate of $0.5\,\mu L\,min^{-1}$. Using this technique, a monolayer of silane-bearing aniline was formed on the substrate via molecular self-assembly. Chemical deposition of the PAni on the modified microchannel walls was performed by filling the microchannel with freshly prepared $1\,M$ HCl solution containing the oxidant (ammonium peroxydisulfate) and aniline in a molar ratio of $0.25 : 1$. This molar ratio was chosen as it has been previously shown that polymerisation of aniline in these experimental conditions produces nanofibres [545] . The pendant aniline on the surface served as the initiation site for polymerisation and was also used to covalently anchor the PAni chain on the substrate [556]. The polymerisation time was fixed to $20\,hours$. After polymerisation, the channels were washed extensively with water to remove any unattached polyaniline nanofibres. The resulting films had good adhesion due to the chemical bonding between the substrate and polymer film. Homogeneous PAni coatings were obtained, covalently attached to the internal walls of microchannels made of PDMS/PDMS or PDMS/glass, see Figure 5.2 on page 163.

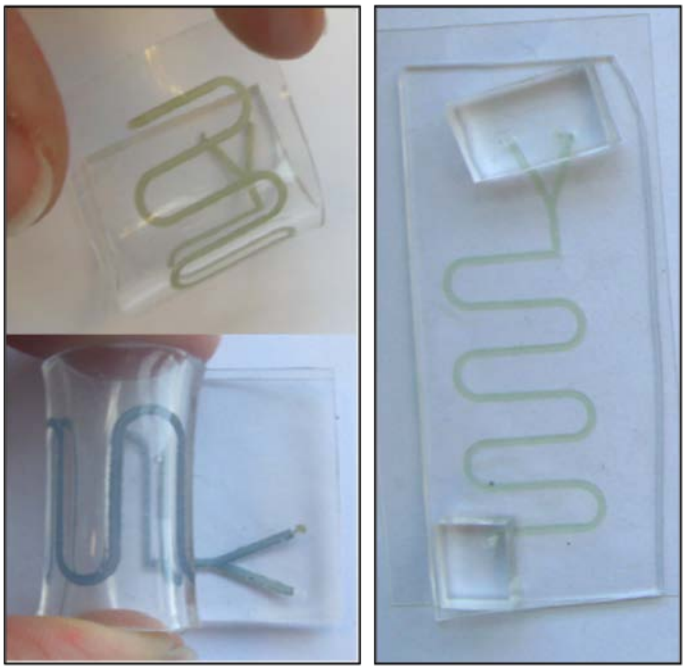

Figure 5.2: Pictures of polyaniline functionalised PDMS/PDMS (left), acidic on the top and basic on the bottom, and glass/PDMS (right) microfluidic devices. The picture on the right shows the PDMS extensions that were attached to the PDMS layer by oxygen plasma. These extensions were configured to secure the connections between the silicon tubes and the inlets of the microchannel and to facilitate sample delivery.

5.2.3 Measurement of Absorbance Spectra of PAni Coatings

Changes in the absorbance spectra of the PAni coatings as different pH solutions flushed inside the microchannel were recorded using two fiber-optic light guides connected to a Miniature Fiber Optic Spectrometer (USB4000 - Ocean Optics) and aligned using an in-house made holder. The in-house designed holder was fabricated using a 3D printer (Dimension SST 768) in black acrylonitrile butadiene styrene co-polymer (ABS) plastic in order to minimise interferences from ambient light. The two parts of the holder (2 identical parts, one to be placed on top of the microfluidic chip, the other underneath) were designed using ProEngineer CAD/CAM software package and fixed together with screws ensuring precise alignment between the two fiber-optics (SI - Figure C.1 on page 229). The Absorbance spectra recorded with Miniature Fiber Optic Spectrometer (USB4000). For clarity, all absorbance spectra recorded were smoothed using Origin software using Savitzky- Golay algorithm.

5.2.4 Digital Image Capture

After the fabrication of the flow channels and subsequent analysis using reference instrumentation (spectrophotometer) the channels were then subjected to analysis via digital imaging techniques. The channel was placed within the field of view of a standard colour camera (Panasonic DMC-FZ38) along with a white background

for subsequent image processing. An XRite professional colour reference chart was also placed within the camera's field of view (see SI - Figure C.2 on page 231) as this experiment was performed under variable ambient lighting conditions.

Solutions of known pH produced by mixing appropriate amounts of hydrochloric acid or sodium hydroxide (pH 2 to 12) were then flushed through the microchannel at a flow rate of $50\,\mu L\,min^{-1}$. At each pH unit step, an image was captured using the colour camera. This process was repeated and multiple images gathered at each unit step to investigate reproducibility.

An additional set of images were similarly captured, in which the flow channel was first filled with a solution of pH 3 and then a droplet of pH 6.5 aqueous solution placed at the opposite inlet where it was encouraged along the microchannel via an applied negative pressure using a microsyringe. This generated a pH gradient inside the microchannel along the channel's length. Therefore, the channel showed two extreme colours at either end coupled with a colour gradient connecting them. The ability to detect this pH gradient point through image processing and analysis was then investigated.

5.2.5 Image Processing

A number of image processing steps were employed in order to analyse the overall channel pH for the calibration procedure, and subsequently additional steps were undertaken to detect the pH gradient along the channel. After capturing an image (see ESI† - Figure C.2a on page 231) a segmentation process identified regions of interest from background areas (see SI - Figure C.2b on page 231). The regions were identified based on their spatial coordinates and were matched between progressive calibration images on this basis. The average Hue component of each region was taken to represent the colour of the channel and reference patches, which were then used for normalisation, and later to generate a calibration plot. Following this, a similar approach was employed to analyse the pH gradient along the channel in which the pH analysis was localised at every point along the channel. A more detailed account of these processing steps can be found within the accompanying supporting information (see Appendix C, Section C.2).

5.3 Results and Discussion

5.3.1 Characterisation of the PAni Coatings

The PAni coatings were characterised by Raman spectroscopy as it permits *in situ* analysis [512] of PAni coating inside the microchannel (see SI - Figure C.4 on page 233). Raman spectroscopy showed that PAni is obtained in its half-oxidised emeraldine state [574]. In addition, Raman spectroscopy was also employed to study

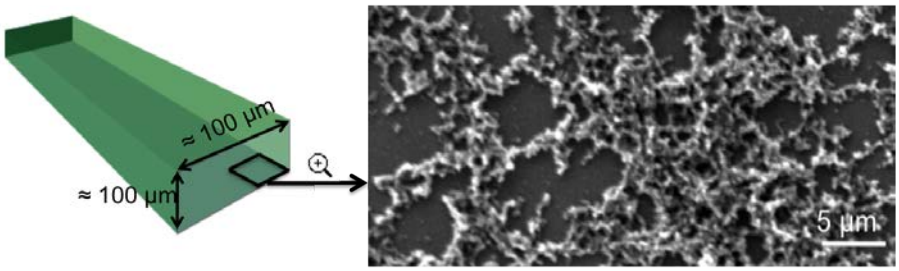

Figure 5.3: Representation of the polyaniline functionalised microchannel (left). SEM image of the polyaniline functionalised glass bottom layer showing a homogeneously covered surface with polyaniline nanofibres (right).

the changes in the bonding structure of the coatings upon doping-dedoping, as very distinct signature bands appear for the quinoid and benzenoid rings, respectively [499, 576]. When a solution of pH 2 is passed through the microchannel, PAni presents the typical bands for the emeraldine salt (ES). When a solution of pH 12 is flushed through the microchannel, the ES bands decrease and the specific quinoid ring bands appear in the spectra, reflecting the dedoped state – emeraldine base (EB).

Scanning electron microscope (SEM) images showed that using the polymerisation technique described in the experimental section, PAni nanofibres were obtained, covalently attached to the inner walls of the microchannels, (Figure 5.3 on page 165). The immediate advantages of having nanofibres (versus bulk PAni) are the high surface area that is exposed to the target molecules and the very short diffusional path lengths [523] which produces enhanced sensitivity coupled with fast response times [525, 524, 555].

5.3.2 pH Measurements

Polyaniline's sensitivity towards pH has been extensively used in recent years for the development of pH sensors due to its intrinsic doping-dedoping pH response [544, 520]. However, to the best of our knowledge this is the first example of the use of polyaniline nanofibres as a pH optical sensor in a microfluidic device, wherein the whole inner wall of the microchannel acts as a sensor enabling the pH to be measured simultaneously at all points within the channel.

The reversible protonation/deprotonation reaction of PAni is of particular interest during the development of the pH sensor. The process occurs on the imine nitrogen atoms as shown in SI - Figure C.5 on page 233. The transformation of Emeraldine Salt (ES) to Emeraldine Base (EB) by deprotonation is accompanied by significant changes in colour. This phenomenon is observed in the case of the PAni coatings when colourless solutions of at varying pH are passed through the microchannel, showing the ability of the covalently bonded PAni nanofibres to rap-

idly respond to changes in their environment (see SI - Figure C.5 on page 233). The changes in the absorbance spectra of the PAni coatings in response to different pH solutions flushed inside the microchannel were recorded using two fiber-optic light guides connected to a Miniature Fiber Optic Spectrometer and aligned using an in-house made cell.

The UV–Vis absorption spectra of PAni films were measured for each pH solution passed through the channel at a flow rate of $50\,ML\,min^{-1}$, see Figure 5.4 on page 167. It is important to note that the absorbance spectrum changes very rapidly after the solution reaches the detection area (approx. 2 s), thereby ensuring a very fast response of the device (see ESI† - videos 1 and 2). Moreover, the signal remains stable during the timescale of the experiment, which was set to 5 minutes. The measurements were done in triplicates with a standard deviation of the absorbance value over the calibration range of 0.001.

As depicted in Figure 5.4 on page 167 the spectrum of the PAni coatings is highly pH dependent and changes in colour from the green (ES) to blue (EB). Increasing the pH from 2 to 12 leads to a shift in the absorption λ_{max} of PAni in the visible region from $420\,nm$ (at pH 2) to $605\,nm$ (at pH 12). This shift is due to doping–dedoping of PAni coatings and can be explained by the different degree of protonation of the imine nitrogen atoms in the polymer chain [509]. More specifically, in a low pH environment, PAni exhibits strong absorbances at approximately $420\,nm$ and $830\,nm$ assigned to polaron and bipolaron transitions. Upon dedoping these transitions disappear and a new absorbance band appears at approximately $600\,nm$. This new band is ascribed to the exciton formation in the quinonoid rings [513] and it is responsible for the blue colour of the PAni coatings. The pH dependence of the absorptions at $605\,nm$ and $832\,nm$ were plotted in Figure 5.4 on page 167 – Inset. The characteristic PAni sigmoid shape curve ($R^2 = 0.996$) was obtained for the absorbance change versus pH, similar to the previous reported results in the case of PAni [519, 574]. The curve is broad, ensuring that the pH dependence of the PAni occurs over a wide range of pH. Therefore, this type of coating can be used for pH sensing across a reasonably broad range, constituting an important advantage over common pH indicator dyes. Since PAni does not fit the expected response curve for an indicator, because of its broad range, the Henderson-Hasselbach equation cannot be applied [530]. In the literature, there have been attempts to introduce an adjusted exponent to fit PAni doping- dedoping behaviour using Henderson-Hasselbach equation, although these attempts were proven to be unsuccessful [520]. Therefore, only an apparent pK_a value can be used to describe the sensor response. As depicted from Figure 5.4 on page 167 – Inset, the apparent pK_a value of PAni coatings is approximately 5, representing the pH value where the two sigmoidals intersect (concentration of ES is approximately equal with the concentration of EB). Most probably this value represents a distribution of pK_a's of PAni units with

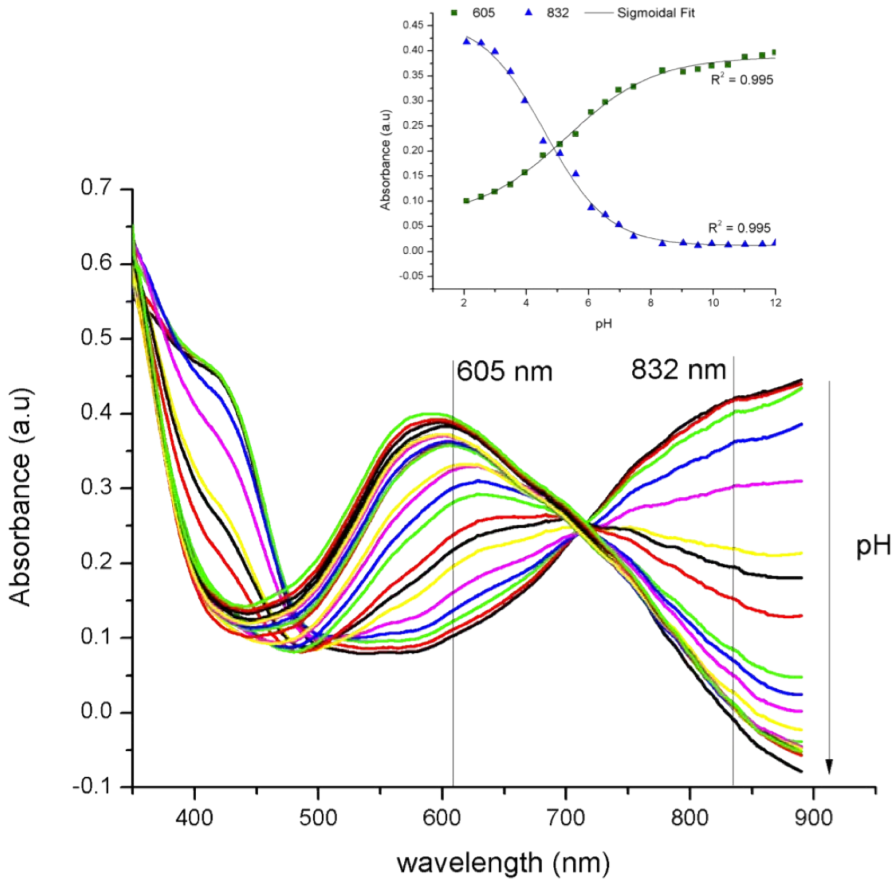

Figure 5.4: Absorbance spectra of the polyaniline coatings in the channel when solutions at different pH are passed through (pH 2-12). Inset - Graph of the absorbance change of polyaniline coatings vs. pH at 605 nm and 832 nm.

differing chain length and local environments [544]. Nevertheless, since important changes in λ_{max} and absorbance were observed in the pH range from 2 to 8, it should be possible to use these PAni coated microchannels for monitoring the pH of, for instance, physiological fluids (gastric juice, saliva, blood) which are important applications for microfluidics at this time.

5.3.3 pH Determination via Colorimetric Imaging Analysis

It has been shown that the channels respond accurately to changes in pH when analysed using a spectrophotometer. However, this work also explored the possibility of performing colorimetric analysis without the need for specialised instrumentation i.e. through the use of a standard digital colour camera. This has the potential to extend the applicability of the sensor, for instance, to point of care microfluidic devices and to low cost diagnostics for the developing world using mobile phones with integrated digital cameras to capture analytical information [537]. The steps taken to extract colorimetric information from the captured images are outlined in detail in the SI - Appendix C.

Processing of the images began with the application of a white balance algorithm. This was possible as the image setting/scene was relatively similar in each case, and included a white region specifically for this purpose. As this study took place in an ambient lighting environment, normalisation of the images in this way was necessary to compensate for shifts in ambient light intensity. For further robustness, the Hue value representing the colour of the channel underwent a colour normalisation process using two of the array of invariant reference patches (i.e. the purple and yellow patches as presented in Figure C.2a on page 231). Next, the average and standard deviation of the channel's normalised Hue value across each of the captured images at corresponding pH unit steps were calculated ($RSD \leq 2.06$). Following this, a calibration plot of the camera's response to different pH solutions was achieved and a sigmoidal model was applied to the data points, see SI - Figure C.6 on page 234. It can be seen from the figure that an excellent fit was achieved ($R^2 = 0.998$, $n = 18$) and subsequently, the resulting mathematical model was used to map the camera response to pH concentration values for gradient analysis.

While spectrophotometer and the camera generate the pH estimations on the basis of 'colour' measurements, the way in which this is achieved is different for both devices. The spectrophotometer can generate a calibration plot at any effective wavelength (i.e. regions of the absorbance spectrum of the dye that change with pH) within its measurement range. For this study, the most dominant peak changes were selected; $605\,nm$ and $832\,nm$, see Figure 5.4 on page 167. In contrast, the camera measures colour across the entire available spectrum, and wavelength specific measurements are not possible except through the rather crude RGB division of the spectrum into three 'Red', 'Green', and 'Blue' (RGB) channels. When conversion into the HSV colour space is applied, the H (Hue) component quantitatively represents the most dominant 'colour' based on the transformation from the captured sRGB data to the target HSV colour space [551], see SI - Figure C.6 on page 234.

Although, individually, each approach generated good quality fits to the calibration data, it was important to establish whether a correlation existed between both detection methods. One way of achieving this was to compare the predicted pH at each unit using the derived mathematical regression models. Figure C.7 on page 235 in the SI presents a plot of the predicted pH using the camera model against the UV-Vis model at $832\,nm$. Clearly, a linear correlation exists when comparing both approaches with a good fit resulting ($R^2 = 0.98$, $n = 18$). Moreover, the difference in slope between this linear fit and the ideal slope (slope = 1) is relatively small at 0.021, suggesting there is little bias or skewness between the two data sets. The correlation between the camera and the UV-Vis model at $605\,nm$ was also investigated. Similar accuracies were achieved with $R^2 = 0.98$ and a difference to the ideal slope of 0.025. From SI - Figure C.7 on page 235 it can be seen that the goodness

of fit of the correlation decreases above c.a. pH 7. This arises from the increasingly small absorbance (colour changes) occurring above this value, see Figure 5.4 on page 167 (inset). Despite this, it is interesting to note that the camera and the spectrometer data remain reasonably well correlated above pH 7, although the scatter is understandably greater, see SI - Figure C.7 on page 235.

5.3.4 Gradient pH Measurements

The main advantage of the digital camera over the spectrometer lies in its ability to rapidly generate spatially distributed information. This should enable the camera to dynamically track changes in pH along the entire length of the fluidic channel. To test this thesis, the microchannel was filled with a pH 3 solution and a second solution of pH 6.5 was introduced at one end, as described in the experimental section and SI - Appendix C. The solutions were allowed to diffuse until a pH gradient visually appeared whereupon an image was captured (Figure 5.5a on page 171).

Following the image processing and data extraction as described above, the images were white balanced and the Hue values at each localised point normalised with respect to the colour reference patches, as described previously for the calibration process. Using the calibration model derived from the sigmoidal regression analysis, the localised Hue values were mapped to their corresponding pH concentrations and a plot of pH concentration over the length of the channel was derived. To reduce noise, a smoothing algorithm based on the Savitzky-Golay filter [548] was applied to the data set. For both Figure 5.5b and Figure 5.5c on page 171, labels are present to denote discrete points along the flow path i.e. points of maximum curvature along the four considered flow bends.

It can be seen visually from Figure 5.5b on page 171 that the pH varies significantly between points '2' and '3' as reflected in the colour gradient. Correspondingly, the analysis presented (Figure 5.5c) shows a dramatic change in pH from ca. pH 3 at point '2' to ca. pH 6.5 at, and beyond, point '3'. Figure 5.5c shows the resulting pH gradient as estimated by processing the colour image with the digital camera algorithm. Close examination of the image reveals the presence of small bubbles, which manifest as slight inconsistencies in the unsmoothed pH data in Figure 5.5c.

To demonstrate the capabilities of the digital imaging approach, changes in the pH along the entire channel were tracked using low-cost digital video imaging, see supplementary information (ESI† – Video 3). In this example, the image section under analysis is bounded by a red square and also enlarged (shown in the top left corner). In addition, a dynamic plot is presented on the right hand side of the video showing the change in pH along the channel. Although the data in Figure 5.5 on page 171 and ESI† – Video 3 represents the pH dynamics of the channel at a single point in time, this process can be easily expanded to enable pH variations to be tracked dynamically along the entire microfluidic system as a function of time.

This capability could have a substantial impact in many areas. For instance, a number of chemical reactions are time critical and require precision when introducing a reagent. By coupling a microfluidic system, PAni and a low cost colour camera, a miniaturised and cost effective solution can be achieved for many chemical and biochemical sensing scenarios that rely on a localised pH to drive the reaction. The speciation state of multibasic acids, or of amino acids could be inferred from a knowledge of pH gradients. Mixing processes involving buffers could be tracked to identify locations of optimum pH for particular processes, and to explore how these locations can be moved, expanded or contracted prior to addition of active reagents. Furthermore, the rapid improvement in price-performance in digital photography through the development of sophisticated, miniaturised and low cost CCD sensors [552, 539, 557] and its increasing integration with mobile phones, provides a powerful technology platform for many new applications. However, while tremendous potential impact of integration of chemical/biological measurements with digital imaging and communications is compelling, for example, in tele-health and personal (point-of-need) diagnostics, the route to winning applications is not clear. Hence, companies like Nokia are sponsoring global competitions with very significant prizes to generate ideas from which they will select the best possible candidate applications [543]. This activity emphasises the rising importance of applying digital imaging to analytical measurements.

5.4 Conclusions

A new, simple, and fast photometric method to measure pH using PAni based coatings in microfluidic devices is presented. pH measurements were performed in continuous flow mode using fiber-optic light guides aligned to the device using an in-house made cell. The main advantage of these sensors is that no reagent indicator is needed to measure the pH, because the PAni acts as the indicator itself, reducing the complexity of pH detection inside microchannels. The functionalisation process is easy and highly reproducible from microdevice to microdevice and over the whole microchannel length. Moreover, it can be easily achieved using different materials as such glass, PDMS, or any other material that allows the introduction of hydroxyl groups on the surface necessary for the present silanisation procedure. Although the time for functionalisation is rather long ($22\,h$), the polyaniline functionalised microchannels are suitable for multiple uses since the coating can be easily regenerated by passing an acidic solution (HCl solution, pH 2) inside the channel. PAni coated microchannels present long-term stability and reproducibility, can be stored at room temperature, exposed to air, empty or filled with a pH 2 solution for over two months without any deterioration in sensor performance.

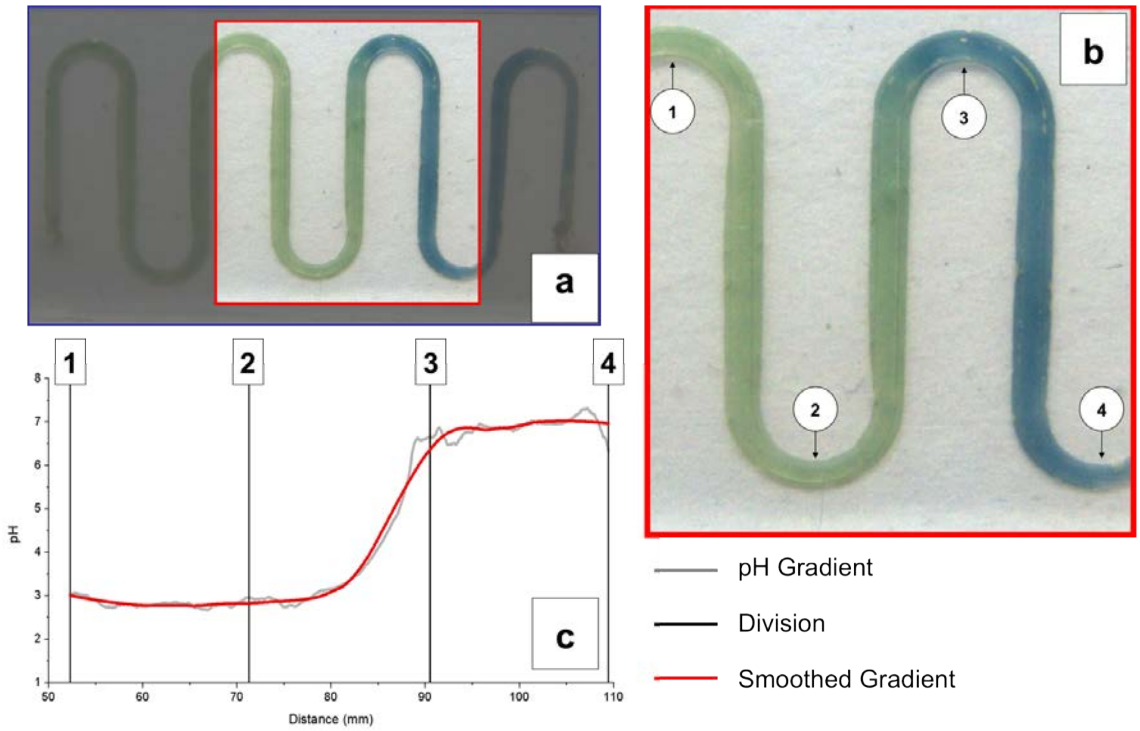

Figure 5.5: (a) Images showing a pH gradient along the microfluidic channel reflected in the changing colour of the PAni coating, red box shows a magnified section in (b), which also identifies specific locations (1-4) highlighted in (c), Plot of the pH gradient along the flow channel generated from the image. The grey line is the raw data from the analysis; the red line has been smoothed using the Savitsky-Golay algorithm.

Since this technique is based on pH responsive coatings, at present, it is not suitable for 3D pH sensing in microchannels but rather 2D (along the length and width of the channel) pH sensing. However, when coupled with imaging techniques, this approach offers a low cost, accurate approach for the tracking of the 2D temporal and spatial dynamics of pH changes along an entire microfluidic channel in real-time, without the need to add a pH sensitive dye to the liquid phase in the channel. The approach of using the colour camera for pH mapping is generic and could be applied for a wide variety of pH responsive systems.

5.5 References

[496] I Alexandre, S Hamels, S Dufour, J Collet, N Zammatteo, F De Longueville, JL Gala, and J Remacle. **Colorimetric silver detection of DNA microarrays**. *Analytical Biochemistry*, **295**(1):1–8, AUG 1 2001.

[497] E. Asijati, B. Kuswandi, N.F. Arifah, Y.I. Kurniawati, and A.A. Gani. **Non-invasive optical chemical sensor based on polyaniline films for detection of ammonia and acetic acid solutions**. In *Sensors and the International Conference on new Techniques in Pharmaceutical and Biomedical Research, 2005 Asian Conference on*, pages 111 – 114, sept. 2005.

[498] SM Barnard and DR Walt. **A Fiberoptic Chemical Sensor With Discrete Sensing Sites**. *Nature*, **353**(6342):338–340, Sep 26 1991.

[499] M Bartonek, NS Sariciftci, and H Kuzmany. **Resonance Raman-Spectroscopy of The Emeraldine Insulator-To-Metal Phase-Transition**. *Synthetic Metals*, **36**(1):83–93, MAY 1990.

[500] Lourdes Basabe-Desmonts, Fernando Benito-Lopez, Han J. G. E. Gardeniers, Rob Duwel, Albert van den Berg, David N. Reinhoudt, and Mercedes Crego-Calama. **Fluorescent sensor array in a microfluidic chip**. *Analytical and Bioanalytical Chemistry*, **390**(1):307–315, JAN 2008.

[501] Fernando Benito-Lopez, Silvia Scarmagnani, Zarah Walsh, Brett Paull, Mirek Macka, and Dermot Diamond. **Spiropyran modified micro-fluidic chip channels as photonically controlled self-indicating system for metal ion accumulation and release**. *Sensors and Actuators B-Chemical*, **140**(1):295–303, Jun 18 2009.

[502] K Berrada, S Quillard, G Louarn, and S Lefrant. **Polyanilines and Substituted Polyanilines - A Comparative-Study of The Raman-**

Spectra Of Leucoemeraldine, Emeraldine and Pernigraniline. *Synthetic Metals*, **69**(1-3):201–204, MAR 1 1995. 13th International Conference on Science and Technology of Synthetic Metals (ICSM 94), SEOUL, SOUTH KOREA, JUL 24-29, 1994.

[503] D Betteridge, WC Cheng, EL Dagless, P David, TB Goad, DR Deans, DA Newton, and TB Pierce. **An Automated Viscometer Based On High-Precision Flow-Injection Analysis .1. Apparatus For High-Precision Flow-Injection Analysis**. *Analyst*, **108**(1282):1–16, 1983.

[504] L Byrne, J Barker, G Pennarun-Thomas, D Diamond, and S Edwards. **Digital imaging as a detector for generic analytical measurements**. *TRAC-TRENDS IN ANALYTICAL CHEMISTRY*, **19**(8):517–522, AUG 2000.

[505] L Byrne, KT Lau, and D Diamond. **Development of pH sensitive films for monitoring spoilage volatiles released into packaged fish headspace**. *IRISH JOURNAL OF AGRICULTURAL AND FOOD RESEARCH*, **42**(1):119–129, JUN 2003.

[506] K. Cantrell, M. M. Erenas, I. de Orbe-Paya, and L. F. Capitan-Vallvey. **Use of the Hue Parameter of the Hue, Saturation, Value Color Space As a Quantitative Analytical Parameter for Bitonal Optical Sensors**. *ANALYTICAL CHEMISTRY*, **82**(2):531–542, JAN 15 2010.

[507] Yi Cheng, Xiaolong Luo, Jordan Betz, Susan Buckhout-White, Omar Bekdash, Gregory F. Payne, William E. Bentley, and Gary W. Rubloff. **In situ quantitative visualization and characterization of chitosan electrodeposition with paired sidewall electrodes**. *SOFT MATTER*, **6**(14):3177–3183, 2010.

[508] Yi Cheng, P. Xiong, C. Steven Yun, G. F. Strouse, J. P. Zheng, R. S. Yang, and Z. L. Wang. **Mechanism and Optimization of pH Sensing Using SnO2 Nanobelt Field Effect Transistors**. *NANO LETTERS*, **8**(12):4179–4184, DEC 2008.

[509] JC Chiang and AG Macdiarmid. **Polyaniline - Protonic acid Doping of The Emeraldine Form to the Metallic Regime**. *Synthetic Metals*, **13**(1-3):193–205, Jan 1986.

[510] YL Chin, JC Chou, TP Sun, WY Chung, and SK Hsiung. **A novel pH sensitive ISFET with on chip temperature sensing using CMOS standard process**. *Sensors and Actuators B-Chemical*, **76**(1-3):582–593,

JUN 1 2001. 8th International Meeting on Chemical Sensors (IMCS-8), BASEL, SWITZERLAND, JUL 02-05, 2000.

[511] JR Clinch, PJ Worsfold, and H Casey. **An Automated Spectrophotometric Field-Monitor For Water-Quality Parameters - Determination Of Nitrate**. *Analytica Chimica Acta*, **200**(1):523–531, SEP 1 1987.

[512] J. Dambrine, B. Geraud, and J-B Salmon. **Interdiffusion of liquids of different viscosities in a microchannel**. *New Journal Of Physics*, **11**:–, JUL 31 2009.

[513] AJ Epstein, JM Ginder, F Zuo, RW Bigelow, HS Woo, DB Tanner, AF Richter, WS Huang, and AG Macdiarmid. **Insulator-To-Metal Transition In Polyaniline**. *Synthetic Metals*, **18**(1-3):303–309, Feb 1987.

[514] Cormac Fay, King-Tong Lau, Stephen Beirne, Ciaran O. Conaire, Kevin McGuinness, Brian Corcoran, Noel E. O'Connor, Dermot Diamond, Scott McGovern, Greg Coleman, Rod Shepherd, Gursel Alici, Geoff Spinks, and Gordon Wallace. **Wireless aquatic navigator for detection and analysis (WANDA)**. *Sensors and Actuators B-Chemical*, **150**(1):425–435, SEP 21 2010.

[515] MA Feres and BF Reis. **A downsized flow set up based on multicommutation for the sequential photometric determination of iron(II)/iron(III) and nitrite/nitrate in surface water**. *Talanta*, **68**(2):422–428, Dec 15 2005. 13th International Conference on Flow Injection Analysis, Las Vegas, NV, APR 24-29, 2005.

[516] Larisa Florea, Fernando Benito-Lopez, Alexandre Hennart, and Dermot Diamond. **Photo-Detection of Solvent Polarities using Non-Invasive Coatings in Capillaries**. *Procedia Engineering*, **25**(0):1545 – 1548, 2011. <ce:title>EurosensorsXXV</ce:title>.

[517] Larisa Florea, Alexandre Hennart, Dermot Diamond, and Fernando Benito-Lopez. **Synthesis and characterisation of spiropyran-polymer brushes in micro-capillaries: Towards an integrated optical sensor for continuous flow analysis**. *Sensors and Actuators B: Chemical*, **175**(0):92 – 99, 2012. <ce:title>Selected Papers presented at Eurosensors XXV</ce:title>.

[518] Xudong Ge, Yordan Kostov, Leah Tolosa, and Govind Rao. **Study on low-cost calibration-free pH sensing with disposable optical sensors**. *Analytica Chimica Acta*, **734**:79–87, JUL 13 2012.

[519] ZF GE, CW Brown, LF Sun, and SC Yang. **Fiberoptic pH Sensor-Based on Evanescent-Wave Absorption-Spectroscopy**. *Analytical Chemistry*, **65**(17):2335–2338, SEP 1 1993.

[520] UW Grummt, A Pron, M Zagorska, and S Lefrant. **Polyaniline based optical pH sensor**. *Analytica Chimica Acta*, **357**(3):253–259, DEC 31 1997.

[521] T Gunnlaugsson, PE Kruger, P Jensen, J Tierney, HDP Ali, and GM Hussey. **Colorimetric "naked eye" sensing of anions in aqueous solution**. *Journal of Organic Chemistry*, **70**(26):10875–10878, DEC 23 2005.

[522] PC Hauser, SS Tan, TJ Cardwell, RE Cattrall, and IC Hamilton. **Versatile Manifold for the Simultaneous Determination of Ions In Flow-Injection Analysis**. *Analyst*, **113**(10):1551–1555, Oct 1988.

[523] JX Huang. **Syntheses and applications of conducting polymer polyaniline nanofibers**. *Pure And Applied Chemistry*, **78**(1):15–27, JAN 2006.

[524] J Huang, S Virji, BH Weiller, and RB Kaner. **Nanostructured polyaniline sensors**. *Chemistry-A European Journal*, **10**(6):1314–1319, MAR 19 2004.

[525] JX Huang, S Virji, BH Weiller, and RB Kaner. **Polyaniline nanofibers: Facile synthesis and chemical sensors**. *Journal of the American Chemical Society*, **125**(2):314–315, JAN 15 2003.

[526] Wen-Ding Huang, Hung Cao, Sanchali Deb, Mu Chiao, and J. C. Chiao. **A flexible pH sensor based on the iridium oxide sensing film**. *Sensors and Actuators A-Physical*, **169**(1):1–11, SEP 10 2011.

[527] A Hugotlegoff and MC Bernard. **Protonation and Oxidation Processes In Polyaniline Thin-Films Studied By Optical Multichannel Analysis And In-Situ Raman-Spectroscopy**. *Synthetic Metals*, **60**(2):115–131, SEP 15 1993.

[528] KS Johnson, CL Beehler, and CM Sakamotoarnold. **A Submersible Flow-Analysis System**. *Analytica Chimica Acta*, **179**:245–257, Jan 31 1986.

[529] V. K. Khanna. **Fabrication of ISFET microsensor by diffusion-based Al gate NMOS process and determination of its pH sensitivity from transfer characteristics**. *Indian Journal of Pure & Applied Physics*, **50**(3):199–207, MAR 2012.

[530] Norbert Klauke, Paul Monaghan, Gavin Sinclair, Miles Padgett, and Jon Cooper. **Characterisation of spatial and temporal changes in pH gradients in microfluidic channels using optically trapped fluorescent sensors**. *Lab on a Chip*, **6**(6):788–793, JUN 2006.

[531] B Kuswandi and R Narayanaswamy. **Polymeric encapsulated membrane for optrodes**. *Fresenius Journal of Analytical Chemistry*, **364**(6):605–607, JUL 1999.

[532] A. Lapresta-Fernandez and L. F. Capitan-Vallvey. **Environmental monitoring using a conventional photographic digital camera for multianalyte disposable optical sensors**. *Analytica Chimica Acta*, **706**(2):328–337, NOV 14 2011.

[533] KT Lau, S Baldwin, M O'Toole, R Shepherd, WJ Yerazunis, S Izuo, S Ueyama, and D Diamond. **A low-cost optical sensing device based on paired emitter-detector light emitting diodes**. *Analytica Chimica Acta*, **557**(1-2):111–116, JAN 31 2006.

[534] KT Lau, S Baldwin, RL Shepherd, PH Dietz, WS Yerzunis, and D Diamond. **Novel fused-LEDs devices as optical sensors for colorimetric analysis**. *Talanta*, **63**(1):167–173, MAY 10 2004.

[535] King Tong Lau, R. Shepherd, Danny Diamond, and Dermot Diamond. **Solid state pH sensor based on light emitting diodes (LED) as detector platform**. *Sensors*, **6**(8):848–859, AUG 2006.

[536] S. Martellucci, A.N. Chester, and A.G. Mignani. *Optical Sensors and Microsystems: New Concepts, Materials, Technologies*. Springer, 2000.

[537] Andres W. Martinez, Scott T. Phillips, George M. Whitesides, and Emanuel Carrilho. **Diagnostics for the Developing World: Microfluidic Paper-Based Analytical Devices**. *Analytical Chemistry*, **82**(1):3–10, JAN 1 2010.

[538] FAA Matias, MMDC Vila, and M Tubino. **A simple device for quantitative colorimetric diffuse reflectance measurements**. *Sensors and Actuators B-Chemical*, **88**(1):60–66, JAN 1 2003.

[539] P. Maxwell. **Test for low cost CMOS image sensors**. In *Test Symposium, 2005. European*, page 222, may 2005.

[540] P Mela, S Onclin, MH Goedbloed, S Levi, MF Garcia-Parajo, NF van Hulst, BJ Ravoo, DN Reinhoudt, and A van den Berg. **Monolayer-functionalized microfluidics devices for optical sensing of acidity**. *Lab on a Chip*, **5**(2):163–170, 2005.

[541] Junichi Miwa, Yuji Suzuki, and Nobuhide Kasagi. **Adhesion-based cell sorter with antibody-coated amino-functionalized-parylene surface**. *Journal of Microelectromechanical Systems*, **17**(3):611–622, JUN 2008. 20th IEEE International Conference on Micro Electro Mechanical Systems (MEMS 2007), Kobe, JAPAN, JAN 21-25, 2007.

[542] B. Nemeth, S. Tsuda, C. Busche, L. Cronin, and D. R. S. Cumming. **ISFET sensor system for real-time detection of extracellular pH oscillations in slime mould**. *Electronics Letters*, **48**(3):143–U20, FEB 2 2012.

[543] Nokia. **The Nokia Sensing X Challenge**. Online (`http://www.nokiasensingxchallenge.org/`).

[544] E Pringsheim, E Terpetschnig, and OS Wolfbeis. **Optical sensing of pH using thin films of substituted polyanilines**. *Analytica Chimica Acta*, **357**(3):247–252, DEC 31 1997.

[545] Junfeng Qiang, Zhuhuan Yu, Hongcai Wu, and Daqin Yun. **Polyaniline nanofibers synthesized by rapid mixing polymerization**. *Synthetic Metals*, **158**(13):544–547, AUG 2008.

[546] Andreas Richter, Georgi Paschew, Stephan Klatt, Jens Lienig, Karl-Friedrich Arndt, and Hans-Juergen P. Adler. **Review on hydrogel-based pH sensors and microsensors**. *Sensors*, **8**(1):561–581, JAN 2008.

[547] R. W. Sabnis, S. Sanders, and LLP. Dempsey. *Handbook of Acid-Base Indicators*. CRC PressINC, 2008.

[548] A Savitzky and MJE Golay. **Smoothing + Differentiation Of Data By Simplified Least Squares Procedures**. *Analytical Chemistry*, **36**(8):1627–&, 1964.

[549] GJ Schmidt and RPW Scott. **Simple and Sensitive Ion Chromatograph For Trace-Metal Determination**. *Analyst*, **109**(8):997–1002, 1984.

[550] A. B. Shrirao and R. Perez-Castillejos. **Simple Fabrication of Microfluidic Devices by Replicating Scotch-tape Masters**. *RSC Publishing: Chips & Tips*, **-**:–, 17 May 2010.

[551] Alvy Ray Smith. **Color gamut transform pairs**. *SIGGRAPH Comput. Graph.*, **12**(3):12–19, August 1978.

[552] H. Tamayama, K. Ito, and T. Nishimura. **Technology trends of high-definition digital still camera systems**. In *VLSI Circuits Digest of Technical Papers, 2002. Symposium on*, pages 100 – 105, 2002.

[553] Quang Thong Trinh, Gerald Gerlach, Joerg Sorber, and Karl-Friedrich Arndt. **Hydrogel-based piezoresistive pH sensors: Design, simulation and output characteristics**. *Sensors and Actuators B-Chemical*, **117**(1):17–26, SEP 12 2006.

[554] CN Tsai, JC Chou, TP Sun, and SK Hsiung. **Study on the sensing characteristics and hysteresis effect of the tin oxide pH electrode**. *Sensors and Actuators B-Chemical*, **108**(1-2):877–882, JUL 22 2005. 10th International Meeting on Chemical Sensors, Tsukuba, JAPAN, JUL 11-14, 2004.

[555] S Virji, JD Fowler, CO Baker, JX Huang, RB Kaner, and BH Weiller. **Polyaniline manofiber composites with metal salts: Chemical sensors for hydrogen sulfide**. *Small*, **1**(6):624–627, MAY 2005.

[556] CG Wu and JY Chen. **Chemical deposition of ordered conducting polyaniline film via molecular self-assembly**. *Chemistry Of Materials*, **9**(2):399–&, FEB 1997.

[557] Feng Xiao, Xuemei Zhang, and Boyd Fowler. **Color processing in camera phones: How good does it need to be?** In *Proc. SPIE 5678, Digital Photography*, **-**, pages 96–104, 2005.

6 Conclusions

"My test of a good novel is dreading to begin the last chapter."

— Thomas Helm

THE WORK PRESENTED IN THIS THESIS has investigated previously unexplored methods of harvesting chemical information using optical detectors. The range of applications examined environmental monitoring, to wearable sensing, towards analysis of chemical gradients within a microfluidic channel. Connecting each piece of work was a question related to the most effective method for chemical sensing, under which two approaches have been proposed. The first is related to the implementation of a sensing model following the classic design approach i.e. the creation and deployment of dedicated devices within the environment with data harvested and transmitted in a real-time manner. However, there are questions related to this model in terms of scalability and cost effectiveness. The second - although investigated on a more exploratory level - considers the concept of using an infrastructure that is currently readily available in many areas, present on most modern devices, and possesses a sensing method which is most likely portable from platform to platform i.e. imaging technology. Three main areas are considered i.e. its potential impact for environmental monitoring, wearable sensing without the need for equipping the wearer with electronics, and detection of dynamics within microfluidic structures.

6.1 Summary

There have been a number of themes running throughout the course of this work. The first is the extraordinary capabilities residing within the molecular research community; the variety and the range of it. Chapter 1 has discussed the potential impact that this ability is having for environmental and health applications. However, it was also pointed out that sensing in these domains almost always takes place on a manual basis i.e. under laboratory conditions. The second theme considers the recent technological advances, its widespread use throughout the world, and its transformative effects on information gathering and exchange. One aspect of this has been in the development of sensing devices capable of gathering information from an environment. The development of WSNs consisting of low power sensor nodes and the overwhelming advancement and availability of vision system has allowed for information to be harvested and transferred in a multitude of forms. A question inexorably arises from both of these themes: why is chemical sensing devices not ubiquitous, and devices not available at the point of delivery? This question is not easily answered and can be attributed to a number of variables. One can relate this to the challenges in crossing the disciplinary divide, which has been discussed in Chapter 1.

Chapter 2 highlighted the difficulties involved in the monitoring, and the frequency of monitoring greenhouse gas emissions from landfill sites. The work presented in this paper has addressed these particular aspects through the investigation of applying an end-to-end autonomous sensing strategy to this process. The adoption of modern technology and wireless infrastructures, middleware management, and development of web-based applications has resulted in the creation of three novel prototypes capable of measuring the major chemical constituents of greenhouse gas (CO_2 and CH_4). The information was ultimately presented via a we-enabled portal page for stakeholders. Further to this, the longevity of these prototypes was investigated and demonstrated through the successful operation of the study which spanned over ca. 16 months. Data gathered throughout this period were analysed and revealed a number of legal breaches across all deployments. In addition, a comparison of the manual sampling technique to autonomous sampling took place using historical data. This highlighted a number of major events that were detected by the autonomous model which was missed when employing the manual approach. Finally, recommendations for future improvements of this model were outlined based on the findings/experience gained through this study.

The work in Chapter 3 explored the feasibility of of a novel approach to chemical sensing networks. Three sensing stations were constructed with a chemo responsive material that changed in colour when in contact with a chemical species; pH in this case. The stations were placed at three locations within a large container filled with water. In addition to this, a mobile sensing platform was developed capable of

traveling through the water body by means of biomimetic fish tail through the use of polypyrrole actuators. The actuators and therefore movements were controlled by on board electronic circuitry which received commands wirelessly. Another on board feature, responsible for chemical sensing allowed users to avoid collision with other objects through the use of a wireless colour camera. The premise of this work was to use the setup and component elements described above and apply them to the investigation of a novel chemical sensor network. One that may address certain issues related to the traditional setup of sensor nodes e.g. requiring independent electronic components, coordination of wireless communications, and also maintenance factors i.e. battery changes. To investigate this, the mobile fish platform was set on two patrols, in both cases to determine the state of the local environment through interrogation of the colorimetric chemical indicators en route by determination of its colour. The first patrol set a reference point where *normal* conditions were known i.e. there was no presence of the target chemical compound. During the second patrol, however, a concentrated contaminant was released (1 M HCl) in the direct location of one of the sensor station which resulted in a change in the pH indicator's colour. Through a series of image processing techniques developed by the student, the colour of the chemo responsive material was selected per station and quantified. Comparison of the data resulting from both patrols resulted in a clear difference or *event* occurring at the very station where the contaminant was released. This demonstrated the ability of this mobile device to detect a chemical contaminant (simulating a pollutant event) by a means other than the device dependent approach which commonly requires a number of efforts for deployment and maintenance.

The work presented in Chapter 4 explored the feasibility of developing a wearable system capable of harvesting chemical information from a user without the need for dedicated electronic circuitry. This was investigated by strategically separating elements that are fundamental to on-body molecular analysis (molecular world) from those that are required to quantify and digitise the information (digital world). In other words, this approach reduced the number of components on the wearer to those necessary for chemical analysis and as a result to limit the effect(s) that such devices may have on the user. The boiler plate components were placed on the wearer and the detection was achieved through a device capable of digital imaging capturing. Initially, a calibration routine was carried out where the chemical device was exposed to 'artificial sweat' solutions with concentrations of various pH. Through image capturing and processing, a mathematical calibration model was achieved for later use. By placing the device on an athlete and allowing them to exercise for a period of ca. 1 hour (including warm up time), their sweat was allowed to come in contact with the colorimetric pH indicators within the device causing them to change in colour. Measurements via a portable pH electrode at the point of interest

took place every 10 minutes along with simultaneously capturing the scene of the indicators via a digital camera. Later, the images were analysed and estimates of the pH were achieved through the aforementioned calibration model. Finally, the data to validate the results from the reference measurement and the camera measurement were compared.

Chapter 5 investigated a novel photometric approach to measuring pH along a microfluidic channel through a novel and low cost imaging approach. The detection mechanism also investigated the determination of a chemical gradient along the entire length of the channel. These features were explored through the creation of a microfluidic chip consisting of a single flow channel. During this process the walls of the channel were functionalised with a reversible chemical transducer i.e. PAni that changes colour with respect to concentrations of pH. A calibration process followed which involved flooding the channel with solutions of various pH concentrations in steps of 0.5 of a pH unit. At each pH stage, parallel analysis of the channel took place using a reference instrument (spectrophotometer, at two wavelengths) and a digital colour camera. In both cases, a mathematical regression model was applied to the data points and a good fit resulted i.e. $R^2 > 0.99$ in each case. A comparison between both approaches was also investigated and yielded that both data sets were highly correlated i.e. $R^2 > 0.98$ with very little difference in comparison to an ideal slope. Another aspect of this work was investigation into the detection of pH concentrations at all points along the channel. The demonstration of this concept took place by firstly inducing a pH gradient along the microfluidic channel along with capturing an image during this time. Analysis was possible through the established camera calibration model and image processing at all locations along the channel. A gradient plot resulted which agreed with observable evidence with respect to the location of changing colours.

6.2 Hypotheses and Contributions

At this point it is important to return to the original hypotheses and outline the contributions of each piece of work. The contributions are summarised in relation to the first hypothesis and then to the second.

The first hypothesis relates to novel methods of harvesting chemical based information through optical detection techniques in a non-invasive fashion. Even though that this has been investigated in the literature in a number of forms, the work presented here addresses this issue in previously unexplored areas and/or using novel techniques, with end applications in mind.

- In order to investigate this premise for landfill gas monitoring, IR sensors were chosen for two constituent gases and encased within an autonomous sensing platform which transmitted new information related to the local chemistry in

a real-time fashion - Chapter 2;

- This concept was then related to the detection of chemical events through the use of a moveable platform (equipped with a digital camera) and a network of stationary stations with a chemo-responsive element affixed - Chapter 3;
- Exploration of this idea for wearable sensing applications was achieved through colorimetric pH patches and extraction of the chemical information by means of capturing and interrogation of digital images - Chapter 4;
- Investigation into the detection of chemical gradients along microfluidic channels via digital imaging under this hypothesis was achieved in Chapter 5;

Emerging from this work was the investigation of a second hypothesis which posed the question if digital imaging approaches could reduce the underlying costs and efforts associated with the development of dedicated devices for optical chemical sensing. Chapter 2 served as exemplar to the efforts required for the development of a chemical sensing system based on the dedicated-device model. Chapter 3 on the other hand investigated this hypothesis directly through the possible reduction of sensing infrastructure for water-based chemical sensing. This concept was also explored in Chapter 4 which demonstrated a capability for harvesting chemical based information from a wearer during exercise without the need for wearable electronics. Finally, the possibility of detecting chemical gradients within microfluidic channels with a low cost approach (i.e. digital imagery) without the need for an array of sensors was investigated in Chapter 5.

While there are many potential advantages that the digital imaging approach can offer chemical sensing applications when compared to the dedicated design approach, it can also suffer from inherent drawbacks. As available resources and the environment under investigation have a substantial impact on the detection approach and choice of detector, it becomes difficult to offer a generic comparison. Nevertheless, a high level comparison is offered in Table 6.1 on page 184, where the language adopted is relative to each approach. Please note that while the contents within the table attempts to offer an objective viewpoint with respect to the sensing criteria, actual sensing implementations under specific conditions may disagree. However, the contents are based on the experience gained during the course of these years (see page viii) in conjunction with the environmental/wearable technologies reviewed previously (Section 1.5, Section 1.6, and 1.7.4).

6.3 Future Work

A number of exciting and novel opportunities exist in the context of chemical sensing in both the environmental and health related domains. The findings and contribu-

Table 6.1: Conceptual comparison of the dedicated-device and digital imaging approaches.

Criteria	**Dedicated Device Approach**	**Digital Imaging Approach**
Sensing Infrastructure	Must be implemented.	Possible to use existing vision systems (e.g. CCTV). Limited to these areas, otherwise must be supplied.
Data Load (Transmission/Storage)	Light. A data point can be limited to a time stamp and sense value.	Heavier. A single image consists of a large number of bytes (i.e. Rows × Columns × # Channels × Data Type)
Processing Requirements	Low. Can be performed on modern microcontrollers.	Higher. Likely to require microprocessors.
Power Requirements (Duty Cycle)	Relatively lower - depends on implementation, e.g. photodiode/PEDD.	High. Image processing techniques likely to require a number of procesing steps. Likely to be processed on server side.
Accomodation of Other Sensor Types	Methods readily exist for others, e.g. electrochemical, pellistor, optical, physical, etc.	Limited to optical sensing.
Expansion of Additional Indicators	Low level implementation required per sensing target and/or sensing type.	Easily accomodated if colorimetric based. A change in the software is required.
Portability	Likely to require calibration from one platform to the next. Variability exists between optical detectors.	Possible if all imaging devices can fully conform to the same colour space, e.g. sRGB. (Premise not explored)
Spatial Sensing	A large number of nodes required to cover the sensing area.	Possibility of one detector if magnification is sufficient and accessible, e.g. satellite spectral data. (Premise not explored for in situ sensing)
Sensitivity/Noise	Can be fine tuned to optimise sensitivity and reduce noise.	Limited. However, spatial averaging offers a greater degree of possible noise reduction.
Choice of Colorimetric Indicator	Greater degree of flexibility. Device can comply with the conditions of the indicator.	Limited as most cameras are standardised and mostly in visible region. Colorimetric indicator must be chosen to comply with imaging device.
Future Proof	Components are likely to be discontinued. Redesing and development maybe needed in this case.	More likely to comply with future imaging technology. See portabilitiy above.
Operational Lifetime	Depends upon chosen battery capacity, energy scavaging, and power usage.	Can last longer if using fixed systems (e.g. CCTV) and possibly magnification. Otherwise may have a shorter deployed life due to power requirements.
Multi-Dimensional Sensing	Must implement an array. Otherwise limited to a single point of data.	Inherently available: 1D with scanners, 2D with cameras.
Additional Uses	Sensor designed to target chosen parameters(s).	Can have multiple functions e.g. traffic/people tracking. A richer data set results.

tions to these domains by means of the work within this thesis have generally been positive. In relation to the specific issues investigated within this work, a number of possible avenues for future explorations is worth discussing.

6.3.1 Paper 1: Landfill Gas Monitoring (Chapter 2)

Relative to the time of this study and subsequent publication, a number of progressional steps have taken place which will be highlighted in this section. The experience gained through the the development of the first prototype generation (Gen #1) has given rise to a number of conceptual improvements to the system design which were suggested at the end of the publication. More than that, the second generation (Gen #2) of the full system is equipped with additional advantages and improvements. One of the primary aims was to drive down the cost whilst achieving the sensing requirements of the project. As a result a new casing was sourced along with an approach of *design for manufacture and assembly*. The resulting design is shown in Figure 6.1 on page 186 with example data harvested from an active landfill site using this system shown in Figure 6.3 on page 188.

The sensing procedure has been changed to suit the findings in the paper i.e. the baseline and purge stages have been omitted along with a reduction of the sample stage to 2 minutes. A result of this has allowed for a higher density of transmitted data in one single SMS text message, see Figure 6.2 on page 187. In this way, the user no longer receives a statistical report, but the full sample data set. Consequently, a more computationally intensive analysis and therefore representation of a single sample can be compiled. Moreover, stakeholders have access to the full dataset from the database.

With a more compact casing, a battery with less capacity was used; from one rated at 12 V 7 Ah to one of 12 V 4 Ah. This immediately meant that the system's longevity within the environment would be reduced. However, through establishing new embedded programming, the system is now capable of lasting for ca. 10.5 weeks without requiring power replenishment. This is a significant improvement from 4.5 weeks i.e. computationally by a factor of 2.3 times longer (on a lower capacity battery).

An improvement in data storage, visualisations, and access took place involving a new feature by Google (in its beta test at the time), which was adopted i.e. Google Fusion Tables (GFT) [564, 565]. This allowed for a framework that could easily backup, share, and present the data. Furthermore, the structure of sharing can easily be achieved in a hierarchical fashion through specific account sharing. For instance, high level EPA officials can have administrative access and share specific datasets with relevant regional inspectors. In addition, they themselves can selectively share data specific information to relevant landfill sites. Other advantages include viewing data in RAW tabulated format, or with many choices of visual tools

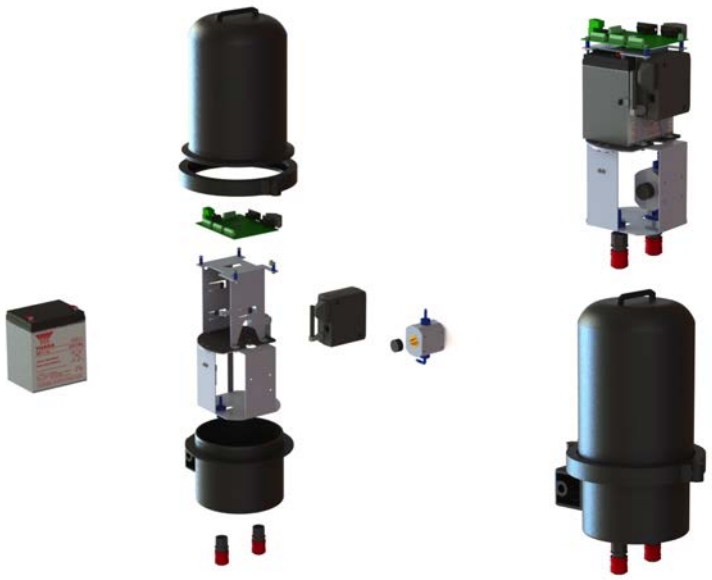

Figure 6.1: Rendered 3D models of landfill generation 2 (Gen #2) in both exploded view (left) and assembled views (right).

including associating data with Google Maps. In addition, the RAW data can be downloaded in CSV format for reports, etc.

Subsequent to these contributions, funding was secured for an additional 2 years to continue this research. During this time three additional Gen #2 systems and two Gen #2 pressure sensing devices (Gen #1 pressure sensing prototype was realised in another study by the student - paper in preparation see page viii) with solar cells for power harvesting. In addition, five Gen #3 systems were designed and created which integrated three sensing targets i.e. CO_2, CH_4, and pressure. Finally, it must be noted that the EPA have purchased a Gen #2 system in 2011 (data from the pilot deployment can be seen in Figure 6.3 on page 188), with additional deployments in Scotland (Glasgow) and Brazil. Furthermore, the project has secured additional funding for commercialisation prospects.

6.3.2 Paper 2: Robotic Fish Platform (Chapter 3)

Since the time of this paper, effort has gone into examining further aspects of the premise primed by this study. One of the first aspects to address was the fish casing. It was found, during development of the first prototype, that assembly of all components into the housing was cumbersome and connection to the actuators was troublesome which required an investment of time. Therefore, effort has been

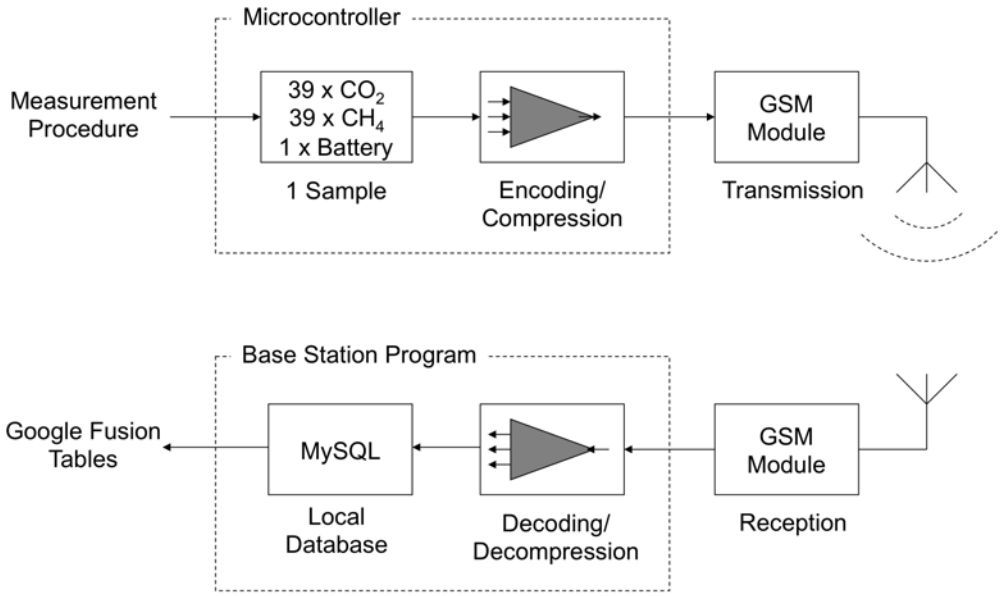

Figure 6.2: Flow diagram presenting the new data handling technique.

invested into the design of the next casing which appears in Figure 6.4 on page 190. It has been designed to allow for greater access to the internal components, integrated supports for said components, and for easier connections to the PPy actuators. Based on this design, more experimentation can be performed without the down time involved in repeated construction.

The significance of the fish like movement (biomimetic approach) generated by the PPy actuators may not have been explicit in the paper as it was not the central focus. For the purposes of the primary aspect of the proposed sensing model, a mechanical motor may have sufficed. However, the project itself was to leave future scope for an additional use i.e. to offer a means for leading water based life away from harmful conditions. This concept follows from the findings of Marras *et al.* at NYU that the movement generated by a fish like movement via a biomimetic robot will encourage other fish to follow [562]. One of the main limitations of this sensing implementation is the PPy actuators. At present, the fish is limited to slow moving streams or practically stationary water areas as the forward movement is not strong in comparison to mechanical motors. The fish in its present configuration may suit catchment areas or aquariums, its use per the proposed target area (i.e. the environment) will not suffice at present. Although, the 'artificial muscle' research domain may offer a stronger propulsion mechanism in the future. For the immediate present, however, a mechanical equivalent may be better suited for the proposed application scenario.

Consideration has also been given towards the design of the sensor station. The desired next step is to achieve quantitative measurements of the contaminant and

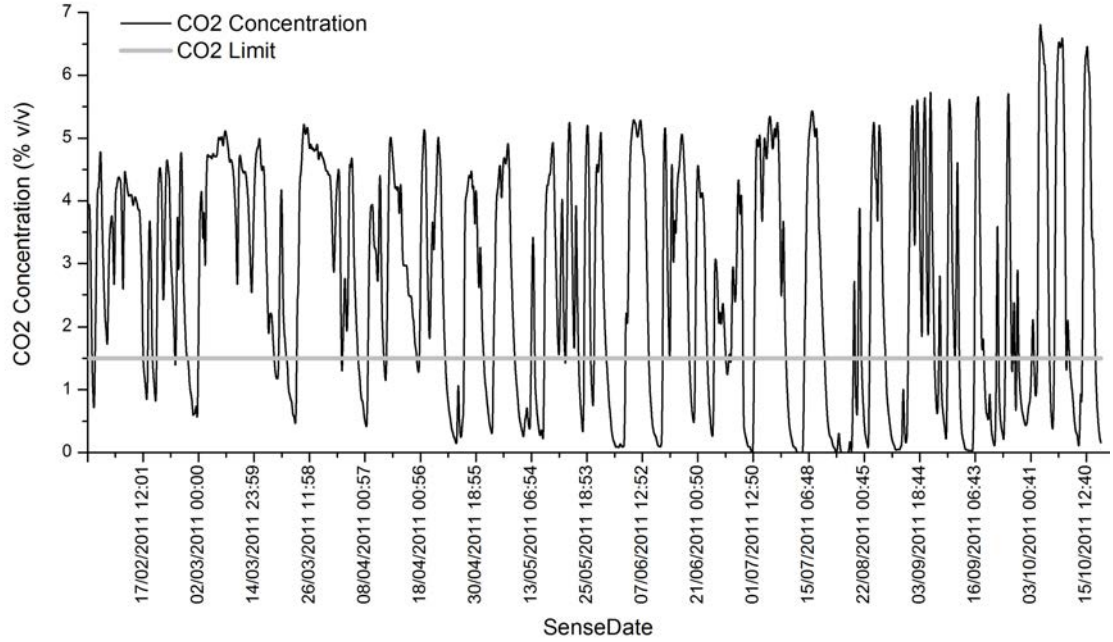

(a) Carbon dioxide (CO_2).

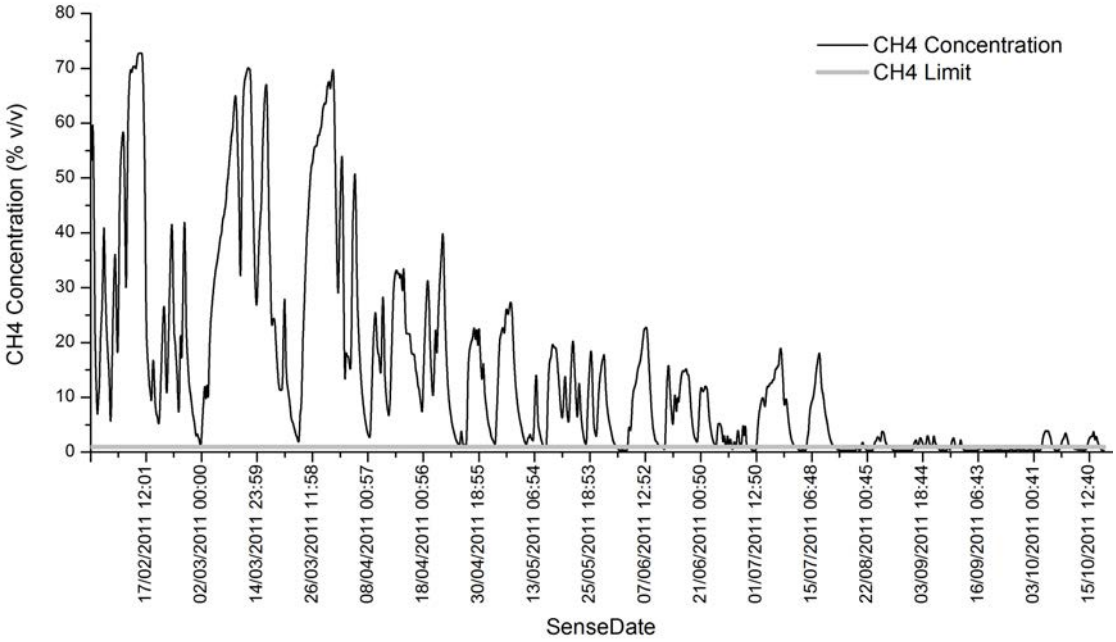

(b) Methane (CH_4).

Figure 6.3: Example of data harvested using the new Gen #2 system.

have the fish track the plume as it travels in a water system. This has involved a redesign of the sensor station which appears as in Figure 6.5 on page 191. The reasons for the design consisting of red coloured ends are twofold. One is that it allows for detection of the sensor station by video process in a water system i.e. with two coloured blobs with the same shape but rotated by 180°. The second allows for the distance between the station and fish platform to be determined by calculating the distance between the centroids of each red end. For instance, in Figure 6.6 on page 191 a sensor station was placed at known distances to the camera which resulted in a plot as seen in Figure 6.7 on page 192. In addition to this, colour bands have been applied to the mid section of the station design with an aim to act as a colour reference and also to identify which station is being interrogated as per Table 6.2 on page 190 and thus determine the position of the platform.This design can also allow for future expansion in terms of multiple indicators for different sensing targets and/or indicators that operate over a limited range. The two-dimensional aspect of the light sensor (camera) can also provide the means for chemical depth profiles within a water body. This can generate valuable information related to the chemistry of a system when compared to single point location sensing nodes. Furthermore, through this design, information related to the flow and direction of a chemical plume may be achievable. This is observable in Figure 3.13b on page 129 when, during patrol, the chemical plume did not (at the time of image capturing) fully react with the entire surface of the indicator, indicating that the plume was strong on one side than the other (similar to Figure 3.10b on page 126 for reference). This is consistent with the experimental procedure and demonstrates that information of a higher localised grade can be achieved, especially if the colour change occurs during interrogation.

One issue with the proposed approach, when compared with a traditional WSN setup, is the potential loss of information at a location when the fish is patrolling elsewhere. One way of addressing this issue may reside in passive temporal logging of the chemistry in a similar way as an auto sampler, discussed in Chapter 1. This may involve methods similar to that introduced in Chapter 5 in conjunction with controlling the flow rate as with the sweat patch in Chapter 4. Potentially, this may allow for temporal mapping and worth investigation. One possible way of triggering a longitudinal sampling regime (logging) would be to equip the fish with an LED to trigger a light actuated control valves as described by Lopez *et al.* [566]. In this way each station may perform temporal measurements can gather historical data since WANDA's previous patrol.

Furthermore, a question that must be addressed is the condition of the water body. For instance, water systems can be turbid and consequently alter the quantitative measurement. The reference patches - which are rotated about the centre i.e. visible from all directions - can offer an additional advantage in determining the

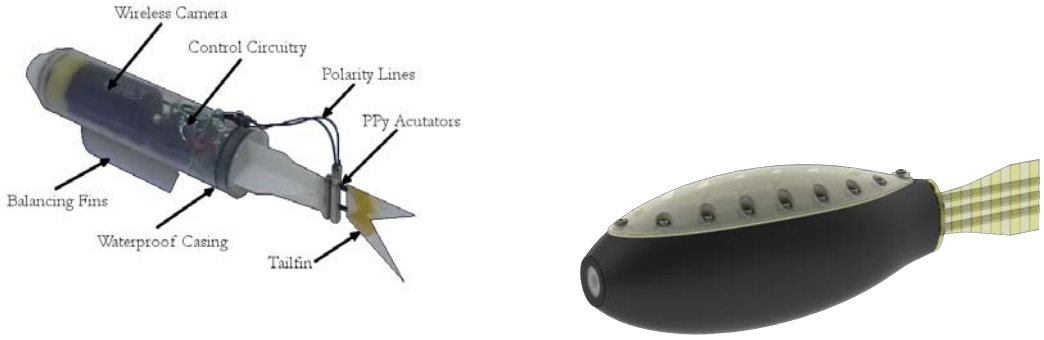

(a) Current fish casing design. (b) New fish casing design.

Figure 6.4: CAD rendering of the next casing for the fish platform.

Table 6.2: Station identification and colour reference band arrangement.

Station ID	**Top band**	**Middle band**	**Bottom band**
1	Red	Green	Blue
2	Green	Red	Blue
3	Red	Blue	Green

turbidity or perhaps the discolouration of the water e.g. algae. These are interesting questions to address in the future. Furthermore, the chemical sensing band is in place to determine the concentration of the chemical measurand and can use the coloured patches as reference to various water conditions.

6.3.3 Paper 3: Sweat Analysis via Imaging Techniques (Chapter 4)

This work does not claim that the adopted approach is optimum for wearable sensing applications. On the contrary, it is not suitable for the richness that accelerometers/IMUs offer for measuring movement; unless the user is always in full view of well equipped camera systems i.e. within stadiums such as those associated with football, tennis, rugby, Olympics, etc. However, that is an different issue and not within the realms of this thesis. This work does offer an interesting alternative to

(a) Basic station construction consisting of two identical ends, red in colour (with one rotated 180 degrees) and connected via a white cylindrically shaped mid section.

(b) Sensor station enhancement with 3 colour bands (bottom 3 - red, green, and blue) and a chemical colorimetric indicator (top - yellow band).

Figure 6.5: Design of the next generation station design.

(a) Camera position at end of pool and at 0 m of measuring tape.

(b) Overhead image with camera, sensor station and measuring tape in pool.

(c) Sensor station position at 1.3 m from camera along measuring tape.

Figure 6.6: Arrangement of camera, measuring tape, and sensing station within the pool area. The sensing station is moved to various positions along the measuring tape to investigate a correlation between actual distance and pixel distance of the station's red end centroids.

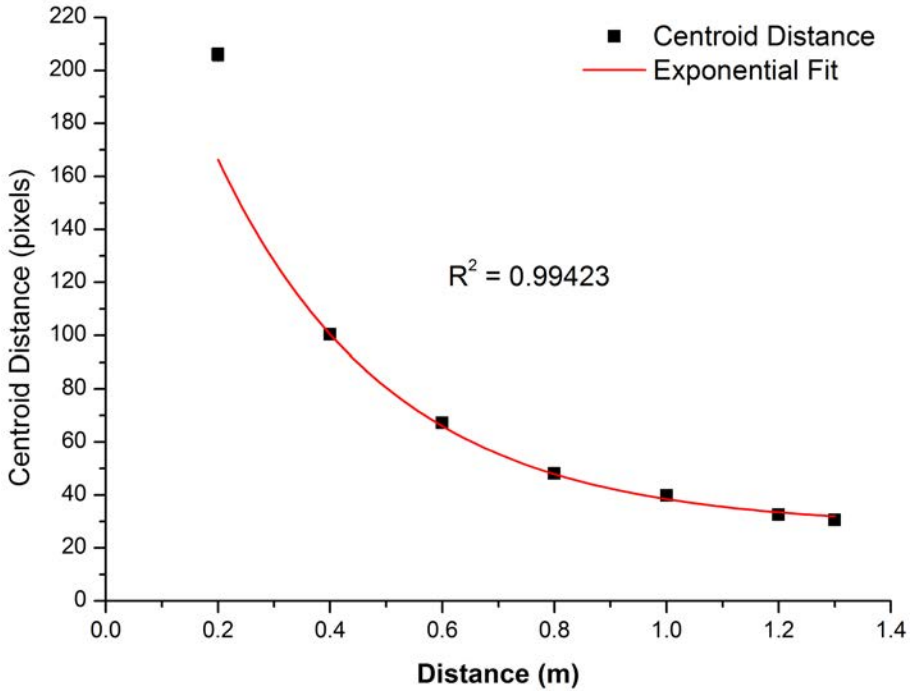

Figure 6.7: Plot relating the distance of a sensor station to the camera. An excellent exponential fit results, $R^2 = 0.99423$, $n = 7$.

gathering chemical information related to a wearer and a number of issues needs to be addressed for future development, some of which is currently in process.

Firstly, the accuracy is a prime factor to address. Although for the purposes of exploring this concept an accuracy of 0.49 of a pH unit may be acceptable, however for future use it may not be suitable for wearable applications; a higher resolution is more desirable. Exploration of other colour spaces e.g. HSV, Lab, or Ycc may offer a higher precision.

Other questions related to digital capturing is also raised, i.e. effects that they may have on the accuracy of the chemical sensing. For example, the distance of the camera to the gels and therefore the effects of digital zooming comes into mind and its various interpolation methods e.g. bilinear, nearest neighbour, bicubic, etc. This prospect is under investigation and in comparison to optical sensing capabilities, as seen in Figure 6.8 on page 193. In addition, the figure shows the patch on a laboratory shaker to investigate the effects of movement to the accuracy of measurements when captured in a video. Further to this, video analysis offers the capability of an inherent higher temporal sampling rate. However, this does raise questions what with the parameters that videos operate on when compared to digital stills e.g. lower resolution, different compression schemes. This warrants investigation, and will be part of the currently ongoing sweat trial, see Figure 6.9 on page 194 for a single video frame.

Improvements related to the gels and processing their data is also desirable. Gels with a dynamic range across the detection range of the camera is more desirable that one changing from one colour to the next one within the visible spectrum. This was

(a) 0x Optical Zoom.

(b) 2x Optical Zoom.

(c) 5x Optical Zoom.

Figure 6.8: Wearable microfluidic patch at various optical zoom levels.

apparent with the Methyl Red dye, relative to the visible spectrum, i.e. it changed from red to orange/yellow which is small when ideally the colour change to suit the camera would translate across the rainbow model of colours. This may be an additional reason why little change was detected by the camera in the paper. In addition to this, a more robust method of combining the dyes to yield a single pH value may improve the accuracy and performance of the system.

Finally, it was previously outlined that the captured images were processed in a semi-autonomous manner, i.e. to maximise the assurance that all relevant pixels were identified for processing without potential errors arising from other sources, e.g. background pixels. For future practical scenarios discussed within the paper, this method will not serve for a real-time autonomous chemical sensing system. To achieve this a fully automatic approach must be investigated. This is one of the challenges associated with the current sweat trial as shown in Figure 6.9 on page 194. In this case a video capturing the entire sweat trial was recorded with the indicators in view at all time. To identify and track the indicator areas within the spatial and temporal domains, algorithms based on object identification and location tracking must be investigated to suit the application scenario. Conceptually this can be achieved through a combination of (but not limited to) a number of processing steps and features extracted from each video frame, e.g. initially by means of template matching [560], or a mean-shift algorithm [561], coupled with contour matching descriptors (e.g. spatial moments), and features matched via SVMs following a training phase. By testing this algorithm on the movement introduced via the shaker shown in Figure 6.8 on page 193, it may provide confidence that it will operate sufficiently in a real-world scenario. This again can be tested on the current sweat trial, albeit on an offline basis using the captured video.

6.3.4 Paper 4: Microfluidic Gradient Analysis (Chapter 5)

Unlike the previous papers, future progression related to this work has not taken place as the final publication took place only very recently (early 2013). However,

(a) Single captured image from the camera.

(b) Arrangement of sweat trial setup.

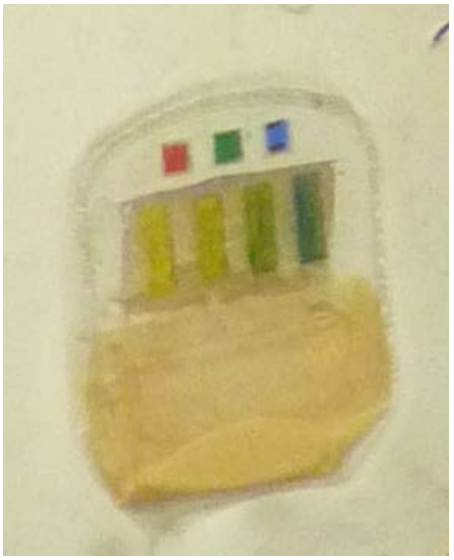

(c) Enlarged image of the sweat patch only.

Figure 6.9: Setup of current sweat trial under investigation.

there are a number of progressions of this work that can take place and will be discussed here.

It was mentioned previously that during development of this work, a bubble was encountered along the channel. This was addressed through a new chip design and not reported in the paper, however it did offer the promise of detecting bubbles along the channel. For instance, Figure 6.10a on page 196 shows a captured image with a bubble formation observable at location '1'. By employing the same analysis technique described within Chapter 5 the location of this bubble can be detected as shown in Figure 6.10b on page 196. The implications of these results indicates that this approach shows promise for the detection of bubbles and may provide a means to address this problematic area of microfluidics. For future investigation of this premise the exact nature of bubble formation will need to be reviewed first, at which point these can be artificially induced along a channel. Detection of these occurrences can then take place in order to either ensure reliable chemical concentration analysis or act as quality assurance protocols in this area. This can potentially aid in experimentally optimising aspects such as flow speed, impact of flow control mechanisms, and overall effects of these on mixing and design of channels. Furthermore, this approach may also provide a basis for flushing out bubbles (away from traditional detection areas) that can interfere with absorption measurements [558]. Another potential advantage of this approach may lie in providing feedback for chemical reaction timing purposes (e.g. for nitrite reactions [559]), which can be affected by environment variables such as temperature; thus possibly resulting in a closed loop system.

The capability of detecting the chemical gradient along a channel has allowed for another question related to this area. This question is related to and stems from a recently reported manuscript by Lagzi *et al.* who described the use of a chemical pH gradient as a transportation mechanism of a droplet for solving a maze [563]. The speed with which the droplet travels along the gradient depends upon the timing of its introduction. This can be seen in the SI (videos) accompanying this paper, i.e. the droplet travels slowly at the start and ends but fastest in the middle of its course. The gradient analysis introduced in this thesis has demonstrated the detection of such a pH gradient and the potential for real time analysis. By integrating both works, a novel approach to optimising the transportation of droplets can potentially be realised. Investigation into this concept has taken place with early results from analysis of a straight channel which can be seen in Figure 6.11 on page 197. It can be seen from the resulting plot that this idea is promising which can lead to a system that can potentially analyse the gradient in a real-time fashion and trigger a pump at optimum times to allow for optimum times of mixing, etc.

Further work in this are can include filtration of spectral reflectance from the surface of the chip, mixing of a number of chemicals and optimising their mixing phases,

or perhaps applying more than one camera (i.e. at different locations/angles) to investigate the possibility of expanding this analysis technique to three-dimensional microfluidic structures.

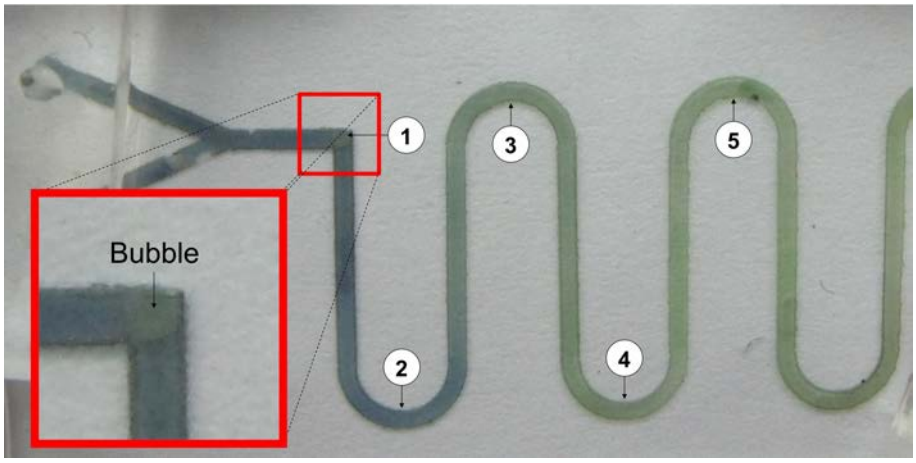

(a) Captured image of microfluidic chip primed with a solution of pH 3 and later injected with a solution of pH 10.5. Labels denote discrete locations along the channel. A bubble is observable at location '1' and emphasised in the red box insert (left).

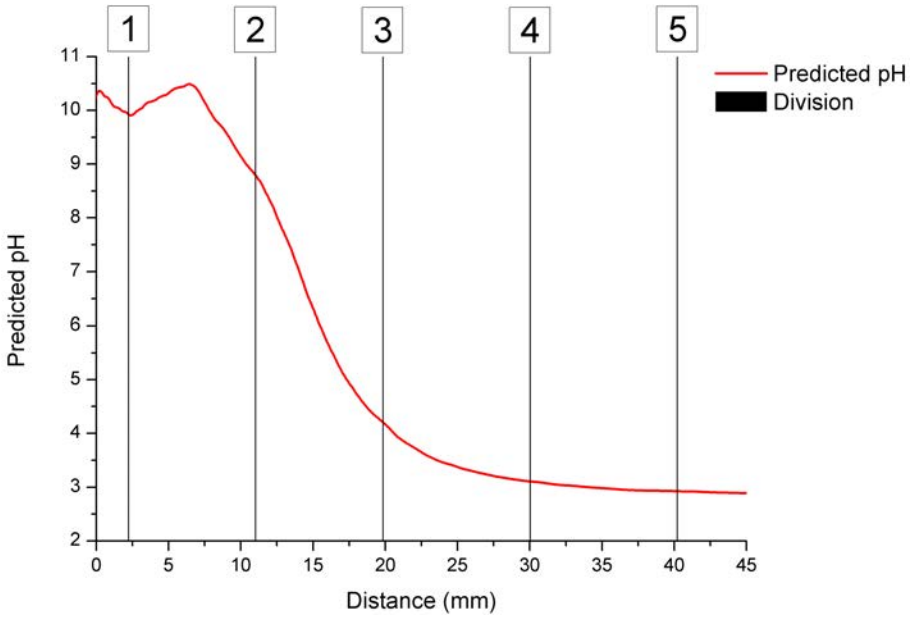

(b) Analysis of the image in (a) where divisions 1-5 correspond to labelled locations along the channel. A deviation in the trend has been detected at point '1' which corresponds to the bubble formation along the channel.

Figure 6.10: Detection of a bubble within a microfluidic chip.

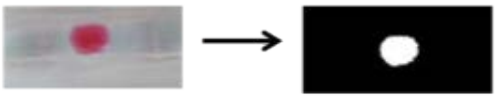

(b) A captured video frame with droplet only (left). Segmented video frame isolating the droplet only (right).

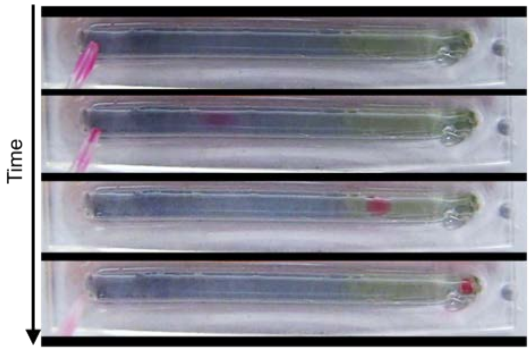

(a) Selected video frames showing the movement of the droplet along the pH gradient.

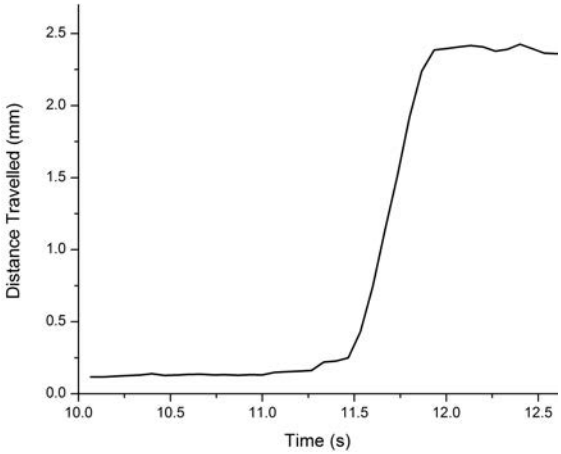

(c) Video analysis results of tracking the droplet distance travelled along the gradient over time.

Figure 6.11: Analysis of tracking a DCM droplet along a microfluidic channel.

6.4 References

[558] C. Slater, J. Cleary, K. T. Lau, D. Snakenborg, B. Corcoran, J. P. Kutter, and D. Diamond. **Validation of a fully autonomous phosphate analyser based on a microfluidic lab-on-a-chip**. *WATER SCIENCE AND TECHNOLOGY*, **61**(7):1811–1818, 2010.

[559] Monika Czugala, Cormac Fay, Noel E. O'Connor, Brian Corcoran, Fernando Benito-Lopez, and Dermot Diamond. **Portable integrated microfluidic analytical platform for the monitoring and detection of nitrite**. *Talanta*, **116**(0):997 – 1004, 2013.

[560] R. Brunelli. *Template Matching Techniques in Computer Vision: Theory and Practice*. Wiley, 2009.

[561] D. Comaniciu and P. Meer. **Mean shift analysis and applications**. In *Computer Vision, 1999. The Proceedings of the Seventh IEEE International Conference on*, **2**, pages 1197–1203 vol.2, 1999.

[562] Stefano Marras and Maurizio Porfiri. **Fish and robots swimming together: attraction towards the robot demands biomimetic locomotion**. *Journal of The Royal Society Interface*, 2012.

[563] Istvan Lagzi, Siowling Soh, Paul J. Wesson, Kevin P. Browne, and Bartosz A. Grzybowski. **Maze Solving by Chemotactic Droplets**. *Journal of the American Chemical Society*, **132**(4):1198–1199, 2010. PMID: 20063877.

[564] Hector Gonzalez, Alon Halevy, Christian S. Jensen, Anno Langen, Jayant Madhavan, Rebecca Shapley, and Warren Shen. **Google fusion tables: data management, integration and collaboration in the cloud**. In *Proceedings of the 1st ACM symposium on Cloud computing*, SoCC '10, pages 175–180, New York, NY, USA, 2010. ACM.

[565] Hector Gonzalez, Alon Y. Halevy, Christian S. Jensen, Anno Langen, Jayant Madhavan, Rebecca Shapley, Warren Shen, and Jonathan Goldberg-Kidon. **Google fusion tables: web-centered data management and collaboration**. In *Proceedings of the 2010 international conference on Management of data*, SIGMOD '10, pages 1061–1066, New York, NY, USA, 2010. ACM.

[566] Fernando Benito-Lopez, Robert Byrne, Ana Maria Raduta, Nihal Engin Vrana, Garrett McGuinness, and Dermot Diamond. **Ionogel-based light-actuated valves for controlling liquid flow in micro-fluidic manifolds**. *LAB ON A CHIP*, **10**(2):195–201, 2010.

A

Landfill Paper: Supporting Information

A.1 Introduction

The work in Chapter 2 presented the efforts involved in the development of an end-to-end system for the monitoring of landfill gas. As this thesis is in publication format, not all of the information for full reproduction/examination could be communicated. To aid in this process, this chapter presents supporting information to the development of the device discussed in Chapter 2. Additional details are presented in the board design, calibration process, commands necessary to describe the workings of the GSM unit, examples of the SMS messages, and database structure for later visualisations.

A.2 Board Design

The design of the control board is central for successful operation. The design was first realised on a bread board implementation and fully tested with target components to develop and test the programming effects. This allowed for robustness of the design and to minimise potential future problems. The design was transferred to a proto-board implementation to complete the first prototype. Once this was fully recognised, finalised, and tested, the design was ported to a PCB implementation.

Figures A.1, A.2, and A.3 presents the schematics drawn in in EagleCAD reflecting the bread-board and proto-board implementations. Routing of the design followed and is shown in Figure A.4. The design was sent to a third party (Beta Layout, Ireland) to be manufactured. Upon reception of the boards the necessary components were soldered onto the board by hand. Testing of each component followed with additional programming parameters for this purpose. The system was finally assembled as described in Chapter 2.

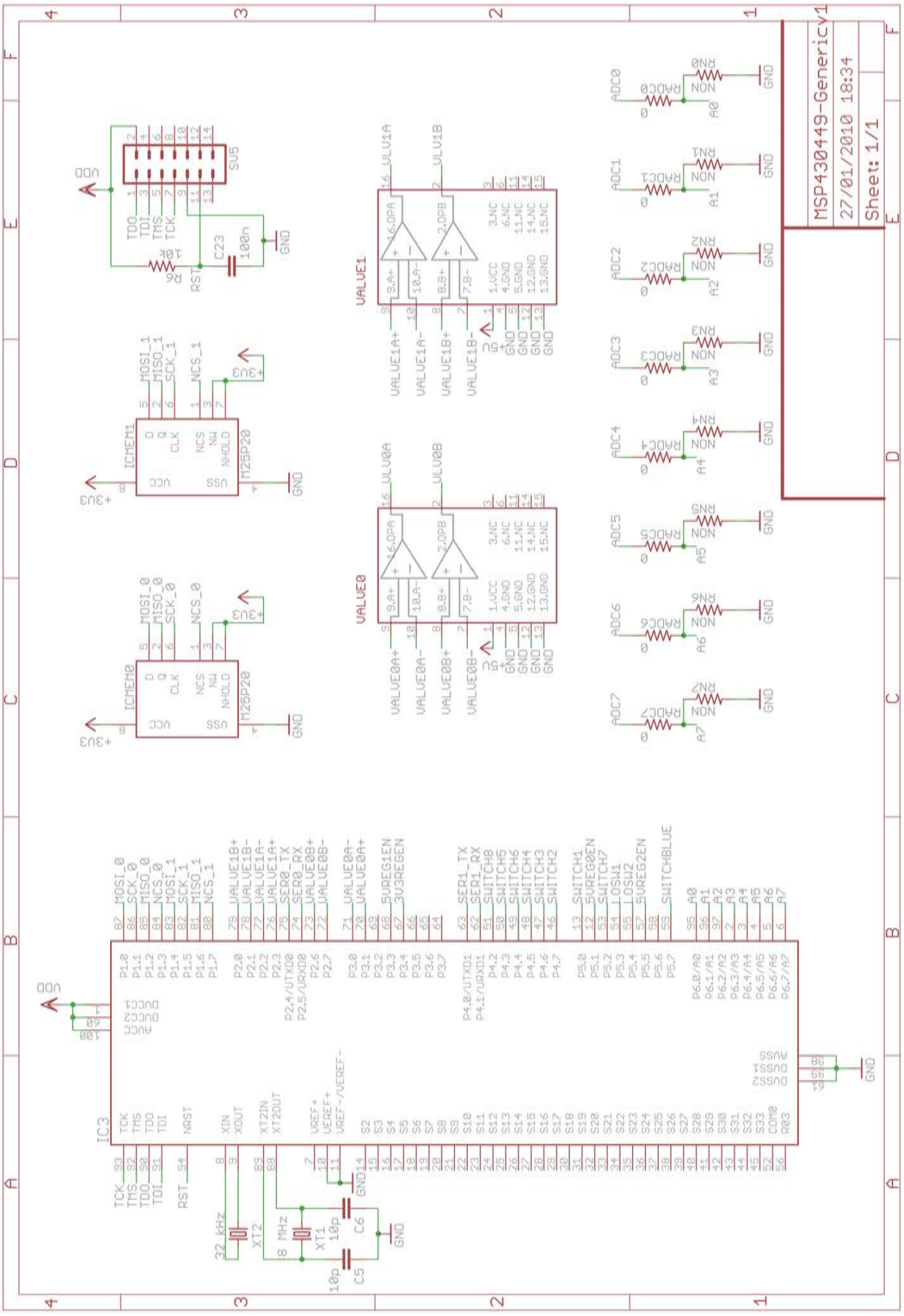

Figure A.1: Landfill electronics board schematic design - Sheet 1.

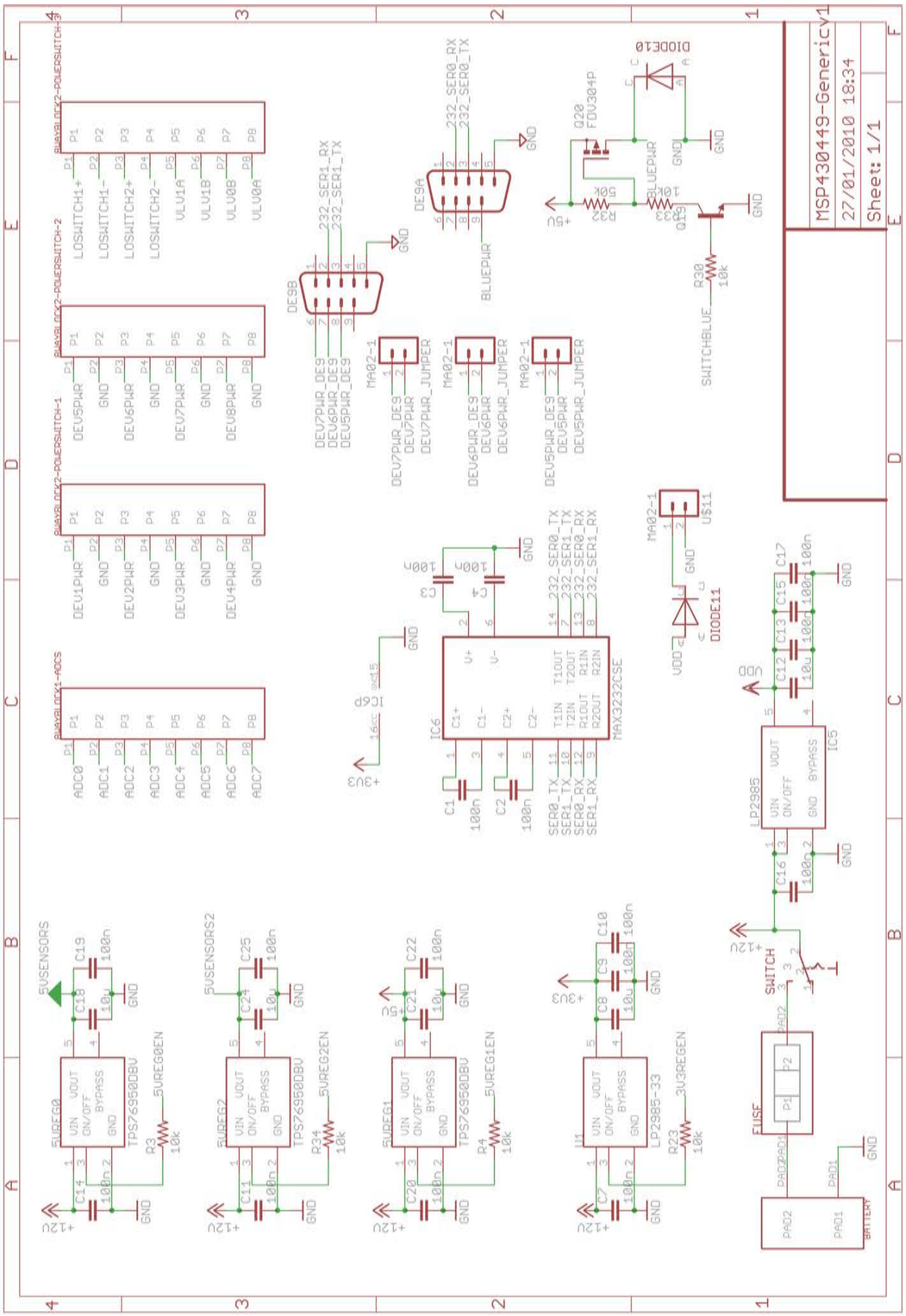

Figure A.2: Landfill electronics board schematic design - Sheet 2.

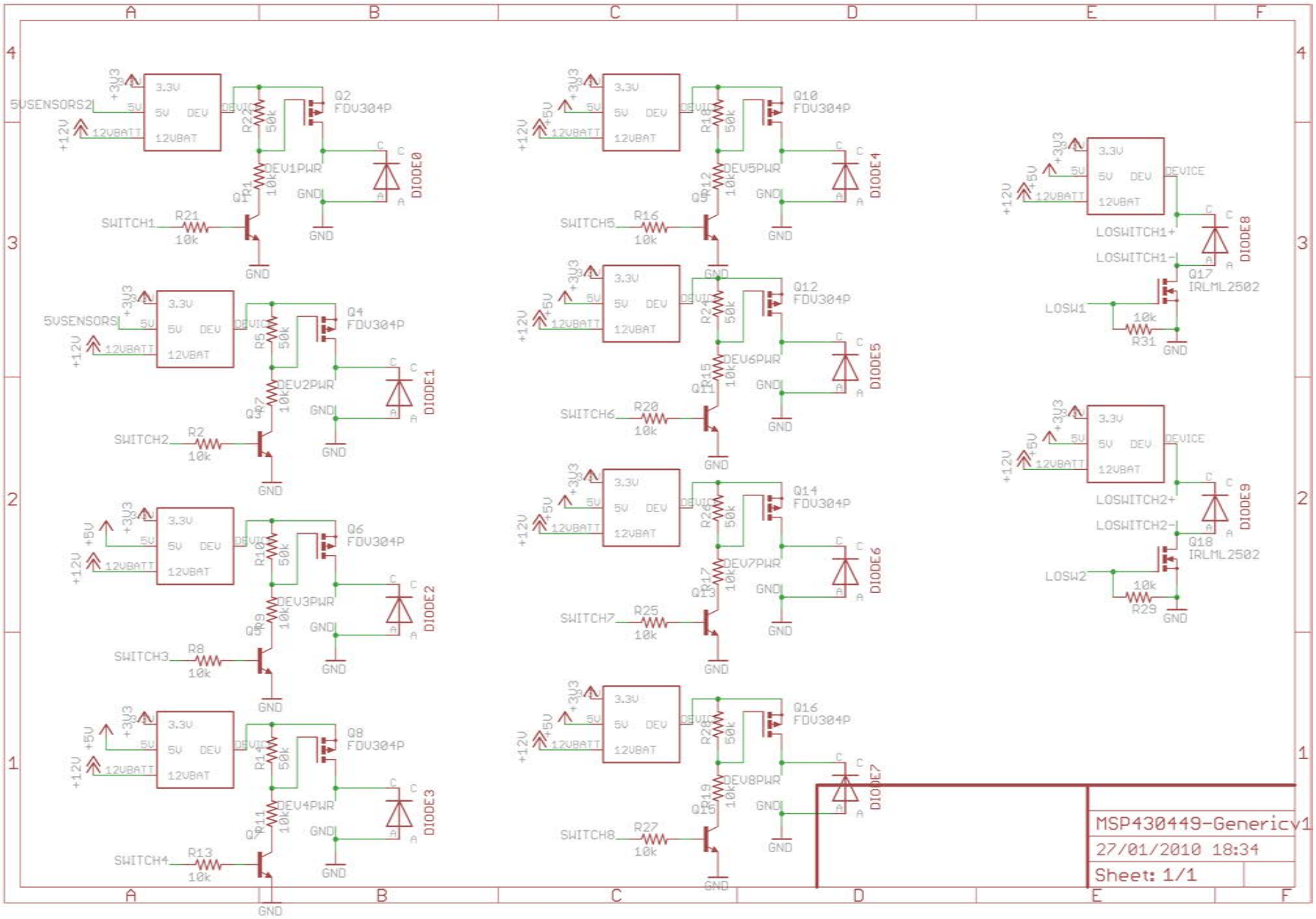

Figure A.3: Landfill electronics board schematic design - Sheet 3.

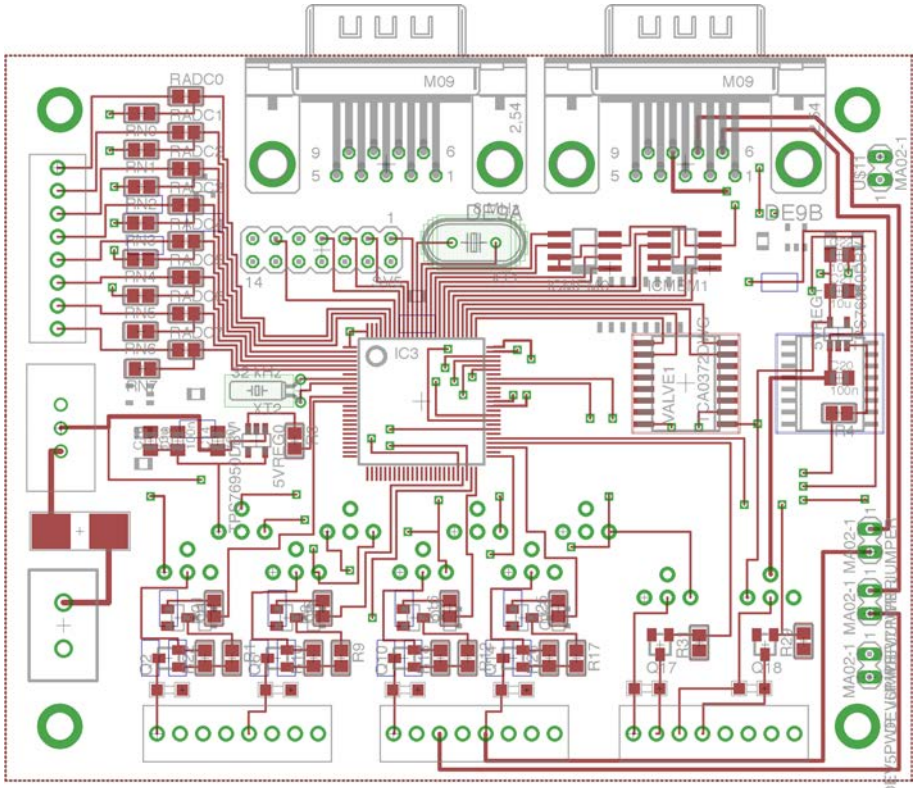

(a) PCB routing design - top view.

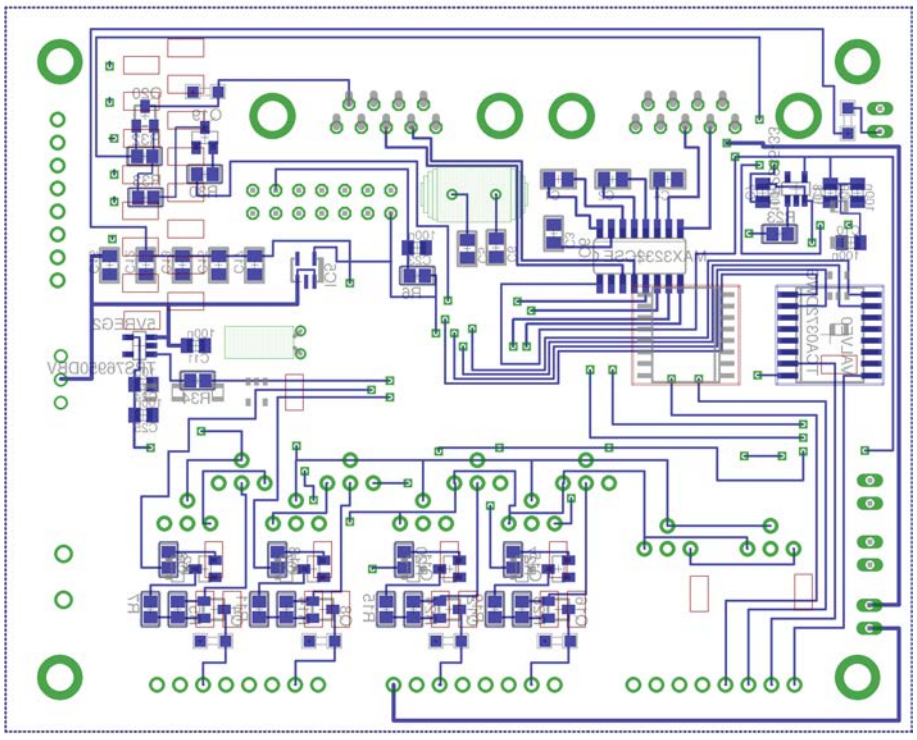

(b) PCB routing design - bottom view.

Figure A.4: Board Design Implementation - routing diagram.

(a) PCB top view.

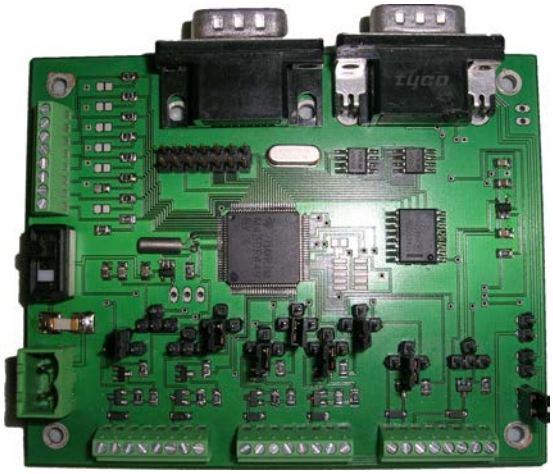

(b) PCB top assembly.

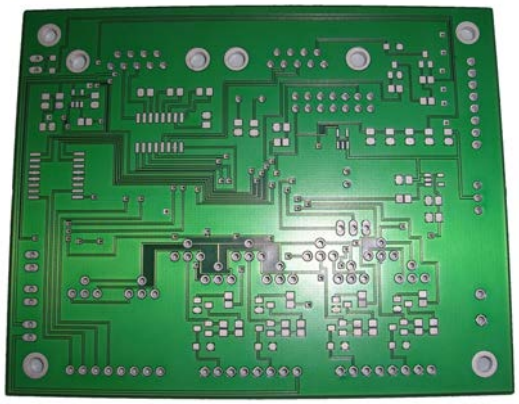

(c) PCB bottom view.

(d) PCB bottom assembly.

Figure A.5: Photographs showing the manufactured PCB before and after the addition of components (assembly).

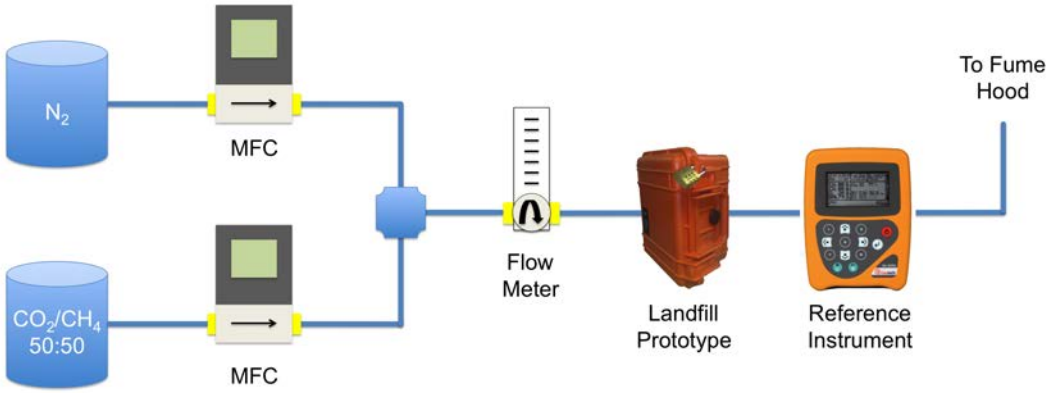

Figure A.6: The calibration process. Nitrogen and Carbon Dioxide + Methane gas sources flow through digital mass flow controllers (MFC) and eventually mix. The sources are mixed, concentrations controlled through the MFC, and finally flowed through the landfill and reference instrument (GA2000 Plus, Geotech).

A.3 Calibration

Figure A.6 presents a digram representing the calibration process in more detail than described in Chapter 2. The purpose of the calibration process was to relate the response of the landfill system (i.e. ADC readings) to known concentrations of CO_2 and CH_4. The current standard adopted by the EPA is through the use of a portable instrument (GA2000). A similar unit (GA2000+) was purchased and calibrated by the manufacturer. Its role in this project was to act as reference to supply known concentrations of both gases to a certainty that the EPA used at the time.

An additional algorithm was written to power on the prototype's sensors and relay ADC readings to the screen for capture by the operator. The flow meter was set to maintain the flow rate of the GA2000 when used on site i.e. 0.6 L/min. Mixtures of nitrogen and CO_2/CH_4 (50:50 ratio) was passed through both the prototype and reference instrument. Once a steady state was reached (as reported by the prototype and GA2000) the resulting ADC values were taken to form a calibration plot and later calculate concentrations of CO_2 and CH_4.

A.4 SMS Messaging

Harvested information by the landfill unit when deployed was communicated to a base station via SMS text messaging. To maintain consistency across all units and also for the creation of an autonomous program on the base station side to parse the received text messages, a template was formed which all units adopted. Algorithm

Algorithm A.1 Text message template that all landfill units follow. Text header begins with '+CMGR' and the text body begins with 'Index'.

```
+CMGR: "<READ_STATUS>","<PHONE_NUMBER>",,"<SENT_DATE_-
TIME>" Index(<SYSTEM_MEMORY_INDEX>), Battery(<ADC_BATTERY>),
Baseline(<ADC_BASELINE_CO2>,<ADC_BASELINE_CH4>), SampleMax(<ADC_-
SAMPLE_CO2>,<ADC_BASELINE_CH4>,<ADC_TEMPERATURE>,<ADC_HUMIDITY>),
PurgeMin(<ADC_PURGE_CO2>,<ADC_BASELINE_CH4>)
```

Algorithm A.2 Example of a text contents transmitted by the landfill units. Text header begins with '+CMGR' and the text body begins with 'Index'.

```
+CMGR: "REC UNREAD","+353876842895",,"10/02/18,11:11:02+00"

Index(2), Battery(3905), Baseline(499,512),
SampleMax(502,515,3071,2143), PurgeMin(497,509)
```

A.1 shows this template where each parameter is represented between the angle brackets. For clarity, an example is presented in Algorithm A.2. The reason for texting ADC values rather than concentration values was two fold. Firstly, it allowed the database to save all ADC values in the event that there was a problem with the conversion. Secondly, it provided a layer of security; the ADC numbers are meaningless should a security breach occur. ADC are relative to the calibration model and this is unknown to any recipient. Finally, this format, e.g. `SampleMax`(a,b,c,d), was chosen so that a human operator could interpret the data. This was the initial use of the texts before a program could be developed.

A.5 GSM Unit Setup

A few steps must take place when setting up the GSM terminal unit for successful operation i.e. to comply with the base station's programming. Algorithm A.3 presents the setup commands for the MC35iT terminal unit. The echo parameter is disabled (ATE0) for simplifying the program i.e. input characters are no longer transmitted back to the user. It must also be placed into text mode (AT+CMGF=1). Finally the AT+CNMI command enables the GSM unit to send an alert once a text message is received. An example of this is provided in Algorithm A.4 containing information that the text message is saved in a certain memory location on the GSM unit, location 7 in this case. The text message is read by a read command (AT+CMGR=7) and it returns the text similar to the example in Algorithm A.2.

Algorithm A.3 Commands used to setup the MC35iT GSM terminal unit for this project.

```
ATE0\r
AT+CMGF=1\r
AT+CNMI=3,1,3,2,1\r
```

Algorithm A.4 Character stream sent by the GSM unit upon receipt of a new text message.

```
\r\n+CMTI: ‘‘MT’’,7\r\n
```

A.6 Database Arrangement

The custom written java program, as described in Chapter 2, places the information gathered by the deployed units onto databases. Chapter 2 has already outlined the process. However, for clarity the database structure is reported here for supporting information. The registry database is shown in Figure A.7 on page 208 and column description provided in Table A.1 on page 207. Similarly, the main data is stored in the ‘landfill’ database as shown in Figure A.8 on page 208 with columns described in Table A.2 on page 209. The data is read from this database and visualised as described within the chapter.

A.7 Power Usage & Sampling Frequency Analysis

The frequency with which the system performs a measurement has a direct impact on the operational lifetime of the device during deployment. The reason for this is

Table A.1: Description of each column within the registry database.

Column Name	Description
id	Row identification
phoneNumber	Identification of the text
deviceName	Differentiates between device types
locationName	Description of the sample location
unit	Identification of the unit used for sampling
latitude	Geographic coordinates of sampling location (latitude parameter)
longitude	Geographic coordinates of sampling location (longitude parameter)
cal	Lists the calibration parameters
startDate	Start date of the deployment
endDate	End date of the deplyoment

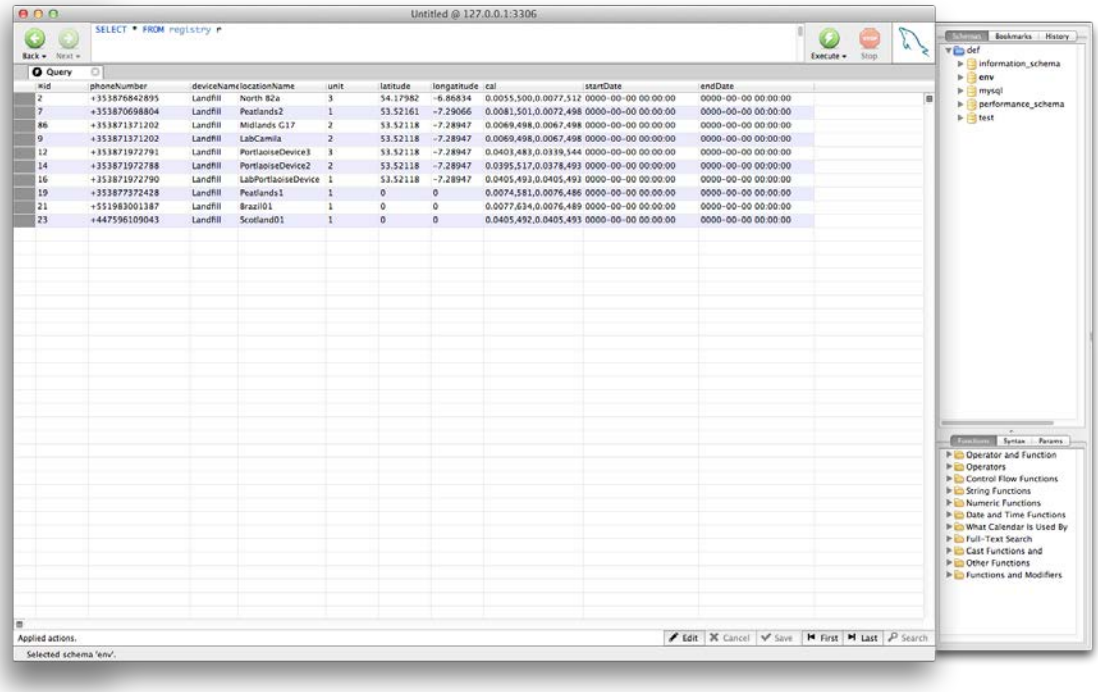

Figure A.7: Screenshot of the registry database when viewed using MySQL Query Browser.

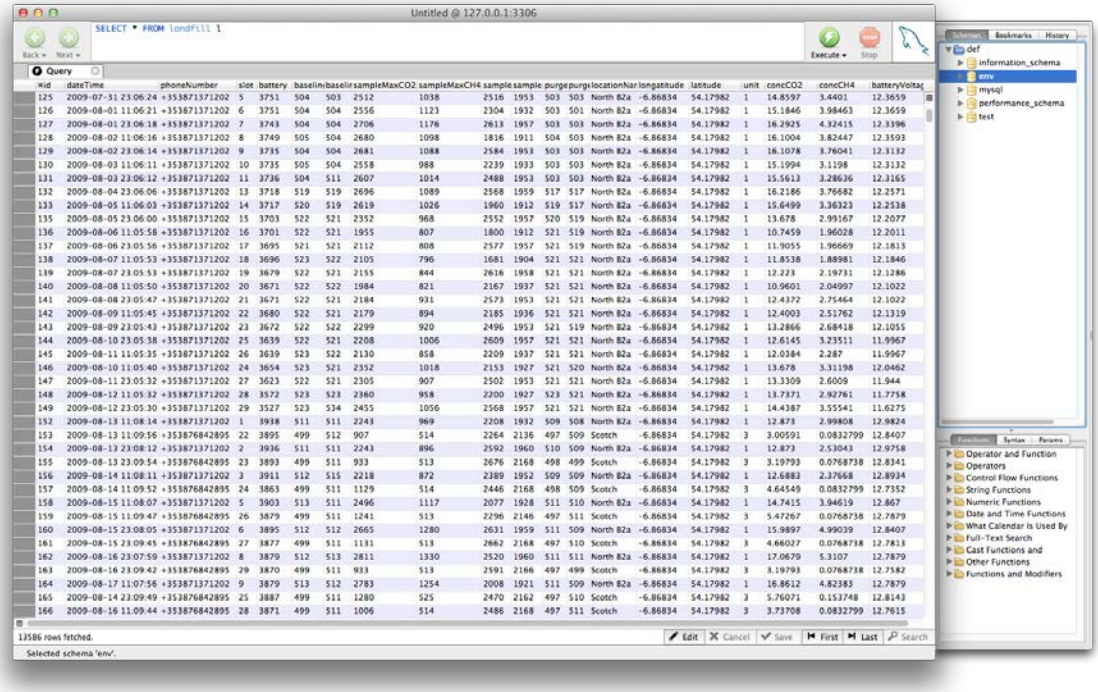

Figure A.8: Screenshot of the landfill database when viewed using MySQL Query Browser.

Table A.2: Description of each column within the landfill database.

Column Name	**Description**
id	Row identification
dateTime	Timestamp of when the sample occurred
phoneNumber	Identification of the text
slot	Relates to the corresponding location stored on device
battery	ADC value of the battery level
baselineCO2	ADC measurements of the CO_2 sensor during baseline process
baselineCH4	ADC measurements of the CH_4 sensor during baseline process
sampleMaxCO2	ADC measurements of the CO_2 sensor during sample process
sampleMaxCH4	ADC measurements of the CH_4 sensor during sample process
sampleMaxTemperature	ADC measurements of the temperature sensor during sample process
sampleMaxHumidity	ADC measurements of the humidity sensor during sample process
purgeMinCO2	ADC measurements of the CO_2 sensor during purge process
purgeMinCH4	ADC measurements of the CH_4 sensor during purge process
locationName	Description of the sample location
longitude	Geographic coordinates of sampling location (longitude parameter)
latitude	Geographic coordinates of sampling location (latitude parameter)
unit	Identification of the unit used for sampling
concCO2	Converted CO_2 concentration values in $\% \, v/v$
concCH4	Converted CO_2 concentration values in $\% \, v/v$
batteryVoltage	Converted battery level values in V

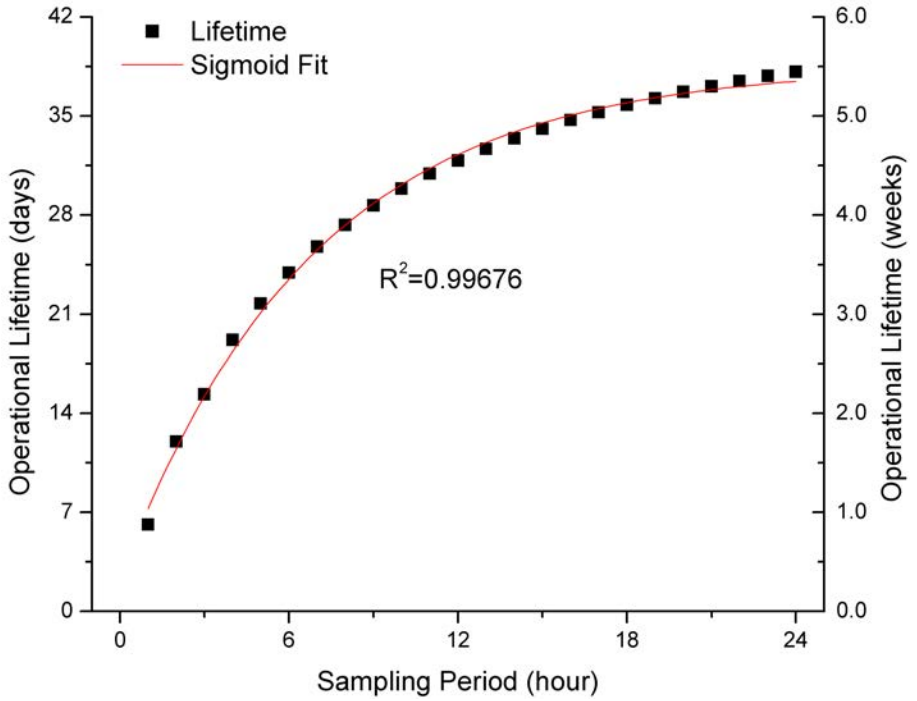

Figure A.9: Results of an ideal simulated power useage analysis showing a relatioship between the projected operational lifetime of the system with respect to a chosen sampling period. The lifetime of the system was based on an active duty cycle of 230.1 mA (average draw), an inactive draw of 6.13 mA, and the system's battery capacitance (12V 7Ah), while varying the sampling period from 1 to 24 hours.

due to the substantially larger power draw when the system is in it's sampling/active state when compared to its stand-by/inactive state, see 2.3.2 for details. To determine the operational lifetime of the system with respect to a chosen sampling period (time between measurements), the results of the power analysis seen earlier in Figure 2.9 on page 97 were noted along with the system's battery capacity (7 Ah), and used as a basis for prediction. Figure A.9 on page 210 shows the results of this analysis when considering a sampling period of 1 to 24 hours. These results indicate that the trend (shown by the sigmoid fit) starts to show a steady state at a sampling period of ca. 24 hours without a significant difference in operational lifetime, relative to a higher sampling frequency. It must be noted that this analysis does not consider other factors effecting the efficiency of the battery, e.g. temperature or aging affects. In addition, it does not account for the fact that as the battery discharges, the electrical potential decreases and some components cannot function at this voltage level, e.g. the system's GSM module. Considering these factors, the practical operational lifetime is likely to be less than that shown in the figure. A 12-hour sampling period indicates a compromise between both linear portions of the graph in terms of maximising the sampling frequency while minimising the efforts/resources involved in maintaining the systems in terms of changing their batteries over multiple deployments.

Table A.3: Calibration parameters for all deployments. The parameters follow the following equation: $[Gas_{conc}\,\%\,v/v] = [Slope \times ADC] + [Intercept]$.

Location	**Start Date**	**End Date**	**System**	**Slope** (CO_2)	**Intercept** (CO_2)	**Slope** (CH_4)	**Intercept** (CH_4)
A_1	28-May-09	08-Oct-09	1	135.4	500	149.2	495
B_1	13-Aug-09	08-Oct-09	3	151.52	510	161.26	497
A_2	20-Nov-09	28-Dec-09	1	133.18	500	156.1	501
C	03-Mar-10	07-Sep-10	2	181.82	500	129.87	512
A_3	10-Mar-10	07-Sep-10	3	144.7	499	156.77	457
B_2	24-May-10	07-Sep-10	1	134.7	500	157.3	501

A.8 System Calibration

Witihin the working chapter (Chapter 2) a single calibration routine was reported for each chemical sensing target, yet multiple systems and deployments were reported. For each deployment (reported in Table 2.1 on page 95) the platforms were calibrated beforehand. Table A.3 on page 211 presents a complete account of the calibration parameters for each deployment reflecting the data presented in Table 2.1 on page 95. In addition, Table A.3 on page 211 also provides information related to which system was deployed at corresponding locations. For instance, system #1 was deployed at locations A_1, A_2, and B_2 which show a very similar calibration parameters, and similarly for system #3. Location C was monitored using system #2, which has a dissimilar calibration parameters than 1 and 2. Overall, this data indicates that the differences in calibration parameters per system (e.g. see system #2) supports an argument for calibrating each system prior to deployment. The similar parameters per system, however, indicates high confidence that the platforms can hold their calibration and little drift was encountered; evident from the slope parameters.

B

WANDA Paper: Supplementary Information

B.1 Introduction

As mentioned previously, cameras have been successfully employed to monitor changes in pH by detecting changes in the colours of pH sensitive indicators. However, this has almost always been achieved under strictly controlled lighting conditions and using the RGB colour space which is inherently sensitive to variations in lighting conditions and, as such, is not suitable for field conditions where the ambient light levels can vary significantly. Other researchers have recently reported the use of an alternative colour space for chemical analysis i.e. the HSV colour space. It is worth mentioning that the the work presented in this thesis is essentially contemporaneous with this report and independent of it. Furthermore, these researchers only exploited the hue component of the HSV colour space.

The concept of placing optical chemical indicators on discrete 'satellite' stations dispersed within a water system for quantitative measurements of the chemical state of an environment is the overarching goal of this work from here on. However, in order to reach this point a number of bench top experiments are necessary to fully explore unanswered questions or 'gaps' left by the literature. The purpose of this chapter is to offer simple experimentation that attempts to establish key elements necessary to the success of the proof of principle study that will be explored in future work. It was therefore important to move away from controlled lighting conditions and perform this experiment under variable ambient lighting conditions. The initial study commences by investigating the camera as a detection system for a chemical change in solution form (Section B.2). After that, the work then progresses towards a detection system for a chemical dye bound within a polymer matrix (Section B.3) . Once these elements are investigated and tested sufficiently, the work can then progress onwards to a proof of principle study i.e. towards the central hypothesis as future work.

B.2 Analysis of pH Using the HSV colour space: Dye in Solution Form

In this section the use of a colour space other than RGB is considered and fully explored whilst operating in uncontrolled lighting conditions. The use of pH indicator dyes are fully documented and well accepted within the literature and often in solution form, although indicator strips (e.g. pH indicator paper) have been in general use for decades. However, normally the dye is not bound to the paper substrate in these test strips, and the dye leaches rapidly out into test solutions. We therefore were interested in polymer formulations that would inhibit dye loss as the test units would be required to survive *in situ* for extended periods of time (days, weeks, or months). However, binding the dye within the polymer matrix is known to affect the dye response characteristics (e.g. its pK_a). It was therefore important to evaluate the performance of the dye using a setup in its simplest form i.e. within a solution and moreover using deionized water. After this, the results may be compared with that of accepted theory within the literature. Once this measurement method has been established the next section addresses the use of this method with a dye bound by a polymer matrix.

B.2.1 Experimental

A pH dye solution was prepared by dissolving 0.7 g of bromocresol green dye in 250 ml of ultra pure water within a 500 ml beaker. In addition, a second solution was prepared but within an acidic environment to gain max (blue - water solution) and min (yellow - acidic solution) reference colours. Above the beaker, a standard burette was held by a retort stand with a concentration of 0.1 M HCl inside. Next, the beaker was placed on a magnetic stirrer and the background (i.e. with respect to the camera's field of view) surrounding the beaker was saturated with white paper to aid in later image segmentation. The wireless colour camera (ZTV ZT830T) was placed ca. 0.3 m away from the beaker. Finally, a laptop PC (Dell Latitude D630) captured the image stream from the video camera via a capture card (Avermedia C038) where a custom written program processed the data.

Figure B.1 shows the experimental setup for this study as described above. Firstly, the an initialisation procedure is activated:

1. Activate the magnetic stirrer;
2. Ensure that the the pixels representing the dye in the beaker are only considered in the image processing program;
3. Setup of a band pass filter on the Hue channel i.e. one that correspond to the max/min reference points of the two prepared solutions to aid in the segmentation process.

After that, a repeated sequence of steps is put in place:

1. Take an aliquot (10 ml) of solution and place it within a new 20 ml vial;
2. Add a sufficient volume of HCl in the burette to the beaker until the hue reading decreases by 0.2 rad;
3. Repeat until the hue value reaches the min reference value i.e. 1 rad.

Figure B.2 shows the custom written image processing and analysis program. The software components involved derived from using the Java programming language and the Java advanced imaging package (JAI). At first, the image stream was captured at a standard size of 640 x 480 pixels, at 15 frames per second (fps), in 24-bit colour depth (8x8x8) and in raw (uncompressed) RGB format. Next, a region of interest was established to surround the coloured solution within the beaker. For every newly captured video frame, the following image processing steps were executed:

1. A transformation of the sub image of the captured frame occurred from the RGB to the HSV colour space [567];
2. A standard region labelling algorithm was implemented on the Hue channel where neighbouring pixels of similar colour were grouped together into regions i.e. labeled as grey levels;
3. Each region was ranked according to its total number of pixels;
4. The largest region was identified to represent the pixels representing the pH dye;
5. Once identified a mask image was created where the identified dye region was set to a white colour (255) and everything else of non interest set to black (0), see top right section of Figure B.2;
6. The generated mask image was applied to the captured image where only pixels representing the dye were put forward for analysis;
7. The average Hue/Saturation/Value values of this region was output to the user via the GUI on a continuous basis for every captured video frame.

Once each aliquot was stored within vials, it was necessary to determine the pH of each sample. This was achieved using a reference pH meter. At first, the pH meter was calibrated with stock solutions of pH 4 and 7 as per instructed method. Subsequently, each sample was analysed and the reported pH by the meter was recorded. Between each sample analysis, the pH probe was cleansed using appropriate wipes (Chem Wipes).

An additional reference method was put in place i.e. a high end bench top spectrophotometer for absorption analysis of each sample. The absorption spectrum

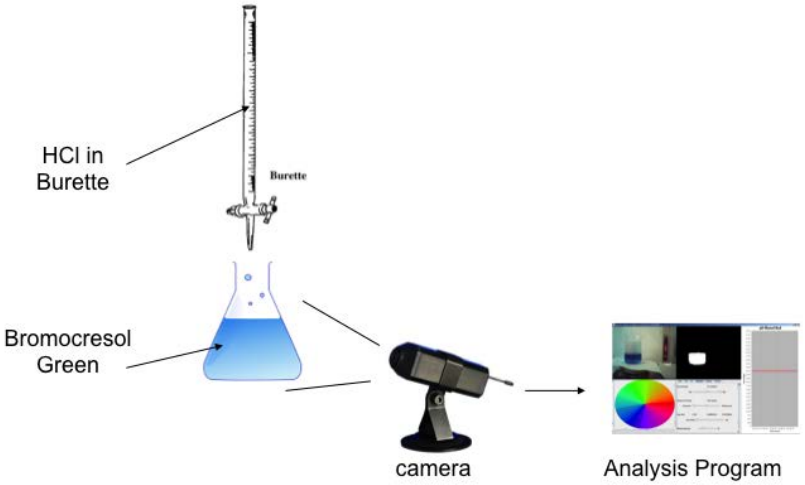

Figure B.1: Experimental setup to investigate an alternative colour space for colorimetric chemical analysis in solution form.

was set from 200 nm to 800 nm in 1 nm increments for completeness. Once the data for all samples were established, a program was written to normalise all the readings about the isosbestic point to account for dilutions of the dye concentration.

B.2.2 Results

B.2.2.1 Spectrophotometer

Figure B.3 shows the UV-Vis plot of all samples taken during the above procedure. This shows the expected progressive decline of the dye at its prominent peak of ca. 617 nm [569] as shown by others in the literature using bromocresol green as an indicator [572]. Moreover, the figure shows that a change in the dye's absorption did in-fact occur when an acid was introduced and furthermore was progressively changed with respect to the concentration of the acid.

The data were processed where the prominent peak changes i.e. at 617 nm [569, 571, 572] were extracted and plotted as a function of pH as shown in Figure B.4 along with a sigmoidal regression (Boltzmann technique) with an excellent fit of $R^2 = 0.99575$. After that, the model derived from the regression was plotted separately and its first derivative was calculated to yield the dye's pK_a value by adopting the same approach as by O'Toole *et al.* [572]. Figure B.5 depicts a plot of the model itself along with the first derivative which reports a pK_a value of 4.98.

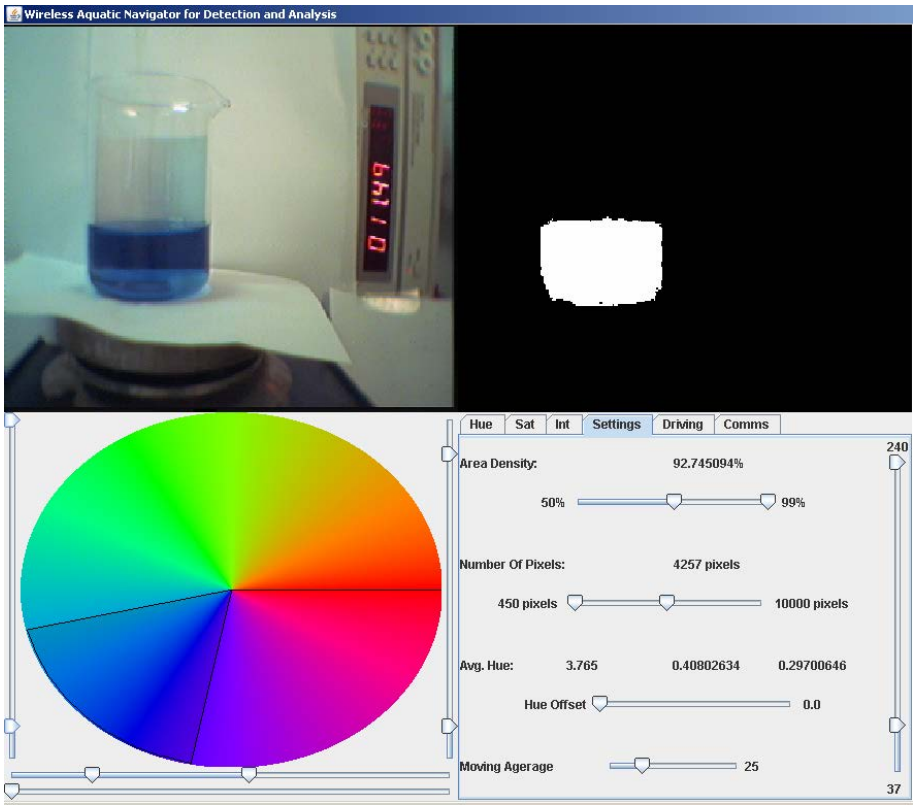

Figure B.2: Screen capture of the real time command and control program. The screen is split into 4 distinct regions. Captured image (top left). Mask image created after image processing (top right). HSV ban pass filter settings (bottom left). Settings and readings panel (bottom right) with controls to apply a region of interest, and output readings of the HSV colour space once the mask is applied to the original image.

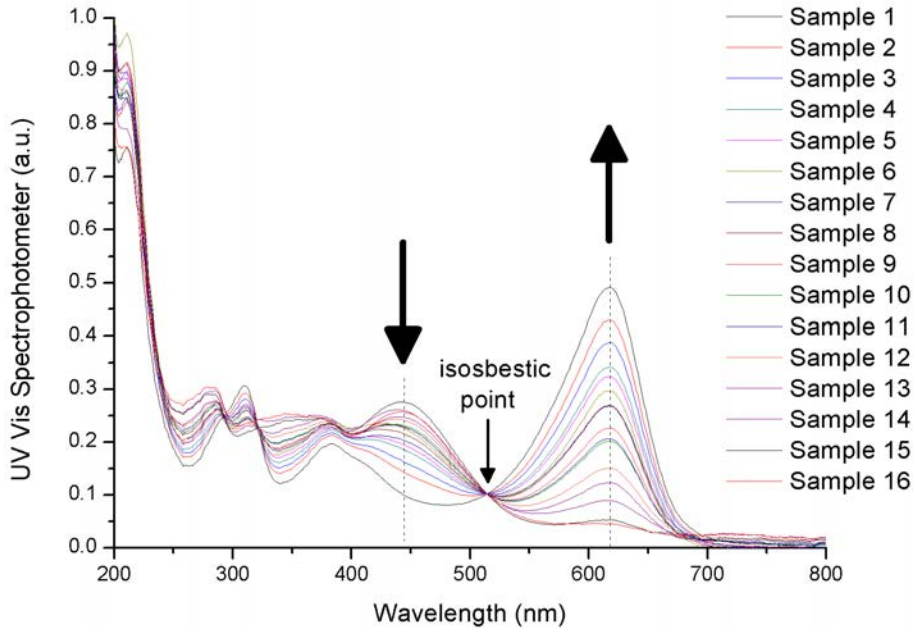

Figure B.3: UV-Vis plot of all aliquots with plots normalised about the isosbestic point. Heavy arrows show the increase and decrease of absorption about two distinct wavelengths shown as dashed lines. The peak absorption is shown at 617nm by the arrow pointing upwards.

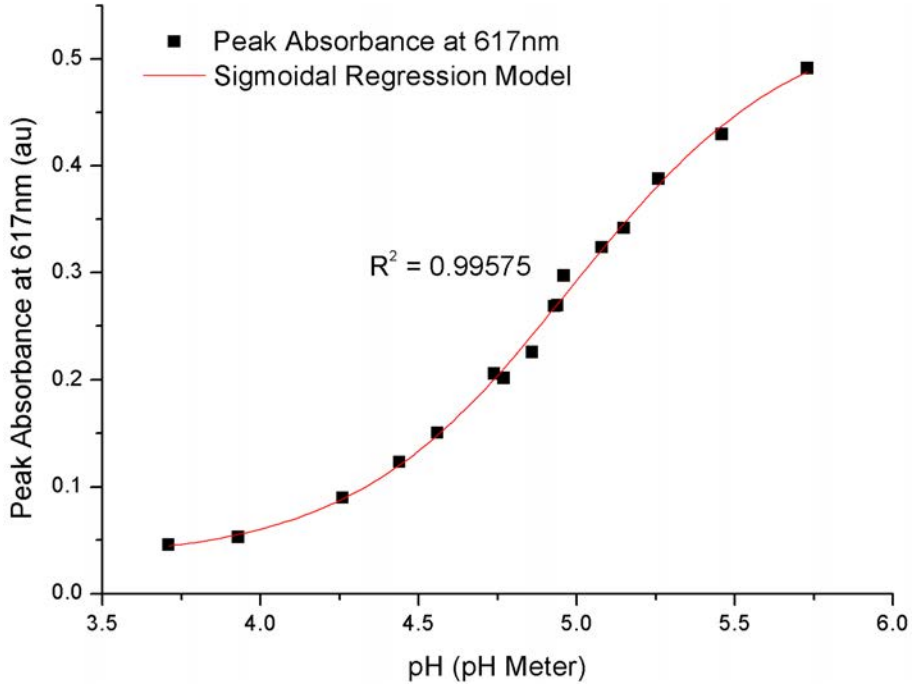

Figure B.4: The absorption of all samples at the peak of 617nm as a function of measured pH. A sigmoidal regressions was applied (Boltzmann) and an excellent fit resulted i.e. $R^2 = 0.99575$.

B.2.2.2 Camera (Hue Component)

As seen earlier, one would expect to see a logarithmic or sigmoidal shape to result [568, 572] from a colorimetric analysis of a pH indicator. Figure B.6 shows the response of the camera's hue component as a function of pH. As expected, one can see that the trend of the points creates this shape and therefore a sigmoidal fit (Boltzmann regression) was applied resulting in an excellent fit with $R^2 = 0.99018$. Calculation of the dye's pK_a value was achieved in the same manner as used previously with the UV-Vis data but instead of analysing one waveband, the analysis considers the hue value instead. Figure B.7 shows the plot of the model along with the first derivative which reports a pK_a value of 4.9 which is slightly higher (i.e. by 0.16) than the reported pK_a value of 4.74 for BCG at room temperature [569, 571], however it is very close to the literature value and more accurate than the UV-Vis approach by 0.9. Although a difference of 0.16 (with respect to that in the literature) may not be significant when compared to an accuracy achieved by others (e.g. a disagreement of 0.24 was achieved by O'Toole *et al.* [572]), its source may have come from a number of variables. One significant issue may stem from the fact that the dye was not examined over the entire pH range and consequently may have

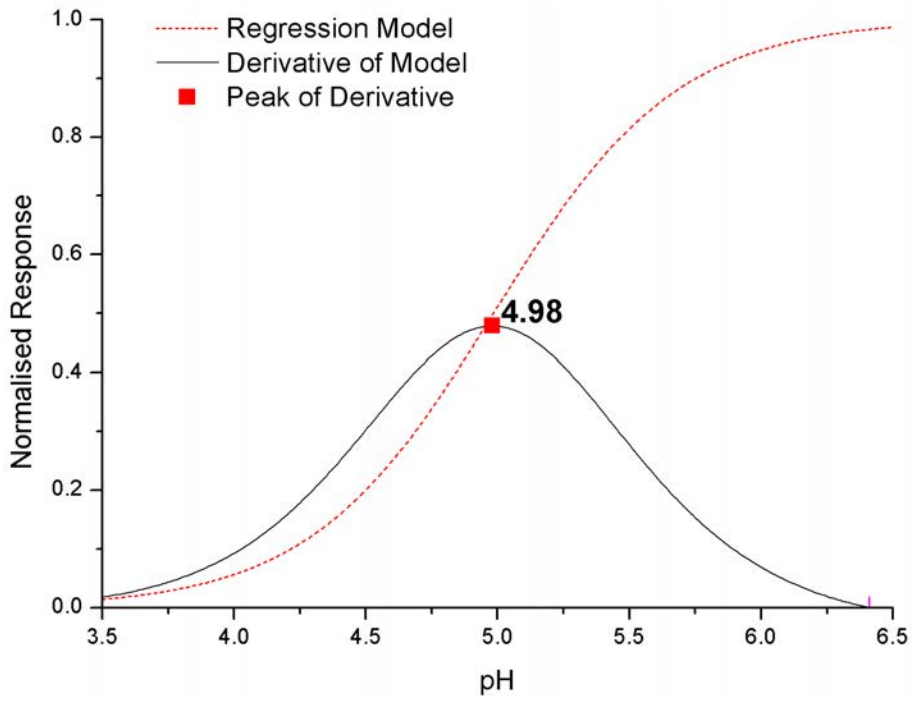

Figure B.5: Model (dashed line) from sigmoidal fit in Figure B.4. 1^{st} derivation (solid line) gives an estimated pK_a value of 4.98.

resulted in a non-symmetrical plot for analysis. Another reason may also be due to the fact that the dye was not completely opaque in solution form and that the image background that came through as transparency (see Figure B.2) may have interfered with the analysis.

B.2.2.3 Camera (Saturation Component)

An additional data analysis step that has not been explored by those in the literature was to examine the Saturation (S) component of the HSV colour space. The value of the Hue (H) component is used for tracing the colour change and hence the concentration of pH; it was felt that the S component could hold some value and show some interesting characteristics of the dye. As mentioned earlier, the saturation component measures the intensity of the colour while the Hue measures the colour itself. Coupled with the fact that many colorimetric dyes such as BCG, shifts from one colour to another, it was believed that while one colour fades (or becomes less intense) another in its spectrum shift becomes more prominent, this changeover point may therefore indicate the pK_a value of the dye. Figure B.8 shows the plot of the Saturation (S) component along with a Gaussian model for best fit. Here one can see that the change in colour intensity occurs at a value of ca. 4.7 from this plot alone. However, to ascertain a quantitative value, the model was inverted (to

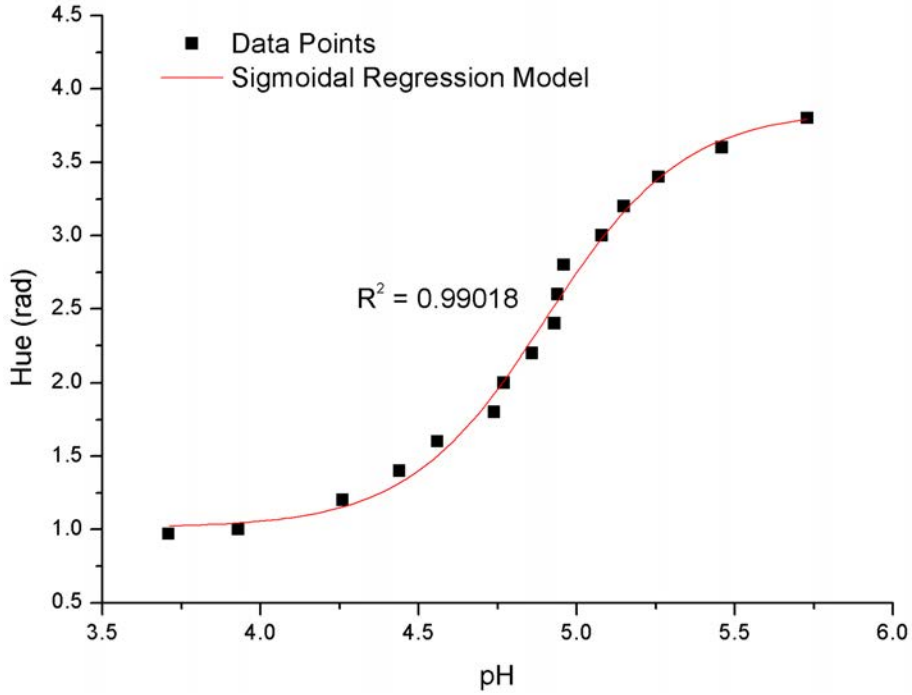

Figure B.6: Hue component plot of camera vs pH. Sigmoidal fit (Blotzmann) yields an excellent fit of $R^2 = 0.99018$.

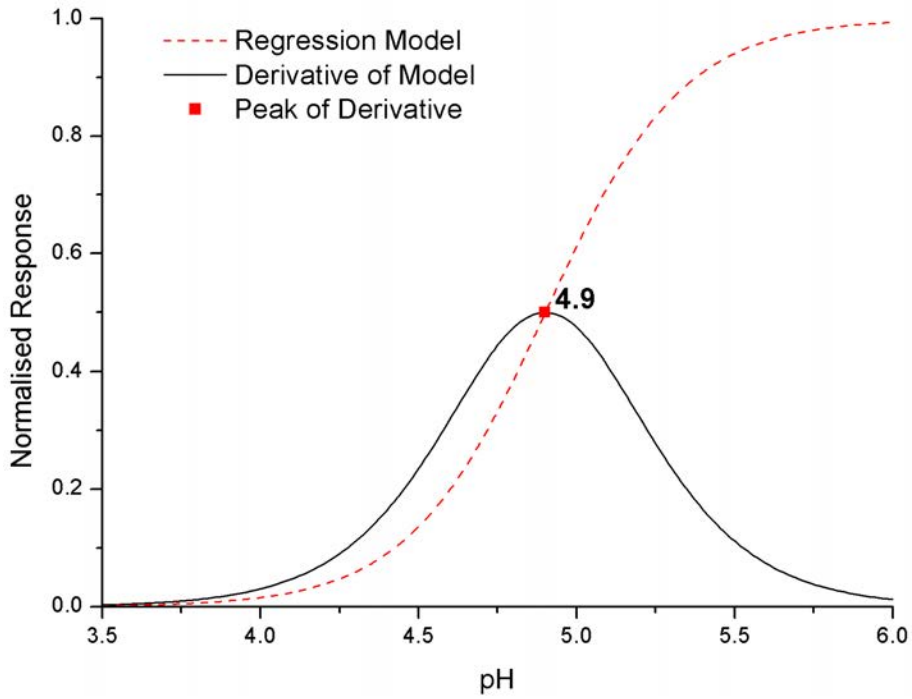

Figure B.7: Model (dashed like) from sigmoidal fit in Figure B.6. 1^{st} derivation (solid line) gives an estimated pK_a value of 4.9.

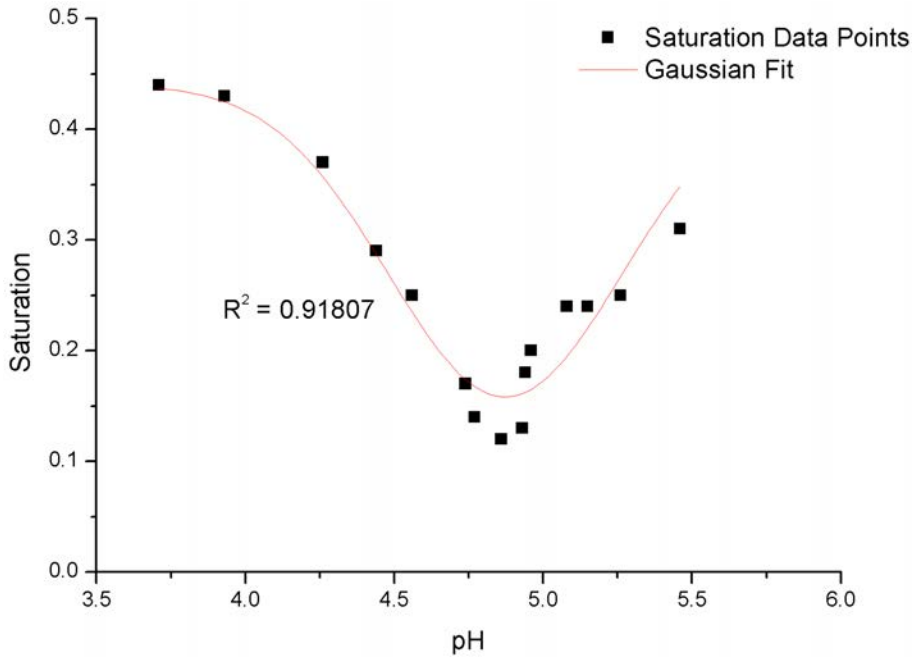

Figure B.8: Saturation component plot of camera vs pH.

comply with the peak detection algorithm), normalised and plotted in Figure B.9. The result of this analysis yields a value of 4.87 which is in excellent agreement with the pK_a value ascertained through the Hue approach.

B.2.2.4 Comparison of Results

Table B.1 lists the differences found in the estimated pK_a using the three methods employed above. Each estimation was compared to the ideal BCG pK_a value of 4.74 at room temperature [569, 571]. The differences are very small albeit closer when using the camera. The reason for this can be attributed to those mentioned previously along with the ability for the camera to take an average over a large number of pixels in comparison to the point measurement of the spectrophotometer; thus reducing noise effects, if present. The message in these results is that the camera has the potential to detect the highest point of colour change and as a result holds promise for more complex indicators to be analysed such as those with multiple dyes comprised of multiple indicators. Furthermore, the literature at present demonstrates that a camera can track colour change and therefore does not account for other colorimetric indicators that do not change wrt colour but wrt colour intensity. These results show that the saturation component tracks changes in colour intensity and therefore may offer the capability to determine colourless to coloured dyes such as phenolphthalein (turning from colourless in acidic solutions and pink in basic solutions).

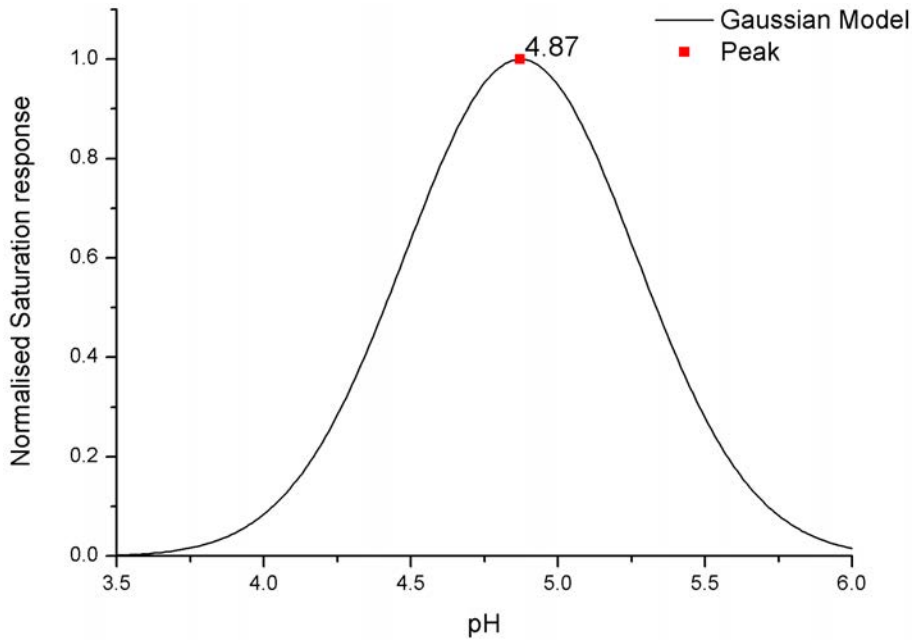

Figure B.9: Gaussian model derived from Figure B.8, inverted and normalised between 0 and 1. Peak analysis yields a value of 4.87 which agrees with the pK_a value of 4.9 ascertained in Figure B.7.

Next, the two methods (absorbance via the spectrophotometer and colour via the camera) were tested for correlation.

Table B.2 gives the measured pH values for all 16 samples using the pH meter along with the predicted pH of both the UV-Vis and camera by means of the models ascertained in Figures B.4 and B.6, respectively. In addition, the data were compared and the relative percentage error (%RE) was calculated as: $\frac{B-A}{B} \times 100$ where B and A take the values obtained using the pH-meter and both sensing devices. It can be seen that the errors were low in both cases i.e. for the UV-Vis instrument (%RE ≤ 1.07 %) and for the camera (%RE ≤ 1.33 %). By means of the predicted pH data it was possible to determine the correlation between both sensing approaches. Figure B.10 shows a plot of the predicted pH for all 16 samples predicted by their models. The figure shows that excellent correlation between the two data sets was obtained ($R^2 = 0.98835$, n=16) and that both approaches are therefore equivalent in terms of measuring pH. It should be mentioned at this point that the UV-Vis approach requires a controlled lighting environment to operate, however the approach adopted via the camera has successfully operated under variable lighting conditions whilst showing a high correlation and a low relative error to the measured pH.

By analysis of both the Hue and Saturation components as a dye changes in colour with respect to a chemical change, it can be seen that one may be able to measure not only the pH of the dye, but also other characteristics of a colorimetric indicator simultaneously i.e. the pK_a through the Saturation component and ultimately through the use of a low cost, off the shelf, digital colour camera. With excellent model fits and very close pK_a approximations to that within the literature,

Table B.1: Comparison of pK_a estimation from all approaches.

Method	Estimated pK_a	Difference to Ideal Value (4.74)
Spectrophotometer	4.98	0.24
Hue	4.9	0.16
Saturation	4.87	0.13

Table B.2: Predictions and percentage relative error of both UV-Vis and Camera sensing approaches.

Sample Number	pH Meter	UV-Vis pH Prediction	Camera pH Prediction	%RE (UV-Vis)	%RE (Camera)
1	5.73	5.75	5.75	-0.42	-0.38
2	5.46	5.43	5.41	0.62	0.97
3	5.26	5.28	5.26	-0.32	-0.07
4	5.15	5.14	5.17	0.25	-0.30
5	5.08	5.09	5.09	-0.11	-0.13
6	4.96	5.01	5.02	-1.06	-1.16
7	4.94	4.94	4.95	0.09	-0.28
8	4.93	4.93	4.89	-0.08	0.77
9	4.86	4.81	4.83	0.95	0.62
10	4.77	4.74	4.76	0.59	0.11
11	4.74	4.76	4.69	-0.32	0.99
12	4.56	4.57	4.61	-0.16	-1.07
13	4.44	4.45	4.50	-0.29	-1.33
14	4.26	4.27	4.32	-0.13	-1.49
15	3.93	3.89	4.10	1.07	-4.29
16	3.71	3.74	3.98	-0.80	-7.25

it has been shown that a camera is a viable chemical measurement unit. The results of the camera were correlated against that of the reference instrument and a high linear correlation was obtained. However, the results of this correlation may not be excellent and this may be due to the fact that the camera considers the full visible spectrum where as the reference instrument only analyses an extremely narrow waveband. In addition, the fact that the UV-Vis was analysing samples of varying concentrations in the dye (due to the removal of aliquots and addition of more acid and base for balance) may explain this slight inaccuracy. Further analysis into this issue may yield for greater accuracy. The important aspect to establish through this process was to investigate if a low cost camera was capable of distinguishing between two extreme pHs in solution form. This concept will now be tested when the dye is bound in a polymer matrix.

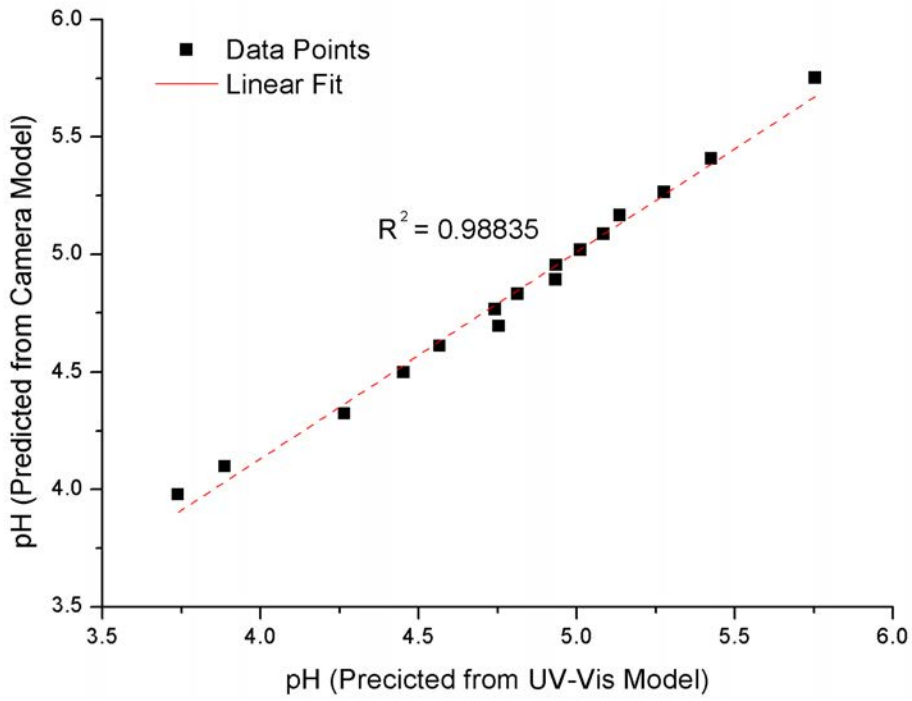

Figure B.10: Correlation plot of reference instrument against analysis of the Hue component when using a low cost camera. A high linear correlation exists between both data sets: $R^2 = 0.98835$.

B.3 Analysis of pH Using the HSV colour space: Dye Bound in Polymer Matrix

It is promising that the camera, using the HSV colour space, has detected differences in pH and resulted in an excellent sigmoidal fit to the reference pH instrument whilst in solution form. The previous results gives confidence for the use of the HSV colour space and especially in uncontrolled lighting conditions. Projecting forward to a proof of principle test of the central hypothesis, i.e. the use of a chemical indicator on satellite stations, it becomes necessary for this sensing approach to be evaluated while the dye is bound within a polymer matrix. Furthermore, as the proof of principle study will qualitatively determine the presence of a chemical within a water system, only two chemical extremes are considered using the same dye but bound within a gel structure to also investigate leaching effects.

B.3.1 Experimental

The procedure followed in this section is very similar to that of the previous study i.e. dye in solution form (Section B.2). Firstly, the choice of dye in this case remained consistent to the previous experiment as bromocresol green and immobilised within a polymer where the preparation was outlined by Benito-Lopez *et al.* [570]. Next, the polymer strip was placed in a petri dish beside a colour reference chart (XRite colour reference chart) on a lab bench. A wireless camera (ZTV ZT830T) is held by

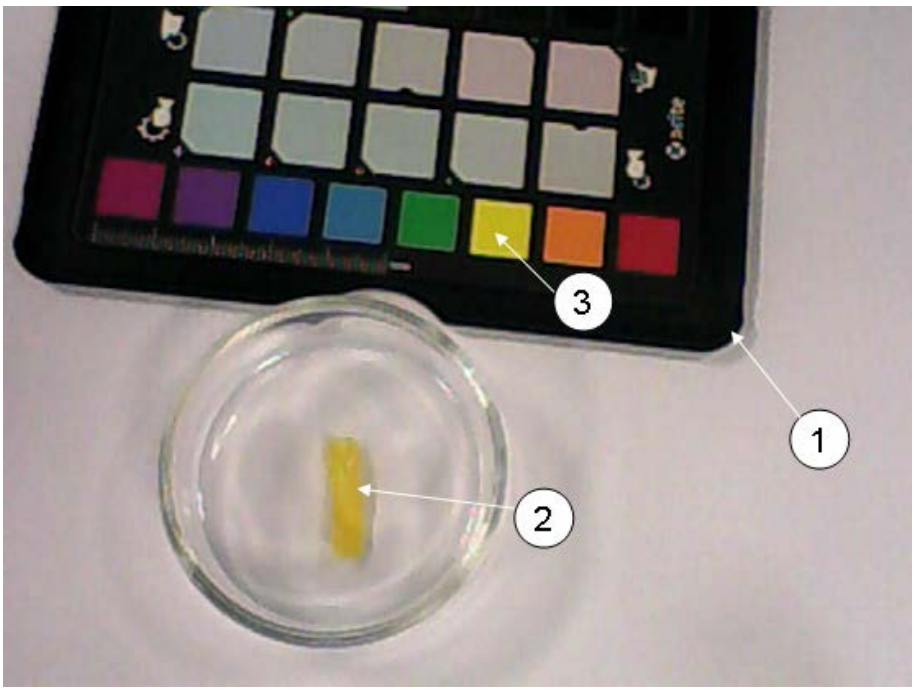

Figure B.11: Dye bound in polymer matrix experimental setup. (1) XRite colour reference chart. (2) Bar code i.e. bromocresol green dye in polymer matrix. (3) Yellow patch used as reference on XRite colour chart.

a retort stand an pointed down with the strip and reference chart in it field of view. The setup can be seen in Figure B.11.

For this procedure, the video was captured in the same format as in the previous section but instead of performing the analysis in real time, the video was captured to file for processing and analysis offline. Once the experimental setup was established, the video was set to record and the following steps were repeated 3 times in total:

1. A 0.1 M solution of KOH was added to the petri dish allowing for the strip to be completely immersed within it;
2. The strip was allowed time to change colour until it appeared blue i.e. until it appeared to stop changing colour;
3. At this point, the excess KOH was emptied and/or soaked up using standard lab blue roll;
4. Next, a 0.1 M solution of HCl was added to the petri dish allowing for the strip to be completely immersed within it;
5. Again, the strip was allowed time to change colour back to its acidic state i.e. yellow.
6. The excess HCl was emptied from the petri dish and/or soaked up.

Image processing was performed offline through the use of a recorded video file as the source. The image processing steps were identical to the precess outlined in the previous section except that it was performed twice on two separate regions and that the values were automatically saved to file. The first process executed was taking the strip as the object of interest. The following run took the yellow patch on the reference chart as the object of interest (see Figure B.11). Both data sets were then taken and plotted on the same graph.

B.3.2 Results

Figure B.12 shows the results of the image analysis of two objects within the camera's field of view. The first plot line (red line) shows the analysis of the yellow reference patch which reports a constant average hue reading of ca. 1 rad. The constancy is notable especially in a busy laboratory environment where there were many lighting effects on the patch through shadowing effects introduced by laboratory personnel. This is the first indication that by using this colour space, one may have a robustness to such lighting effects.

The second plot line (blue line) shows the change in the hue channel when the dye was exposed to two different chemicals i.e. KOH and HCl and repeated 3 times. The kinetics of the reaction are very different when one compares the first against the second and third. It was concluded that this can be attributed to the fact that the strip was not fully hydrated and so it took longer for the ion exchange to fully interact with the dye molecules. By analysis of the second and third reactions, one can see that the reaction times are significantly faster. Moreover, the reproducibility of the reaction is very consistent i.e. reporting ca. 3.5 rad in its alkaline state and ca. 0.9 rad in its acidic state. Overall, the results look very promising and allows for this work to be used in the proof of principle study in future work.

B.4 Conclusions

Overall the results show that the camera, using the HSV colour space, can in-fact convey information from the molecular word and is viable as a chemical detector and furthermore can give promising results even under variable lighting conditions. The results from the first experiment (solution form) showed that the use of the Hue parameter of the HSV colour space can be used as a quantitative measurement of pH when in use with a colorimetric dye as it followed an expected sigmoidal response. Furthermore, simple analysis of the Saturation (S) component of the HSV colour space warrants further investigation as it has strongly indicated the pK_a value of the dye at the point when the two colours changeover. Later, as the focus

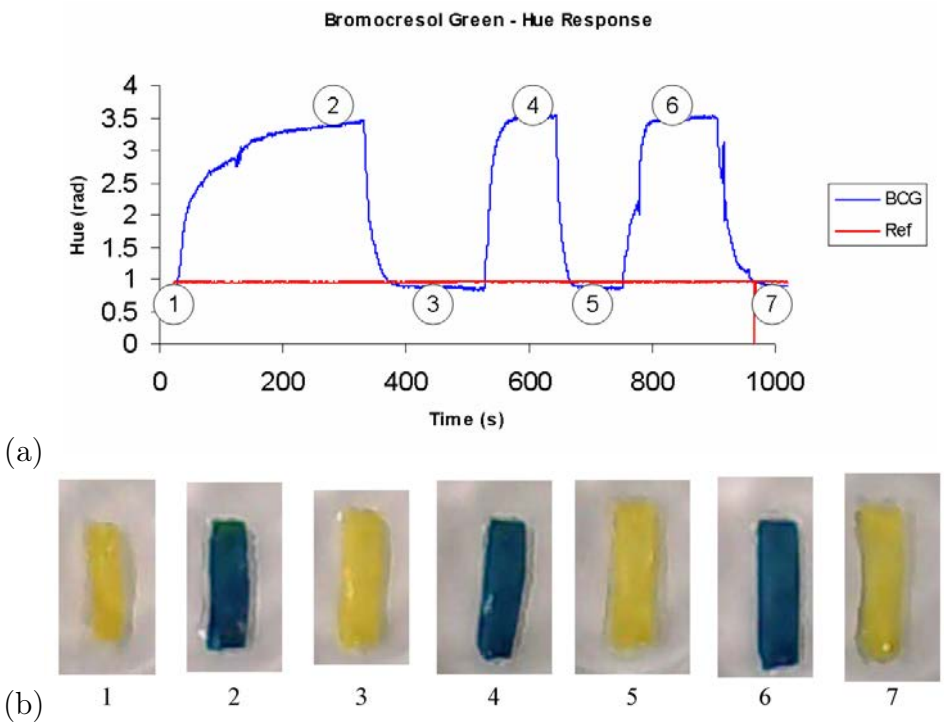

Figure B.12: (a) Response plot of polymer bar code to repeated exposures of 0.1 M HCl and 0.1 M KOH. (b) Video frames of bar code colour at different times during the experiment.

moves towards the requirements of the proof of principle study i.e. a reproducible, qualitative measurement of pH using a camera in ambient lighting conditions, the second experiment showed that a colorimetric dye immobilised within a polymer matrix can successfully be used as a qualitative indication of the presence of a chemical. Therefore, this work is now ready to qualify the presence of a localised chemical plume within a water body and analyse multiple stationsi.e. as preliminary to Chapter 3.

B.5 References

[567] Alvy Ray Smith. **Color gamut transform pairs**. In *SIGGRAPH '78: Proceedings of the 5th annual conference on Computer graphics and interactive techniques*, pages 12–19, New York, NY, USA, 1978. ACM.

[568] Soren Sorensen. **Enzymstudien. II Mitteilung. Uber die Messung und die Bedeutung der Wasserstoffionenkoncentration bei enzymatischen Prozessen**. *Biochemische Zeitschrift*, **21**:131 – 304, 1909.

[569] R. W. Sabnis; S. Sanders; LLP. Dempsey. *Handbook of Acid-Base Indicators*. CRC Press, 2007.

[570] F. Benito-Lopez, S. Coyle, R. Byrne, C. O'Toole, C. Barry, and D. Diamond. **Simple Barcode System Based on Inonogels for Real Time pH-Sweat Monitoring**. In *Body Sensor Networks (BSN), 2010 International Conference on*, pages 291 –296, 2010.

[571] D.R. Lide. **CRC Handbook of Chemistry and Physics**. *CRC Press*, **1**:8–19, 2004.

[572] Martina O' Toole, King Tong Lau, and Dermot Diamond. **Photometric detection in flow analysis systems using integrated PEDDs**. *Talanta*, **66**(5):1340 – 1344, 2005.

C

Microfluidic pH Mapping Paper: Supplementary Information

C.1 Materials and Methods

Aniline (BDH), HCl (Fisher Scientific), ammonium persulfate (Aldrich), N-[3- (Trimethoxylsilyl)propyl]aniline (Aldrich), sodium hydroxide (Aldrich) were used. The aniline monomer was purified by vacuum distillation before use. Other chemicals were used as received.

Raman Spectroscopy was employed to study the chemical features of the polyaniline coatings inside the microchannel. Raman spectra were taken with a Perkin Elmer RamanStation at 2 cm^{-1} resolution, 3 s per scan and 10–20 collections. A 785 nm laser line was used as it can detect both doped and dedoped features in polyaniline.

Scanning Electron Microscopy (SEM) was carried out at an accelerating voltage of 20 kV on a S-4300 Hitachi system. For imaging purposes the PDMS layer of the PDMS/glass microchannel was removed. The glass layer containing the polyaniline film was coated with 10 nm Au prior to imaging.

UV-Vis Spectroscopy was used to study the pH dependence of the polyaniline coatings. The absorbance spectra were recorded using 2 fiber-optic light guides connected to a Miniature Fiber Optic Spectrometer (USB4000 - Ocean Optics) and aligned using an in-house made cell (see Figure C.1 on page 229). The light source used was a Deuterium – Halogen light source (Top Sensor Systems).

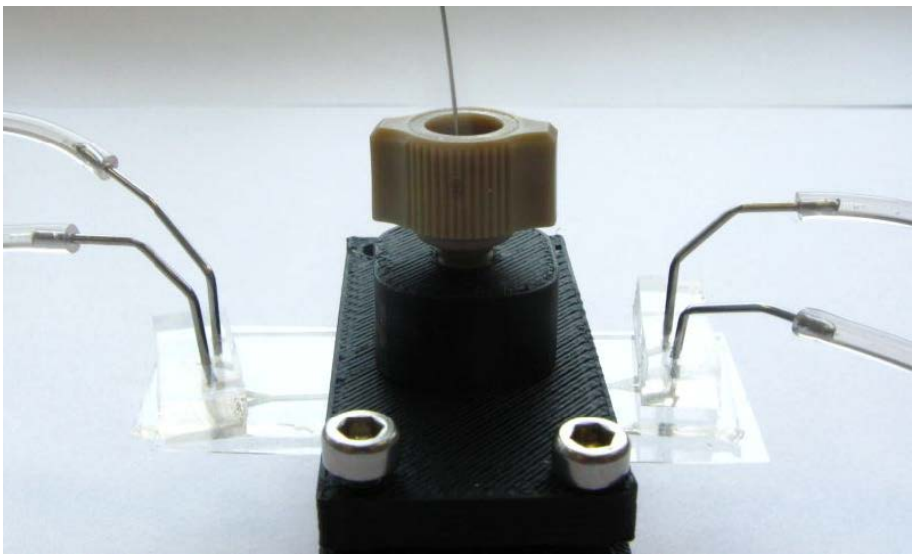

Figure C.1: In house designed holder used for absorbance measurements of the PAni coatings.

C.2 Digital Image Capture

Throughout the calibration routine, the images were captured using a Panasonic DMC-FZ38 digital colour camera which was held in a fixed position via a retort stand at a distance of 7 cm from the microchannel / reference chart to fully capture the image scene, see Figure C.2a on page 231. The camera was set to capture in RAW format to eliminate possible image artefacts and at a resolution of 4016 $\times$ 3016 (12 $MPixels$). The other camera settings were as follows: F-Number (2.8), Max aperture (F2.8), No Flash and a Focal Length of 4.8 mm.

Once the images were captured, they underwent a segmentation process where pixels representing the flow channel and reference patches were identified and separated into image regions. This was achieved through the use of an Interactive Segmentation Toolkit [581]. Although an unsupervised/automatic segmentation algorithm was possible, it was felt that this supervised approach was more robust to misclassifications and as a result, it fully ensured the location and determination of the reference patches and channel regions. A binary mask image resulted from this process with black pixels representing areas of non interest (e.g. the background) and white regions representing the reference colour patches and the flow channel. Finally, a binary erosion algorithm was applied to remove possible boundary pixels and also any isolated white pixels i.e. to ensure robustness for subsequent processing steps, see Figure C.2b on page 231.

Next, it was necessary to identify each region separately for correct analysis. Therefore, a connected component algorithm was applied to the binary mask image which assigned a unique region identification number to each image area with connected white pixels. This allowed for each of the reference patches and flow channel to be analysed separately at a later stage. Subsequently, due to the consist-

ency across all images (from the experimental constraints) it was possible to easily identify each region based on their spatial coordinates within the image. As a result, each patch was identified correctly in all instances via their calculated centroid locations in each subsequent image.

After that, the calibration images were taken and processed. Initially, the original images underwent a white balance process in order to compensate for possible changes in the ambient lighting environment. This involved generation of the histograms for each of the Red, Green, and Blue channels of the captured sRGB colour space. Next, a binary threshold was determined at either end of each histogram. Pixel counts that used less than 0.05% of the total image pixels were discarded at each histogram ends and the histograms were stretched to the boundary i.e. 0 and 255. The images were then reconstructed. Next, a copy of this image was made and transformed from the captured sRGB colour space into the HSV (Hue, Saturation and Value) colour space [583]. Following this, the binary mask image was applied to the HSV image through a simple pixel-by-pixel binary AND operation on the Hue channel alone. Finally, the colour of each region was ascertained by calculating its Hue average and saving it to an external file in CSV (comma separated value) format for all regions within each image for later analysis.

The gradient analysis step took place in much the same way as with the calibration image processing. However, instead of calculating the Hue average over the entire flow channel region, a localised average was considered at discrete points along the channel's path. This was achieved by firstly isolating the flow channel region alone via its bounding box and using that to crop the image thereby removing the reference patches. Here, a medial axis transformation was applied to this singular binary region resulting in an 8-connected contour line alone the centre of the channel at a width of 1 pixel [584, 582], see Figure C.3 on page 231. After this, the starting point was identified to be at the most extreme upper left white pixel of the contour. Next, a binary circular mask image with a diameter of 35 pixels was created and combined (binary AND operation) with the binary mask image of the channel at the starting point. The resulting mask was, in turn, applied to the Hue channel at the same location. Finally, the average Hue value at this sub region was calculated and saved to a CSV file. The process was repeated at every pixel location along the contour with all values saved to file.

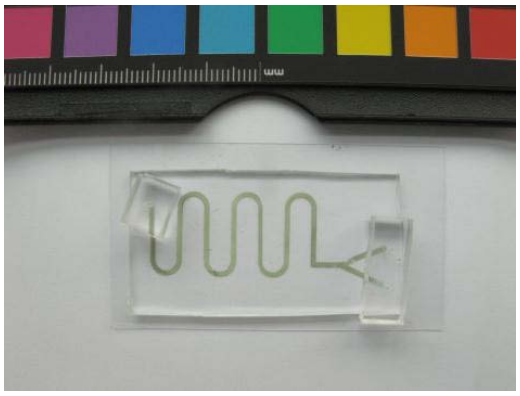

(a) Picture of a captured image during the experimental procedure showing the colour reference chart/patches and flow channel.

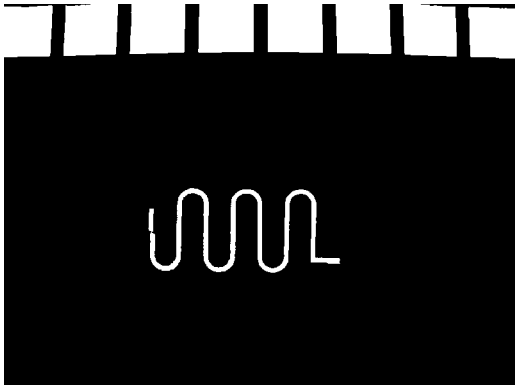

(b) Mask image after image processing algorithms were applied.

Figure C.2: Segmentation process.

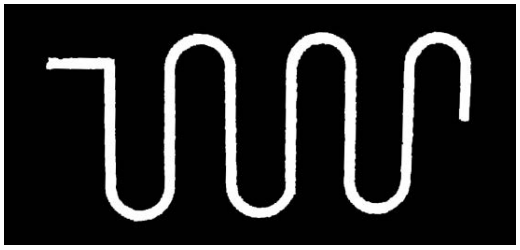

(a) Processed images showing the mask region of the flow channel.

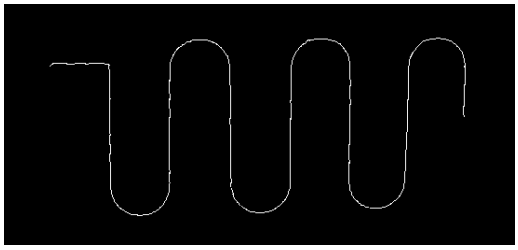

(b) The result of applying a medial axis transformation.

Figure C.3: Image processing depicting the medial axis transformation process.

C.3 Characterisation of Polyaniline (PAni) Coating by Raman Spectroscopy

Raman spectroscopy is a very powerful technique for the analysis of intrinsically conducting polymers. Here, Raman spectroscopy is employed to study the chemical structure of the coating as this technique permits in situ analysis of the polyaniline coating inside the microchannel. In the case of polyaniline, Raman spectroscopy can also be used to study its doping-dedoping behaviour as very distinct signature bands appear for the quinoid and benzenoid rings respectively.

Figure C.4 on page 233 presents the Raman spectra of a polyaniline functionalised microchannel taken after a solution of pH 2 (HCl, $10^{-2}\,M$) and pH 12 (NaOH, $10^{-2}\,M$), respectively are passed inside the microchannel. For comparison, the spectrum of a bare PDMS microchannel is also shown (black). For low pH values the polymer exists in the doped state, emeraldine salt (ES). Increasing the pH causes a change in the bonding structure of the material, and at high pH values PAni is present in its dedoped state – emeraldine base (EB). Signature bands between 1300 cm^{-1} and 1400 cm^{-1} appear for the doped material (Figure C.5 on page 233 – in green). These are less significant at higher pH values, and strong bands between 1400 cm^{-1} and 1500 cm^{-1} reflect the dedoped state (Figure C.5 on page 233 – in blue).

In particular, in the case of EB, an important peak can be observed at 1454 cm^{-1} and is characteristic to C=N stretching vibration of the quinoid units [574, 575, 576, 577, 578]. Other bands at 1596 cm^{-1} and 1164 cm^{-1}, are assigned to C-C stretching [574, 577] and C-H bending modes [574, 575], respectively, centered on the quinoid ring. Another new peak at 1221 cm^{-1} appears in the spectra of polyaniline upon dedoping and is assigned to C–N stretching vibrations of the benzenoid units [574, 577] (the EB form consists of both C=N and C-N bonds). In the case of ES, the most important band appears at 1340 cm^{-1} and can be assigned to a C-N• + polaron stretch [574, 577, 579, 580] while the band at 1172 cm^{-1} is characteristic to the C–H in-plane bending of the benzenoid ring [574, 578]. Both C - C stretching vibrational modes, in the benzenoid and quinoid rings, are seen at 1612 cm^{-1} and 1588 cm^{-1}, respectively [577], in the case of polyaniline spectra taken at pH 2. This suggests that minor fractions of non protonated quinoid rings are still present in the structure. It has been shown before that the Raman Intensity is enhanced in the case of EB compared with ES when a 785 nm laser is used [578]. The PAni coating may also be partially excited to the EB form by the incoming laser radiation resulting in resonant enhancement of the lines originating from the quinoid ring [577]. The specific vibrations of PDMS can also be found in the spectra of polyaniline coatings since polyaniline is attached to the inner walls of the PDMS/ glass microchannel. The CH_3 bending vibrations appear at 1263 cm^{-1} and 1412 cm^{-1} [573]. Other

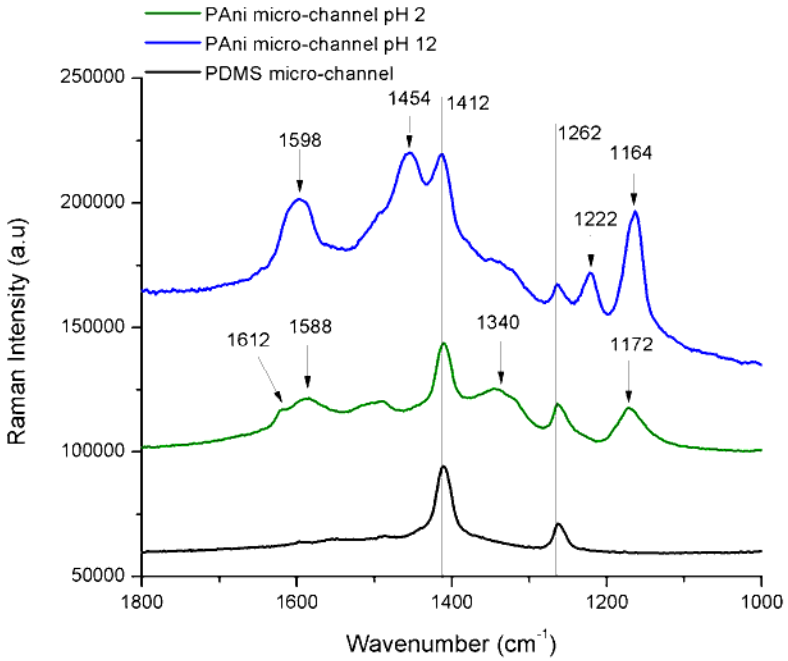

Figure C.4: Raman Spectra of unfunctionalised PDMS microchannel (black), PAni functionalised microchannel after being filled with a pH2 HCl solution (green) and PAni functionalised microchannel after being filled with a pH12 NaOH solution (blue).

bands specific to the PDMS layer are also present: Si-O-Si symmetric stretching (490 cm^{-1}), Si-C symmetric stretching (708 cm^{-1}), CH3 symmetric stretching (2904 cm^{-1}), and CH3 asymmetric stretching (2964 cm^{-1}) [573], but not shown here.

C.4 pH Measurements

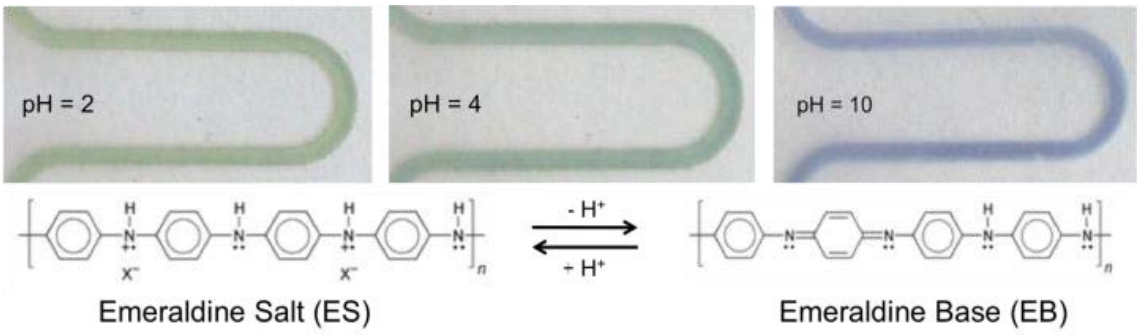

Figure C.5: Photos of a microchannel loop when solutions of different pHs are flushed through the channel. The photos are accompanied by a scheme showing the differences in the chemical structure of polyaniline (two different states: Emeraldine Salt and Emeraldine Base).

C.5 pH determination via colorimetric imaging analysis

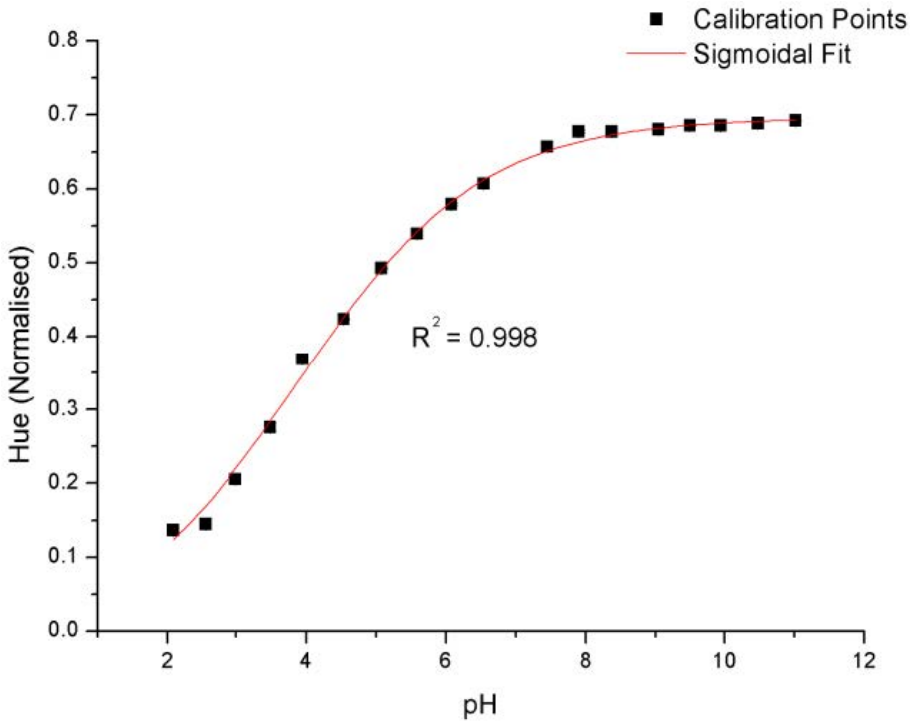

Figure C.6: Calibration plot of the camera and channel to changing pH. Points represent the normalised average Hue value of the channel's colour across multiple images and the error bars (occluded by the points) represent their standard deviation. The line is a sigmoidal fit after applying Boltzmann's regression technique ($R^2 = 0.998$, $n = 18$).

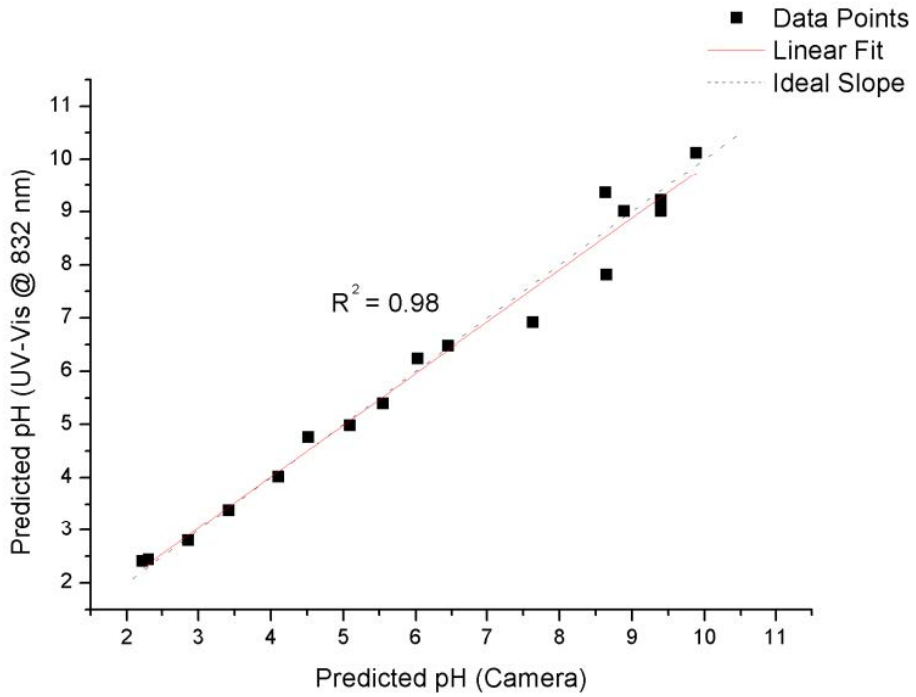

Figure C.7: Plot showing the correlation between predicted pH using the camera and UV-Vis at 832 nm. The line represents a linear fit ($R^2 = 0.98$, $n = 18$).

C.6 References

[573] SC Bae, H Lee, ZQ Lin, and S Granick. Chemical imaging in a surface forces apparatus: Confocal Raman spectroscopy of confined poly(dimethylsiloxane). *Langmuir*, 21(13):5685–5688, JUN 21 2005.

[574] K Berrada, S Quillard, G Louarn, and S Lefrant. Polyanilines and Substituted Polyanilines - A Comparative-Study Of The Raman-Spectra of Leucoemeraldine, Emeraldine And Pernigraniline. *Synthetic Metals*, 69(1-3):201–204, MAR 1 1995. 13th International Conference on Science and Technology of Synthetic Metals (ICSM 94), SEOUL, SOUTH KOREA, JUL 24-29, 1994.

[575] Y Furukawa, T Hara, Y Hyodo, and I Harada. Vibrational-Spectra Of Polyaniline And Its N-15-Substituted And H-2-Substituted Derivatives In As-Polymerized, Alkali-Treated And Reduced States. *Synthetic Metals*, 16(2):189–198, Nov 1986.

[576] A Hugotlegoff and MC Bernard. Protonation and Oxidation Processes In Polyaniline Thin-Films Studied By Optical Multichannel Analysis And In-Situ Raman-Spectroscopy. *Synthetic Metals*, 60(2):115–131, Sep 15 1993.

[577] J Laska, R Girault, S Quillard, G Louarn, A Pron, and S Lefrant. Raman spectroscopic studies of polyaniline protonation with bis(2-ethylhexyl) hydrogen phosphate. *Synthetic Metals*, 75(1):69–74, Nov 1995.

[578] T Lindfors and A Ivaska. Raman based pH measurements with polyaniline. *Journal of Electroanalytical Chemistry*, 580(2):320–329, JUL 1 2005.

[579] C Liu, JX Zhang, GQ Shi, and FE Chen. Doping level change of polyaniline film during its electrochemical growth process. *Journal of Applied Polymer Science*, 92(1):171–177, APR 5 2004.

[580] R. Mazeikiene, A. Statino, Z. Kuodis, G. Niaura, and A. Malinauskas. In situ Raman spectroelectrochemical study of self-doped polyaniline degradation kinetics. *Electrochemistry Communications*, 8(7):1082–1086, JUL 2006.

[581] Kevin McGuinness and Noel E. O'Connor. A comparative evaluation of interactive segmentation algorithms. *Pattern Recognition*, 43(2):434–444, FEB 2010.

[582] J.R. Parker. *Algorithms for Image Processing and Computer Vision*. IT Pro. Wiley, 2010.

[583] Alvy Ray Smith. Color gamut transform pairs. *SIGGRAPH Comput. Graph.*, 12(3):12–19, August 1978.

[584] TY Zhang and CY Suen. A Fast Parallel Algorithm For Thinning Digital Patterns. *Communications of the ACM*, 27(3):236–239, 1984.